

**MECHANISMS AND SPECIFICITY OF LENTIVIRUS
NEUROTOXICITY.**

Isabella Starling

Thesis submitted for the degree of
Doctor of Philosophy
Preclinical Veterinary Sciences
Royal (Dick) School of Veterinary Studies
University of Edinburgh
1998



TABLE OF CONTENTS

Declaration	i
Acknowledgements	ii
Abbreviations	iii
Abstract	vi
CHAPTER 1: INTRODUCTION	1
1.1. INTRODUCTION TO LENTIVIRUSES.	2
1.1.1. Description and history of MVV.	2
1.1.2. Genomic description of Lentiviruses.	3
1.1.2.1. <i>Structural genes.</i>	3
1.1.2.2. <i>Regulatory genes.</i>	4
1.1.3. Cellular tropism of MVV and HIV.	9
1.1.4. The MVV life cycle	9
1.2. PATHOLOGY OF MVV AND HIV INFECTION.	10
1.2.1. Lungs.	10
1.2.2. Joints.	11
1.2.3. Central Nervous System	12
1.3. LENTIVIRAL INVASION OF THE CNS.	14
1.3.1. Neurotropism of MVV and HIV.	14
1.3.2. Mechanisms of HIV and MVV entry to the CNS.	15
1.4. NEUROPATHOGENESIS OF LENTIVIRAL INFECTIONS.	18
1.4.1. Direct action of viral fragments.	18
1.4.1.1. <i>gp120</i>	18
1.4.1.2. <i>Tat</i>	19
1.4.1.3. <i>Rev</i>	20
1.4.1.4. <i>Nef</i>	21
1.4.1.5. <i>gp41</i>	21
1.4.2. Indirect causes of neurodegeneration	21
1.4.2.1. <i>Quinolinic acid (QA).</i>	21
1.4.2.2. <i>An NMDA-like neurotoxin.</i>	22
1.4.2.3. <i>Cytokines.</i>	22
1.4.2.3.1. <i>Cytokine receptors in the CNS.</i>	23
1.4.2.3.2. <i>TNFα in HIV and MVV infection.</i>	24
1.4.2.3.3. <i>IL-1β and IL-6 in HIV and MVV infection.</i>	25
1.4.2.3.4. <i>TGFβ in HIV and MVV infection.</i>	27
1.4.2.4. <i>Arachidonic Acid (AA) and its metabolites</i>	28
1.4.2.5. <i>Nitric Oxide</i>	29
1.4.2.6. <i>Neuroleukin and vasoactive intestinal polypeptide (VIP)</i>	30
1.4.2.7. <i>Free radicals</i>	30
1.4.2.8. <i>Platelet Activating Factor (PAF)</i>	30
1.4.3. Inflammation and immunological mechanisms in the CNS	32
1.4.3.1. <i>Microgliosis.</i>	32
1.4.3.1.1. <i>Description and functions of microglia.</i>	32
1.4.3.1.2. <i>Microgliosis.</i>	33
1.4.3.2. <i>Astrocytosis.</i>	34

1.4.3.2.1. <i>Types of astrocyte.</i>	34
1.4.3.2.2. <i>Functions of astrocytes.</i>	35
1.4.3.2.3. <i>Astrocytosis.</i>	36
1.4.3.3. <i>The role of the immune response</i>	38
1.5. INTRODUCTION TO EXPERIMENTS	39
CHAPTER 2: MATERIALS AND METHODS	43
2.1. CELL CULTURES	44
2.1.1. PBMC and macrophage (MØ) cell preparation.	44
2.1.2. Rat cortical cultures (RCC).	45
2.2. VIRAL INFECTION OF MACROPHAGES AND PBMCs.	45
2.2.1. 50% Tissue Culture Infectivity dose (TCID ₅₀)	45
2.2.2. MVV infection of PBMCs and macrophages in vitro.	46
2.2.3. Proliferation assay	46
2.3. STEREOTAXIC INJECTIONS	47
2.3.1. PBMC and macrophage cell preparations.	47
2.3.2. MVV and HIV tat peptide injections	48
2.3.3. Sterotaxic injections in scid mice.	50
2.3.4. Stereotaxic injections in rats.	50
2.4. IMMUNOCYTOCHEMISTRY	51
2.4.1. Detection of viral expression in macrophages.	51
2.4.2. Immunocytochemical and histological processing.	51
2.5. ELECTRON MICROSCOPY (EM)	55
2.6. IMAGE ANALYSIS.	55
2.6.1. Degree of astrocytosis and gliosis is scid mice.	55
2.6.2. MVV and HIV tat peptide induced lesions.	56
2.7. RCC TOXICITY ASSAYS.	56
2.7.1. Application of MVV tat peptide.	56
2.7.2. Application of the macrophage culture supernatant.	56
2.7.3. Lactate Dehydrogenase (LDH) assay	57
2.7.4. MTS assay	57
2.8. RT-PCR OF CYTOKINE mRNA FROM CULTURED MACROPHAGES.	58
2.8.1. Isolation and Reverse Transcription (RT) of mRNA from MVV infected and uninfected macrophages.	58
2.8.2. Polymerase Chain Reaction (PCR)	59
2.8.3. Agarose gel electrophoresis.	60
2.8.4. Southern Blotting	61
CHAPTER 3: A MODEL OF MVV ENCEPHALOPATHY IN SCID MICE	64
3.1. INTRODUCTION	65
3.2. EXPERIMENTAL DESIGN.	66
3.3. RESULTS.	67
3.3.1. Viral infection of macrophages.	67
3.3.1.1. <i>p25 expression in vitro</i>	67
3.3.1.2. <i>p25 expression in vivo</i>	67
3.3.2. Degree of inflammation in injected scid mice brains.	70
3.3.2.1. <i>Effects of free virus</i>	70

3.3.2.2. <i>Survival of injected macrophages</i>	72
3.3.2.3. <i>Acute inflammation caused by live macrophages</i>	73
3.3.2.4. <i>Acute inflammation caused by killed macrophages</i>	83
3.3.2.5. <i>Chronic inflammation caused by live macrophages</i>	85
3.3.2.6. <i>Intracerebral injection of PBMCs</i>	87
3.3.2.7. <i>Intravenous injection of macrophages and PBMCs</i>	90
3.3.2.8. <i>Effect of MK801 on acute inflammation caused by live macrophages</i>	90
3.3.3. Cytokine profile of uninfected and MVV infected macrophages.	92
3.3.3.1. <i>RT-PCR</i>	92
3.3.3.2. <i>Southern blotting.</i>	92
3.4. DISCUSSION	94
CHAPTER 4: <i>IN VITRO</i> NEUROTOXICITY OF MVV INFECTED MACROPHAGE PRODUCTS AND LENTIVIRAL TAT.	101
4.1. INTRODUCTION	102
4.2. EXPERIMENTAL DESIGN	102
4.3. RESULTS.	103
4.3.1. Characterisation of rat cortical cell cultures	103
4.3.2. <i>In vitro</i> neurotoxicity of macrophage supernatants.	103
4.3.3. <i>In vitro</i> neurotoxicity of MVV tat peptide.	105
4.3.3.1. <i>Effects at 24 hours</i>	105
4.3.3.2. <i>Effects at 48 hours</i>	106
4.3.3.3. <i>Effects at 72 hours</i>	106
4.4. DISCUSSION	113
CHAPTER 5: <i>IN VIVO</i> NEUROTOXICITY OF LENTIVIRAL TAT.	114
5.1. INTRODUCTION	115
5.2. EXPERIMENTAL DESIGN.	115
5.3. RESULTS.	115
5.3.1. Lesion characteristics	115
5.3.2. Morphometric analysis.	125
5.3.2.2. <i>Time course</i>	130
5.3.2.3. <i>Neuroprotection experiments</i>	130
5.3.3. Electron Microscopy	135
5.4. DISCUSSION.	138
CHAPTER 6: DISCUSSION	141
6.1. EFFECTS OF MVV INFECTED MACROPHAGES ON <i>SCID</i> CNS.	142
6.2. EFFECTS OF MACROPHAGE PRODUCTS AND MVV TAT PEPTIDE ON NEURONS <i>IN VITRO</i>.	146
6.3 EFFECTS OF LENTIVIRAL TAT PEPTIDES <i>IN VIVO</i>.	147
6.4. CONCLUSIONS AND FUTURE DIRECTIONS	150
BIBLIOGRAPHY	151

TABLE OF FIGURES

Fig. 1.1: Diagram of a mature MVV virion	6
Fig. 1.2: The MVV genome and encoded proteins	7
Fig. 1.3: Transactivating protein Tat of MVV	8
Fig. 1.4: Proposed mechanisms of HIV entry into brain	18
Fig. 1.5: Neurotoxic mechanisms of lentiviral neurodegeneration	33
Fig. 2.1: Single letter amino acid codes of peptides used	49
Fig. 2.2: Immunocytochemical detection of tissue antigens	53
Fig. 2.3: Experimental protocol for immunocytochemistry on free-floating sections	54
Fig. 2.4: The Polymerase Chain Reaction	62
Fig. 3.1: p25 immunoreactivity in MVV infected macrophages <i>in vitro</i>	69
Fig. 3.2: Effect of MVV injection on GFAP and F4/80 staining in <i>scid</i> striatum	71
Fig. 3.3: Detection of injected CD14 positive MØ in <i>scid</i> striatum	74
Fig. 3.4: GFAP staining of <i>scid</i> mouse striatum 1 week post-operatively	75
Fig. 3.5: F4/80 staining of <i>scid</i> mouse striatum 1 week post-operatively	76
Fig. 3.6: Effect of MØ number on GFAP staining of <i>scid</i> striatum	79
Fig. 3.7: Effect of MØ maturity on GFAP staining of <i>scid</i> striatum	80
Fig. 3.8: Effect of live MØ on GFAP staining in <i>scid</i> striatum	81
Fig. 3.9: Effects of live MØ on GFAP and F4/80 induction in <i>scid</i> striatum	82
Fig. 3.10: Effects of killed MØ on GFAP and F4/80 induction in <i>scid</i> striatum	84
Fig. 3.11: Chronic effects of MØ on GFAP and F4/80 staining of <i>scid</i> striatum	86
Fig. 3.12: Effects of PBMCs on GFAP staining of <i>scid</i> striatum	88
Fig. 3.13: Degree of proliferation of PBMCs from MVV infected sheep	89
Fig. 3.14: Effect of MK801 on GFAP and F4/80 induction in <i>scid</i> striatum	91
Fig. 3.15: Densitometry analysis of cytokine cDNA obtained from uninfected and MVV infected macrophages	94
Fig. 4.1: <i>In vitro</i> effect of MØ supernatant on neuronal MTS reduction at 24 hours	104
Fig. 4.2: <i>In vitro</i> effect of MVV tat peptide on neuronal LDH release at 24 hours	108
Fig. 4.3: <i>In vitro</i> effect of MVV tat peptide on neuronal MTS reduction at 24 hours	109
Fig. 4.4: <i>In vitro</i> effect of MVV tat peptide on neuronal LDH release at 48 hours	110

Fig. 4.5: <i>In vitro</i> effect of MVV tat peptide on neuronal MTS reduction at 48 hours	111
Fig. 4.6: <i>In vitro</i> effect of MVV tat peptide on neurons LDH release at 72 hours	112
Fig. 5.1: NeuN lesion caused by 1 μ l MVV tat peptide	118
Fig. 5.2: NeuN staining of rat striatum	119
Fig. 5.3: GFAP induction by MVV tat peptide	120
Fig. 5.4: OX42 induction by MVV tat peptide	121
Fig. 5.5: Loss of Diaphorase staining induced by MVV tat peptide	122
Fig. 5.6: Loss of PV immunoreactive neurons induced by MVV tat peptide	123
Fig. 5.7: Loss of ChAT immunoreactive neurons induced by MVV tat peptide	124
Fig. 5.8: Effect of intra-striatal injection of lentiviral tat peptides on NeuN staining at 30 minutes	126
Fig. 5.9: Effect of intra-striatal injection of lentiviral tat peptides on GFAP staining at 30 minutes	127
Fig. 5.10: Effect of intra-striatal injection of lentiviral tat peptides on NeuN staining at 1 hour	128
Fig. 5.11: Effect of intra-striatal injection of lentiviral tat peptide on GFAP staining at 1 hour	129
Fig. 5.12: Progress over time of the NeuN lesion induced by MVV tat peptide	131
Fig. 5.13: Progress over time of the GFAP lesion caused by MVV tat peptide	132
Fig. 5.14: Effect of neuroprotectants on the MVV tat peptide induced NeuN lesion at 1 hour	133
Fig. 5.15: Effect of neuroprotectants on the MVV tat peptide induced GFAP lesion at 1 hour	134
Fig. 5.16: Electron microscopy of neurons at the site of the lesion caused by MVV tat peptide	136
Fig. 5.17: Electron microscopy of glial cells at the site of the lesion caused by MVV tat peptide	137

Declaration

I declare that this thesis was composed entirely by myself as was the execution of the studies, with the exception of the Southern blots, carried out by Bahram Ebrahimi, and the proliferation assay, performed by Lawrence Dickson. The work in this thesis was carried out under the supervision of Prof. G. Arbuthnott and Dr. G. Harkiss.

Isabella Starling

Acknowledgements

I would like to thank my supervisors Gordon Arbuthnott and Gordon Harkiss for their support and encouragement during my PhD, and the MRC for their funding. I would also like to thank Ann Wright, Linda Norrie, Liz Hutton, Cali Ingham, Sue Hood and Gordon Goodall for their help with immunocytochemical and electron microscopy techniques, Bahram Ebrahimi and Zhidong Zhang for their help with RT-PCR and southern blotting, Colin Warwick for his excellent advice on graphics, Jeremy Bradshaw for his computer knowledge, Gillian May for her help with the neuronal cultures, all the staff at the Medical Microbiology Transgenic Unit and the Marshall Building, and last but not least Lawrence Dickson for his technical assistance, his sheep handling skills and his patience!

Abbreviations

AA	Arachidonic Acid
ABC	Avidin Biotin Complex
ACh	Achetylcholine
ADC	AIDS Dementia Complex
AIDS	Acquired Immundeficiency Syndrome
β-APP	beta Amyloid Precursor Protein
ATP	Adenosine Triphosphate
BBB	Blood Brain Barrier
BIV	Bovine Immunodeficiency Virus
BMVECs	Brain Microvascular Endothelial Cells
ChAT	Choline Acetyl Transferase
CNS	Central Nervous System
CSF	Cerebrospinal Fluid
Da	Daltons
DAB	3'3'-diaminobenzidine
DMEM	Dulbecco's Modified Eagle's Medium
DMSO	Dimethyl Sulphoxide
DNA	Deoxyribonucleic Acid
cDNA	copy DNA
dsDNA	double stranded DNA
ECM	Extracellular Matrix
EDTA	Ethylenediaminetetraacetic Acid
EIAV	Equine Infectious Anaemia Virus
EM	Electron Microscopy
EtBr	Ethidium Bromide
FCS	Fetal Calf Serum
FITC	Fluorescein Isothiocyanate
FIV	Feline Immunodeficiency Virus
FMOC	9-fluorenylmethoxy-carbonyl
GABA	Gamma Amino Butyric Acid
GFAP	Glial Fibrillary Acidic Protein
HBSS	Hank's Balanced Salt Solution
HIV	Human Immunodeficiency Virus
HRP	Horseradish Peroxidase
5-HT	5-Hydroxytryptamine
HTLV	Human T Lymphotropic Virus
IFNγ	Interferon gamma
IgG	Immunoglobulin
IL-1α	Interleukin-1 alpha
IL-1β	Interleukin-1 beta
IL-6	Interleukin-6
kDa	Kilodaltons

LDH Lactate Dehydrogenase
L-gln L-Glutamine
LIP Lymphocytic Interstitial Pneumonitis
L-NAME N^G-nitro-L-arginine methyl ester
LS Lamb Serum
LT Leukotrienes
LTR Long Terminal Repeat
m Metres
M Molar
MCP Macrophage Chemotactic Protein
M/E Mecaptoethanol
MHC Major Histocompatibility Complex
MK801 (+)-5-methyl-10,11-dihydro-5H-dibenzo[a,d]cyclohepten-5,10-imine maleate
µm Micrometres
µM Micromolar
min Minutes
ml Millilitres
MMLV Moloney Murine Leukemia Virus
MØ Macrophage
mol Moles
MS Multiple Sclerosis
αMSH alpha Melanocyte Stimulating Hormone
MTS 3-(4,5-dimethylthiazol-2-yl)-5-(3-carboxymethoxyphenyl)-2-(4-sulphophenyl)-2H-tetrazolium, inner salt
MVV Maedi Visna Virus
NAD Nicotinamide Adenine Dinucleotide
NADH Nicotinamide Adenine Dinucleotide, reduced form
NADPH Nicotinamide Adenine Dinucleotide Phosphate, reduced form
NBQX 2,3-dihydroxy-6-nitro-7-sulphamoyl-benzo-(F)-quinoxaline
NBT Nitro Blue Tetrazolium
NGF Nerve Growth Factor
NMDA N-Methyl-D-aspartate
nm Nanometres
nmol Nanomoles
NIP Non-specific Interstitial Pneumonitis
NO Nitric Oxide
NOS Nitric Oxide Synthase
NSS Normal Sheep Serum
ORF Open Reading Frame
PAF Platelet Activating Factor
PAP Peroxidase-Anti-Peroxidase
PB Phosphate Buffer
PBMCs Peripheral Mononuclear Cells
PBS Phosphate Buffered Saline
PG Prostaglandins

PGE₂ Prostaglandin E2
PGF_{2α} Prostaglandin F2 alpha
PMS Phenazine Methosulfate
P/S Penicillin and Streptomycin
PV Parvalbumin
QA Quinolinic Acid
RCC Rat Cortical Cultures
RNA Ribonucleic Acid
mRNA messenger RNA
ssRNA single stranded RNA
rt room temperature
RT Reverse Transcription
RT-PCR Reverse Transcriptase - Polymerase Chain Reaction
SA-OMVV South African Ovine Maedi Visna Virus
Scid Severe Combined Immunodeficient
SDW Sterile Distilled Water
SIV Simian Immunodeficiency Virus
SOD Superoxide Dismutase
SPBS Sterile Phosphate Buffered Saline
SS Somatostatin
SSC Standard Saline Citrate
SSPE Standard Salt Phosphate EDTA
TAE Tris Acetate EDTA
TAR Trans-activation Responsive
TBS Tris Buffered Saline
TCID₅₀ 50% Tissue Culture Infective Dose
TGFβ Transforming Growth Factor beta
TNFα Tumour Necrosis Factor alpha
TX Triton-X-100
V-CAM1 Vascular Cell Adhesion Molecule 1
VIP Vasoactive Intestinal Peptide

MECHANISMS AND SPECIFICITY OF LENTIVIRUS NEUROTOXICITY

Abstract

Lentiviruses such as Maedi-Visna Virus (MVV) in sheep and Human Immunodeficiency Virus (HIV) often cause a variety of neurological symptoms in later stages of infection. In sheep, MVV infection results in paralysis and ataxia, with post-mortem investigations revealing astrocytosis, demyelination and axonal damage. At present it is unclear how such neurodegeneration is mediated as MVV, like HIV, does not directly infect neurons. There is much debate as to the mechanisms involved in lentivirus related brain damage, centred around three main possibilities. Firstly, there may be a direct detrimental action of a viral fragment on neuronal cell types. Secondly, MVV infected cells may be releasing diffusible mediators such as cytokines which could cause neural damage or act on astrocytes and microglia causing them to produce factors to induce neurodegeneration. Thirdly, the prospect of an immune response occurring within the brain, involving infected macrophages or microglia, is highly probable.

In order to investigate the possible mechanisms at work in lentivirus induced neurodegeneration, several sets of experiments were carried out. Firstly, a putative model of MVV encephalopathy was established in severe combined immunodeficient (*scid*) mice. *Scid* mice lack T and B cells and are thus unable to mount any immune response. Blood derived macrophages were obtained from healthy sheep and infected with MVV *in vitro*. These were intracerebrally injected into *scid* mice, as were uninfected macrophages, in order to assess the occurrence of any neural cell damage. Cell preparations of peripheral blood mononuclear cells (PBMCs), uninfected, supplemented with virus, or obtained from productively MVV infected sheep, were also administered to *scid* mice in the same manner, to evaluate the role of immune cells in causing any neurodegeneration. The results show that the administration of MVV infected macrophages produces greater gliosis and

astrocytosis in the brains of these mice as compared to those injected with control uninfected macrophages or vehicle. However, the injections of PBMCs did not cause any detectable differences in astrocytes and microglia between the groups. No neuronal loss or demyelination was evident with any of the injections. These results suggest that neural cell disruption in MVV encephalopathy may be due to the presence of MVV infected macrophages in the Central Nervous System (CNS) of infected sheep, acting indirectly through the release of diffusible mediators.

To investigate further the underlying causes of these changes, the possible detrimental contribution of cytokines in this model was evaluated through the use of the reverse transcriptase-polymerase chain reaction (RT-PCR) of MVV infected and uninfected blood derived macrophages *in vitro*. The results show an increase in the levels of the pro-inflammatory cytokine interleukin-1 beta (IL-1 β) mRNA in MVV infected macrophages. Interpretation of this model therefore suggests that MVV exerts an indirect disruptive effect on neural cells via the release of pro-inflammatory cytokines from infected macrophages, causing microgliosis and astrocytosis which in turn lead to major disturbances of brain function.

The possibility of a neurotoxic action of a viral product was also investigated. Peptides derived from the basic region of the transactivating protein Tat from both MVV and HIV have previously been shown to be lethal to neurons *in vivo* and *in vitro*, through a mechanism believed to involve Nitric Oxide (NO)-mediated glutamate neurotoxicity and cytokines. The actions of the MVV tat peptide when injected intracerebrally in rats are diminished one week post-operatively by the N-methyl-D-aspartate (NMDA) receptor antagonist (+)-5-methyl-10,11-dihydro-5H-dibenzo[a,d]cyclohepten-5,10-imine maleate (MK801) and the Nitric Oxide Synthase (NOS) inhibitor N^G-nitro-L-arginine methyl ester (L-NAME). Here, its short term effects were examined and its neurotoxic mechanisms probed through the use of *in vivo* stereotaxic injections and pharmacologic manipulations. The results show that the MVV and HIV tat peptides were very rapidly neurotoxic, causing neuronal cell death within 0.5 hours, and displayed a distinctive and unusual lesion profile. Changes in astrocytes and microglia were also observed. The acute effects of the MVV tat peptide were blocked by MK801, an NMDA receptor antagonist. However,

the administration of L-NAME, a NOS inhibitor, alpha melanocyte stimulating hormone (α MSH), a TNF α inhibitor, or 2,3-dihydroxy-6-nitro-7-sulphamoyl-benzo-(F)-quinoxaline (NBQX), a non-NMDA glutamate receptor antagonist, did not reduce the volume of the lesion. This suggests that the MVV tat peptide acts at the NMDA receptor to cause cell death either directly or via an excitotoxic mechanism.

The findings of the current experiments show that macrophages infected with MVV cause activation of astrocytes and microglia in the brains of *scid* mice. These changes may be detrimental to the normal function of the CNS. Furthermore, they may be caused by the increased release of pro-inflammatory cytokines, especially IL-1 β from infected macrophages. The acute *in vivo* neurotoxic capability of a peptide derived from the lentiviral protein Tat was also demonstrated and may contribute further to neurodegeneration occurring in MVV infection of sheep.

CHAPTER 1: INTRODUCTION

1.1. INTRODUCTION TO LENTIVIRUSES.

1.1.1. Description and history of MVV.

Maedi Visna Virus (MVV) and Human Immunodeficiency Virus (HIV) belong to the *Lentivirinae* subfamily of the *Retroviridae* family of viruses which also includes Caprine Arthritis Encephalitis Virus (CAEV), Feline Immunodeficiency Virus (FIV), Bovine Immunodeficiency Virus (BIV) Simian Immunodeficiency Virus (SIV), and Equine Infectious Anaemia Virus (EIAV). MVV is prototypic of the lentivirus family and causes a very slow disease in sheep, characterised by a long interval between the time of infection and the onset of clinical signs. Maedi, literally meaning dyspnoea, was first described by Sigurdsson in 1954 (Sigurdsson 1954b), as was visna, meaning wasting (Sigurdsson 1954a), after a particularly severe outbreak in Iceland, caused by the importation of infected European sheep. MVV occurs throughout the world and usually affects animals between 3 and 5 years old when they are at their most agriculturally productive (Dawson 1980). The disease progresses slowly, with an incubation period of 1 to 3 years, and can affect the Central Nervous System (CNS), lungs, joints and mammary glands.

In sheep with Maedi, the respiratory rate will increase severely after exercise, and will eventually stay high even at rest. Hollowed flanks and a dry cough are also evident. If no secondary bacterial infections occur, then death ensues from anoxia. Visna affected animals usually suffer the onset of symptoms slightly earlier, usually around 2 years old. A similar loss of body condition occurs, with emaciation despite normal appetite, and the animal shows an unsteady gait. Trembling facial muscles is another characteristic, and paresis in the hind limbs eventually leads to paraplegia. Other symptoms can include ataxia, mastitis, particularly in lactating animals, synovitis and arthritis. Eventually, chronic pneumonitis or paralysis induced by a progressive demyelinating encephalitis causes death.

In 1967, a single virus, MVV, was shown to be the causative agent of both sets of symptoms (Gudnadottir *et al.* 1966). This virus was later shown to be a retrovirus (Lin *et al.* 1971). The disease was shown to be transmitted horizontally through respiratory exudates, particularly where housing conditions were cramped, and from ewe to lamb via colostrum and milk (Narayan *et al.* 1985), and could result in the whole

of the flock becoming infected from the addition of just one diseased animal (Palsson 1976).

Several countries have instrumented plans to eradicate MVV with varying degrees of success. In Holland, the removal of infected ewes and lambs from flocks failed to stop the spread of the disease (Houwers *et al.* 1984). The slaughter of all infected animals from affected farms, as has been practised in Iceland, has however resulted in the elimination of MVV (Palsson 1976). In the United Kingdom, pedigree flocks are subject to an accreditation scheme, controlling the number of flocks affected by MVV to under 5%. However, some countries still have no control programs and infectivity of flocks by ruminant lentiviruses can often reach 100% (Crawford *et al.* 1981).

1.1.2. Genomic description of Lentiviruses.

Lentiviruses possess a positive sense single stranded (ss)RNA genome (Brahic *et al.* 1977), an RNA dependant DNA polymerase (reverse transcriptase) (Lin *et al.* 1970) and replicate via a DNA intermediate (Haase *et al.* 1973). Molecular cloning has enabled the analysis of nucleotide sequences of MVV and their comparison with other lentivirus genes, both structural and regulatory. Lentiviruses differ from other retroviruses by possessing a more complex genome structure. Six strains of MVV have been sequenced to date. Four of the strains have been derived from the 1514 Icelandic strain (Sonigo *et al.* 1985; Braun *et al.* 1987; Staskus *et al.* 1991), one from Britain (EV-1) (Sargan *et al.* 1991) and the other from South Africa, termed Ovine Maedi Visna Virus (SA-OMVV) (Querat *et al.* 1990). All are broadly similar but retain minor differences. Two species of HIV, HIV-1 and HIV-2 have been identified, but unless otherwise specified all data presented here will refer to HIV-1 since this type has been the most extensively studied. Also present in the lentiviral genome are a TATA box and a long terminal repeat (LTR) at both ends of the genome, containing initiation sites for positive strand DNA synthesis (Carey *et al.* 1993).

1.1.2.1. Structural genes.

The functions of the structural genes *gag*, *pol* and *env* of MVV, CAEV and HIV are broadly similar. In common with other lentiviruses, MVV is characterised by a large structural *env* gene which codes for two envelope glycoproteins (Narayan *et al.*, 1993).

Gp135, (gp120 in HIV), is the highly glycosylated surface glycoprotein which contains the receptor-binding site of the virus. This is non-covalently attached to the highly hydrophobic transmembrane glycoprotein gp46, (gp41 in HIV), which contains the fusion domain of the virus envelope (Crane *et al.* 1991). The *gag* gene encodes the major structural proteins: p30 (or p25) - the core protein, p16 - the matrix protein, and p14 - the nucleoprotein (Vigne *et al.* 1982). *Pol* encodes the reverse transcriptase, an endonuclease and a protease (Narayan *et al.*, 1993, Figs. 1 and 2). All the structural proteins are cleaved from precursors during the replication and maturation of the virus.

1.1.2.2. Regulatory genes.

Lentiviral regulatory proteins are encoded by the small open reading frames (ORFs) *vif*, *rev* and *tat* (Fig. 2) MVV Tat, the *tat* gene product, is a transactivating protein, of 10 (Davis *et al.* 1989) or 11 kDa (Gourdou *et al.* 1989). MVV Tat is encoded from one exon, whereas HIV Tat requires transcription from two exons (Arya *et al.* 1985). It has been reported that Tat is necessary for efficient viral replication and enhanced viral transcription. However, the function of Tat seems to vary between lentiviruses. SIV (Arya *et al.* 1987), BIV (Pallansch *et al.* 1992), EAIV (Derse *et al.* 1991) and HIV (Arya *et al.* 1985) Tat strongly transactivate the viral LTR, by binding to a TAR (trans-activating responsive) binding sequence. In these viruses it acts as a switch which initiates the expression of all viral genes, allowing more frequent initiation and more efficient elongation during transcription (Gourdou *et al.* 1989). In contrast, CAEV (Harmache *et al.* 1995), FIV (Sparger *et al.* 1992) and MVV (Carruth *et al.* 1994) Tat proteins are only weak transactivators. Furthermore, these viruses do not contain TAR elements. Instead, Tat may bind to AP-1, AP-4 or CBF sequences in the LTR (Gabuzda *et al.* 1989; Sutton *et al.* 1997). These findings suggest that, at least for MVV, FIV and CAEV, the regulatory gene product Tat may have functions other than in the effective replication of the virus. Lentiviral Tat proteins contain three essential domains: the acidic amino terminal, necessary for effective transactivation, a cysteine rich domain, necessary for Tat dimerisation, and the carboxy terminal region, necessary for nuclear localisation (Steffy *et al.* 1991, Fig. 3).

Rev is encoded by exons at both ends of the *env* gene to form a 19 kDa polypeptide (Mazarin *et al.* 1990). Deletion of Rev results in a replication incompetent virus (Toohey *et al.* 1994). It is believed to aid the expression of incompletely spliced

env mRNA coding for the envelope glycoprotein (Tiley *et al.* 1990). There exists little sequence homology between HIV and MVV Rev.

Little is known of the 29kDa protein encoded by *vif*, however, its deletion results in reduced CAEV and HIV production and infectivity. In CAEV, Vif appears to act at the stage of virus formation and release, whereas HIV Vif plays a role in reverse transcription by the virus (Ma *et al.* 1994; Goncalves *et al.* 1996).

In addition, the SA-OMVV possesses an extra novel ORF W, not found in the other strains of MVV (Querat *et al.* 1990). HIV also has four more regulatory ORFs: *vpr*, *vpu*, *tev* and *nef*, which are not present in MVV. The *nef* gene product seems to play an important role in HIV infectivity, by its degradation of CD4 molecules, and individuals infected with *nef* deficient virus generally remain healthy (Sinclair *et al.* 1997).

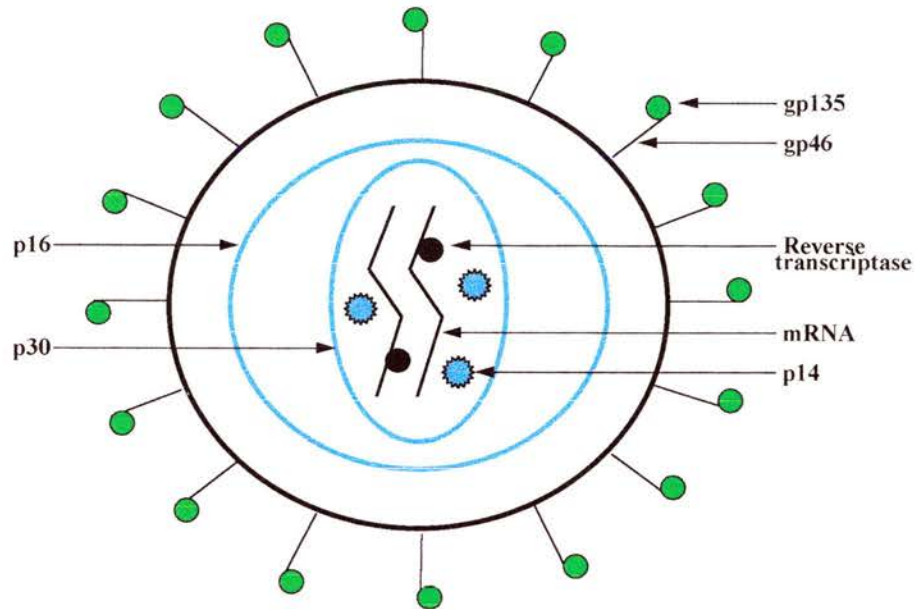


Fig. 1.1: Diagram of a mature MVV virion

Mature virions measure approximately 80-120 nm in diameter with the nucleoid measuring 40 nm. The length of the protruding envelope glycoprotein is 8 nm.

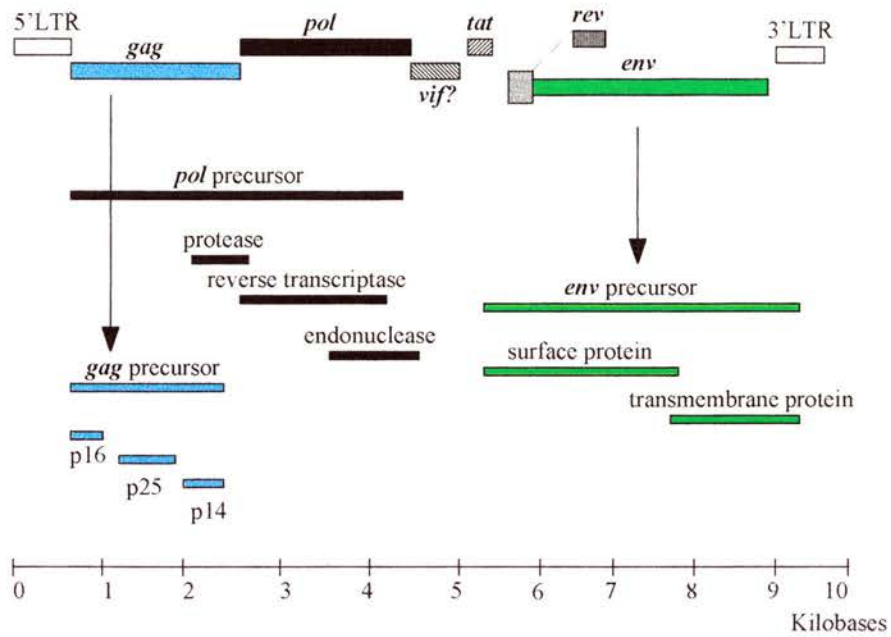


Fig. 1.2: The MVV genome and encoded proteins.

Synthesis and processing of MVV structural proteins are cleaved from precursor polyproteins during maturation and replication of the virus. Relative nucleotide positions are indicated by the scale bar. From Carey and Dalziel (1991).

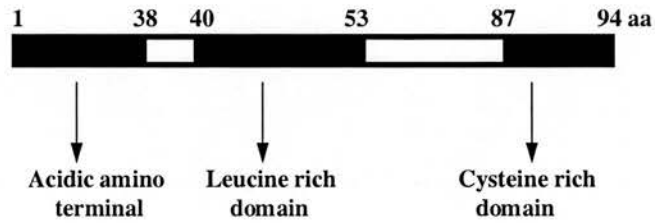


Fig. 1. 3: Transactivating protein Tat of MVV

The acidic amino terminal contains the domain essential for effective transactivation of M
cysteine rich domain is necessary for Tat dimerisation and contains the neurotoxic fragment of th
The carboxy terminal is also needed for nuclear localisation of the protein.

1.1.3. Cellular tropism of MVV and HIV.

MVV primarily infects cells of the monocyte/macrophage lineage *in vivo* (Gendelman *et al.* 1985) but can also infect other cell types *in vitro* including sheep choroid plexus cells, lung epithelia, astrocytes, oligodendrocytes, microglia and fibroblasts (Narayan *et al.* 1982). Studies performed on infection of fibroblasts *in vitro* show that the virus first binds to a specific cellular receptor. This receptor is as yet uncharacterised but MHC class II antigens have been reported to bind MVV, and soluble class II molecules can inhibit infection of choroid plexus cells (Dalziel *et al.* 1991). The presence of MHC class II molecules alone is not sufficient, however, as T and B lymphocytes possess such molecules but do not become infected. Antibodies to an unidentified 50 kDa protein from sheep choroid plexus cells can also block infection in culture, and this protein may represent another constituent of the MVV receptor (Crane *et al.* 1991).

The life cycle of MVV is also linked to the stage of maturation of the cell (Gendelman *et al.* 1986). Monocytes are believed to be latently infected, possibly providing a reservoir of infection and allowing viral persistence in the host. Macrophages in infected tissues, however, are laden with virus particles. Indeed it has been demonstrated that virus replication depends on cellular factors present in the mature macrophage (Gabuzda *et al.* 1989). MVV infection of lymphocytes has been reported (Georgsson *et al.* 1979), and specifically of T-helper cells (Jolly *et al.* 1989). HIV, by contrast, mainly infects T-helper cells, via association with the CD4 receptor, as well as cells of the monocyte/macrophage lineage. In HIV positive patients, approximately 10% of T cells are infected with the virus. However, levels of virus in the blood are low, approximating 1 in 10^5 or 10^6 cells for both viruses.

1.1.4. The MVV life cycle

Following binding of MVV to its cellular receptor, the virus is internalised through pH-independent fusion of the transmembrane glycoprotein with the plasma membrane of the cell. The virus is subsequently uncoated and the ribonucleoprotein complex is liberated into the cytosol (Narayan *et al.*, 1993). Reverse transcription of viral ssRNA ensues with the formation of double-stranded (ds)DNA, probably through

the binding of tRNA^{lys}_{1,2} to the primer binding site of the LTR (Sonigo *et al.* 1985). Entry of proviral DNA into the nucleus and incorporation of viral DNA into host cell DNA follow. Thus, MVV integrates itself into the host cell genome. Once this has been accomplished levels of proviral DNA continue to rise, resulting in synthesis of genomic and spliced mRNA. Viral proteins are then produced and MVV assembly occurs by budding from the plasma membrane.

Less is known about the *in vivo* infection of monocytes/macrophages, where replication of the virus seems to be blocked to some extent. Binding of MVV to macrophages *in vivo* occurs via an uncharacterised receptor but also via Fc receptors when the virus is already bound to an antibody (Jolly *et al.* 1989). The whole Fc-IgG-virion complex is then internalised into the macrophage. It is not known whether proviral DNA integrates into macrophage DNA. A further difference exists in the *in vivo* packaging of virus, which occurs through budding of the endoplasmic reticulum into intracytoplasmic vacuoles in the macrophage (Narayan *et al.* 1982).

1.2. PATHOLOGY OF MVV AND HIV INFECTION.

1.2.1. Lungs.

One of the most extensive descriptions of the pathology of lungs in naturally occurring Maedi comes from Sigurdsson's first account of the disease (Sigurdsson 1954b). The carcass of the diseased sheep is thin with some occasional serous fluid present in the abdomen. When the thorax is opened the lungs collapse less than usual and are four to five times heavier than in a normal individual. Both the tracheobronchial and the mediastinal lymph nodes are greatly enlarged. The lung tissue is dry and diffusely thickened and differs in colour from healthy lungs, ranging from greyish yellow to greyish blue. At the microscopic level, the alveoli are infiltrated with numerous macrophages and the alveolar septa are thickened. The smooth muscle at the alveolar ducts appears thickened. Cellular exudates are composed mainly of alveolar macrophages with relatively few lymphocytes. The pathological changes are confined to the lymph nodes and the lungs, with the bronchial tree being free of lesions.

HIV positive patients often present respiratory complications. Often, these are due to opportunistic bacterial, fungal and viral infections as well as increased incidences of pulmonary malignancies and lymphoma. The discussion of these diseases is beyond

the scope of this work, but some pulmonary complications occur due to HIV infection alone, particularly in children. The major manifestations of these disorders are lymphocytic interstitial pneumonitis (LIP) and non-specific interstitial pneumonitis (NIP). In individuals affected by LIP, the main symptoms are the insidious onset of dyspnoea, a non-productive cough and fever (Andiman *et al.* 1985; White *et al.* 1989). In HIV positive children with LIP, the onset of disease usually occurs in the second or third year of life and is observed as pulmonary lymphoid hyperplasia with hyperplasia of bronchus-associated tissue and lymphoid infiltration of the lung parenchyma (Schneider 1996). Histologically, LIP is characterised by infiltration of small lymphocytes and plasma cells along lymphatic vessels and into the alveolar septae (Halprin *et al.* 1972). NIP is less well characterised and symptoms are usually mild, involving a non-productive cough (Ognibene *et al.* 1988). The pathology of infected lungs showing NIP reveals nodular lymphoid aggregates around the bronchioles with interstitial fibrosis, loose alveolar septal fibrosis and diffuse alveolar damage (Travis *et al.* 1992). Infiltrates of mononuclear cells and lymphocytes are distributed along the pleura and the interlobular septae as well as along the bronchioles and blood vessels (Travis *et al.* 1992). The prognosis for these disorders is good, as both respond to treatment with steroids, but inevitably other more serious pulmonary disorders occur in these patients which are often fatal.

1.2.2. Joints.

Lentiviruses are associated with disorders of joints, resulting in synovitis and arthritis. Symptoms of joint disease are most frequently seen in goats infected with CAEV, but are also present in sheep infected with MVV and HIV positive patients (Crawford *et al.* 1981; Oliver *et al.* 1981a; Dalton *et al.* 1990). In HIV positive individuals with musculoskeletal symptoms, the largest joints, such as the knee and elbow, are the most frequently affected. The most common manifestation of HIV-induced joint problems is articular arthralgia causing intermittent or persistent pain in the affected joints (Buskila *et al.* 1990). AIDS-associated arthritis, an unclassified inflammatory articular disease, is also described in HIV positive individuals, and appears to be a reactive phenomenon caused by the action of immune complexes on the synovium, as opposed to a direct action of the virus (Berman *et al.* 1988).

The main joint affected in CAEV and MVV is the carpus, followed by the tarsal joints. Tissue surrounding the articulations becomes visibly swollen causing lameness in the infected animal. On post-mortem examination, the affected joints are edematous. Hyperplasia of the synovial membrane is evident with periarticular fibrosis and areas of mineralisation and necrosis. These features are also present in sub-synovial tissues. Erosion and necrosis of cartilage and bone present another trait of affected joints (Oliver *et al.* 1981b; Cutlip *et al.* 1985). The most striking feature however, is the infiltration of lymphoid cells and macrophages into synovial tissue. Of the lymphoid cells, CD8⁺ T-cells are the preponderant cell type in the synovium at all stages of the disease (Anderson *et al.* 1994). This is paralleled in HIV associated arthritis (Espinoza *et al.* 1990).

1.2.3. Central Nervous System

The CNS lesions observed in visna appear to be mainly inflammatory in nature with invasion of inflammatory cells along the ventricular system. In naturally occurring and experimental visna, there is a marked pleocytosis in the cerebrospinal fluid (CSF) with the main invading inflammatory cell type being the macrophage followed by reactive lymphocytes and eventually phagocytes (Sigurdsson 1954a; Georgsson *et al.* 1977; Georgsson *et al.* 1982; Georgsson *et al.* 1979) although some reports have identified T-cells as the preponderant cell type (Torsteindottir *et al.* 1992). Inflammatory lesions consisting of increased cellular infiltrates and glial cell abnormalities appear in the frontal lobes, cerebellum, thalamus, mesencephalon, pons and medulla but are rarer in the occipital lobes (Sigurdsson 1954a). Scattered foci of activated microglial nodules and astrogliosis are the most prevalent features of MVV neuropathology although some neuronal damage is also observed. Secondary degeneration of nerve cells in the CNS has been described, observed as chromatolysis and sclerosis (Sigurdsson 1954a).

Ultrastructural studies on the brains of experimentally infected sheep have been carried out at various stages after infection. In the shorter term (Georgsson *et al.* 1977), one month post-injection, no virions are found within the CNS, but cellular infiltrates are found perivascularly, with a widening of the extracellular spaces. Astrocytes are found to be swollen and axonal damage is observed without myelin breakdown. In those

brains recovered years after experimental infection (Georgsson *et al.* 1982), intense inflammation is observed around the ventricular system and the choroid plexus. The ependymal lining appears destroyed and inflammation is further observed in the neuroparenchyma, especially in the corpus callosum, the fasciculus subcallosus and the hippocampi with some infiltration of the meninges. In areas showing particularly intense inflammation, axonal degeneration and primary demyelination are evident accompanied by liquefactive necrosis. In the spinal cord, neuronal degeneration in naturally occurring visna is especially prevalent in the cervical segments (Sigurdsson 1954a). Later work on experimental visna indicates spinal cord lesions in grey matter (Georgsson *et al.* 1977) and white matter (Georgsson *et al.* 1982), with axons stripped of myelin sheaths and secondary demyelination evident as axonal atrophy without myelin degradation. In areas of primary demyelination, astrocytes with densely packed microfilaments are evident, as well as the presence of macrophages.

The neurological symptoms resulting from HIV infection culminate in Aids Dementia Complex (ADC). Early ADC is characterised by slowing of motor and cognitive functions, as well as tremor and gait unsteadiness. In later ADC, forgetfulness, a worsening of the intellectual impairment, apathy, motor weakness and hypokinesia become apparent, eventually resulting in overt dementia and loss of motor control (Navia *et al.* 1986; Price *et al.* 1988). Cases of paediatric AIDS result in the child suffering developmental delay and failing to reach milestones. Spasticity is also common.

The neuropathology observed in HIV infected individuals has been divided into HIV encephalitis and HIV leukoencephalopathy in the CNS, with vacuolar myelopathy occurring in the spinal cord. HIV encephalitis is characterised by the spread of inflammatory cell infiltrates, and the presence of multinucleated giant cells, consisting of fused HIV infected and uninfected microglial cells (Sharer *et al.* 1986; Budka 1986; Dickson 1986). HIV leukoencephalopathy is characterised by intense reactive astrocytosis, where astrocytes become activated and overexpress glial fibrillary acidic protein (GFAP), and diffuse white matter pallor, probably due to loss of myelin (Budka 1991). Multinucleated giant cells are present, as in HIV encephalitis, but there appears to be less infiltration of inflammatory cells.

Spinal cord abnormalities are detectable in both adult and paediatric HIV positive individuals. In adult patients this consists of vacuolar myelopathy with

swelling within the myelin sheath of axons, and only a thin layer of myelin surrounding the underlying vacuoles (Petito *et al.* 1985). In areas of intense vacuolation, axonal degeneration is observed. As in HIV encephalopathy, spinal cord myelopathy is accompanied by an infiltration of macrophages expressing HIV antigens, with some macrophages demonstrating active ingestion of myelin (Eilbott *et al.* 1989). In paediatric AIDS, corticospinal tract degeneration is evident, with loss of myelin or axonal degeneration or both (Dickson *et al.* 1989). This may be a consequence of pathological changes within the CNS, extending to the spinal cord by the mechanism of Wallerian degeneration. Both HIV encephalitis and HIV leukoencephalopathy preferentially affect subcortical regions of the brain, with pathology occurring mainly in areas such as the basal ganglia, pons and cerebral white matter. Neuronal loss is also evident in these areas, but can extend to the cerebral cortex and the cerebellum (Everall *et al.* 1991). Neurons that are not completely lost display dilated and vacuolated dendrites, with less spines and decreased length and branching (Masliah *et al.* 1992). Paediatric HIV encephalitis is manifest preponderantly by astrocytic gliosis, with mineralisation of the basal ganglia and brain atrophy (Belman *et al.* 1986).

1.3. LENTIVIRAL INVASION OF THE CNS.

1.3.1. Neurotropism of MVV and HIV.

Although it is well established that MVV infects monocytes/macrophages and HIV infect monocyte/macrophages and T-helper cells, it is necessary, for the purposes of understanding the neurodegeneration involved in HIV dementia, to elucidate the neural cell types which become infected with HIV. Co-localisation studies performed on post-mortem brains, simultaneously identifying viral antigens and specific cell type markers have revealed that the main type of cells infected in both MVV and HIV are glial cells as well as circulating macrophages (Wiley *et al.* 1986; Kure *et al.* 1990a; Vaseux *et al.* 1987; Stoler *et al.* 1986; Stowring *et al.* 1985). In HIV, the main type of glial cell expressing viral antigens is the microglial cell (Wiley *et al.* 1986; Kure *et al.* 1990a; Kure *et al.* 1990b; Vaseux *et al.* 1987; Stoler *et al.* 1986). Microglia have also been shown to support HIV and MVV infection *in vitro* (Cheng-Mayer *et al.* 1987; Chiodi *et al.* 1987; Dewhurst *et al.* 1987; Jordan *et al.* 1991; Tornatore *et al.* 1994;

Watkins *et al.* 1990; Bagasra *et al.* 1996; Wigdahl *et al.* 1987; B. Ebrahimi, personal communication).

Other types of glial cells, notably astrocytes and oligodendrocytes, have also been shown to express MVV and HIV viral antigens *in vivo* (Epstein *et al.* 1985; Gyorkey *et al.* 1987; Kohleisen *et al.* 1992; Pumarole-Sune *et al.* 1987; Saito *et al.* 1994; Tornatore *et al.* 1994; Stowring *et al.* 1985), although the evidence for this is not as emphatic as for the infection of microglia. Reports of astrocyte infection are rare in adult HIV encephalitis but do seem to be a more prominent feature in paediatric AIDS cases, where astrocytes generally appear to be more involved in the pathologic process, and may thus play a more pivotal role in the neuropathogenesis of HIV (Blumberg *et al.* 1994). *In vitro*, astrocyte infection by HIV is restricted, the virus only expressing early regulatory gene products but no structural genes (Blumberg *et al.* 1994; Ma *et al.* 1994). Further doubt regarding the productive infection of astrocytes also arises from the finding that immunocytochemical markers for some HIV antigens, in particular the *nef* gene product, are expressed at low levels in the uninfected nervous system (Saito *et al.* 1994).

Neurons do not seem to support MVV replication, although MVV antigens have been detected in cells that cannot be morphologically identified as microglia, astrocytes or oligodendrocytes and thus could be neurons (Stowring *et al.* 1985). Similarly, there are a few reports of HIV infection of neurons *in vivo* (Bagasra *et al.* 1996; Stoler *et al.* 1986; Wiley *et al.* 1986), although there is little evidence that neurons support HIV replication *in vitro*.

Although it is known that HIV infects lymphocytes via an association of the envelope glycoprotein gp120 with the CD4 receptor on T-helper cells, little is known as to the mechanism by which HIV infects microglia. Some authors report the blocking of HIV infection of brain derived microglia with CD4 antigens (Jordan *et al.* 1991) suggesting that the same mechanism which mediates HIV entry into lymphocytes is at play in microglia. This is supported by the finding that microglia can be stained *in situ* for CD4 antigens and that CD4 specific RNA is detected in these cells (Funke *et al.* 1987). However, other authors report that glial cell infection is not CD4 dependant (Ma *et al.* 1994; Harouse *et al.* 1989; Kunsch *et al.* 1989). Moreover, neurons have been shown to express the CD4 molecule (Funke *et al.* 1987), but as has previously been discussed, do not seem to be productively infected by HIV. It is possible that CD4 does

play a role in the binding of the virus to microglial cells, but that there may also be another mode of entry of HIV into glial cells. This may involve the presence of a second receptor on microglial cells, which would allow infection of these by HIV. Indeed, recently, the chemokine receptors CCR5 and CCR3 have been proposed as microglial co-receptors for HIV (He *et al.* 1997).

1.3.2. Mechanisms of HIV and MVV entry to the CNS.

Much has still to be elucidated regarding the entry of HIV and MVV into the CNS. There is little evidence of cell-free entry of MVV into the brain although freely circulating virus has been detected in the brains of HIV positive patients. Levels of free virus, however, do not correlate with the extent of dementia whereas the number of infected cells does. Indeed, there is little evidence that HIV or MVV infect brain microvascular endothelial cells (BMVECs), which would provide a direct route of infection to the CNS. Lymphocytotropic strains of HIV have been shown to infect BMVECs *in vitro* (Moses *et al.* 1994). However, it is rarely found that BMVECs are infected on post-mortem analysis and macrophage tropic strains of HIV, which have more neuroinvasive potential, are not found to infect BMVECs (Nottet *et al.* 1996b). It is more likely that lentiviruses gain access to the CNS via the Trojan Horse mechanism, disguised under the cover of infected monocytes (Peluso *et al.* 1985).

HIV infected monocytes have been shown to produce elevated levels of the cytokines TNF α and IL-1 β (Tyor *et al.* 1992; Wesselingh *et al.* 1993). These have in turn been shown to upregulate the cell adhesion molecules E-selectin and vascular cell adhesion molecule-1 (V-CAM1) on BMVECs (Staunton *et al.* 1988; Osborn *et al.* 1989; Bevilacqua *et al.* 1987). Molecules on the cell surface of monocytes, sialylated and sulfated fucosylated lactosamine oligosaccharides and antigen-4 integrins (Bevilacqua *et al.* 1993; Varki 1994; Elices *et al.* 1990), can bind to E-selectin and V-CAM1 to allow the transendothelial migration of monocytes across the BBB (Carlos *et al.* 1991; Hakkert *et al.* 1991). E-selectin and V-CAM1 also promote BMVEC adhesion to other cells including polymorphonuclear cells, memory T-cells, lymphocytes, basophils and eosinophils (Bevilacqua *et al.* 1987; Shimizu *et al.* 1991; Dobrina *et al.* 1991; Bochner *et al.* 1991). Therefore it is possible that agents are released by infected monocytes that act as specific chemoattractants for other monocytes to allow the preferential permeation

of these cells across the BBB. Levels of Transforming Growth Factor beta (TGF β), a powerful monocyte attractant molecule, are elevated in cases of HIV encephalitis (Wahl *et al.* 1987; Wahl *et al.* 1991), as are the levels of expression of the chemokines MIP1 α and MIP1 β which also act as chemoattractants for monocytes as well as subpopulations of lymphocytes (Schmidtmayerova *et al.* 1996). Induction of MIP1 α and MIP1 β (macrophage inflammatory protein-1 α and β) is also upregulated in HIV infected monocytes. Furthermore, activated BVEMCs have been shown to produce increased levels of MCP a macrophage chemotactic protein (Rollins *et al.* 1990). In addition to these molecules, HIV infected monocytes produce leukotrienes (LT) which have been shown to increase BBB permeability (Black *et al.* 1985).

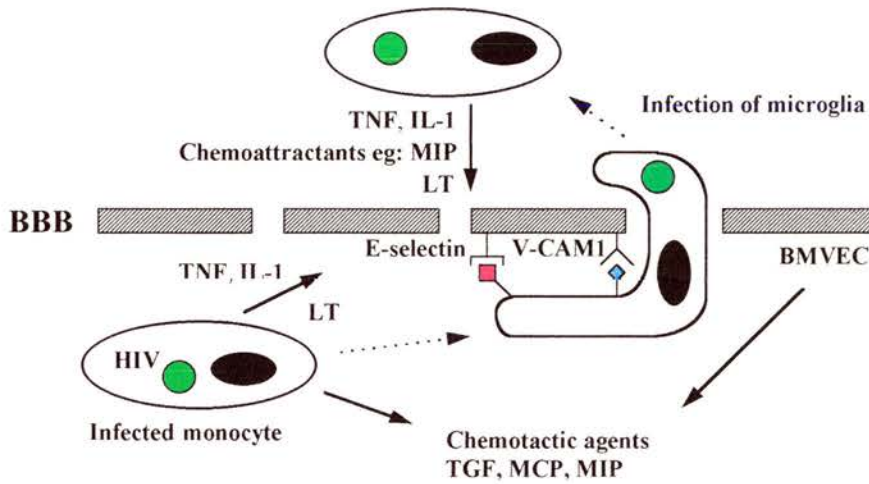


Fig. 1. 4: Proposed mechanism of HIV entry into brain.

BBB: Blood Brain Barrier, BMVECs: Brain Microvascular Endothelial Cells, TNF: Tumour Necrosis Factor α , IL-1: Interleukin 1β , LT: Leukotrienes, TGF: Transforming Growth Factor β , V-CAM1: Vascular Cell Adhesion Molecule 1. Infected monocytes release $TNF\alpha$ and $IL-1\beta$ which upregulate the cell adhesion molecules E-selectin and V-CAM1, whilst also releasing chemotactic agents to recruit further infected cells. V-CAM1 and E-selectin then bind molecules on the surface of infected monocytes and permit their migration across the BBB. Once entry to the CNS has been achieved, resident microglia become infected with HIV and release $TNF\alpha$ and $IL-1\beta$ to sustain the expression of V-CAM1 and E-selection on BVEMCs, as well as chemoattractants which diffuse across the BBB, and leukotrienes which increase the permeability of the BBB. Activated BMVECs may also release MCP, Monocyte Chemotactic Protein.

1.4. NEUROPATHOGENESIS OF LENTIVIRAL INFECTIONS.

Several hypotheses have been put forward regarding the causes of the neuropathology observed in MVV and HIV. Firstly, it is possible that viral proteins may be exerting direct detrimental effects on cells in the CNS. Secondly, cells infected with HIV or MVV may be releasing agents that cause neural damage, or act on resident cells of the CNS causing these to produce neurodegeneration. Thirdly, although the brain has long been regarded as immunologically privileged, there is now increasing evidence that immunological responses do occur within the CNS in response to invading pathogens, and that these may have deleterious consequences on surrounding brain tissue.

1.4.1. Direct action of viral fragments.

Several MVV and HIV proteins have been volunteered as neurotoxic agents.

1.4.1.1. *gp120*

The HIV envelope glycoprotein gp120 has been intensely investigated as a possible neurodegenerative agent, probably due to the fact that it is located on the surface of lentiviruses, and thus would be one of the first elements to come in contact with host cells, and that it is shed extracellularly upon infection of cells. Gp120 has been shown to be directly neurotoxic to various neuronal cultures including cortical, hippocampal, retinal ganglion and cerebellar granule cell cultures (Brenneman *et al.* 1988; Brenneman *et al.* 1994; Corasaniti *et al.* 1995; Dawson *et al.* 1994; Meucci *et al.* 1996; Mucke *et al.* 1995; Dawson *et al.* 1993; Ushijima *et al.* 1993; Sweetnam *et al.* 1993). The neurotoxic mechanism involved in gp120 killing of neuronal cultures has been ascribed to excessive extracellular calcium influx to neurons, via the L-type voltage sensitive calcium channel (Lo *et al.* 1992; Lipton 1991). Gp120 has also been reported to act at the NMDA receptor of neurons, a receptor for glutamate, which, when inappropriately activated, as in some disease states, can cause a superfluous amount of glutamate release, causing adjacent neurons to die (Sweetnam *et al.* 1993). Indeed, inhibition of the NMDA receptor by MK801 results in lower neurotoxic rates of gp120 (Corasaniti *et al.* 1995; Lipton 1992a). However, gp120 has only been reported as a weak agonist of the NMDA receptor and is more likely only to act synergistically with

other NMDA receptor activators (Lipton 1991). Another mechanism that may be at play in the gp120 induced killing of neurons is apoptosis, whereby the affected cell is induced to self destruct with minimal damage to surrounding cells (Aggoun-Zouaoui *et al.* 1996; Muller *et al.* 1992). However, some studies do not report any *in vitro* gp120 induced neurotoxicity, whilst others have only found a harmful effect of gp120 when neurons are co-cultured with microglia, astrocytes or macrophages (Lipton 1992b), indicating that the sole presence of gp120 is not sufficient to elicit considerable neurotoxicity. In these cases gp120 causes the release of neurotoxins from macrophages or microglia (Giulian *et al.* 1993). Gp120 has also been found to damage astrocytes in culture, causing changes in GFAP immunoreactivity and some astrocytic cell death (Benos *et al.* 1994; Pulliam *et al.* 1993; Levi *et al.* 1993).

In vivo experiments consisting of stereotaxic injections have also demonstrated the neurotoxic capability of gp120 (Hill *et al.* 1993; Lipton *et al.* 1995), including neuronal loss, decreases in glucose utilisation and impairment of memory function (Kimes *et al.* 1991; Glowa *et al.* 1992). However, this capacity seems to vary greatly, depending on the age of the experimental animal as well as the method and site of administration of gp120 (Bagetta *et al.* 1994). In cases where gp120 is found to cause toxicity to neurons, this seems to be mediated by an apoptotic mechanism. More convincing evidence for the neurotoxic potential of gp120 *in vivo* comes from the development of transgenic mice overexpressing gp120 where neuronal damage is evident (Toggas *et al.* 1994). This is manifest by the drop-out of cortical neurons, vacuolar degeneration of dendrites and a decrease in the number of presynaptic terminals of neurons. Astrocytosis and microgliosis are also observed. None of these changes occur in wild type mice or in transgenic control mice overexpressing β -galactosidase. These neurotoxic changes occur from 7 days post-natally in gp120 transgenic mice. This correlates with the time of development of NMDA receptors in mice (MacDonald *et al.* 1993), therefore reinforcing the putative role of these receptors in mediating gp120 induced neurodegeneration.

1.4.1.2. Tat

The transactivating protein Tat has also been found to be neurotoxic *in vitro* and *in vivo*. Studies on HIV infected lymphocytes have shown that Tat can be released from these cells *in vitro* (Ensoli *et al.* 1990). Furthermore, Tat can be taken up by uninfected

cells when it is present in their culture medium (Frankel *et al.* 1988; Mann *et al.* 1991), and may move from infected cells to uninfected cells via cell to cell contact resulting in the transactivation of the adjacent uninfected cell (Helland *et al.* 1991; Marcuzzi *et al.* 1992a; Marcuzzi *et al.* 1992b). These findings suggest that, at least some of the time, Tat is present extracellularly and may have an effect on different cell types.

Application of HIV Tat to hippocampal neurons in rodent brain slices results in the depolarisation of neurons (Magnuson *et al.* 1995). Tat also depolarises rat glioma and murine neuroblastoma cells (Sabatier *et al.* 1991). This is mediated by non-NMDA glutamate receptors on neurons since it can be blocked by the excitatory amino acid antagonist kynurenate. These findings, and the observation that Tat bears some sequence homology with snake venom neurotoxins (Garry *et al.* 1992), imply that Tat may be having a direct action on neuronal cell types which may result in neurotoxicity. Indeed, the *in vitro* application of HIV and MVV Tat or tat peptide, derived from the basic cysteine rich region of Tat, to rodent cortical cell cultures results in cell death as measured by Lactate Dehydrogenase (LDH) assay (Strijbos *et al.* 1995b) and trypan blue exclusion (Magnuson *et al.* 1995; Sabatier *et al.* 1991). In both cases, neurotoxicity is attenuated by the administration of NMDA receptor antagonists, and involves calcium influx. However, HIV Tat has also been found to cause neuronal death in culture by apoptosis (New *et al.* 1997) and to alter the normal organisation of astrocytes in culture although no astrocytic cell death ensues (Kolson *et al.* 1993)

In vivo, HIV and MVV Tat and tat peptides are also neurotoxic when injected stereotaxically into rat and mouse striatum (Gourdou *et al.* 1990; Hayman *et al.* 1993; Sabatier *et al.* 1991). Infusion of the tat peptide results in neuronal loss, microglial activation, macrophage invasion and astrocytosis. Similarly to the *in vitro* findings, this neurotoxicity can be diminished by the co-administration of MK801, an NMDA receptor antagonist, and by L-NAME, a NOS inhibitor, suggesting that the mechanism causing neuronal cell death is NO-mediated glutamate neurotoxicity via NMDA receptors. Also *in vivo*, the blocking of TNF α reduces the neurotoxic effects of lentiviral Tat (Philippon *et al.* 1994), suggesting that this cytokine is involved as a neurotoxic mediator.

1.4.1.3. Rev

Few experiments have been performed on the neurotoxic capability of Rev. One investigation, however, has revealed that, when injected into mice intracerebroventricularly, the basic domains of HIV and SIV Rev do cause neurotoxicity (Mabrouk *et al.* 1991). Like Tat, Rev contains numerous arginine residues and an unusual basic domain, which may confer it a neurotoxic ability. HIV Rev is also abundantly expressed in glial cells in the brains of HIV positive patients and correlates with the level of dementia (Ranki *et al.* 1995).

1.4.1.4. Nef

As for gp120, Tat and Rev, the HIV *nef* gene product has been shown to exhibit sequence and structural homology to other known neurotoxins. In this case, Nef resembles a scorpion neurotoxin which interacts with K⁺ channels (Werner *et al.* 1991). However, no studies on any neurotoxic potential of Nef have been published, although some investigators ascribe it a potential neurotoxic role since it is produced in abundance in glial cells during restricted HIV infection of astrocytes (Werner *et al.* 1991; Ranki *et al.* 1995)

1.4.1.5. gp41

The transmembrane protein gp41 has similarly been suggested to have a neurotoxic role since it resembles natural peptides with cytopathic abilities and has itself been found to be neurotoxic in culture (Miller *et al.* 1991).

1.4.2 Indirect causes of neurodegeneration

Although the viral fragments listed above have neurotoxic properties, little cell free virus is detected in HIV and MVV infection. This suggests that a direct action of viral proteins may not be the single cause of lentiviral neurodegeneration, although this possibility should not be discounted especially since gp120 and Tat are released from infected macrophages. It is more likely that any direct effects of viral proteins are accompanied by indirect effects of infected cells. These effects may be due to the combined release of viral proteins such as gp120 and Tat, and soluble mediators such as cytokines, from infected macrophages. These may be directly neurotoxic or may affect microglia and astrocytes, causing them to release neurotoxic substances, thus perturbing

the local microenvironment in the CNS, and interfering with the natural homeostasis achieved by the normal interaction of neurons with microglia, astrocytes and oligodendrocytes.

1.4.2.1. Quinolinic acid (QA).

Levels of QA have been shown to be elevated in patients with ADC and are positively correlated with the level of dementia (Heyes *et al.* 1992). Furthermore, levels of secreted QA by macrophages are elevated when these cells are activated and infected with HIV (Nottet *et al.* 1996a). QA is an agonist at the NMDA receptor, and has been found to be neurotoxic, albeit at relatively high doses, both *in vitro* and *in vivo* (Schwarcz *et al.* 1983; Kim *et al.* 1987). Thus, although it is unlikely that the presence alone of small amounts of QA is sufficient to result in neurotoxicity, it is possible that QA acts in concert with other infected cell-secreted factors, for example Tat or gp120, to cause neurotoxicity via the NMDA receptor. Another detrimental action of QA may result from its synthesis. The precursor for QA is L-tryptophan, an amino acid which also participates in the synthesis of the neurotransmitter 5-hydroxy-tryptamine (5-HT). Increased production of QA in HIV may result in a depletion of tryptophan, and thus 5-HT, to further add to CNS dysfunction.

1.4.2.2. An NMDA-like neurotoxin.

Biochemical, physical and pharmacological evaluations of lentivirus induced neurotoxicity *in vitro* point to an unknown substance released from HIV infected macrophages that may be responsible for neuronal injury. These investigations point to an element that is protease-resistant, therefore not a protein or cytokine, heat-stable, therefore not a free radical, which is neither a glycolipid nor an amino-acid, but is blocked by NMDA receptor antagonists, although is not a classical NMDA receptor agonist as it lacks a COO- moiety. It is also cationic and less than 500 Da in mass (Giulian *et al.* 1990; Giulian *et al.* 1993). It is possible that this substance modulates the NMDA receptor in some way or increases extracellular levels of NMDA receptor agonists to incur neurotoxicity. Recently this substance has been characterised as a neurotoxic amine called NTox (Giulian *et al.* 1996). This is not an established neurotoxin, but has been found to be neurotoxic when injected *in vivo*. Furthermore, NTox can be extracted from CNS tissue of HIV positive individuals.

1.4.2.3. Cytokines.

Cytokines are a large family of cellular mediators which are widely believed to play an important role in the regulation of tissue homeostasis and integrity, either via local influences or by the recruitment of other factors from the circulation. Typically, they are expressed at very low levels in healthy situations, but their expression can change markedly in disease states and in response to tissue stress. Their actions cover a broad range of activities, some known to act as trophins, others as toxins and yet others as both depending on the level of their expression, and they are secreted by a wide range of different cell types. The size and structure of cytokines has provoked controversy as to whether they are able to penetrate the BBB, but it is now firmly established that cytokines are synthesised and expressed within the CNS, or cells isolated from the CNS. There exists a veritable plethora of cytokines, but for the purposes of this thesis only a few will be discussed, those that seem to play a role in response to central nervous tissue damage and disease states, in particular IL-1 β , IL-6, TNF α , and TGF β .

1.4.2.3.1. Cytokine receptors in the CNS.

Receptors for IL-1 α and β , IL-6 and TNF α have been characterised in brain, but their precise cellular location is unclear. Two receptors for IL-1 α and β , types I and II, exist in the CNS. Some reporters attribute the actions of IL-1 α and β in the brain exclusively to the type I receptor (Sims *et al.* 1993). However, other investigators have shown that the actions of IL-1 β , when administered directly to the brain, can be inhibited by antibodies to the IL-1 type II receptor (Luheshi *et al.* 1993). This treatment does not have any effect on the actions of IL-1 α , suggesting that the two isoforms of IL-1 may be acting at the two different receptors. Detection of the IL-1 type I receptor locates it predominantly in the dentate gyrus of rodents (Takao *et al.* 1990). In the brain, as well as peripheral tissues, a naturally occurring antagonist to the actions of IL-1 exists (IL-1ra), although its functions are unknown (Licinio *et al.* 1991).

In human cells, IL-6 binds to a 80 kDa glycoprotein which associates with a 130 kDa glycoprotein (gp130) for signal transduction (Taga *et al.* 1989). IL-6 receptors are expressed in rodent brain and are localised in the hippocampus, hypothalamus, the internal capsule, the optic tract and the piriform cortex (Schobitz *et al.* 1992). These receptors are also expressed in cultured neurons and glial cells (Sawada *et al.* 1993). Interestingly, like some other cytokine receptors, the extracellular portion of the IL-6

receptor can be released as a ligand binding protein. However, unlike other cytokine receptors, the binding of the free receptor to its ligand fails to cause inactivation of the ligand and instead increases the affinity of the interaction between the IL-6 receptor and gp130 (Hopkins *et al.* 1995).

TNF α binds two distinct receptors p55 and p75 (Smith *et al.* 1994), which are linked to different signal transduction pathways (Tartaglia *et al.* 1991), and may modulate different effects of TNF α . In the CNS, TNF receptors are widely distributed (Smith *et al.* 1992). TNF α receptor subtypes also show homology with Fas/Apo-1 cell surface receptors, which are implicated in programmed cell death of many types of cell (Suda *et al.* 1993).

Three types of receptors have been identified for TGF β (Derynck 1994). Evidence suggests that the type I and II receptors act as the principal signal transducer elements and that the type III receptor plays a role in presenting TGF β to the other two receptors (Miyazono *et al.* 1994).

1.4.2.3.2. TNF α in HIV and MVV infection.

The role of the pro-inflammatory cytokines TNF α , IL-1 β and IL-6 in the neuropathogenesis of HIV has been the subject of much research. TNF α has been reported to be elevated in the CSF of patients suffering from HIV dementia as compared to HIV positive patients with no dementia (Grimaldi *et al.* 1991; Perrella *et al.* 1992), although this correlation is not always present (Vitkovic *et al.* 1994). *In situ* detection of mRNA for TNF α has also found that the message for this cytokine is expressed in the brains of HIV positive individuals, but not in uninfected individuals (Nuovo *et al.* 1996), and that expression of TNF α mRNA positively correlates with the level of dementia in HIV positive individuals (Wesselingh *et al.* 1993). Interestingly TNF α mRNA is not always co-localised in cells expressing HIV antigens, suggesting that it may be released from other cell types in response to HIV infection. In post mortem brains, TNF α mRNA expression is observed in microglia and occasionally astrocytes (Tyor *et al.* 1992). *In vitro*, activation of astrocytes results in the release of a substance resembling TNF α (Robbins *et al.* 1987). HIV infected activated monocytic cells have been shown to produce increased levels of TNF α *in vitro* (Merrill *et al.* 1989; Molina *et al.* 1989). Astrocytes have also been found to produce higher levels of TNF α when infected with HIV but only when these are co-cultured with macrophages (Fiala *et al.*

1996). Similarly, TNF α is upregulated in glial cells and human cultured monocytes, when exposed to HIV gp120 (Koka *et al.* 1995; Clouse *et al.* 1991), and rises in T-cells exposed to HIV Tat (Buonaguro *et al.* 1992). Cultured sheep microglia infected with MVV also display increased levels of TNF α as revealed by RT-PCR (B. Ebrahimi, personal communication). Supernatant from these infected cells also causes the death of mouse trigeminal ganglion cells.

TNF α has been proposed as a mediator in causing demyelination in Multiple Sclerosis (MS) and Human T-lymphotropic Virus 1 (HTLV1) associated myelopathy (Brosnam *et al.* 1988; Moore *et al.* 1989) and has been implicated as a neurotoxin in animal models of stroke (Liu *et al.* 1994). Indeed, TNF α has been found to be neurotoxic to human neuronal cultures (Westmoreland *et al.* 1996) via the AMPA glutamate receptor (Gelbard *et al.* 1993), or by the binding of TNF α to the p55 receptor on neurons. Human neuronal cells can also be killed *in vitro* by TNF α via the mechanism of apoptosis (Talley *et al.* 1995). Furthermore, rodent oligodendrocytes are killed by TNF α *in vitro* (Robbins *et al.* 1987; Selmaj *et al.* 1988). TNF α also induces the proliferation of astrocytes (Barna *et al.* 1990), and can change their profile of cytokine release (Benveniste *et al.* 1994). *In vitro*, TNF α has also been reported to protect neurons against excitotoxic, metabolic and oxidative stresses (Barger *et al.* 1995; Cheng *et al.* 1994), possibly by the stabilisation of calcium homeostasis together with suppression of the accumulation of free radicals and the induction of the neuroprotective proteins calbindin and Mn-superoxide dismutase (Warner *et al.* 1991). However, the sheer weight of evidence seems to point to a definite detrimental action of increased levels of TNF α on neuronal cells.

The possibility of a neuroprotective role of TNF α has also been suggested *in vivo* since knockout mice deficient in both TNF α receptors display greater cellular responses to middle cerebral artery occlusion and seizure induced damage to hippocampal neurons than their wild-type counterparts (Bruce *et al.* 1996). In these same mice, microglial activation is also decreased. In another transgenic model of disease, mice with a disruption in the gene encoding TNF α show a greater vulnerability to autoimmune-mediated demyelination (Liu *et al.* 1998). This model suggests that TNF α may be exerting an anti-inflammatory role. However, other reports seem to confirm the pro-inflammatory role of TNF α . Transgenic mice overexpressing TNF α

develop more severe symptoms of the demyelinating disease experimental allergic encephalomyelitis than their wild type counterparts (Taupin *et al.* 1997). The overexpression of TNF α alone does not seem to directly damage myelin or oligodendrocytes, but appears to be mediated by excessive prolonged activation of microglial cells.

1.4.2.3.3. *IL-1 β and IL-6 in HIV and MVV infection.*

The cytokines IL-1 β and IL-6 are normally expressed in some CNS cells. Immunocytochemically, IL-1 β is found mainly in endothelial cells, microglia and macrophages (Tyor *et al.* 1992) but it can also be detected in astrocytes and oligodendrocytes (da Cunha *et al.* 1993b). IL-6 is detectable in macrophages, astrocytes, endothelial cells and microglia (Van Snick 1990). As with TNF α , reports of increased levels of IL-1 β and IL-6 in the CSF of HIV positive demented patients are inconsistent, some investigators reporting increased levels (Gallo *et al.* 1989; Perrella *et al.* 1992), others not (Weller *et al.* 1991). *In situ* detection of IL-1 β in the brains of AIDS patients has shown greater levels of IL-1 β immunoreactivity in these individuals as compared to HIV negative controls (Tyor *et al.* 1992). IL-6 expression does not seem to alter, although some reporters have found that microglia stain positively for IL-6 in AIDS brains but not in control brains (Vitkovic *et al.* 1994), as well as in the spinal cord of patients with AIDS (Yoshioka *et al.* 1994). *In vitro*, levels of IL-1 β and IL-6 are upregulated in human glial cells and monocytes when these are treated with HIV gp120 (Koka *et al.* 1995; Clouse *et al.* 1991). HIV infected astrocytes co-cultured with macrophages also produce higher levels of IL-6 (Fiala *et al.* 1996). IL-1 β levels are also increased in HIV infected monocytes (Harouse *et al.* 1991; Molina *et al.* 1989), and in sheep microglia infected with MVV (B. Ebrahimi, personal communication).

The pro-inflammatory cytokines IL-1 β and IL-6 do not seem to be neurotoxic *per se*, since their direct application to brain cells *in vitro* and *in vivo* does not always result in cell death. *In vitro* low concentrations of IL-1 β can be neuroprotective whereas higher concentrations are neurotoxic (Araujo *et al.* 1993; Lapchak *et al.* 1993). *In vivo*, infusion of large quantities of IL-1 β directly into the brain of rodents causes neuronal loss and microglial activation (Bourdiol *et al.* 1991).

Moreover, IL-1 β exerts a neurotoxic intensifying action when other excitotoxic factors are present (Strijbos *et al.* 1995a). Levels of IL-1 β and IL-6 are increased

following brain damage, and IL-1 β mRNA is rapidly upregulated following experimental ischemia (Olsson *et al.* 1987; Minami *et al.* 1992). IL-1 β has also been shown to release arachidonic acid, a precursor for pro-inflammatory eicosanoids (Rothwell *et al.* 1993). These can mediate glutamate action at the NMDA receptor and have been shown to positively enforce glutamate release presynaptically. Furthermore, IL-1 β causes increases in intracellular calcium levels and causes the production of NO from glial cells, both of which are factors involved in excitotoxic cell death (Rothwell *et al.* 1993). IL-1 β can also activate astrocytes, possibly leading them to secrete excitotoxins (Lee *et al.* 1993). The study of these cytokines in other neurological diseases also points to their possible neurodegenerative role. Inhibitors of IL-1 β have been shown to reduce neuronal injury in animal models of stroke and Parkinson's disease where glutamate neurotoxicity is believed to be at play (Rothwell *et al.* 1993). In Alzheimer's disease, IL-1 β and IL-6 are synthesised in the amyloid plaques characteristic of the disease (Griffin *et al.* 1989; Strauss *et al.* 1992), and IL-1 β can induce the production of β -APP, a protein involved in the deposition of these plaques in the brain (Gray *et al.* 1993). As for IL-1 β , IL-6 has been proposed as a neurodegenerative cytokine, since it has been shown to increase levels of intracellular calcium (Qiu *et al.* 1995). Furthermore, transgenic mice which overexpress IL-6 develop severe neurological problems resulting in ataxia, tremors and seizures, suggesting that this cytokine is potentially lethal to cells in the CNS when its levels are unchecked (Campbell *et al.* 1993).

1.4.2.3.4. TGF β in HIV and MVV infection.

Three isoforms of TGF β exist but the most extensively studied form in the CNS is TGF β -1. The mRNA for TGF β -1 is constitutively expressed in astrocytes, microglia and oligodendrocytes but not neurons, under normal conditions (da Cunha *et al.* 1993a). The detection of the protein, however, is rare in healthy brains (da Cunha *et al.* 1992). Post-mortem examination of AIDS brains have revealed the presence of TGF β -1 immunoreactivity (da Cunha *et al.* 1995). The extent and localisation of this immunoreactivity correlate with levels of IL-1 β . These findings are supported by *in vitro* evidence that IL-1 β stimulates the expression of TGF β -1 by astrocytes, oligodendrocytes and microglia (da Cunha *et al.* 1993b).

To investigate the role of TGF β -1 in normal and pathologic conditions, transgenic mice overexpressing TGF β -1 in astrocytes under the control of the GFAP promoter have been studied (Wyss-Coray *et al.* 1995). Such mice develop increased levels of extracellular matrix proteins (ECM), such as laminin, fibronectin and heparan sulfate proteoglycan. These substances are suspected to be involved in the deposition of β -amyloid, a substance which forms plaques in the brains of patients suffering Alzheimer's disease (Fillit *et al.* 1995; Finch *et al.* 1993). Many of these mice do not survive to adults but those that do most often become hydrocephalic. Furthermore, when they are immune-challenged, these mice more readily develop symptoms of experimental autoimmune encephalitis, with greater levels of mononuclear cell infiltrates in the CNS and more overt clinical signs than their wild-type counterparts.

However, in *in vitro* cultures of astrocytes, TGF β -1 has been found to enhance production of IL-6, Nerve Growth Factor (NGF), a trophic element for some neurons, and suppress proliferation of astrocytes as well TNF α production from these cells, suggesting that some functions of TGF β -1 may be protective to neurons (Lindholm *et al.* 1992; Benveniste *et al.* 1994). TGF β -1 also downregulates the proliferation of microglial cells and alters their pattern of cytokine release (Suzumura *et al.* 1993). Furthermore, TGF β -1 can promote the survival of various types of neurons, such as motor neurons, midbrain dopaminergic neurons and hippocampal neurons when these are grown in culture (Ishihara *et al.* 1994; Krieglstein *et al.* 1995; Martinou *et al.* 1990). The application of TGF β -1 to cortical cell cultures also conferred on neurons a degree of resistance to toxicity (Krieglstein *et al.* 1995; Chao *et al.* 1994) and can protect neurons against excitotoxic and ischaemic insults *in vivo* (McNeill *et al.* 1994; Prehn *et al.* 1993). These findings suggest that steady states of TGF β -1 production may be neuroprotective, but that upmodulation of this cytokine, as in HIV infected neuroglial cells in response to increased levels of IL-1 β , may be detrimental and further contribute to CNS disruption already evoked by other cytokines.

Taken together these findings suggest that TNF α and other pro-inflammatory cytokines may be involved in lentiviral induced neurodegeneration by two mechanisms: firstly, by being directly released from infected macrophages and microglia to cause neurotoxicity, secondly by being upregulated in microglia and astrocytes by diffused viral proteins such as Tat and gp120, which would cause an internal disruption to these

cells as well as the concomitant discharge of proinflammatory cytokines and other mediators to neighbouring cells.

In addition, IL-1 β and TNF α causes the up-regulation of HIV gene expression in neural cells, by enhancing the liberation of the NF κ B protein from its inhibitor protein I κ B, allowing NF κ B to bind to the enhancer region of the HIV LTR (Swingler *et al.* 1992). In MVV, up-regulation of gene expression is believed to occur through the Jun and Fos proteins binding to AP-1 or CBF sites of the viral LTR (Gabuzda *et al.* 1989, Sutton *et al.* 1997). Thus, a vicious circle of cytokine mediated neurotoxicity and viral gene amplification may be established in lentiviral encephalopathies.

1.4.2.4. Arachidonic Acid (AA) and its metabolites

Macrophages are highly enriched in lipids and, as part of their role in the immune system, naturally phagocytose cellular debris. Membrane phospholipids are metabolised by the formation of arachidonic acid, which is subsequently degraded either by the cyclooxygenase pathway to produce prostaglandins (PG) and thromboxanes (TX), or through the lipoxygenase pathway to produce leukotrienes (LT). These have been proposed as toxins in some neurological diseases as they can affect neuronal function and interfere in the regulation of cytokines (Egg *et al.* 1980; Merrill *et al.* 1983). In cases of HIV encephalitis, levels of the prostaglandins PGE₂ and PGF_{2a} have been found to be elevated in the CSF (Griffin *et al.* 1994). *In vitro*, gp120 has been shown to produce increases of arachidonic acid metabolites in cultures of monocytes (Wahl *et al.* 1989), and amounts of these molecules are also raised in co-cultures of astrocytes with HIV infected macrophages (Genis *et al.* 1992). Prostaglandins have recently been found to stimulate glutamate release from astrocytes, via a calcium dependant mechanism (Bezzi *et al.* 1998). Since excessive glutamate is toxic to neurons, prostaglandins may be exerting an indirect neurotoxic effect. As yet, however, neither prostaglandins, thromboxanes or leukotrienes have been shown to be directly neurotoxic. Nevertheless, since they seem to disrupt the normal regulation of cytokine production, they may be causing increased levels of the pro-inflammatory cytokines previously mentioned, thus adding further weight to the neurotoxic threat of these mediators.

1.4.2.5. Nitric Oxide

As has previously been mentioned NO plays a role in certain types of cell death, by the mechanism of NO mediated glutamate neurotoxicity. Much attention has

therefore focused on whether NO may be having a detrimental effect in lentiviral encephalopathies. NO has been shown to be released from HIV infected macrophages (Bukrinsky *et al.* 1995) and may therefore also be released from other infected cell types. NO has also been shown to be released from blood derived macrophages when these are exposed to the HIV envelope glycoprotein gp120 (Pietraforte *et al.* 1994). Increased levels of NO have also been found to be elevated in peripheral blood mononuclear cells and polymorphonuclear lymphocytes in HIV positive individuals, especially those displaying signs of HIV encephalopathy (Torre *et al.* 1995). *In vitro*, gp120 induced neurotoxicity in the presence of glutamate and extracellular calcium in rodent primary cortical cultures can be reduced by inhibitors of NO formation (Dawson *et al.* 1993). Moreover, soluble NO has been shown to be toxic to rodent oligodendrocytes. Thus, it seems that increased levels of NO in HIV infection may lead to damage of healthy tissues, for example by the exhaustion of antioxidants, or by its role in glutamate toxicity to brain cells. However, the ability of HIV infection to increase levels of NO is not always paralleled in human studies. Levels of the inducible form of NOS are not elevated in post-mortem sections of individuals with HIV encephalitis (Bagasra *et al.* 1997), and levels of nitrite or nitrate, by products of the synthesis of NO, in the CSF of HIV positive patients are not always consistent, as some reporters find no significant differences in occurrence (Milstien *et al.* 1994), whilst others do (Baldeweg *et al.* 1996). Furthermore the ability of human macrophages, as opposed to rodent macrophages, to synthesise increased levels of NO has been questioned. Human macrophages have less of the enzyme pyruvyltetrahydropterin synthase, which causes rate limitation in the activity of NOS (Fuchs *et al.* 1994). Instead large amounts of neopterin are produced, evident in the CSF of HIV infected patients (Fuchs *et al.* 1989). Neopterin has been shown to enhance programmed cell death caused by TNF α (Fuchs *et al.* 1995).

1.4.2.6. *Neuroleukin and vasoactive intestinal polypeptide (VIP)*

Gp120 shares sequence homology with the neurotrophic factors neuroleukin and VIP. It may be that gp120 competes with the receptors for these substances and thus diminishes the production of neurotrophins necessary for the survival and well-being of neurones and astrocytes (Lipton 1992a)

1.4.2.7. Free radicals

NO, OH and O₂ can all be produced by astrocytes, macrophages and microglia, and can cause neuronal damage by the disruption of cellular proteins, nucleic acids and membrane peroxidation through their oxidative properties. Normally they are counterbalanced by Nerve Growth Factor (NGF) or metabolised by Super Oxide Dismutase (SOD), but the oxidant-anti-oxidant equilibrium may be disrupted by lentivirus infection (Jackson *et al.* 1990).

1.4.2.8. Platelet Activating Factor (PAF)

Yet another molecule that has been implicated in HIV encephalitis due to its augmented levels in HIV positive patients with dementia is PAF (Gelbard *et al.* 1994). PAF is directly neurotoxic to cultures of human fetal neurons and rat retinal cultures, via its actions on NMDA receptors (Gelbard *et al.* 1994). It has also been shown to be produced in co-cultures of astrocytes and HIV infected monocytes (Genis *et al.* 1992).

1.4.3. Inflammation and immunological mechanisms in the CNS

For many years, the brain has been considered an immunologically privileged site, due to the presence of the BBB preventing the migration of immune mediating cells into the CNS. Recently, however, more and more evidence points to the likelihood of cells within the CNS, in particular microglia, being able to mount an intrinsic response to invading pathogens, with concomitant detrimental side effects on other cell types in the brain. This mechanism has been put forward as one of the main contenders in the demyelination observed in MS, where it is hypothesised that cells are mounting an immune response to myelin, and thus destroying it (Hartung 1993). It is therefore possible that the invasion of the CNS by macrophages infected with lentiviruses triggers the outbreak of an inflammatory response from neuroglial cells, which may at the same time stimulate the invading macrophages to produce increased levels of neurotoxins, whilst also causing damage themselves by the release of neurotoxic factors due to their activated state.

1.4.3.1. Microgliosis.

1.4.3.1.1. Description and functions of microglia.

Microglia were first characterised by del Rio Hortega in 1932 and, despite much controversy, are now generally accepted as the resident macrophages of the CNS. They arise from monocytes during development and express some of the same markers as macrophages (Perry *et al.* 1985). Monocytes migrating to the CNS can give rise to other populations of macrophages in the CNS such as perivascular macrophages and the macrophages of the choroid plexus and meninges, but by far the largest is the microglial cell population. The main difference between these types of brain macrophages is the presence of MHC class II antigens on perivascular macrophages and those in the choroid plexus, which are down-regulated in microglia. Microglia can vary morphologically, having a simple stellate form in areas lacking a BBB, a branched and ramified form in grey matter, or a more linear pattern running along axon fibres in white matter (Perry *et al.* 1994). Similarly, the distribution of microglia can vary. They are at their most dense in areas of grey matter, particularly in the substantia nigra and pallidum, but occur much more rarely in white matter regions such as the brainstem and cerebellum (Lawson *et al.* 1990). However, the general pattern of distribution seems to remain homogeneous, as

microglia are usually evenly spaced, and do not seem to touch each other (Perry *et al.* 1985). This suggests that they may be under the influence of astrocytes and neurons, as well as each other, through the means of diffusible mediators.

As for astrocytes, microglia perform important supportive functions for neurons. It is generally believed that microglia in a resting state act as monitors of the extracellular environment. However, they are known to react rapidly to any pathological changes, even when these are very subtle, such as disruptions in ion homeostasis (Gehrmann *et al.* 1993). Microglia possess a variety of receptors for CNS signalling molecules, for example noradrenaline, ATP and ACh, and can therefore react to any changes in the signalling patterns involving these molecules (Walz *et al.* 1993; Langosch *et al.* 1994; Priller *et al.* 1995; Whittemore *et al.* 1993). One of the ways in which this may be accomplished is by the presence of an inward rectifying potassium channel (Kettenman *et al.* 1990; Kettenman *et al.* 1993). As the resident macrophages of the CNS, they also have the capability to scavenge cellular debris in an effort to maintain tissue homeostasis (Streit *et al.* 1988a). However, as a result of this ability, macrophages that are activated in response to tissue damage or soluble mediators may have deleterious effects on surrounding bystander cells.

1.4.3.1.2. *Microgliosis.*

The activation and proliferation of microglia, microgliosis, occurs rapidly in reaction to injury. This response occurs in injury models which preserve or destroy the BBB. Injection of a neurotoxin, kainic acid, into the brain of rodents causes the activation of microglia within three days of the lesion (Marty *et al.* 1991). Similarly, axotomy of the facial nerve causes the proliferation and hypertrophy of microglia within a few days, accompanied by synaptic stripping of neurons (Streit *et al.* 1988b; Graeber *et al.* 1988). Microgliosis also causes the expression of several marker molecules in microglia. These include MHC class I and II antigens, TNF α , IL-6 and TGF β (Streit *et al.* 1989; Buttini *et al.* 1996; Kiefer *et al.* 1993). *In vitro*, activated microglia have also been shown to release reactive oxygen intermediates (ROI), NO, proteases, arachidonic acid derivatives, excitatory amino acids, quinolinic acid and the cytokines TNF α , IL-1 β , IL-6 and TGF β (Banati *et al.* 1993; Colton *et al.* 1987). This points to a detrimental action of microgliosis, since many of these substances have been shown to be neurotoxic, although levels of TGF β may be neuroprotective. The induction of

microgliosis can also be achieved by the administration of cytokines including IL-1 β , IL-6, TNF α and IFN- γ (Wekerle *et al.* 1986; Fagan *et al.* 1990; Campbell *et al.* 1993). The cytokine TGF β , on the other hand, seems to exert an inhibitory effect on the hypertrophy and hyperplasia of microglia (Suzumura *et al.* 1993).

1.4.3.2. Astrocytosis.

1.4.3.2.1. Types of astrocyte.

Astrocytes represent one of the most heterogeneous cell populations of the CNS. They vary morphologically and phenotypically. At first, two kinds of astrocyte were defined on the basis of shape, the fibrous and the protoplasmic astrocyte (Privat *et al.* 1986). Differentiation of astrocytes in the rat optic nerve on the basis of phenotype has also revealed two sets, type I and type II, although these do not necessarily correspond to the two types revealed by morphological characterisation (Raff 1989).

Astrocytes, unlike neurons, are not structurally independent, but form syncytial-like networks connected by gap junctions (Kettenman *et al.* 1983). These neuroglial cells are found throughout the brain, but occur particularly surrounding vascular structures, on the surface of the brain and around neuronal cell bodies and synapses. Specialised intramembrane structures found in astrocytes, termed assemblies, differ in their frequency between these locations. Thus high concentrations of these assemblies are found in astrocytes investing the vasculature of the CNS and in astrocytes forming the surface of the brain, but only low concentrations of these assemblies are found in astrocytes located around synapses and even lower levels near cell bodies (Landis *et al.* 1974; Landis 1981; Landis *et al.* 1982). Furthermore the shape of astrocytes may change in response to neurotransmitters, neuronal interactions and physiological stresses (Hatten 1985; Cornell-Bell *et al.* 1990b; Hatton 1990).

Astrocytes also differ regionally, their shape differs in white matter and in grey matter, as do their patterns of expression of various proteins and enzymes. Most astrocytes express receptors for neurotransmitters (Murphy *et al.* 1987) but, for example, in the cerebellum astrocytes additionally express somatostatin (SS) mRNA, whereas in the cortex and striatum, astrocytes express mRNA for proenkephalin as well as the enkephalin peptide, but do not produce cholecystokinin (Shinoda *et al.* 1989; Denis-Donini *et al.* 1984). This suggests that astrocytes may be differing based on the neuronal population of a particular area of the CNS. The glutamate receptor on the cell

surface of astrocytes is also expressed heterogeneously *in vitro*, and the expression of the enzyme glutamine synthetase in astrocytes varies between the developing and mature rodent brain (Hallermeier *et al.* 1984; Holzwarth *et al.* 1994; Wilkin *et al.* 1990). The capability of astrocytes to secrete the cytokines IL-1 β and TNF α also differs, as these cytokines are expressed either alone or together in some but not all astrocytes (da Cunha *et al.* 1993b).

1.4.3.2.2. *Functions of astrocytes.*

Astrocytes were long regarded as bystanders to most functions of the CNS and merely assigned a supportive role for neurons. Increasing research has found that this is not the case and that while astrocytes do indeed provide neurons with structural support, by playing a role in neuronal migration, neurite outgrowth, synaptogenesis and synaptic plasticity, they also confer functional support by the maintenance of tissue homeostasis, the regulation of water, ion and amino acid neurotransmitter metabolism, energy and nutrition balance, maintenance of the BBB and modulation of immune and inflammatory responses (Norenberg 1994). Furthermore, some of the functions of astrocytes are positively beneficial to neurons, particularly with regard to the metabolism of ammonia, glutamate, free radicals and metals, substances which are toxic to neurons.

Astrocytes are the only cells in the CNS which express the enzyme glutamine synthetase (Mearow *et al.* 1989). This enzyme catalyses the formation of glutamine from glutamate, and consumes the resulting by-product of ammonia, detoxifying it in the process (Mearow *et al.* 1989; Mennerick *et al.* 1994). Astrocytes also take up glutamate released from synaptic junctions of neurons as well as the inhibitory neurotransmitter γ -amino-butyric acid (GABA). Glutamate analogues can depolarise astrocytes via ligand-gated receptors, but these are not responsive to NMDA (Bowman *et al.* 1984; Kettenman *et al.* 1993; Tang *et al.* 1986).

Potassium homeostasis within the CNS is another function of astrocytes. Potassium is taken up by astrocytes in regions where its concentration is high and is redistributed either to areas where potassium levels are low or, if potassium concentrations are uniformly high throughout the brain, for example due to diffuse neuronal activity, potassium is released into the circulation by the astrocytic end-feet present on blood vessels (Gardner-Medwin 1983; Paulson *et al.* 1987). Potassium is

also extruded from astrocytes when these uptake glutamate and sodium (Brew *et al.* 1987). A possible pathological consequence of this may therefore be the inhibition of glutamate uptake into astrocytes in the presence of high extracellular potassium causing the build-up of extracellular glutamate and possible excitotoxicity (Barbour *et al.* 1988).

The presence of carbonic anhydrase in astrocytes contributes to the metabolism of CO₂ within the CNS and maintenance of uniform pH. Normal neuronal metabolism releases CO₂. This is taken up by astrocytes and degraded into bicarbonate, which is exchanged with endothelial cells for sodium and chloride. The simple diffusion of CO₂ from neurons to the circulation would cause disturbances in pH, and possible cell damage. The presence of astrocytes thus enables the elimination of CO₂ without pH changes (Landis 1994).

Astrocytes, however, do not serve merely to control the extracellular environment in the CNS. The binding of glutamate to receptors on astrocytes causes increases in levels of free intracellular calcium. These oscillations can propagate to neighbouring astrocytes and to neurons causing modulations of intracellular calcium levels. Therefore, the activity of neurons influences the activity of astrocytes which in turn induce changes in neuronal responses (Charles *et al.* 1991; Cornell-Bell *et al.* 1990a; Dani *et al.* 1992; Nedergaard 1994). Thus a bi-directional flow of information between neurons and astrocytes occurs, similar to the signalling capabilities of neuronal networks.

1.4.3.2.3. Astrocytosis.

Astrocytosis is defined as hypertrophy, increases in size, and hyperplasia, increases in density, of astrocytes. Astrocytosis is most usually indicated by an increase in immunocytochemical staining for GFAP, a subunit of an intermediate filament present only in astrocytes. Some investigators have questioned this method as a tool for measuring astrocytosis since the intensity of GFAP staining depends on its polymerisation and therefore may not reflect the amount of protein present (Lipsky *et al.* 1987). Nevertheless, it is still the most commonly used detection method for the presence of astrocytosis. Mechanical injury to the brain causes astrocytosis within one to three days of the procedure (Landis 1994). Astrocytosis can also occur, however, in response to axonal degeneration at a site distant from the astrocyte, for example in the spinal cord after sciatic nerve transection (Murray *et al.* 1990). This suggests that

astrocytosis can occur in response to changes in normal neuronal function. Furthermore, GFAP expression occurs over a large area in response to local injury. This is probably due to the communication between astrocytes and not just reactions to changes in the extracellular environment since astrocytosis in this situation occurs more readily in the grey matter than in the white matter, whereas the pattern would be more uniform if diffusible elements were at play (Landis 1994). This also presents further evidence as to the heterogeneity of astrocytes and their differing responses to injury, which must therefore be taken into account when studying pathological changes in injured or diseased brains.

The early changes in astrocytes are reflections of their homeostatic functions. Within seconds to minutes of injury the normal metabolic activities of astrocytes can become disrupted. The normal regulation of potassium levels becomes overstretched and due to osmotic equilibrium, astrocytes swell. As a consequence of disrupted potassium uptake, local blood flow may decrease leading to deficiencies in oxygen availability. This in turn can cause the increase of bicarbonate metabolism in astrocytes, leading to further swelling. Furthermore, astrocytes may switch to anaerobic glycolysis. Normally, astrocytes metabolise glycogen to provide glucose for neurons when blood flow decreases, but this may be lost during astrocytosis causing a lack of glucose. Lactate also builds up in astrocytes causing further swelling as well as acidosis of the extracellular matrix, which may be further detrimental to neuronal function (Kraig *et al.* 1990; Staub *et al.* 1990). The decrease in glutamate uptake may lead to excitotoxicity of neurons, as well as overstimulation of astrocytes to cause calcium influx and ultimately astrocytic death (Kimmelberg *et al.* 1990). The swelling of astrocytes will cause an increase in their volume and thus will further distort any mechanical injury, as well as eventually causing an increase in intracranial pressure, which further serves to reduce the perfusion of brain tissue.

Within hours of mechanical injury to the brain, increases in GFAP staining are seen. Increases in astrocyte number and density are observed. Accompanying these changes is the expression of MHC classes I and II on astrocytes, which do not normally express these molecules. This is particularly true in viral infections (Olsson *et al.* 1987; Suzumura *et al.* 1986). *In vitro*, astrocytes can be stimulated to express MHC class II molecules in response to interleukins, interferons, TNF α and TGF β (Hertz *et al.* 1990; Johns *et al.* 1992).

After several days following a lesion to the brain, astrocytosis can decrease reflecting a return to steady state functions. However, if an injury is severe, hypertrophy and hyperplasia of astrocytes persist, and there is some evidence that at this stage astrocytes undergo mitosis (Miyake *et al.* 1992). There is also evidence that astrocytes can migrate from other areas of the CNS to the site of the lesion. Ultimately, astrocytic responses are deemed to exert a curative action following injury, re-establishing tissue homeostasis and lending support to neurons by secreting members of the NGF family. However, astrocytic scars are a common result of injury to the brain, and these can often be detrimental to the regeneration of axons. During development, astrocytes guide the establishment of axons, but this function is lost once cellular connectivity is established. Indeed, *in vitro* the presence of astrocytes past a certain stage of maturity can inhibit the progress of axons. Furthermore in injured spinal cords, axons do not regrow past astrocytes at the site of injury (Liuzzi *et al.* 1987). This suggests that astrocytes can exert both regenerative and detrimental actions once an injury has been established, and may participate in the degeneration of neurons in during injury.

In summary, there is compelling evidence that microglial and astrocytic activation in response to injury can have detrimental inflammatory effects within the CNS. Since astrocytosis and microgliosis are a common neuropathological finding in MVV and HIV infection, the role of any detrimental effects of these cells must be evaluated.

1.4.3.3. *The role of the immune response*

Much research has focused on immune mechanisms occurring in MVV and HIV infection. Much of this work is beyond the scope of this thesis, but several points need to be addressed in order to understand better lentiviral infection of the CNS. The diseases caused by MVV and HIV differ in one vital respect. Whereas HIV causes the depletion of CD4⁺ T cells, sheep infected with MVV seem to mount a good humoral and cellular immune response throughout the progress of the disease. The importance of this variation must be taken into account when considering parallels between the two lentiviral diseases, as well as when designing any experiments or animal models to investigate lentiviral neurodegeneration. The question remains however, as to how much of the damage encountered in lentiviral encephalopathies can be attributed to the effects of immune cells. Nathanson *et al* (1993), for example, have found that the

blocking of the immune response by cyclosporin A and cycloheximide in sheep experimentally infected with visna, reduced the extent of neuropathology observed as compared to sheep infected with visna with no immunosuppression. However, there is still much debate as to the relevance of this since the major cell type that infiltrates the CNS is the macrophage and not lymphocytes. Other investigators have proposed that HIV infection of macrophages only results in the release of neurotoxins when these are immune-activated by endogenous regulatory factors (Nottet *et al.* 1995a).

In HIV, a switch from a Th1 type immune response to a Th2 type immune response may occur. These responses are characterised by different cytokine profiles. A down-regulation of the cytokines IL-4 and IL-10, which ordinarily exert an inhibitory action on the number and action of macrophages, is usually encountered. This may be due to the killing of CD4⁺ T cells by the virus (Nottet *et al.* 1995a). Indeed, some investigators have found that levels of pro-inflammatory cytokines such as TNF α rise whilst levels of other cytokines such as IL-4 are decreased in the brains of patients with HIV (Wesselingh *et al.* 1994), and that this unbalance may further contribute to any neurodegeneration.

In any case, the role of immunological responses both within the brain, incorporating astrocytosis and microgliosis, and outwith the CNS, including the circulating lymphocytes and their cytokine profile, needs to be taken into consideration, both when evaluating post-mortem damage to the CNS in lentiviral infection, and when designing any experimental models of the diseases.

1.5. INTRODUCTION TO EXPERIMENTS

Recently, a model of HIV encephalopathy has been described in *scid* mice (Tyor *et al.*, 1992). These mice lack T and B cells and are thus unable to mount an immune response. Their manipulation therefore allows the investigation into how much a pathology relates to non-immune mechanisms. Gendelman and colleagues have shown that the injection of HIV infected human macrophages into these mice causes astrocytosis, the presence of multinucleated giant cells and the death of neurons via apoptosis (Persidsky *et al.* 1996; Persidsky *et al.* 1997). These are all hallmarks of the naturally occurring disease and the model therefore presents a valuable experimental tool for the study and manipulation of HIV infection of the brain.

In MVV, as previously mentioned, the immune response seems to play a more significant role in the development of lesions within the CNS. To assess whether neurodegeneration in MVV is entirely a factor of immunological responses, a similar model of MVV encephalopathy in *scid* mice is investigated here. Firstly, the ability of MVV infected and uninfected ovine macrophages to cause neurodegeneration was investigated through the injection of these cells into the striatum of *scid* mice. The contribution of immune cells was also investigated by the administration of these in the same manner to *scid* mice. The presence of neurons, activated astrocytes and microglia was then ascertained through the immunocytochemical detection of these in fixed *scid* brain tissue, and any changes in the relative density of these cells between mice receiving MVV infected or uninfected cells was assessed through the use of image analysis.

The contribution of mediators released from virally infected cells was also probed. Firstly, the reverse transcriptase - polymerase chain reaction (RT-PCR) was carried out on MVV infected and uninfected macrophages to determine whether infection of these cells caused their activation. Cytokine induction was used as a measure of monocyte/macrophage activation. Therefore, the amounts of mRNA being synthesised for the pro-inflammatory cytokines IL-1 β , IL-6, TNF α and TGF β was assessed by RT-PCR in uninfected and macrophages infected with MVV *in vitro*. Secondly, the possible neurotoxicity of the supernatant from these cells was also tested, by the incubation of rat cortical cell cultures (RCC) with the supernatant from MVV infected and uninfected macrophages.

Since the Tat protein has been shown to be released by HIV infected cells, the effects of this lentiviral protein were also investigated by the application of both an MVV and HIV tat peptide, derived from the basic region of each Tat protein, to rat cortical cultures *in vitro*. Acute *in vivo* neurotoxicity assays were also carried out, by the injection of MVV and HIV tat peptides to rat striatum. The neurotoxic mechanisms of the MVV tat peptide were further probed by the administration of MK801, an NMDA receptor antagonist, NBQX, a non-NMDA receptor antagonist, L-NAME, a NOS inhibitor and α MSH, a TNF α inhibitor.

CHAPTER 2:

MATERIALS AND METHODS.

2.1. CELL CULTURES

2.1.1. PBMC and macrophage (MØ) cell preparation.

All procedures were carried out under sterile conditions in a laminar flow hood. For the macrophage cell preparation, blood was collected from healthy sheep, in 50 ml tubes containing 500 units heparin (10 units per ml), and centrifuged at 200g for 20 min. The buffy coat, the layer between plasma and red blood cells, was removed with a pasteur pipette, and resuspended in 10 ml sterile Phosphate Buffered Saline (SPBS), and underlaid with 10 ml Ficoll Hypaque (Lymphoprep, Nycomed, Birmingham, UK). The solution was again centrifuged at 200g for a further 20 min, resulting in the accumulation of PBMCs at the interface of the SPBS and the Lymphoprep. These were harvested with a pasteur pipette and washed twice in SPBS, by centrifugation at 150g, resuspension and centrifugation at 100g. At this stage, PBMCs destined for injection were ready for infection with MVV. Some PBMCs were also obtained from sheep experimentally infected with MVV. Cells destined for macrophage cell preparations were washed once further in the culture medium, with one centrifugation at 100g. The culture medium consisted of RPMI 1640 (Gibco/Life Technologies, Paisley, UK) containing 0.4 mM L-glutamine (L-gln), to which was added 0.04 mM HEPES (BDH, Lutterworth, UK), 20 units/ml of penicillin and streptomycin (P/S, BDH), 0.01 mM of mercaptoethanol (M/E, BDH), 10% fetal calf serum (FCS, Gibco) and 10% lamb serum (LS, Seralab, Crawley Down, UK). Flasks for macrophage cultures were coated with a 2% gelatin solution for 1 hour, dried and incubated with plasma from the buffy coat spin for 30 minutes at 37°C. Cells were plated out at a density of 5×10^6 cells/ml. Care was taken to ensure that cells and serum taken from each blood sample were not mixed with any other, in order to minimise the risk of a mixed lymphocyte reaction occurring in the cell preparations. Once the cells were plated out, they were incubated for one hour or overnight at 37°C, in 95% air, 5% CO₂, to enable the macrophages to stick to the flask, at which time the non-adherent cells were washed off with a solution of RPMI containing 2% FCS. The resulting macrophage cell preparation was then maintained at 37°C in humidified atmosphere of 95% air, 5% CO₂, for the appropriate amount of time until infection and injection into the *scid* mice.

2.1.2. Rat cortical cultures (RCC).

All procedures were carried out in sterile conditions in a laminar flow hood. Embryonic day 17 rats were used. Brains were dissected out in Hank's Balanced Salt Solution (HBSS, Gibco) on ice, and the cortices removed and chopped. These were then incubated with a mixture of trypsin and DNase (5000 IU DNase, Sigma, Poole, UK; 0.9% trypsin, Sigma, in 10 ml HBSS) for 12 min at 37°C. A trypsin inhibitor (ovomucoid, Sigma, 0.9% in 10 ml HBSS) was then added and the solution centrifuged at 200g for 5 min. The supernatant was removed, 10 ml DNase added (5000 IU in HBSS), the mixture homogenised, and spun at 200g for a further 10 min. The resulting pellet was then resuspended in 10 ml of culture medium and passed through a piece of 200 nm gauze to remove any remaining large pieces of tissue. The culture medium consisted of Dulbecco's Modified Eagle's Medium (DMEM, Sigma) supplemented with 0.01% Bovine Serum Albumin (BSA, Sigma), 0.03 mg/ml putrescine (Sigma), 200 µg/ml apo-transferrin (Sigma), 10 µg/ml insulin (Sigma), 6.7 ng/ml selenium (Sigma), 5.5 ng/ml tri-iodo thyronine (Sigma), 12.6 ng/ml progesterone (Sigma), 200 ng/ml corticosterone (Sigma), 0.5 mM L-gln (Gibco). A sample of cells were then counted on a haemocytometer, and the solution suspended in the appropriate volume of culture medium to give 5×10^5 cells/ml. Cells were then plated out in 24 well plates (Corning, Stone, UK). These had previously been incubated for 1 hour with a solution of poly-D-lysine (0.01 mg/ml, Sigma), washed in HBSS once and dried. Cultures were maintained at 37°C in a humidified environment of 95% air, 5% CO₂. After 24 hours, the culture medium was renewed, and changed every two days.

2.2. VIRAL INFECTION OF MACROPHAGES AND PBMCs.

2.2.1. 50% Tissue Culture Infectivity dose (TCID₅₀)

All procedures involving manipulation of virus and infected cells were carried out in a Class II Microbiological safety cabinet. Sheep chondrocytes were used to determine the TCID₅₀ of the virus supernatant used. Sheep chondrocytes were removed from storage in liquid nitrogen, thawed quickly and kept on ice. The culture medium of DMEM supplemented with 0.5 mM L-gln, 20 units/ml P/S and 10% FCS was slowly

added to the suspension of cells to dilute out the cryoprotectant, up to a final volume of 10 ml, and centrifuged gently at 100g for 5 min. The cells were then resuspended in cold culture medium, transferred to tissue culture flasks and maintained at 37°C in a humidified atmosphere of 95% air, 5% CO₂. Once the chondrocytes had reached confluence, they were washed in versene and removed from the tissue culture flask by adding a solution of 0.05% trypsin and 0.02% versene, spun at 100g, resuspended in culture medium and seeded in 96 well plates (Corning) at sub-confluent density. The cells were then maintained in the same conditions until they reached 60%-70% confluence. Doubling dilutions of the virus supernatant were then added to wells, in quadruple replicates. The cells were then observed every day and checked for the formation of syncytia indicating productive infection of the chondrocytes. When syncytia were readily observed in large numbers, the culture medium was removed from the wells and the cells fixed in neat methanol. Once fixed, the methanol was removed and the chondrocytes stained with a solution of GIEMSA (BDH) diluted 1:5 in water, to identify the wells containing syncytia. Each well was checked for the presence or absence of syncytia, to determine the concentration of virus at which 50% of wells showed the appearance of syncytia. This then enabled the calculation of the viral concentration in the original inoculum.

2.2.2. MVV infection of PBMCs and macrophages *in vitro*.

Macrophages were infected with MVV by removing the culture medium and replacing it with 2 ml of supernatant culture medium from 1514 strain infected sheep chondrocytes for 5 min, then adding 3 ml of warm fresh culture medium for overnight incubation. PBMCs were infected by incubation with 2 ml of the supernatant culture medium for 3 hours prior to injection.

2.2.3. Proliferation assay

In order to establish whether the lymphocytes obtained from sheep productively infected with MVV were responding to the addition of virus under tissue culture conditions, a proliferation assay was carried out. This involved the collection of blood

from the same MVV infected sheep whose PBMCs were injected into *scid* mice. Blood was collected into universal glass tubes containing glass beads and gently inverted for 10 min. The resulting fibrin clot was then removed, and the blood divided into 50 ml centrifuge tubes, supplemented with SPBS to a volume of 40 ml. As before, this solution was underlaid with 10 ml Lymphoprep and centrifuged at 200g for 20 min. The cells at the resulting interface between the SPBS and the Lymphoprep were removed and suspended in a solution of RPMI containing 1% FCS up to a volume of 20 ml. This was then centrifuged at 200g for 10 min. The cell pellets obtained at this stage were then washed twice in 10 ml of RPMI with 1% FCS, and spun again at 150g for 5 minutes. Following resuspension in culture medium RPMI containing 0.4 mM L-gln and supplemented with 0.01 mM M/E and 10% FCS, a sample of the cells were counted. The remaining cells were then recentrifuged and resuspended in the culture medium at 10^6 cells/ml.

Cells were then seeded in 96 well plates. Fresh culture medium was used as a negative control. Differing concentrations of ConA (50 μ g/ml, 25 μ g/ml, 12.5 μ g/ml, 6.25 μ g/ml, 3 μ g/ml and 1.5 μ g/ml), a known mitogen serving as a positive control, and virus supernatant (diluted 1:2, 1:4, 1:8, 1:16, 1:32, and 1:64) were then added to the wells containing cells. These were incubated together for 5 days in a humidified 95% air, 5% CO₂ atmosphere at 37°C. Proliferation was measured by pulsing the cells with 1 μ Ci/well of tritiated thymidine followed by incubation for 5 hours. This molecule is incorporated into any new DNA formed as a result of proliferative activity. Cells were harvested onto glass fibre mats, scintillant added and the value of radioactive disintegrations per minute scored on a Wallac Microbeta counter.

2.3. STEREOTAXIC INJECTIONS

2.3.1. PBMC and macrophage cell preparations.

To obtain cells for injection, PBMCs were washed twice in SPBS, by centrifugation at 100g and resuspension, counted on a haemocytometer and resuspended in the appropriate volume of SPBS. Macrophages were also washed twice in SPBS, before being scraped off the flask. A sample of cells was diluted 1:1 in 0.01% trypan blue to assess cell viability, and the unstained, live cells counted, to allow the

resuspension of the macrophages in the correct volume of SPBS for injection. Macrophages were obtained at various stages of maturity, namely 24 hours in culture, 2 days in culture, 4 days in culture and 1 week in culture, and were injected at different densities of 2×10^3 cells/ μl , 5×10^3 cells/ μl and 7×10^3 cells/ μl . Similarly, PBMCs were injected at differing concentrations of 10^5 cells/ μl , 5×10^5 cells/ μl , and 10^6 cells/ μl .

2.3.2. MVV and HIV tat peptide injections

Injections were made of 20 μg (9.6 nmol) of the MVV or 20 μg (9 nmol) HIV tat peptides. All the substances used for intracerebral injection were dissolved in sterile saline and administered in 1 μl . The MVV tat peptide and the ovalbumin peptide were synthesised by standard FMOC chemistry, desalted and purified, as previously described (Hayman *et al.* 1993). The HIV tat peptide was obtained from the MRC AIDS directed programme (Fig. 2.1). In the neuroprotection experiments, 20 μg (25 nmol) L-NAME (Research Biochemicals International, St. Albans, UK) was co-injected with the MVV tat peptide, as was 10 μg (6 nmol) αMSH (Sigma). MK801 (Research Biochemicals International) was administered intraperitoneally at a dose of 0.01 mmol/kg one hour before the injection, as was NBQX (Tocris Cookson, Bristol, UK) at a dose of 30 mg/kg. Control intracerebral injections were also made with 5 μg (56.8 nmol) ibotenic acid (Sigma), 0.9% sterile saline, 100 μg (61.9 nmol) ovalbumin peptide, 20 μg (25 nmol) L-NAME, and 10 μg (6 nmol) αMSH .

Peptide	Amino acid code
MVV tat peptide	(Ac)-MWKHKGAAVRRNCGRLC-(NH ₂)
HIV tat peptide	CFTTKALGISYGRKKRRQRRRPPQG SQTHQVSLSKQ
HIV(43-72) tat peptide	LGISYGRKKRRQRRRPPQGSQTHQV SLSKQ
HIV(48-72) tat peptide	GRKKRRQRRRPPQGSQTHQVSLSKQ
α MSH	N-(Ac)-SYSMEHFRWGKPV-(NH ₂)
Ovalbumin peptide	(Ac)-ISQAVHAAHAEINEAG (NH)

Fig. 2.1: Single letter amino acid code of the peptides used.

(Ac): Acetylated, (NH): Amidated.

2.3.3. Sterotaxic injections in *scid* mice.

Scid mice were obtained from the University of Edinburgh Medical Microbiology Transgenic Unit. All injections were performed under sterile conditions in a laminar flow hood. Male adult mice were anaesthetised by intraperitoneal injection of Hypnorm/Hypnovel (0.1-0.15 ml per mouse). Although no stereotaxic frame was available, anaesthetised mice showing no paw withdrawal reflexes were kept immobile through the use of a clamped tooth bar. The Hamilton syringe used to make the injections was attached to a micrometer supported by an arm fitting to a solid base. Injections of 1 μ l of the macrophage and PBMC cell solutions to the striatum were made approximately 1 mm laterally to Bregma. After the surgery, the mice were returned to their sterile isolators and left to recover for 3, 7 or 21 days. Following a lethal injection of pentobarbitone (Sagatal, Vet Drug Co., Falkirk, UK, 1 ml/kg), mice were transcardially perfused with 10 ml of heparinised saline followed by 50 ml of fixative containing 4% paraformaldehyde and 0.05% gluteraldehyde in 0.1 M Phosphate Buffer (PB) pH 7.4. Their brains were removed and placed in a 50/50 solution of fixative and 20% sucrose overnight at 4°C.

2.3.4. Stereotaxic injections in rats.

Male Sprague Dawley rats were anaesthetised using halothane and placed in a stereotaxic frame. The injection site was determined following the coordinates: 0.7 mm anterior, 2.5 mm lateral to Bregma and -5 mm ventral from the surface of the brain (Paxinos and Watson, 1986). Once the injection was made, the Hamilton syringe used to make the injections was left in place for 5 min in order to minimise needle reflux. At the appropriate time after the injection, the experimental animals were injected with a lethal dose of pentobarbitone (Sagatal, 1 ml/kg) and transcardially perfused, firstly with 50 ml of warm saline and then with 300 ml of a fixative solution containing 4% paraformaldehyde, 0.05% gluteraldehyde in 0.1 M PB pH 7.4. Their brains were dissected out and placed in a 50/50 mixture of 20% sucrose and fixative solution overnight at 4°C.

2.4. IMMUNOCYTOCHEMISTRY

2.4.1. Detection of viral expression in macrophages.

Indirect immunofluorescence against the viral antigen p25 was employed to determine the presence of MVV in infected macrophages. Cultured infected and uninfected macrophages were washed twice in SPBS, scraped off the culture flask into 1 ml of SPBS and cytopun onto slides. The resulting deposit of cells on the slides was then washed twice in HBSS, and fixed with a solution of ice-cold 80% acetone in 0.15 M sodium chloride (NaCl) for 2 min. The cells were allowed to air dry, before being blocked in PBS containing 0.01% Tween (Sigma) and 10% normal sheep serum (NSS) for 30 min, to minimise any non-specific binding of the antibody. This solution was then shaken off, the cells washed once in PBS containing 0.01% Tween and 2% NSS, and incubated for 1 hour in a humidified environment at room temperature with a monoclonal antibody against p25 (VPM 70, University of Edinburgh, UK), diluted 1:5000 in the wash solution. Following removal of the antibody, the cells were washed five times in the same wash solution as previously. The biotinylated secondary antibody sheep-anti-mouse, diluted 1:400 in the wash solution, was then applied for 1 hour at room temperature. The cells were then again washed in PBS containing 0.01% Tween. Avidin conjugated to the fluorescent marker Fluorescein isothiocyanate (FITC, Sigma), diluted 1:400 in PBS with 0.01% Tween and 2% NSS, was applied for 1 hour at room temperature to the preparation to visualise any positive cells. These were finally washed twice in PBS containing 0.01% Tween, mounted in PBS containing 15% glycerol and examined under ultraviolet microscopy.

2.4.2. Immunocytochemical and histological processing.

Coronal sections of brain 50 μm thick were cut on a freezing microtome. Free-floating sections were reacted histologically in multiwell plates. On sections obtained from rats injected with the HIV or MVV tat peptides, immunocytochemistry was routinely performed for Glial Fibrillary Acidic Protein (GFAP), to reveal astrocyte activation (McQueen *et al.* 1990); the neuron specific nuclear protein NeuN (A60), to assess neuronal damage (Mullen *et al.* 1992); and the type 3 complement receptor (OX42), to estimate microglial activation (Robinson *et al.* 1986). In addition, on

samples from animals perfused 7 days after injection of the MVV tat peptide, immunocytochemistry was performed for Parvalbumin (PV), a calcium binding protein co-localising to gamma amino butyric acid (GABA)-ergic interneurons (Kita *et al.* 1990), and Choline Acetyl Transferase (ChAT) to reveal acetylcholine-containing neurones (Bolam *et al.* 1984). The NADPH-Diaphorase histochemical method was also performed for the detection of NOS containing neurons (Dawson *et al.* 1991), by incubation with a solution containing 2.5 mg of Nitro Blue Tetrazolium (NBT, Sigma) and 25 mg NADPH (Sigma) in 25 ml PBS-TX pH8, for 45 min at 37°C. NOS reduces the NADPH resulting in the deposition of a blue formazan dye.

On sections recovered from *scid* mice, immunocytochemistry was performed for F4/80, an antibody against activated mouse microglial cells; GFAP, to detect astrocytes; Myelin Basic Protein (MBP), to estimate any possible myelin loss; neurofilament (NF) to reveal neurons; MAC3, an antibody against CD14, to detect injected macrophages; and p25 to detect MVV.

The antibodies to GFAP (Dako, Ely, UK), OX42 (Serotec, Oxford, UK), NeuN (a gift from W. Staines, University of Ottawa, Canada), PV (a gift from Prof. P. Emson, University of Cambridge, UK), F4/80 (Serotec), MBP (a gift from Prof. P. Brophy, University of Edinburgh, UK) and NF (Genosys, Cambridge, UK) were revealed using the ABC method (Vectastain ABC and ABC Elite kits, Vector, Peterborough, UK) with 3,3'-diaminobenzidine (Vector) as the chromogen. p25 immunocytochemistry was carried out in the same manner but in the presence of a 'mouse blocking' kit, (Histomouse, Vector), due to the use of a monoclonal antibody in mouse tissue. The antibody to ChAT neurons (Boehringer-Mannheim, Lewes, UK) was revealed using the PAP method. The MAC3 antibody (a gift from Dr. J. Hopkins, University of Edinburgh, UK) was biotinylated and therefore revealed by avidin peroxidase without the need for the addition of a secondary antibody. Sections were mounted on gelatin coated slides, dried, dehydrated through alcohols, except for the Diaphorase sections, cleared in xylene and mounted in DPX (BDH). Diaphorase sections were cleared in xylene and mounted in Permount (Sigma).

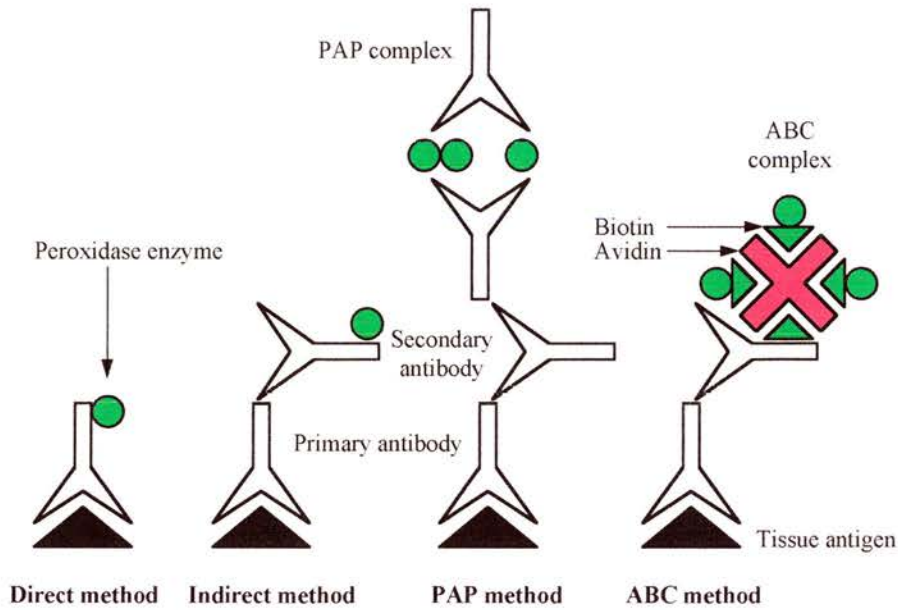


Fig. 2.2: Immunocytochemical detection of tissue antigens.

The primary antibody (IgG class) is raised in species x against the antigen A (x-anti-A). The secondary antibody is raised in species y against the IgG of species x (y-anti-x). The PAP complex is raised in species x against horse radish peroxidase (HRP), and attaches to the spare binding site of y-anti-x. The secondary antibody for the ABC reaction is biotinylated, and attaches the biotin of the ABC complex. The presence of the peroxidase enzyme is visualised with the chromogen DAB, resulting in a dark brown deposit.

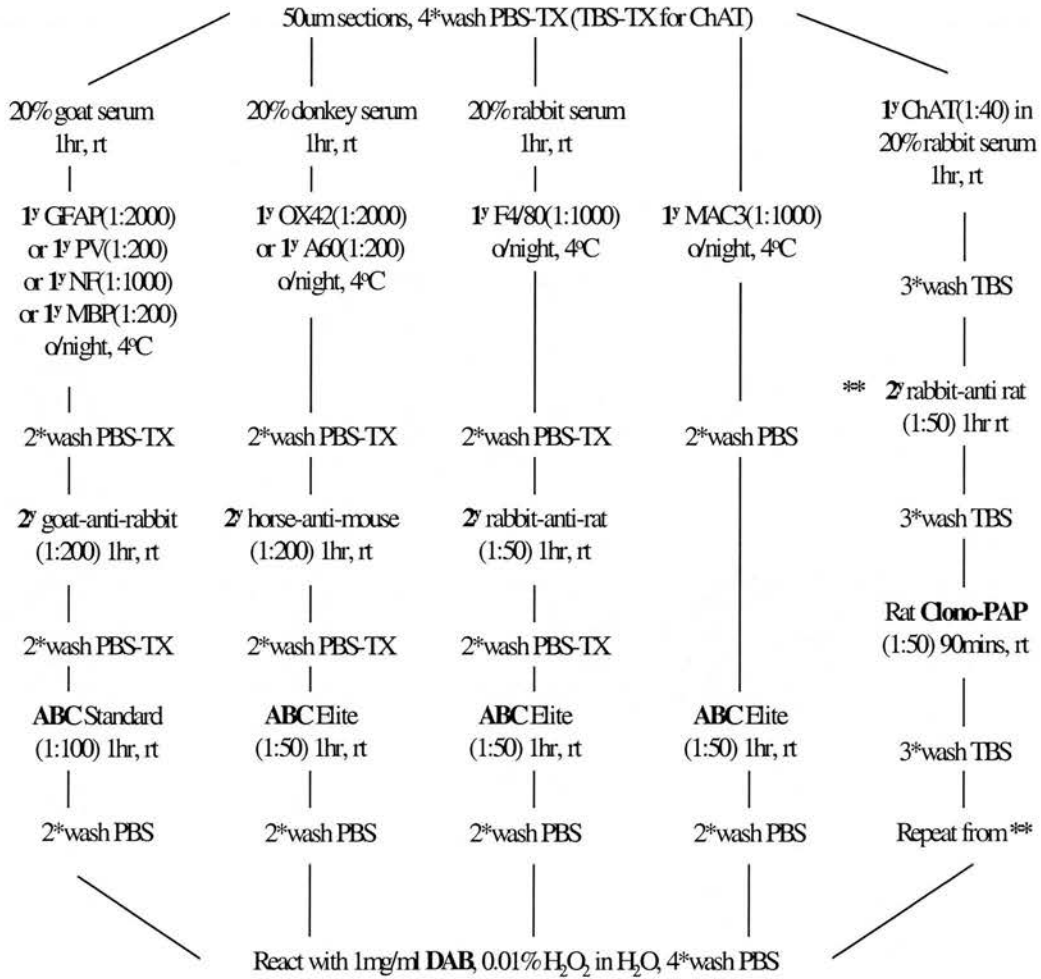


Fig. 2.3: Experimental protocol for immunocytochemistry on free-floating sections

1^y: Primary antibody. 2^y: Secondary antibody. PBS: 0.05% Phosphate Buffered Saline. PBS-TX: PBS containing 0.03% Triton-X-100. TBS: Tris Buffered Saline. rt: room temperature.

2.5. ELECTRON MICROSCOPY (EM)

EM necessitates the good ultrastructural preservation of tissue. Animals destined for EM analysis were therefore perfused with a fixative solution of 4% paraformaldehyde, 1% glutaraldehyde. Sections 70 μm thick were cut on a vibratome. Sections washed 6 times for 10 min in PB. Some sections were processed for A60 immunocytochemistry. These were freeze-thawed to enhance the penetration of reagents. Sections were first washed in sodium borohydride to reduce any background staining, and then in increasing concentrations (5%, 10%, and 20%) of DMSO in PB for 10 min. Most of the liquid was then removed, leaving just a covering layer, and the sections frozen on dry ice (approx. 40 sec) and thawed at 4°C. This was repeated 3 times. Sections were then washed and processed for A60 following the ABC protocol, except that the secondary antibody and ABC solutions were applied for longer (8-12 hours). After the DAB stage, sections were washed 6 \times 10 min in PB. Sections were then laid flat on slides and 1% osmium tetroxide (OsO_4) applied for 40 min. Four washes of 10 min in PB were followed by a rinse in water. Sections were then passed through alcohols, 50% ethyl alcohol for 5 min, 70% ethyl alcohol containing 1% uranyl acetate in the dark for 40 min, 95% ethyl alcohol for 15 min and 100% ethyl alcohol for 2 \times 10 min. Propylene oxide was then applied for 2 \times 10 min and the sections then immersed in resin for 12 hours and mounted. Thin sections of the areas of interest were cut and observed under EM (Totterdell *et al.* 1992). Photographs of representative areas of the lesion were taken and compared with control areas.

2.6. IMAGE ANALYSIS.

2.6.1. Degree of astocytosis and gliosis in *scid* mice.

The degree of astocytosis and gliosis in injected brains was measured through the use of a CCD camera attached to a microscope and an Apple Mac. The NIH Image 1.44 software was used to capture the image of a section. The area of GFAP and F4/80 immunoreactivity was first measured on the injected side, by density slicing the image, ensuring that all positively stained cells were identified. This was then repeated on the unlesioned side of the same section, without changing the parameters. The subtraction

of the unlesioned side area from the lesioned side area then provided the value of the area of overall GFAP and F4/80 immunoreactivity for that section. This procedure was applied to all sections showing a visible difference in staining between the injected and uninjected sides of each brain section. The total volume of GFAP and F4/80 immunoreactivity per brain was then calculated based on the number of sections showing a difference in staining combined with the numerical value of the total area of immunoreactivity.

2.6.2. MVV and HIV tat peptide induced lesions.

Sections were examined under the light microscope and camera lucida drawings were made of the lesioned area stained with NeuN or GFAP. These were then scanned into the NIH Image 1.57 software package on an Apple Macintosh computer, and quantified by measuring the area of the drawing. The volume of the lesion was then calculated by the multiplication of the lesioned area by the number and thickness of sections containing the lesion.

2.7. RCC TOXICITY ASSAYS.

2.7.1. Application of MVV tat peptide.

After 4 days in culture, the RCC culture medium was removed and either the MVV tat peptide (235 nM), the ovalbumin peptide (235 nM) or culture medium added to the cells. After 24 hours the cell cultures were then assayed for cell death, either by measuring Lactate Dehydrogenase release (LDH, see section 2.7.3), or the MTS assay, (see section 2.7.4).

2.7.2. Application of the macrophage culture supernatant.

Supernatant from uninfected and MVV infected 1 week old macrophage cell cultures was removed and applied to the cortical cell cultures before being left for 24 hours in cell culture conditions. Toxicity of the supernatant was measured using the MTS assay.

2.7.3. Lactate Dehydrogenase (LDH) assay

LDH is an enzyme released by cells upon lysis and is therefore an indicator of cell death. Released LDH from cell cultures catalyses the formation of NADH and pyruvate from NAD⁺ and lactate. Using a cytotoxicity assay (CytoTox 96™, Promega, Southampton, UK), the amount of NADH formation can be measured using a reaction which converts a tetrazolium salt into a red formazan dye. The amount of colour is proportionnal to the number of lysed cells.

Rat cortical cell cultures were incubated with the MVV tat peptide, ovalbumin or culture medium for 24 hours. To measure the spontaneous release of LDH (LDH₀), 50 µl of the cultured cells in each condition was transferred to 96 well plates. The cells were then washed once in HBSS, culture medium containing 0.1% Triton-X-100 added to lyse the cells which were then left for 15 min. The culture plate was then gently shaken and 50 µl of the lysed cell solution added to the remaining wells of the 96 well plates. This gives the value of maximum LDH release (LDH₁). Control wells were also set up, containing culture medium alone and culture medium with 0.1% Triton-X-100 but no cells. The substrate solution of the cytotoxicity assay (50 µl) was then added to each well and the plate left for 30 min wrapped in foil to minimise any light interference. The stop solution (50 µl) was then added and the absorbance of each well at 490 nm read, blanking on the control wells. The value of LDH release was then calculated following the formula:

$$\% \text{ LDH release} = (\text{LDH}_0) / (\text{LDH}_0 + \text{LDH}_1) \times 100$$

2.7.4. MTS assay

MTS (3-(4,5-dimethylthiazol-2-yl)-5-(3-carboxymethoxyphenyl)-2-(4-sulfophenyl)-2H-tetrazolium, inner salt) is a compound that is reduced by dehydrogenases found in metabolically active cells, into a formazan. The quantity of formazan can be measured by its absorbance at 490 nm and is directly proportionnal to the number of living cells in culture. The CellTiter 96™ AQueous Non-Radioactive Cell Proliferation Assay (Promega) was used to determine the number of viable cells in culture, based on the reduction of MTS in the presence of an electron coupling reagent

(phenazine methosulfate, PMS). After the RCC cultures had been incubated with the MVV tat peptide or macrophage supernatant, 100 μ l of the MTS/PMS (333 μ g/ml MTS, 25 μ M PMS) solution was added to the culture medium in each well, and left in culture conditions for 4 hours. A sample of culture (100 μ l) medium from each well was then transferred to wells of a 96 well plate and the absorbance read at 490 nm. The relative amount of cell death was then calculated based on the subtraction of cell viability measurement from 100%.

2.8. RT-PCR OF CYTOKINE mRNA FROM CULTURED MACROPHAGES.

2.8.1. Isolation and Reverse Transcription (RT) of mRNA from MVV infected and uninfected macrophages.

RT involves the making of DNA from an RNA template. RNA is extracted from cells or tissues of interest, to which is added a reverse transcription enzyme, in this case obtained from the Moloney Murine Leukemia Virus (MMLV), in the presence of dNTPs and either random hexamers or specific primers. The use of random hexamers would result in the transcription of all mRNA molecules present in the tissues or cells of interest, creating a cDNA library. The use of specific primers for genes of interest, on the other hand, results only in the transcription of mRNA for these genes. Random primers were used here to create cDNA from which specific genes were amplified in a subsequent polymerase chain reaction (PCR).

Macrophages were cultured for 1 week as previously described. mRNA from uninfected macrophages and macrophages infected with MVV overnight was extracted, with the aid of an RNeasy kit (QIAGEN, Crawley, UK). All collection tubes and eppendorfs were autoclaved to ensure that they were “clean”, i.e. RNase free. Cells were first washed in SPBS twice to remove any culture medium. They were then lysed in the culture vessel with 600 μ l of the RNeasy lysis buffer RLT containing 10 μ l/ml β -mercaptoethanol (Sigma). This buffer contains guanidinium isothiocyanate which denatures and inactivates any RNases to ensure isolation of intact RNA. The homogenate was then transferred to a clean eppendorf, to which was added 600 μ l of 70% ethanol. The presence of ethanol allows appropriate binding conditions for the adherence of RNA to the silica gel in the RNeasy spin column. This solution was then

applied onto an RNeasy spin column and microfuged for 15 sec at 10000 rpm. The flowthrough was discarded and 700 μ l of the wash buffer RW1 applied to the spin column and centrifuged as before. Once again, the flowthrough was discarded and 500 μ l of the wash buffer RPE was applied to the spin column and centrifuged. This was repeated but centrifuged for 2 min. The wash buffers are high in salt content and therefore wash away smaller RNA molecules, allowing the remaining RNA to be relatively richer in larger RNA molecules. At this stage, the mRNA was eluted with 20 μ l of Sigma water, spun for 1 min at 10000 rpm. The mRNA obtained (13 μ l) was then added to the RT mix, containing 5 μ l of 5 \times RT buffer (provided with the RT enzyme), 1.5 μ l (3 pM) random primers, 2.5 μ l (0.05 mM) dNTPs and 1 μ l (1 mM) DTT. This solution was then heated at 80°C for 3 min to melt the secondary structure of the RNA, and cooled on ice for 3 min to prevent reannealing. The RTase enzyme (Gibco) was then added (1 μ l), along with 1 μ l of RNasin (Gibco), an RNase inhibitor, and incubated at 45°C for 1 hour. The RTase enzyme was then heat inactivated at 95°C for 5 min, giving the solution of cDNA.

2.8.2. Polymerase Chain Reaction (PCR)

The PCR is an enzyme mediated amplification of DNA. Using primers for specific genes of interest, it allows the denaturation of DNA, followed by attachment of primers to binding sites and copying of the DNA. Forward and reverse primers are specifically designed to bind to certain sequences on opposite strands of the DNA molecule. A DNA polymerase can then generate a complimentary strand of DNA to that of the original DNA which results in a copy of the original DNA which can itself be duplicated. Here, primers for the cytokines TNF α , IL-1 β , IL-6 and TGF β were used. In order to be able to semi-quantitate the amount of DNA subsequently obtained, PCR for a house keeping gene, the alpha subunit of the (Na/K) ATPase pump, was also performed as its concentration is kept constant in cells.

The cDNA (1 μ l) obtained from the RNA of cultured uninfected and MVV infected macrophages was added to 48 μ l of the primer mix. For the cytokines this consisted of 1 μ l (2 pM) of both the forward and reverse primers (Genosys), 2 μ l (2

mM) of magnesium chloride (MgCl_2), 5 μl of the 10 \times PCR buffer (Gibco), 5 μl (0.1 mM) of dNTPs and 34 μl of sterile distilled water (SDW). For the ATPase reaction, the primer mix consisted of 32.5 μl of SDW, 1 μl (2 pM) of each of the primers, 5 μl (0.1 mM) of dNTPs, 5 μl of the 10 \times PCR buffer and 3.5 μl (3.5 mM) of MgCl_2 . The solution was then overlaid with 30 μl of mineral oil, to prevent evaporation. The eppendorf tube containing the mixture was then heated to 95°C to hot start the PCR reaction, and then maintained at 80°C while 1 μl (1 Unit) of the DNA polymerase Taq Pol (Boehringer Mannheim), obtained from the bacterium *Thermus aquaticus*, was added to the solution. The PCR was then started by heating the mixture to 95°C for 1 min to denature the DNA, cooling to 55°C for 2 min to allow specific binding of the primers to binding sites on the DNA, followed by heating to 72°C to permit the DNA polymerase to use the annealed primers to initiate copying of the DNA strand. PCRs for IL-6, IL-1, ATPase and $\text{TNF}\alpha$ were run over 33 cycles, and 31 cycles for $\text{TGF}\beta$. cDNA was also sampled from different cycle points. This was performed to enable the semi-quantification of cytokine cDNA against the equivalent cycle points of ATPase cDNA. For ATPase, IL-1, IL-6 and $\text{TNF}\alpha$, samples of cDNA were obtained at 27, 31 and 35 cycles. For $\text{TGF}\beta$, cDNA was obtained at 23, 27, 31 and 35 cycles. At the end of the cycles, the mixture was maintained at 72°C for 5 minutes to enable the formation of equal length chains of DNA. All reactions were run with a negative control consisting of the above mixtures without the addition of cDNA, to detect any cross contamination.

2.8.3. Agarose gel electrophoresis.

To visualise the DNA obtained by PCR, it was run on an agarose gel to which was applied an electrical current. A 1.6% solution of agarose (Sigma) was prepared in Tris-acetate buffer (TAE), composed of 0.04 M Tris-acetate and 0.001 M EDTA and heated to dissolve the agarose. Ethidium bromide (EtBr, 50 μg) was then added to the 100 ml agarose solution, which was then poured into a mould to cool and harden. The gel was run in TAE, and 10 μl of cDNA mixed with 5 μl of loading dye placed in the wells of the hardened gel. A voltage of 100 mV was then applied across the gel for at least 1 hour. The PCR bands fluoresced when viewed under ultraviolet light, due to the presence of EtBr.

2.8.4. Southern Blotting

In order to semi-quantify the amount of DNA obtained from RT-PCR, the agarose gel was probed with radioactive markers. The gel was first soaked in 0.4 N NaOH for 20 min on a rotary platform to denature the DNA. DNA was then transferred to a nylon membrane (GeneScreen Plus[®], NEN[™] Life Science Products, Hounslow, UK) from the gel via capillary action. The membrane was then rinsed twice in Standard Saline Citrate (SSC) buffer for 5 min each and dried at 80°C between two pieces of 3 MM paper (Whatman, Maidstone, UK) to fix the DNA onto the membrane. The membrane was then washed with 2 × Standard Salt Phosphate EDTA (SSPE) buffer and incubated with 10 ml of the hybridisation mix for 1 hour at 65°C. A further 5 ml of hybridisation mix containing 50 µl of herring sperm DNA, was added to block any non-specific attachment of the DNA probe to the membrane, the ³²P labelled probe was then added and the membrane incubated overnight at 65°C. The membrane was then washed twice in 2×SSPE for 5 min, and then twice in 2×SSPE containing 1% SDS at 65°C for 30 min each to remove any unbound radiolabelled probe. The membrane was finally washed in 0.1% SSPE for 3 min before being exposed to X-ray film (X-OMAT[™] ARC, Kodak) to obtain an autoradiograph.

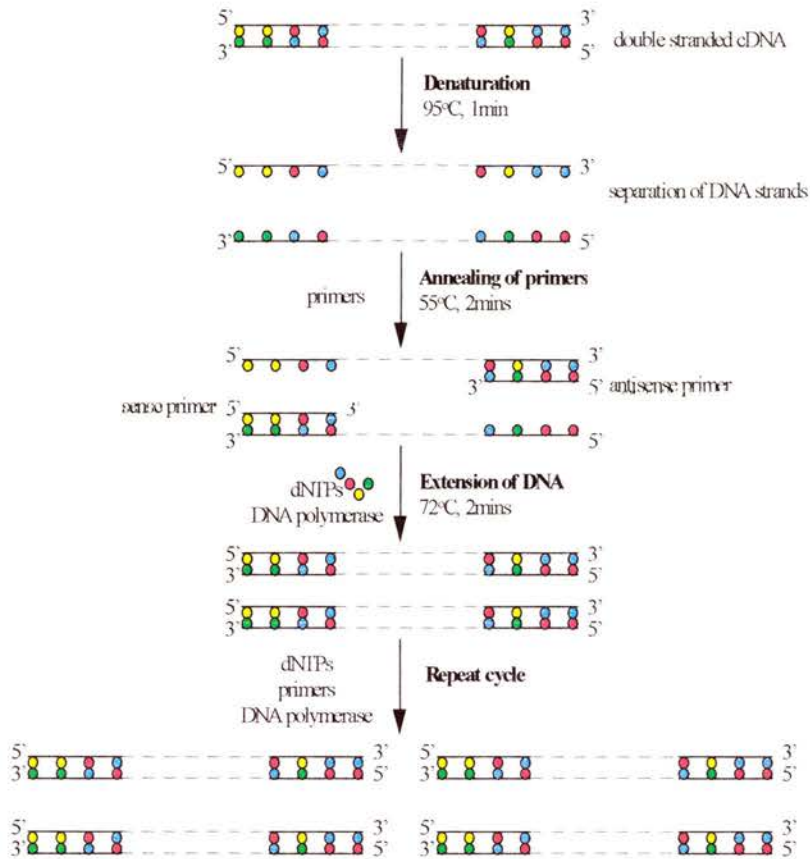


Fig. 2.4: The Polymerase Chain Reaction.

DNA is first denatured to separate the strands, which allows the primers to anneal to the specific 5' and 3' ends of the DNA. These then elongate through the action of a DNA polymerase to form 2 copies of the original strand of DNA. This cycle is repeated as many times as is necessary to obtain enough DNA to visualise on an agarose gel.

2.9 STATISTICAL ANALYSIS

Data was analysed using the SPSS statistical package. The comparison of data from more than two groups was analysed using a one-way ANOVA and post-hoc Bonferroni's and Duncan test. Statistical analysis of data obtained from two groups only was carried out using a one-way ANOVA, if experimental numbers were high, or a Student's t-test, if experimental numbers were low.

CHAPTER 3:

A MODEL OF MVV ENCEPHALOPATHY IN *SCID* MICE

3.1. INTRODUCTION

MVV infection of sheep shows the invasion of virally infected macrophages into the CNS, accompanied by neuropathological changes manifest as demyelination, astrogliosis and liquefactive necrosis. Some investigators attribute the mechanisms of this neurodegeneration to the action of viral proteins on neuronal cell types, or to the release of diffusible mediators such as cytokines from infected cells. Other investigators propose that circulating immune cells may gain access to the CNS in MVV infection and be responsible for the observed brain damage. Since the progression of disease in sheep is slow, a small animal model of MVV infection would be useful to the understanding of the mechanisms involved in lentivirus mediated neurodegeneration. In pursuit of this aim, *scid* mice were used to investigate the role of macrophages in the development of neurodegeneration and to establish a preliminary putative model of MVV encephalopathy. These mice are immunodeficient in that they lack T and B cells. They can therefore allow the experimental isolation of immune responses, and permit the investigation into how a pathology relates to factors other than cell- or antibody-mediated immune mechanisms. Macrophages and PBMCs were infected with MVV *in vitro* and injected into the CNS of *scid* mice. The effects of free virus injection were also evaluated. Neuropathological changes were subsequently revealed immunocytochemically, to detect any changes in the normal organisation of astrocytes, microglia and neurons. In this thesis, significant increases in GFAP and F4/80 staining will be referred to as inflammation.

Several pro-inflammatory cytokines, in particular TNF α , IL-1 β , IL-6 as well as the anti-inflammatory cytokine TGF β have been implicated in the pathological processes of HIV infection, as well as other neurological diseases. *In vitro* and *in vivo*, TNF α , IL-1 β and IL-6 have been shown to cause astroglial and microglial proliferation, and can also cause neuronal death (Campbell *et al.*, 1993; Hertz *et al.*, 1990; Barna *et al.*, 1990; Gelbard *et al.*, 1993). The actions of TGF β appear to be more neurotrophic (Chao *et al.*, 1995), although the actions of this cytokine may be detrimental at high concentrations. The profile of TNF α , IL-1 β , IL-6 and TGF β mRNA synthesis was investigated in uninfected ovine macrophages and macrophages infected with MVV *in vitro*, through the use of RT-PCR. This was carried out in order to evaluate any

upregulation of these cytokines caused by MVV infection, as a measure of virus-induced macrophage activation.

3. 2. EXPERIMENTAL DESIGN.

Scid mice were injected intracerebrally with free virus, live macrophage cell suspensions, killed macrophage preparations or PBMCs. Macrophages were obtained from healthy sheep and cultured for 1, 2, 4 or 7 days prior to infection and injection. Macrophages were infected with MVV supernatant overnight *in vitro*. Killed macrophages were similarly prepared, but underwent 3 cycles of freeze-thawing to rupture their membranes. PBMCs were obtained from healthy sheep and infected *in vitro* on the same day of collection and injection, or directly from diseased sheep and supplemented with virus *in vitro*. Uninfected and MVV infected cells were stereotactically injected, at different densities, into the left striatum of *scid* mice, which were then left to recover for 3 days, 7 days or 3 weeks. Microglial and astrocyte activation, as well as the presence of neurons and myelin, were revealed by immunocytochemistry on free-floating sections. The degree of microglial and astrocyte activation, and therefore inflammation, in the brains of *scid* mice was quantified by image analysis. The effects of free virus on *scid* mouse brain were similarly detected, and the presence of MVV within the brains of injected mice was assessed using an antibody against the viral protein p25.

The stereotaxic injection method used in these experiments was difficult to perfect due to the small size of the experimental mice which, due to their immunosuppression, do not routinely achieve normal wild type proportions, and because of the need for all procedures to be carried out in a sterile environment. Therefore, some of the experimental numbers were small and the results subject to variability.

For RT-PCR analysis, mRNA was extracted from cultures of 1 day, 2 day, 4 day and 1 week old uninfected and MVV infected macrophages *in vitro*, from which cytokine cDNA was amplified by RT-PCR. Samples of cDNA were loaded onto an agarose gel containing EtBr, and a current of 100mV applied across the gel. Fluorescent bands corresponding to the appropriate size of cytokine DNA were visualised under ultraviolet light. The gel obtained from the migration of cDNA obtained from 1 week old macrophages was transferred onto a nitrocellulose membrane and probed with

radiolabeled markers, since it showed differences in the levels of pro-inflammatory cytokines between uninfected and MVV infected macrophages. This Southern blot was then semi-quantified against levels of the housekeeping gene ATPase. This was achieved by density measurements of autoradiographs to determine the level of ATPase in uninfected and MVV infected macrophages, reflecting differences in the amount of RNA obtained from each population of macrophages. Levels of cytokine expression were then normalised against each background level.

3.3. RESULTS.

3.3.1. Viral infection of macrophages.

3.3.1.1. p25 expression in vitro

Measurement of the TCID₅₀ for the MVV virus showed that 50% of sheep chondrocytes in culture developed syncytia when the virus supernatant solution was diluted 1:4096. Therefore the TCID₅₀ approximated 2.05×10^5 viral particles per ml. The number of macrophages in each culture flask varied between 5×10^4 and 15×10^4 cells, therefore the addition of 2 ml of virus supernatant solution was theoretically able to infect all the cells present. Productive infection was demonstrated by the immunocytochemical detection of the p25 protein in macrophages cytopun onto slides (Fig. 3.1). Infected cell populations displayed positive immunofluorescence for the protein but uninfected macrophages did not.

3.3.1.2. p25 expression in vivo

In animals injected with free virus, TCID₅₀ measurements revealed there to be 8.388×10^8 viral particles per ml. Since 1 μ l was injected, each animal received approximately 8.4×10^5 viral particles. Results of p25 staining of *scid* mouse brain sections surrounding the injection site did not conclusively show the presence of viral particles in *scid* mouse striatum. This may be due to difficult detection methods of the viral p25, as the antibody used was a mouse monoclonal used in mouse tissue, or to the clearance of virus from brain parenchyma. However, since neuronal nuclei were

detectable using another mouse monoclonal antibody (NeuN), it seems unlikely that the only reason for not detecting p25 was technical difficulties with the method used.

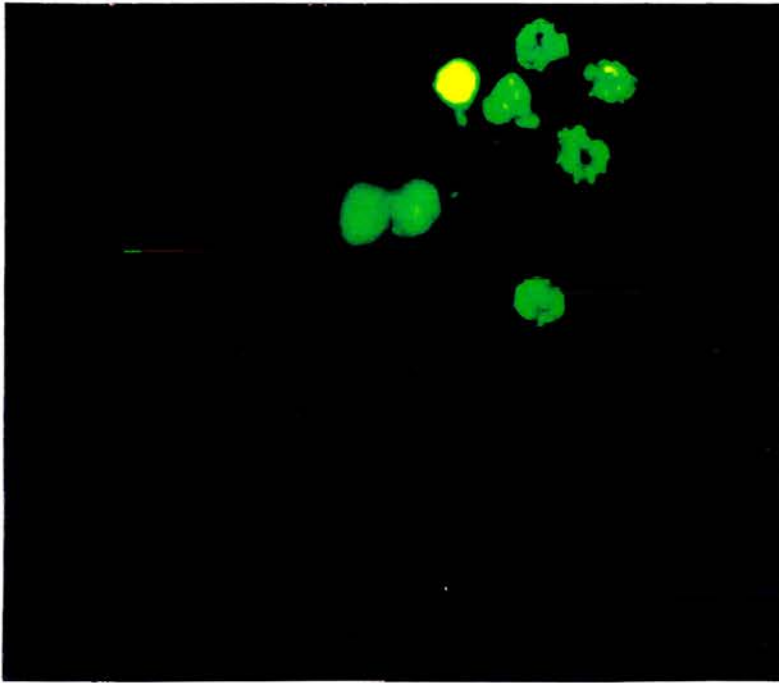


Fig. 3.1: p25 immunoreactivity in MVV infected macrophages *in vitro*.

Macrophages infected with MVV *in vitro* displayed positive immunofluorescence for the viral protein p25, but uninfected macrophages did not.

3.3.2. Degree of inflammation in injected *scid* mice brains.

3.3.2.1. Effects of free virus

The injection of free MVV into *scid* mouse striatum caused some inflammation one week post-operatively as revealed by immunocytochemistry for GFAP and F4/80. GFAP staining showed that MVV caused greater astrocytosis than control medium, although this was not statistically significant as revealed by a Student's t-test ($p=0.1$, Fig. 3.2). F4/80 immunocytochemistry showed the presence of activated microglial cells in *scid* mouse striatum injected with MVV, but the level of these was not significantly different to that of *scid* striata injected with control medium only (Student's t-test, $p=0.3$, Fig. 3.2). Thus the inflammatory effects of free virus are not definite. Although some inflammation is suspected by the apparent increase in GFAP staining, this is not statistically significant.

Furthermore, the lesion volumes incurred by the injection of free virus are low when compared to lesions caused by the injection of live macrophages (Figs. 3.6-3.9). This suggests that free virus alone does not have as severe effects on *scid* brain parenchyma as the injection of macrophages infected with MVV.

The lack of staining of *scid* striata with an antibody directed against p25 suggests that minimal amounts of virus remain in striatum after injection. This may be due to clearance of the virus from the brain. This result concurs with previous reports demonstrating the lack of notable effects of free lentivirus on nerve cells and suggests the need for cellularly released inflammatory mediators in lentiviral neurodegeneration.

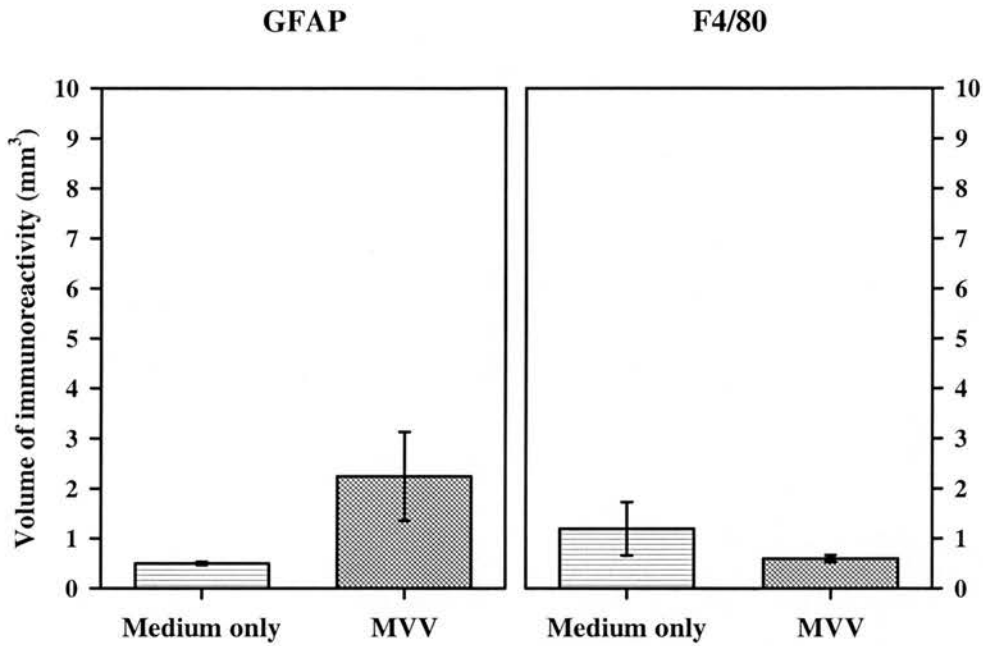


Fig. 3.2: Effect of MVV injection on GFAP and F4/80 staining in *scid* striatum

Animals were sacrificed one week post-operatively. The injection of MVV alone ($n=3$) to *scid* mouse striatum appeared to cause greater astrocytosis than the injection of control medium ($n=3$), although this was not statistically significant (Student's t-test, $p=0.1$). The volume of F4/80 immunoreactivity was also not significantly different between the injection of MVV alone ($n=3$) and control medium ($n=3$, Student's t-test, $p=0.3$). Results: Mean \pm SEM.

3.3.2.2. Survival of injected macrophages

Immunocytochemistry for MAC3 (CD14) showed that the macrophages injected intracerebrally into *scid* mice were still present in the striatum of these mice one week post-operatively (Fig. 3.3). Most were confined to the area surrounding the injection site, but some were occasionally found to have migrated a small distance away from the location of the syringe. In some animals where the injection strayed into the lateral ventricle, MAC3 positive cells were found at the border of the injected ventricle and striatum, but some were also found in the contralateral ventricle and striatum. These animals were not included in the image analysis for GFAP and F4/80 staining because macrophages were present on both sides of the brain.

Immunocytochemistry for p25 in the brains of *scid* mice injected MVV infected macrophages did not conclusively reveal positive staining. The antibody used has been shown to work on cells infected with MVV and cytopun onto slides, but problems of detection may have prevented the detection of p25 in mouse sections. The antibody used, the only antibody available, was a monoclonal and was used in mouse tissue. Detection of p25 in *scid* mice striata in animals injected with MVV infected macrophages, using a kit specifically designed to detect monoclonal antibodies in mouse tissue, did not reveal the presence of this marker. Technical difficulties alone cannot serve to explain the lack of p25 staining, as the above method successfully marked a monoclonal neuronal antibody (NeuN).

The absence of p25 staining may reflect a disappearance of MVV from *scid* mouse brain, but may also reflect other factors such as virus latency *in vivo*. Previous experiments have shown that, in other tissues, MVV becomes down-regulated once *in vivo*. Indeed, the injection of MVV to the joints of sheep results in the appropriate pathology. However, MVV becomes undetectable shortly following injection. Furthermore, if p25 were residing only in the injected macrophages then the antibody may not have been able to sufficiently penetrate the cells. The localisation, however, of ovine macrophage markers within the CNS of *scid* striatum would suggest the continued presence of injected macrophages.

3.3.2.3. Acute inflammation caused by live macrophages

Immunocytochemical detection of activated astrocytes and microglia seemed to reveal a greater degree of astrogliosis and microgliosis in the striata of *scid* mice injected with MVV infected macrophages as compared to those receiving uninfected macrophages, when observed one week post-operatively. This was evident as greater numbers of cells displaying GFAP and F4/80 immunoreactivity *in vivo* (Figs. 3.4 and 3.5). Figure 3.4 shows greater levels of GFAP immunoreactivity in *scid* mouse striatum caused by the injection of MVV infected macrophages as compared to uninfected macrophages. Similarly, Figure 3.5 shows greater F4/80 immunoreactivity in *scid* mouse striatum receiving MVV infected macrophages, as compared to the striatum receiving uninfected macrophages. Furthermore, both control and MVV infected macrophages appeared to cause greater GFAP staining than the injection of free virus alone. This suggests a greater detrimental action of macrophage products on brain parenchyma as compared to MVV alone and may point to the need for cellularly released agents in causing neurodegeneration.

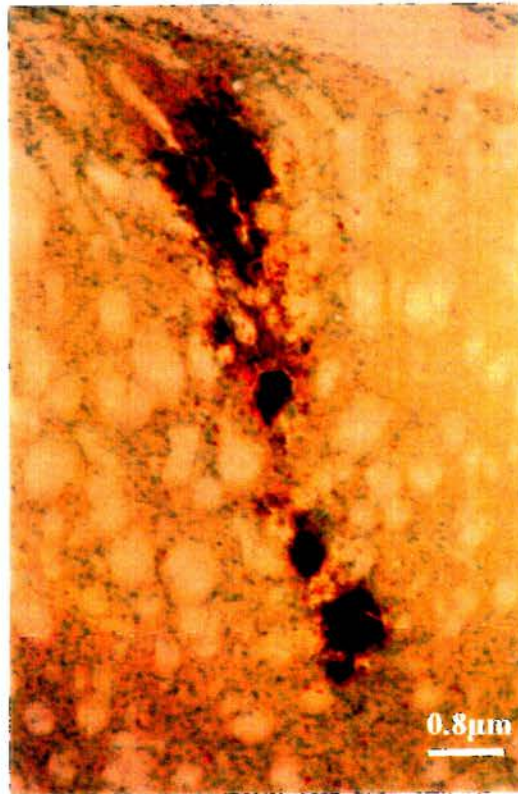


Fig. 3.3: Detection of injected CD14 positive MØ in *scid* striatum

The injected macrophages, 5×10^3 cells/ μl , were visible in the striatum one week post-operatively. Most macrophages remained close to the site of injection although some were found to migrate short distances within the striatum, away from the needle tract.

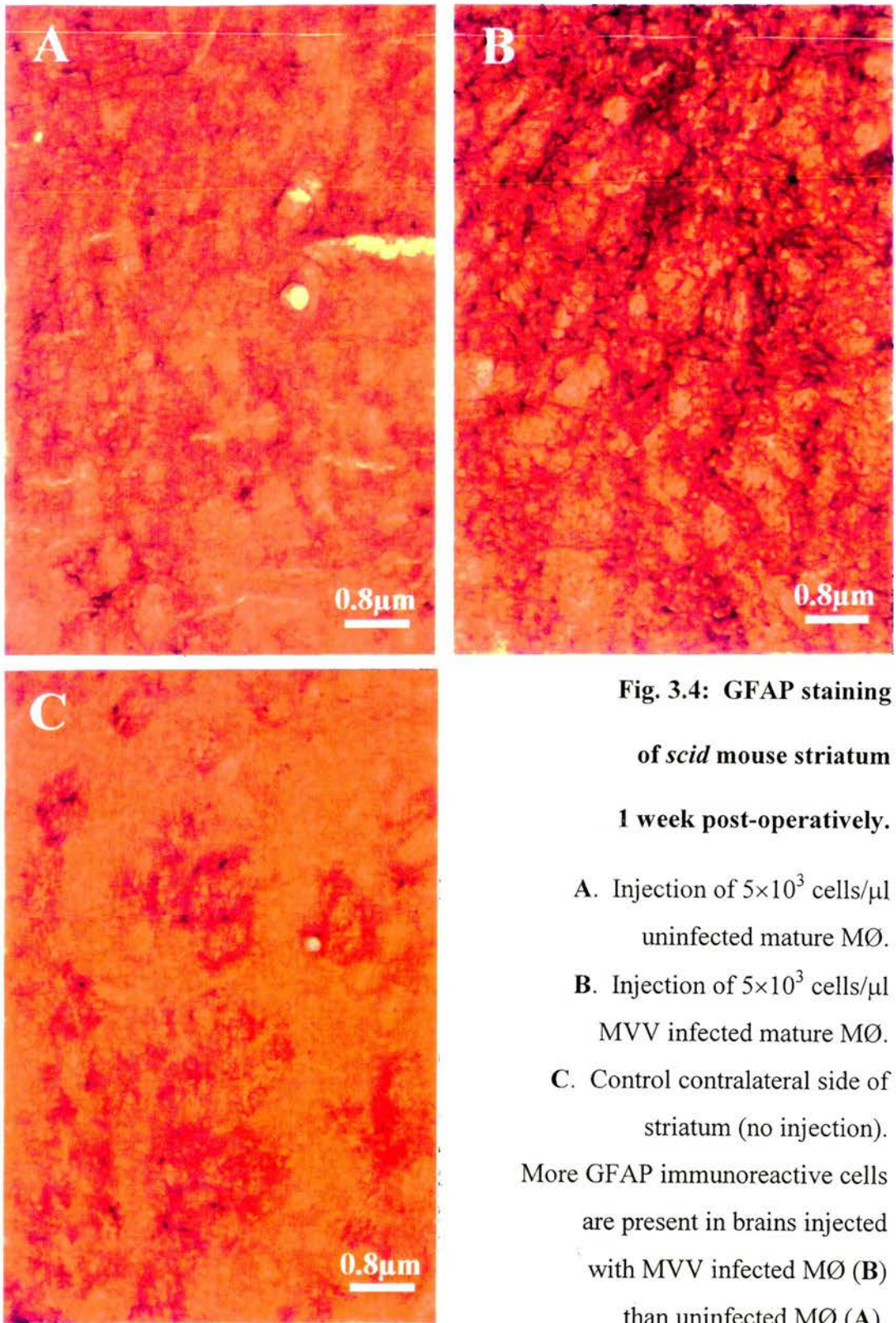


Fig. 3.4: GFAP staining of *scid* mouse striatum 1 week post-operatively.

- A. Injection of 5×10^3 cells/ μ l uninfected mature MØ.
 - B. Injection of 5×10^3 cells/ μ l MVV infected mature MØ.
 - C. Control contralateral side of striatum (no injection).
- More GFAP immunoreactive cells are present in brains injected with MVV infected MØ (B) than uninfected MØ (A).

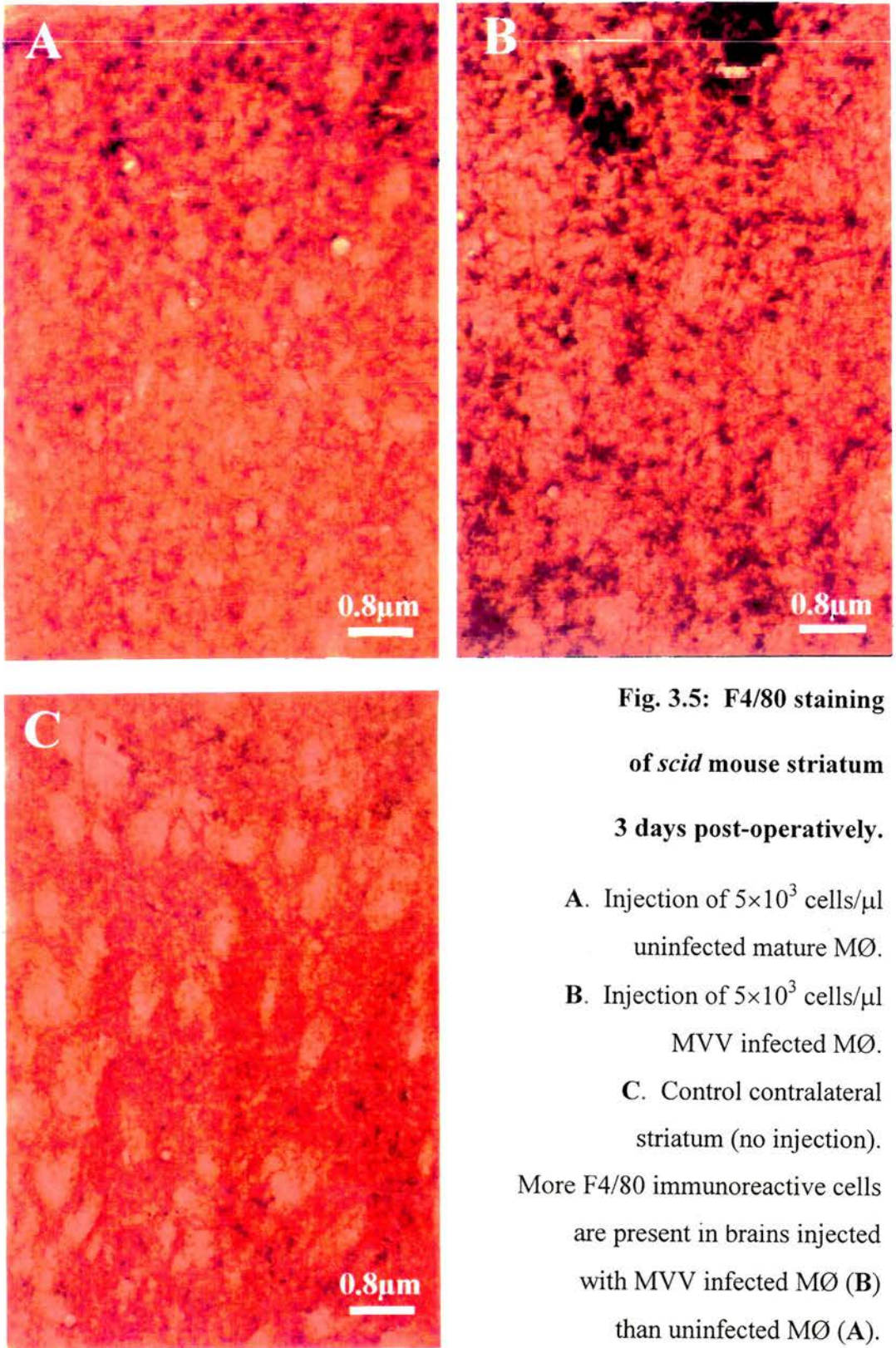


Fig. 3.5: F4/80 staining of *scid* mouse striatum 3 days post-operatively.

- A.** Injection of 5×10^3 cells/ μl uninfected mature M \emptyset .
- B.** Injection of 5×10^3 cells/ μl MVV infected M \emptyset .
- C.** Control contralateral striatum (no injection).

More F4/80 immunoreactive cells are present in brains injected with MVV infected M \emptyset (B) than uninfected M \emptyset (A).

These observations were confirmed by image analysis determining the area occupied by activated astrocytes and microglia. Firstly, the inflammation caused by live 1 day old MVV infected macrophages appeared to be dose dependant. Therefore, the increase in GFAP immunoreactivity rose with the number of cells injected in *scid* mouse striata (Fig. 3.6). Cells injected at 2×10^3 and 5×10^3 cells/ μ l caused less inflammation than cells injected at 7×10^3 cells/ μ l (one-way ANOVA, $p < 0.01$, post-hoc Duncan test $p < 0.05$). This result suggests that diffusible mediators released from macrophages may be causing neurodegeneration. Since the injection of 5×10^3 uninfected macrophages/ μ l caused the least background level of astrocytosis with the greatest amount of cells, this number of cells per preparation was used in all future experiments.

Secondly, the maturity of the macrophage cell preparation was determined as being important in the degree of astrocytosis and microgliosis caused in *scid* mouse striatum one week post-operatively. MVV infected macrophages maintained *in vitro* for 1, 2, or 4 days, and injected into *scid* mice striata, did not cause significant differences in GFAP expression, when compared to the administration of their uninfected counterparts (Fig. 3.7). However, when macrophages were cultured for 1 week and injected into *scid* mouse striata, the inflammation measured by GFAP staining was greater with MVV infected macrophages than with uninfected macrophages (Fig. 3.7). A single factor ANOVA comparing the mean GFAP lesion area in mice receiving macrophages at different maturities shows a significant effect of maturity on lesion volume ($p < 0.001$). Post-hoc analysis indicates that the group receiving MVV infected mature macrophages was significantly different to all the other groups, including those receiving uninfected mature macrophages (Duncan test, $p < 0.05$). Similarly, when F4/80 staining is compared after injection of 1 week old macrophages and 1 week macrophages infected with MVV, the MVV infected cells cause significantly more staining (Fig. 3.8, Student's t-test, $p < 0.05$). Thus, the maturity of injected macrophages appears to be important in causing neurodegeneration in this model, and probably reflects changes in cellular machinery present at different stages of development of the macrophage. This may reflect the ability of the macrophage to sustain viral replication and/or the capability to secrete inflammatory mediators or viral products. Although inflammation was readily observed and confirmed by semi-quantification of the lesioned

areas, no loss of neuronal or myelin markers was observed acutely after the administration of MVV infected macrophages to *scid* mouse striata.

As described in the methods section, macrophages were removed from the culture flasks by gentle scraping. When these cells were counted using trypan blue exclusion, most (approximately 90%) of the cells still appeared live. However, in an effort to ensure the maximal survival of macrophages injected into *scid* striata, experiments were also carried out removing macrophages from the culture flask using warm versene. Results show that similar significant increases in GFAP and F4/80 induction were observed with the injection of MVV infected macrophages as opposed to the injection of uninfected macrophages, one week post-operatively (one-way ANOVA, $p < 0.05$, Fig. 3.9).

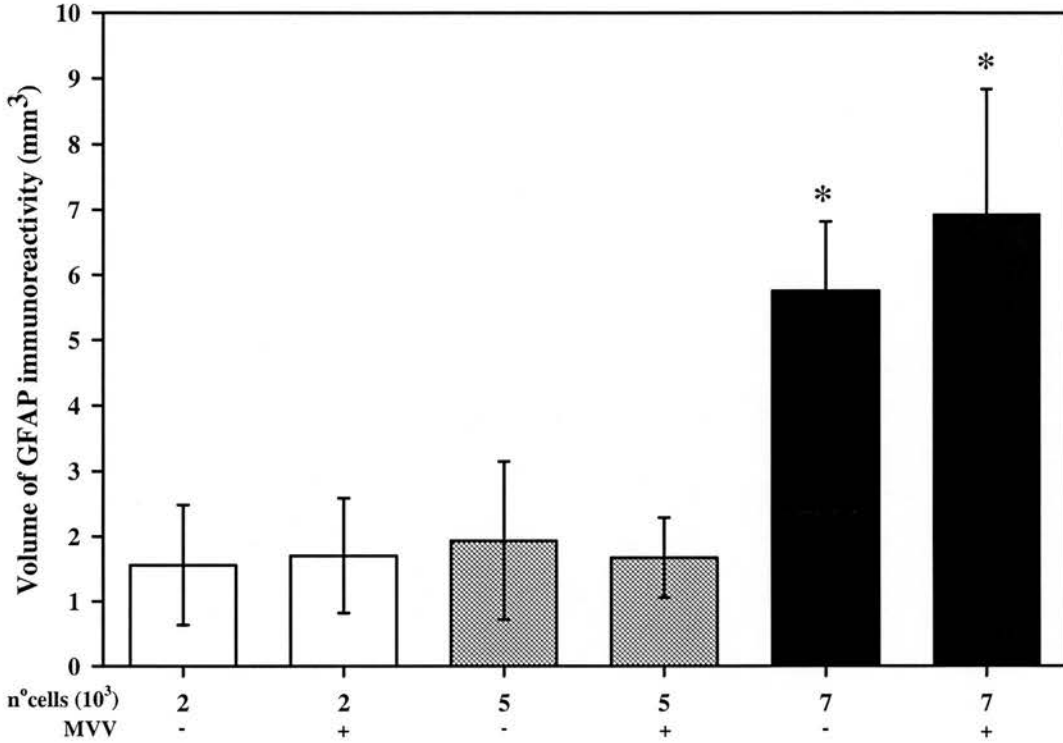


Fig. 3.6: Effect of MØ number on GFAP staining of *scid* striatum

1 day old MØ were injected intracerebrally at different densities: 2×10^3 cells/ μ l (n=3 MVV-, n=3 MVV+), 5×10^3 cells/ μ l (n=3 MVV-, n=5 MVV+) and 7×10^3 cells/ μ l (n=3 MVV-, n=3 MVV+). All mice were perfused one week post-operatively. MVV-: uninfected MØ, MVV+: MØ infected with MVV *in vitro* overnight prior to injection. A single factor ANOVA shows GFAP immunoreactivity to be greater in animals receiving uninfected and MVV infected macrophages at 7×10^3 cells/ μ l ($p < 0.01$ and post-hoc Duncan test $*p < 0.05$), than in animals receiving macrophages in lesser numbers. Results: Mean \pm SEM.

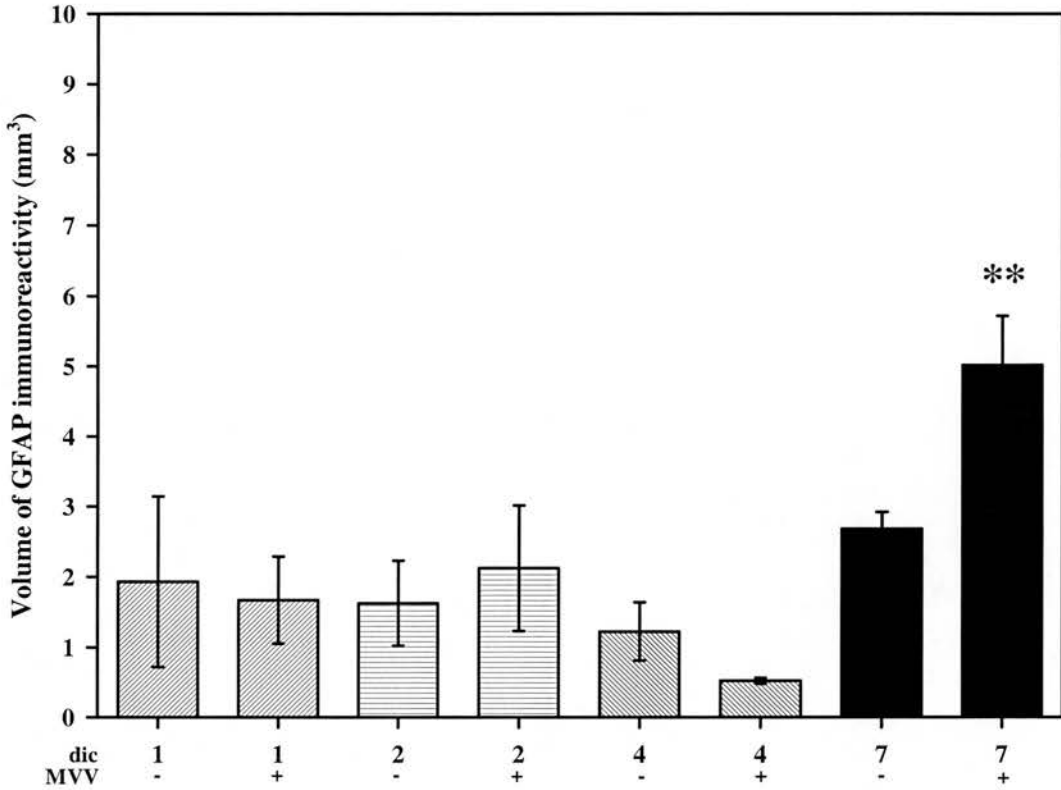


Fig. 3.7: Effect of MØ maturity on GFAP staining in *scid* striatum

MØ were injected after 1 day in culture (dic, n=3 MVV-, n=5 MVV+), 2 dic (n=3 MVV-, n=2, MVV+), 4 dic (n=3 MVV-, n=2 MVV+) or 7 dic (n=11 MVV- and MVV+) at densities of 5×10^3 cells/ μ l. All mice were perfused one week post-operatively. MVV-: uninfected MØ, MVV+: MØ infected with MVV *in vitro* overnight prior to injection. None of the injections of immature macrophages caused any significant differences between uninfected and MVV infected groups, however, mature, 7 dic, MØ infected with MVV caused greater astrocytosis than all the other groups (one-way ANOVA, $p < 0.001$, post-hoc Duncan test, $**p < 0.05$). Results: Mean \pm SEM.

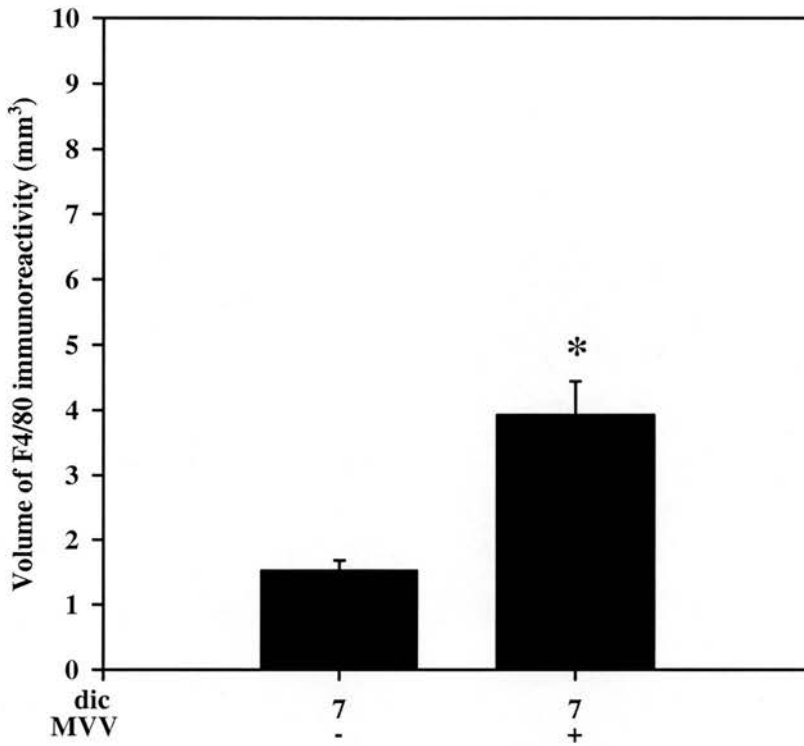


Fig. 3.8: Effect of live MØ on F4/80 staining in *scid* striatum.

Mice were perfused 3 days post-operatively. MVV-: uninfected MØ (n=2), MVV+: MØ infected with MVV *in vitro* overnight prior to injection (n=3). The volume of F4/80 immunoreactivity was significantly greater in mice injected with MVV infected MØ (Student's t-test, * $p < 0.05$). Results: Mean \pm SEM.

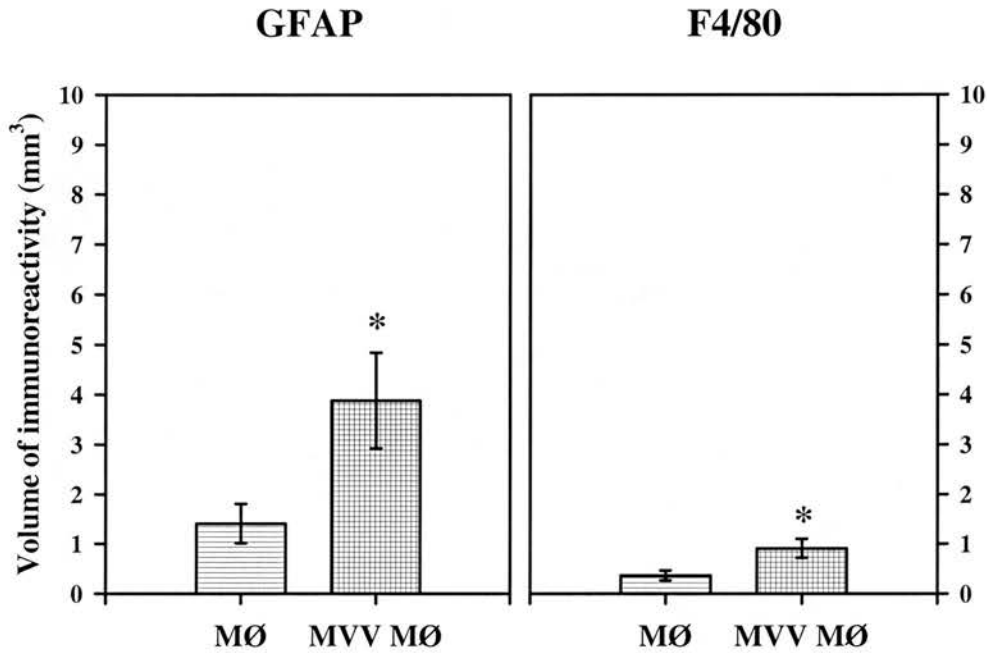


Fig. 3.9: Effects of live MØ on GFAP and F4/80 induction in *scid* striatum

Mice were perfused one week post-operatively. Macrophages were grown for 1 week *in vitro*, infected with MVV overnight and removed from the tissue culture flask with warm versene. MVV infected macrophages (MVV MO, n=5) caused significantly more GFAP and F4/80 induction than uninfected macrophages (MO, n=5, one-way ANOVA, * $p < 0.05$). Results: Mean \pm SEM.

3.3.2.4. Acute inflammation caused by killed macrophages

Since the administration of live MVV infected macrophages to the striatum of *scid* mice caused greater inflammation than the administration of uninfected live macrophages, experiments were also carried out to evaluate the inflammation caused by killed macrophages. These were prepared in exactly the same manner, but received three freeze-thaw cycles immediately prior to injection, thus disrupting membrane integrity.

Results show that inflammation was greater in the striata of mice receiving MVV infected killed macrophages as opposed to those receiving uninfected killed macrophages (Fig. 3.10). The increase in F4/80 immunoreactivity was statistically significant (Student's t-test, $p < 0.01$), although the apparent parallel increase in GFAP immunoreactivity did not reach statistical significance (Student's t-test, $p = 0.2$). However, the GFAP lesion volumes observed with killed MVV infected macrophages are very low (approximately $0.5\text{-}1\text{mm}^3$) compared to lesion volumes observed with live MVV infected macrophages ($4\text{-}8\text{mm}^3$). These levels of inflammation are minimal compared to the effects of live macrophages. Therefore, the results obtained with live macrophages cannot be explained by their death once injected into *scid* striata.

Since the membrane integrity of the injected macrophages was disturbed, the effects of the injection of killed macrophages cannot be attributed to released diffusible mediators. However, the disruption of macrophage membranes would necessarily involve the leakage of many intracellular molecules into the injection medium. These may include diverse agents such as proteases, possibly upregulated by MVV infection, which may cause inflammation in brain parenchyma. The effects on brain tissue of many intracellular components of macrophages are not documented, therefore it is not possible to attribute any of the effects of killed macrophages on *scid* striata to particular mediators. It is, however, plausible to comment that there may exist a mediator, upregulated in live macrophages to cause acute inflammation in *scid* mouse brain, which may also be present in the injection of killed macrophages, to cause similar inflammation.

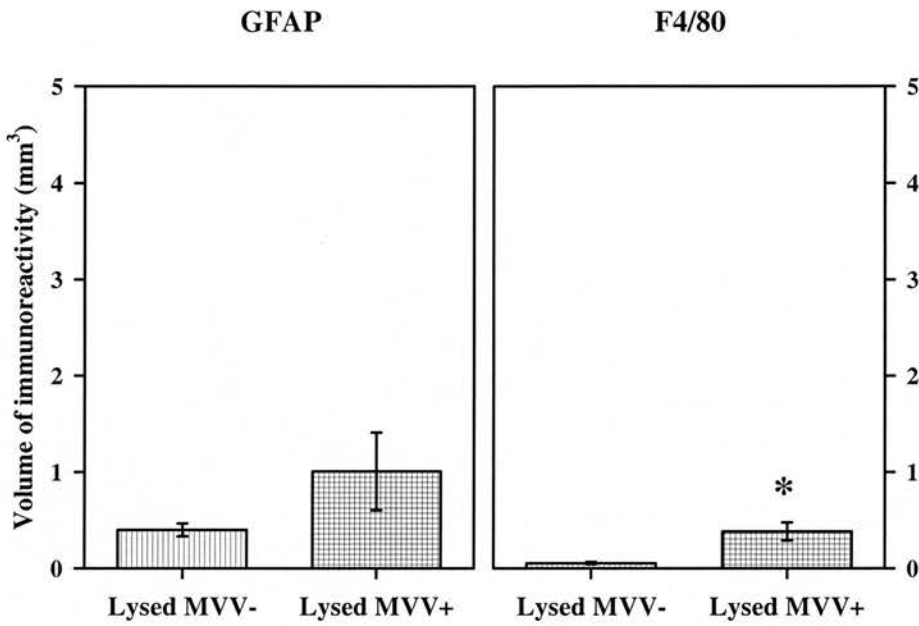


Fig. 3.10: Effects of killed MØ on GFAP and F4/80 induction in *scid* striatum

Animals were sacrificed 1 week post-operatively. The injection of lysed MVV infected MØ (Lysed MVV-, n=6) caused greater astrocytosis than the injection of control uninfected lysed MØ (Lysed MVV+, n=6), although this was not statistically significant (Student's t-test, $p=0.2$). However, the volume of F4/80 immunoreactivity was significantly greater in the same mice injected with lysed MVV infected MØ (n=6) than in those injected with control uninfected lysed MØ (n=6, Student's t-test, $*p<0.01$). Results: Mean \pm SEM.

3.3.2.5. Chronic inflammation caused by live macrophages

Since the intracerebral injection of live macrophages in *scid* mice caused greater acute inflammation when these were infected with MVV, the longer term effects of live macrophages on *scid* mice parenchyma were also investigated. Cells suspensions of live macrophages were prepared and injected in exactly the same manner as previously, but experimental animals were left to recover for 21 days post-operatively. *Scid* brain tissue was immunocytochemically processed as before.

The results show that the inflammation persists over 3 weeks (Fig. 3.11). Indeed, increases in GFAP immunoreactivity appear greater in mice injected with MVV infected live macrophages than with uninfected live macrophages, although this failed to reach statistical significance (Student's t-test, $p=0.6$). The increase in F4/80 immunoreactivity in these mice, however, was much more striking. The near fourfold increase of F4/80 staining following injection of live, infected macrophages as compared to live uninfected macrophages was highly statistically significant (Student's t-test, $p<0.001$).

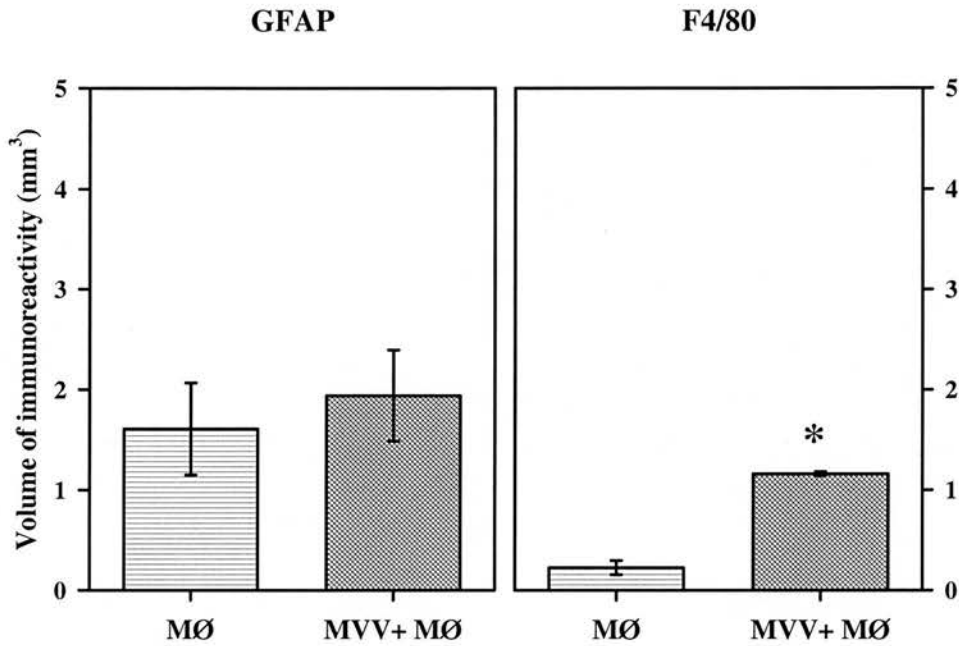


Fig. 3.11: Chronic effects of MØ on GFAP and F4/80 staining of scid striatum

Mice were injected intracerebrally with MØ cultured for 7 days, uninfected (MØ, n=8) or infected with MVV (MVV+ MØ, n=8). Animals were perfused 3 weeks post-operatively. Astrocytosis appeared greater in mice injected with MVV infected MØ than in those injected with uninfected MØ, although this was not statistically significant (Student's t-test, $p=0.6$). The volume of F4/80 immunoreactivity, however, was significantly greater in the same mice injected with MVV infected macrophages as compared to those receiving uninfected macrophages (Student's t-test, $*p<0.001$). Results: Mean \pm SEM.

3.3.2.6. Intracerebral injection of PBMCs

In the naturally occurring disease, lymphocytes and T cells, in addition to macrophages, are found to invade the brains of MVV infected sheep and indeed, many researchers attribute the neurodegeneration involved in MVV to the detrimental actions of these cells. In an effort to investigate the role that these cells may play in causing neuroinflammation, PBMCs were harvested from healthy sheep and supplemented with virus, or harvested from productively infected sheep and supplemented with virus. These cells were then injected in the same manner as in previous experiments and the levels of astrocytosis and microgliosis evaluated in identical fashion.

Results show, surprisingly, that no variations in GFAP expression were observed between the groups of mice receiving uninfected PBMCs, virus supplemented PBMCs and PBMCs harvested from productively infected sheep and supplemented with virus (Fig. 3.12, one-way ANOVA, $p=0.2$). Cells were injected at differing higher densities than for the macrophage cell preparation in order to attempt to deliver the same numbers of monocyte/macrophages as in the previous experiments. Monocyte/macrophages in PBMC cell preparation routinely account for about 10% of the total cell count, and the number of cells/ μl was adjusted accordingly.

The observation of no significant differences between the PBMC groups is surprising since these cells have widely been implicated in MVV induced neurodegeneration. However, in an attempt to resolve this apparent contradiction, a proliferation assay was carried out, in order to evaluate whether the cells were responding to the addition of MVV. The subsequent results show that, although capable of proliferation in response to a known mitogen, ConA, PBMCs did not proliferate in response to the addition of virus supernatant (Fig.3.13). This may be due to the killing of PBMCs by the virus or to inadequate amounts of viral antigen. These results, therefore, cannot discount the possibility of some neuroinflammatory action of PBMCs, as has previously been reported, and the present experiments would need to be repeated.

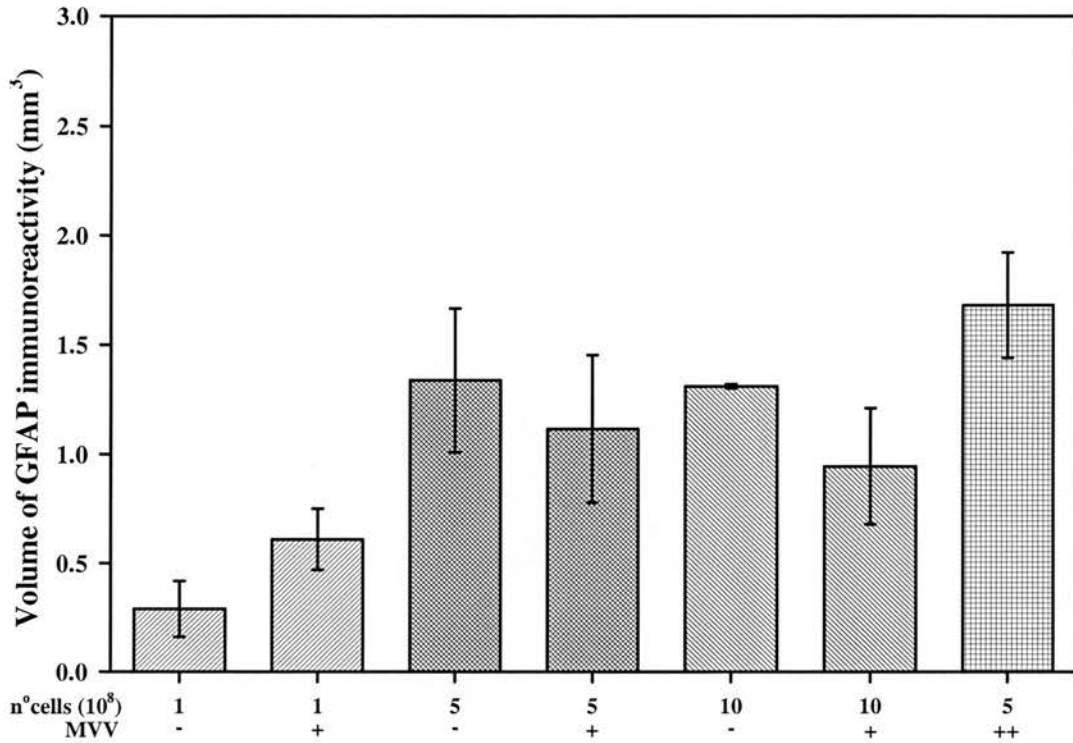


Fig. 3.12: Effects of PBMCs on GFAP staining of *scid* striatum

PBMCs were injected at different densities: 1×10^8 cells/ μ l (n=3 MVV-, n=2 MVV+), 5×10^8 cells/ μ l (n=7 MVV-, n=4 MVV+, n=3 MVV++) and 1×10^9 cells/ μ l (n=2 MVV-, n=3 MVV+). MVV-: uninfected cells, MVV+: virus supplemented cells, MVV++: cells obtained from productively infected sheep and supplemented with virus. All mice were perfused one week post-operatively. No significant differences in degrees of astrocytosis was observed between any of the groups (one-way ANOVA, $p=0.2$). Results: Mean \pm SEM.

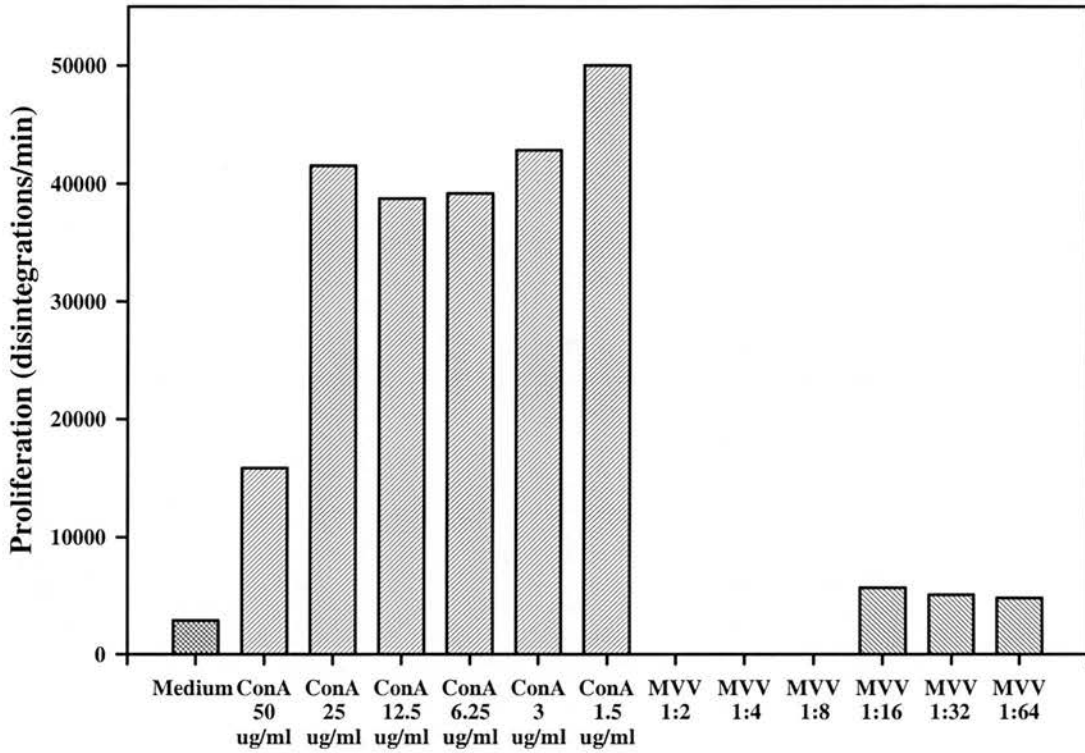


Fig. 3.13: Degree of proliferation of PBMCs from MVV infected sheep. PBMCs were capable of proliferating as shown by the addition of ConA to their medium, but only displayed a limited rate of proliferation in response to the addition of virus supernatant solution to their medium.

3.3.2.7. Intravenous injection of macrophages and PBMCs

In an effort to mimic further the natural MVV disease, macrophages and PBMCs were injected into the tail vein of *scid* mice. No increases in GFAP staining, at 7 days post-transfer, were observed in the brains of *scid* mice injected intravenously with 7 day old uninfected or MVV infected macrophages, or in those injected with PBMCs from productively MVV infected sheep (data not shown). Furthermore, staining for antigens located on macrophages and PBMCs did not reveal the presence of any of the injected cells in the CNS of the *scid* mice. This may be due to the inaccuracy of the injection method, the relatively small amount of time between injection and sacrifice, or the sequestration of macrophages in other tissues.

3.3.2.8. Effect of MK801 on acute inflammation caused by live macrophages

The potential protection by the NMDA receptor antagonist MK801, of neuroinflammation caused by MVV infected macrophages was also probed. Animals receiving MK801 were injected intraperitoneally 1 hour prior to the administration of MVV infected macrophages. The results show that MK801 reduces the volume of both the GFAP and F4/80 lesion present in treated mice (one way ANOVA, $p < 0.05$, post-hoc Duncan test, $p < 0.05$, Fig. 3.14).

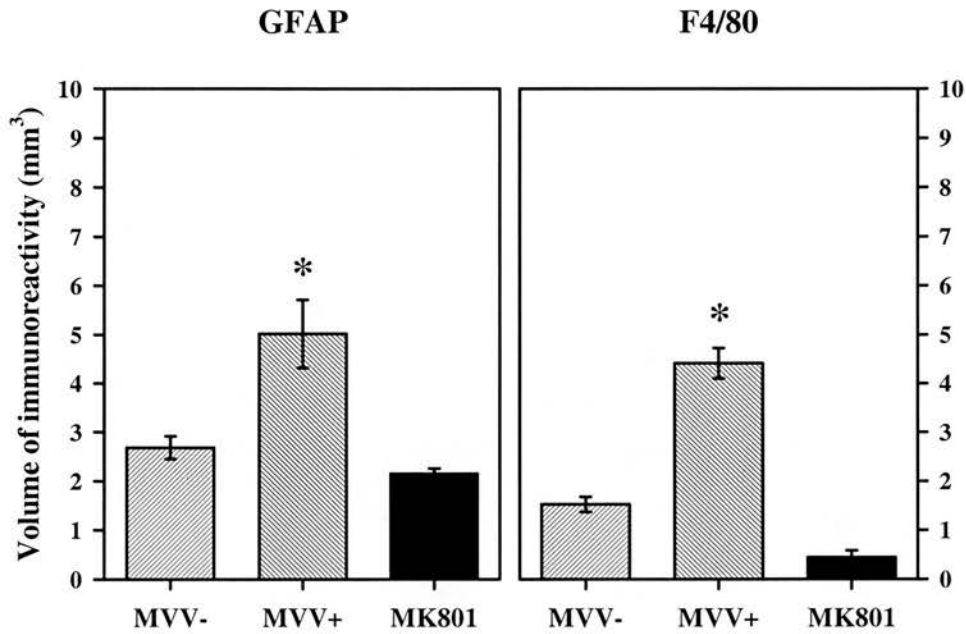


Fig. 3.14: Effect of MK801 on GFAP and F4/80 induction in *scid* striatum

Animals received 5×10^3 mature macrophages in $1 \mu\text{l}$ and were perfused 1 week post-operatively. MK801 was injected i.p. 1 hour pre-operatively. MVV-: uninfected macrophages (n=11), MVV+: macrophages infected with MVV *in vitro* (n=11), MK801: MK801 treated animals receiving MVV infected macrophages (n=3). A one way ANOVA showed a significant effect of treatment on lesion volume ($p < 0.005$) and post-hoc analysis indicated a greater GFAP and F4/80 lesion volume in animals receiving MVV infected macrophages as compared to those receiving uninfected macrophages or treatment with MK801 (Duncan test, $*p < 0.05$). Results: Mean \pm SEM.

3.3.3. Cytokine profile of uninfected and MVV infected macrophages.

3.3.3.1. RT-PCR

RT-PCR successfully isolated mRNA from uninfected and MVV infected 1 day, 2 day, 4 day and 1 week old macrophages, and amplified DNA for the cytokines IL-1 β , IL-6, TGF β , TNF α and the housekeeping gene ATPase from this mRNA. When the cDNA obtained from the PCR was run on an agarose gel, no appreciable differences were found in the levels of cDNA for the cytokines TNF α , IL-1 β , IL-6 or TGF β between uninfected and MVV infected macrophages cultured for 1, 2 or 4 days. However, levels of TGF β and IL-1 β appeared higher in samples obtained from 1 week old macrophages infected with MVV than in uninfected 1 week old macrophages. Since the difference in cytokine profile between uninfected and MVV infected macrophages appeared evident on the agarose gel, it was probed in a southern blot.

3.3.3.2. Southern blotting.

In order to semi-quantify the levels of DNA for each cytokine in 1 week old macrophages, the gel was probed with specific radioactive markers. Viewing of the autoradiograph obtained from the Southern blot, and densitometry reading of the appropriate bands seemed to confirm that levels of the cytokines IL-1 β and possibly TGF β were upregulated in MVV infected macrophages as compared to uninfected macrophages.

Integrated intensity (II) readings of ATPase bands obtained on the Southern blots showed approximately the same levels of ATPase at 35 cycles in uninfected cells (252.934) and MVV infected cells (264.94). Levels of cytokine cDNA were semi-quantified against these levels of overall cDNA, as shown by ATPase cDNA levels. Accordingly, II values obtained from cytokine cDNA from uninfected cells were divided by II readings from uninfected ATPase levels (252.934), and II values obtained from MVV infected cDNA samples were divided by the MVV infected ATPase densitometry reading (264.934). Thus cytokine cDNA bands from uninfected and infected samples were normalised against the appropriate amounts of total cDNA levels. The ratios of cytokine cDNA obtained from MVV infected macrophages against cytokine cDNA obtained from uninfected macrophages were then calculated for each cytokine.

TNF α cDNA levels were not upregulated in MVV infected macrophages as compared to uninfected macrophages. The II ratio of cDNA obtained from MVV infected cells (II_{MVV}) to cDNA acquired from uninfected macrophages (II_{CONT}) was 1.19 at 27 cycles, 1.17 at 31 cycles and 0.77 at 35 cycles. Similarly, IL-6 cDNA levels were not consistently different between uninfected and MVV infected macrophages. The $II_{MVV} : II_{CONT}$ ratios were 2.21 at 27 cycles, 1.04 at 31 cycles and 1.02 at 35 cycles.

However, TGF β cDNA levels appeared slightly increased in MVV infected macrophages. The $II_{MVV} : II_{CONT}$ band reading ratios for TGF β were 0.86 at 27 cycles, 1.17 at 31 cycles and 1.78 at 35 cycles. Likewise, IL-1 β cDNA was definitely increased in MVV infected macrophages compared to uninfected macrophages: $II_{MVV} : II_{CONT}$ ratios equalled 3.4 at 27 cycles, 2.5 at 31 cycles and 2.5 at 35 cycles, corresponding to a near threefold increase in cDNA levels (Fig. 3.15).

Cytokine cDNA	Cycles	$I_{MVV} : I_{CONT}$	Mean $I_{MVV} : I_{CONT}$
TNF α	27	1.19	1.04
	31	1.17	
	35	0.77	
IL-1 β	27	3.4	2.8
	31	2.5	
	35	2.5	
IL-6	27	2.21	1.42
	31	1.04	
	35	1.02	
TGF β	27	0.86	1.27
	31	1.17	
	35	1.78	

Fig. 3.15: Densitometry analysis of cytokine cDNA obtained from uninfected and MVV infected macrophages.

Cytokine cDNA integrated intensity values were calculated from bands obtained in Southern blots and normalised against total levels of ATPase cDNA. TGF β and IL-6 cDNA levels are slightly higher in MVV infected macrophages as compared to uninfected macrophages, but TNF α levels remain unchanged. Levels of IL-1 β cDNA are definitely elevated in MVV infected macrophages when compared to their uninfected counterparts.

3.4. DISCUSSION

The current experiments suggest a possible role for macrophages infected with MVV in causing neurodegeneration. The injection of live MVV infected macrophages into *scid* mouse striatum caused greater GFAP and F4/80 induction, when compared to uninfected macrophages, one week post-operatively. The increase in GFAP staining appears to be an acute transitory phenomenon, not lasting beyond one week post-operatively. The induction of microgliosis, however, persists and is still significant 3 weeks post-operatively. The effects of free virus injection are not clear cut, as, although some increase in GFAP staining appears to be incurred when compared to the injection of control medium, this is not statistically significant. F4/80 staining is likewise not significantly altered. The injection of freeze thawed, killed macrophages previously infected with MVV up-regulated F4/80 staining, as compared to uninfected macrophages, but had no significant effect on GFAP induction. Furthermore, the injection of free virus and killed macrophages caused smaller lesions than the injection of live macrophages.

The aim of these experiments was to investigate whether MVV infected macrophages had any effects on brain parenchyma in the absence of other cell-mediated immune effectors. The results suggest that macrophages infected with MVV may cause acute GFAP expression, therefore transitory astrogliosis, and more chronic F4/80 induction and therefore microgliosis. These effects seem to depend on the state of maturation of the injected macrophages as older macrophages, maintained 1 week *in vitro*, cause greater neuroinflammation than younger macrophages, maintained for fewer days *in vitro*. This may be due to the increased capability of macrophages, as opposed to monocytes, to support viral infection and gene expression (Gendelman *et al.*, 1986). The acute gliosis reflected by elevated GFAP expression may be due to the actions of mediators released by MVV infected macrophages. Astrocytes represent a relatively malleable population of cells within the CNS and the lack of persistent astrogliosis may reflect a return to steady state functions of astrocytes following the initial insult.

The persistence of microgliosis within the striata of *scid* mice injected with MVV infected macrophages may, however, reflect more severe changes in CNS functions, an increased recruitment of blood borne macrophages to the CNS, or both.

The activation of microglia over a period of 3 weeks post-inoculation in *scid* striatum is taken to be the most significant event in these experiments. This continuance may represent the establishment of lesions in the natural disease, and contribute to the symptoms of neurologic MVV infection. The putative importance of activated microglia in the pathogenesis of MVV induced CNS lesions has also been recently highlighted independently, by the correlation of activated microglia and severity of lesion patterns in experimentally MVV infected sheep (Bergsteinsdottir *et al.*, 1998). These investigators attribute a significant degree of importance to the expression of MHC antigens on activated microglia in the induction of CNS lesions. Although activated microglia were only detected in the present *scid* mice experiments by the induction of F4/80, an investigation into the MHC expression profile of these activated microglia would be worthwhile. Nevertheless, the present findings reinforce a role for microglia in the response of the CNS to the challenge of MVV infected cells, and the establishment of neuropathology in the absence of other cell-mediated immune effectors.

The lack of significant effects of free virus on *scid* striata, as well as the lack of demonstrable p25 antigen in *scid* brains one week post-operatively, would suggest either that not enough virus was delivered to the striata of *scid* mice, although the amount of viral particles delivered was calculated at over 800 000, or that virus was being cleared from *scid* mouse CNS. It is also possible that the lack of p25 staining may be due to the down-regulation of MVV *in vivo*. Although MVV can infect cells readily *in vitro* and replicate, the effects *in vivo* may be different. This has been observed in other tissues where the injection of MVV into joints causes pathology characteristic of MVV infection, but no viral markers can be detected shortly after the injection. Similarly, in a recent report involving the intracerebral inoculation of sheep with MVV, few viral antigens were located in the CNS of diseased sheep, but neuropathology characteristic of visna infection was evident (Bergsteinsdottir *et al.*, 1998). A similar phenomenon may be at work in *scid* mice injected with MVV infected macrophages or free virus. The virus may initiate inflammation, but then become latent, causing the down-regulation of viral proteins, including p25.

Although no firm conclusions as to the effects of free virus on *scid* CNS can be upheld, it would seem plausible to suggest that, because of the actions of live macrophages, diffusible mediators may be necessary to the induction of GFAP and

F4/80. The injection of killed macrophages also caused a slight increase in GFAP staining as well as a significant increase in F4/80 induction, when these were infected with MVV. However, the injection of killed macrophages caused smaller GFAP and F4/80 lesion volumes than the injection of live macrophages to *scid* striatum. This would suggest that, although killed macrophages may be having some effect on *scid* parenchyma, this effect is minimal. Thus, the effects of live macrophages may incorporate an effect of killed macrophages, since some macrophages may perish during the injection process. However, live macrophages have a greater effect on *scid* GFAP and F4/80 expression, therefore it is unlikely that these effects are due to the artefact of injecting 'dead' macrophages.

The lysis of uninfected and MVV infected macrophages necessarily involved, by the freeze thawing method used here, the spillage of cellular contents into the injection medium. The actions of many of these cellular components are not documented and therefore no conclusions are possible as to what may be causing F4/80 induction by killed macrophages. However, if an inflammatory mediator is responsible for the neurodegeneration caused by live macrophages, then this mediator may also be present in the injection medium of killed macrophages, and may be exerting similar effects.

The administration of MK801 prior to the injection of macrophages caused the reduction of GFAP and F4/80 induction caused by MVV infected macrophages. This suggests that any putative mediator released by MVV infected macrophages to cause increases in GFAP and F4/80 staining, may be acting through glutamate receptors. The presence of glutamate receptors on astrocytes is suspected, as excitatory amino acids can depolarise astrocytes *in vitro* (Bowman *et al.*, 1984). The effect on microglia may be an indirect effect, as there is little evidence to suggest the presence of glutamate receptors on microglia. The inhibition of astrocyte activation by MK801, may secondarily inhibit the actions of activated astrocytes on surrounding cells and, consequently, microglia. Thus, microglia may be upregulated by activated astrocytic mediators, for example cytokines, as well as by macrophage effectors, and that inhibition of the effects of astrocytes by MK801 may, in turn, cause less microglial activation. However, the actions of MK801 warrant further investigation, as the experimental numbers using MK801 were low.

The injections of PBMCs in these experiments did not cause significant increases in GFAP or F4/80 staining. This does not, however, discount any effects of immune cells on *scid* brain. Further experiments using the injection of MVV reactive lymphocytes would be required to clarify the role of circulating immune cells in causing inflammation in *scid* striata. Indeed, neuronal loss or myelin disruption may require the presence of both macrophages and PBMCs in brain parenchyma. Neither of these events were observed with the injection of MVV infected macrophages alone.

Preliminary investigations into the cytokine profile of MVV infected macrophages as compared to uninfected macrophages revealed an upregulation of IL-1 β mRNA, and a possible increasing effect on the expression of TGF β and IL-6 mRNA. Levels of TNF α mRNA were unchanged. The probing of the pattern of cytokine expression was intended primarily as a tool for the measure of activation of macrophages destined for injection into *scid* mice, but may also offer clues as to the identity of a pro-inflammatory mediator contributing to the lesions seen in *scid* mice. MVV infection of ovine cells has been shown to alter cytokine mRNA patterns both *in vitro* and *in vivo*. Indeed, mRNA levels for the cytokine interleukin-8 (IL-8) are increased in alveolar macrophages infected with MVV *in vitro* (Legastelois *et al.*, 1998). Accompanying this effect is an increase in levels of IL-1 β mRNA. *In vivo* experiments from the same laboratory using naturally MVV infected tissue also show elevated levels of IL-8 mRNA in macrophages. In these cells, virus expression was not always evident, suggesting that cytokine induction may be a downstream predictor of virus activated cells, following clearance of MVV from macrophages. Similarly, TGF β expression has been found to be increased in the alveolar and interstitial macrophages of naturally MVV infected sheep (Moreno *et al.*, 1998). The immunohistochemical detection of TGF β correlated with the occurrence of early lesions in the lungs of these sheep, and, as for IL-8, followed a distinct expression pattern. The current finding of a near three-fold increased expression of IL-1 β mRNA in blood borne macrophages following MVV infection *in vitro* is therefore taken as an indicator of cellular activation in response to MVV infection. This finding may also serve to compensate for the lack of p25 expression in macrophages once injected into *scid* mouse striatum. It is possible to speculate that MVV infection of macrophages *in vitro* initiates a cascade of events,

including changes in cytokine expression, which may persist after the clearance or down-regulation of the virus *in vivo*.

The induction of IL-1 β mRNA in MVV infected macrophages *in vitro* may suggest its release upon transplantation of macrophages into *scid* mouse brain tissue. It is appealing to propose that this cytokine may be involved in causing the astrocytosis and microgliosis observed in *scid* parenchyma following the injection of MVV infected macrophages. Indeed, IL-1 β has been found to have a variety of effects on brain cells, including astrocytes, microglia and neurons (Campbell *et al.*, 1993; Hertz *et al.*, 1990; Barna *et al.*, 1990; Gelbard *et al.*, 1993; Chao *et al.*, 1995), and is generally accepted as a pro-inflammatory mediator. However, further experiments would be needed to clarify the presence of ovine IL-1 β in *scid* parenchyma following MVV infected macrophage transplantation, in order to assign any role to this cytokine in causing neuroinflammation in the experiments carried out in this thesis. Furthermore, species specificity may prevent any actions of ovine cytokines on murine cells. In particular, recombinant ovine TNF α and IL-6 have been shown only to have limited effects on some murine cell lines. Recombinant ovine TNF α does not cause cytotoxicity to murine L929 cells *in vitro* (Green *et al.*, 1993) and recombinant ovine IL-6 does not induce the proliferation of murine B9 myeloma line cells, in contrast to the effect of murine IL-6 (Ebrahimi *et al.*, 1995). However, in the same investigations, murine L929 cells do show activity attributable to TNF α , which is blocked by antibodies to the ovine recombinant protein, and the IL-6 studies used recombinant ovine pre-protein. Thus, ovine cytokines may be capable of exerting effects on these murine cell lines, albeit at higher concentrations than needed for the endogenous cytokines. Moreover, the effects of these recombinant proteins have not been studied on any other murine cell types, such as astrocytes and microglia. The investigation of the effects of ovine cytokines on murine cells would certainly prove valuable in the context of the present experiments.

In summary, the experiments carried out here seem to suggest a possible role for macrophages infected with MVV in causing astrocytosis and microgliosis in the absence of other cell-mediated immune responses *in vivo*. Astrocytosis and microgliosis are characteristics of the natural MVV disease (Georgsson *et al.*, 1977), but these experiments do not confirm that macrophages are solely responsible for the observed changes in brain parenchyma. The induction of astrocytic and gliotic responses in *scid*

CNS may involve a cellularly released mediator. The identity of such a mediator cannot conclusively be suggested as a cytokine, although levels of IL-1 β mRNA are increased in MVV infected macrophages. The inhibitory action of MK801 suggests that any putative mediator may act through glutamate receptors. This is at odds with the proposal of a cytokine as a detrimental effector, and raises the possibility that a viral protein may be playing a role in the inflammation observed, possibly in concert with any cytokine action. The actions of MVV peptides on CNS cells are addressed in the next chapter.

CHAPTER 4:

***IN VITRO* NEUROTOXICITY OF MVV INFECTED MACROPHAGE PRODUCTS AND LENTIVIRAL TAT.**

4.1. INTRODUCTION

In the *scid* mouse model of MVV encephalopathy described in the previous chapter, no neuronal loss was observed in the brains of mice injected with MVV infected macrophages. However, in naturally occurring MVV, areas of necrosis are regularly found, particularly in the vicinity of invading macrophages. Neuronal loss is also common in HIV encephalopathy. Many candidates have been proposed as neurotoxic agents in lentiviral encephalopathies, including cytokines and the lentiviral proteins Tat and envelope glycoproteins. Since the previous experiments showed that MVV infected macrophages caused greater CNS inflammation than uninfected macrophages when injected into *scid* mice, the supernatant from these cells was applied to neurons *in vitro* and neuronal cell death evaluated. Since the lentiviral protein Tat has also been shown to be released from HIV infected cells, the neurotoxic potential of a lentiviral tat peptide derived from the basic region of MVV Tat protein was also probed *in vitro*.

4.2. EXPERIMENTAL DESIGN

The neurotoxic potential of macrophage supernatants and MVV tat peptide was evaluated *in vitro*. Cultures of E17 rat cortical neurons were established and maintained in serum free medium for 5 days prior to application of supernatant or peptides. Supernatant was removed from mature 1 week old uninfected and MVV infected macrophages and applied to the neurons *in vitro*. Cell death was measured using an assessment of cell viability based on the reduction of MTS. MVV tat peptide (235 nM) and control ovalbumin peptide (235 nM) were applied to neuronal cells of the same plate, and cell death evaluated using both the MTS assay, and LDH release.

4.3. RESULTS.

4.3.1. Characterisation of rat cortical cell cultures

Preliminary experiments were carried out to set up rat cortical cultures enriched in neurons. Initially, cells obtained from E17 rats were plated out and maintained in serum containing medium (10% Fetal Bovine Serum). Efforts were made to control the presence of glial cells in these cultures by the application of 10 μ M cytosine arabinoside, a proliferation inhibitor, to wells after 24 hours *in vitro*. However, repeated experiments using cytosine arabinoside at 10 μ M and lower concentrations, resulted in the disappearance of neurons as well as glial cells. However, without the addition of cytosine arabinoside, glial cells proliferated in abundance at the expense of neuronal numbers. This was revealed by immunostaining of cultures with antigens directed against the neuronal protein NeuN, the microglial marker OX42 and the astrocytic marker GFAP. Optimisation of neuronal numbers was achieved by initially plating cortical cells in culture medium containing 5% FBS, and maintaining them *in vitro* using chemically defined, serum free medium. Cells cultured in this manner were predominantly NeuN positive, with a few OX42 and GFAP positive cells present in each well.

4.3.2. *In vitro* neurotoxicity of macrophage supernatants.

Supernatant from 1 week old cultured MVV infected and uninfected macrophages was removed and applied to rat cortical cultures. The supernatant from MVV infected macrophages caused significantly greater neurotoxicity to RCC *in vitro* after 24 hours, as compared to the supernatant from uninfected macrophages (Student's t-test, $p < 0.005$, Fig. 4.1). The increase in cell death was approximately 4-fold. This was measured using the MTS assay which gave an average value of cell death of 43% for the supernatant from MVV infected macrophages, as compared to an average value of 10% for the supernatant obtained from uninfected macrophages.

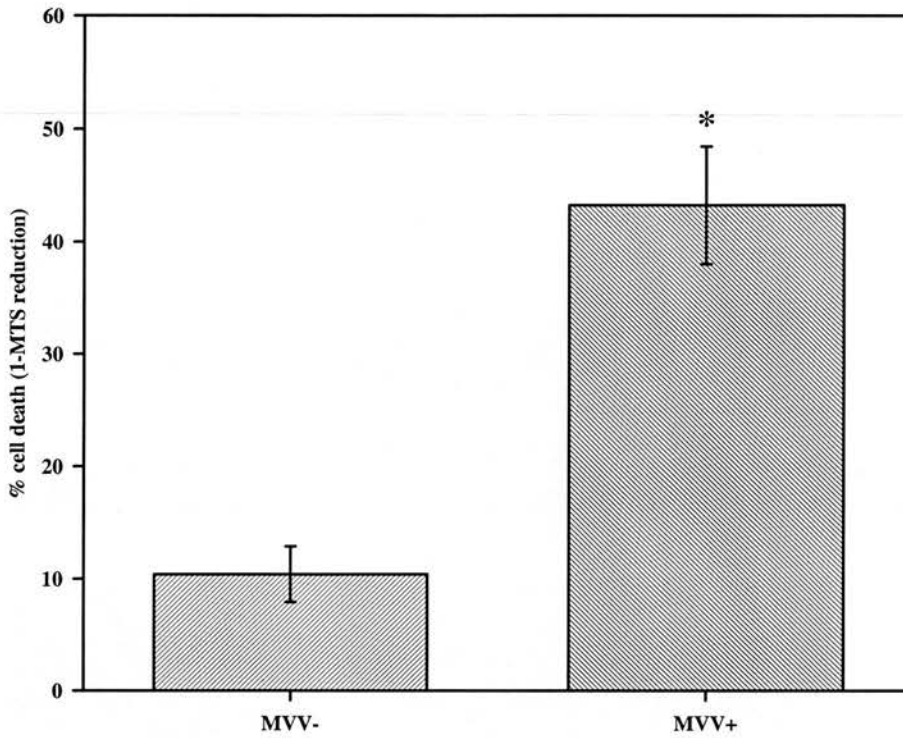


Fig. 4.1: *In vitro* effect of MØ supernatant on neuronal MTS reduction at 24 hours.

Supernatant from uninfected (MVV-, n=6) and MVV infected (MVV+, n=6) mature MØ was applied to RCC for 24 hours. Cell death was measured using the MTS assay. Supernatant from infected MØ produced significantly more cell death than supernatant from uninfected MØ (Student's t-test, * $p < 0.005$). Results: Mean \pm SEM.

4.3.3. *In vitro* neurotoxicity of MVV tat peptide.

MVV tat peptide (235nM) was applied to RCC in 12 replicates after 5 days in culture. At the same time, ovalbumin peptide (235nM) was applied to 12 wells of the same plate, and the remaining wells received a medium change. These were then left for 24, 48 or 72 hours in culture conditions. Cell death was measured by an estimate of LDH release, or by the amount of MTS reduction.

Preliminary data analysis revealed that intrinsic levels of cell death in wells receiving a medium change alone varied between experiments. In some experiments, cell death was much higher than in others. This may have been due to many causes including, for example bacterial infections and excessive tissue disruption during the dissection and trypsinisation procedures. In an effort to preserve the homogeneity of samples studied, an arbitrary level of background cell death was determined, above which samples were discarded. Therefore, if the average level of cell death in wells receiving a medium change was above 25%, the data from that experiment was discarded.

4.3.3.1. *Effects at 24 hours*

After 24 hours, the level of LDH release from neurons treated *in vitro* with MVV tat peptide appeared greater than those treated with ovalbumin peptide or medium alone (Fig. 4.2). LDH release from cells treated with MVV tat peptide rose to 25%, and LDH release from cells treated with ovalbumin peptide increased to 21%. The average background cell death in wells receiving only a medium change was 17%. A statistical one-way ANOVA revealed that there was indeed a significant difference between the three treatment groups ($p < 0.001$). Subsequent post-hoc data analysis also showed that LDH release from cells treated with MVV tat peptide was significantly greater than LDH release from cells treated with control ovalbumin peptide and those receiving only a medium change (Modified LSD [Bonferroni's] test, $p < 0.05$). LDH release corresponds to total amount of cell death, therefore the incubation of neurons with MVV tat peptide caused greater numbers of cells to die than did the administration of ovalbumin peptide or a medium change.

In parallel experiments, cell death was evaluated using an MTS assay, based on the degree of cell viability (Fig.4.3). In these experiments, cell death increased both in wells treated with MVV tat peptide and in wells treated with control ovalbumin peptide,

as compared to wells receiving only a medium change. A single factor ANOVA revealed that the three treatments caused significant differences in MTS reduction in neurons ($p<0.01$). However, subsequent post-hoc statistical analysis did not reveal any differences between treatment with MVV tat peptide and control ovalbumin peptide. Both treatments, however, did cause lesser MTS reduction, and therefore greater neuronal cell death, than a medium change alone (Modified LSD [Bonferroni's] test, $p<0.05$).

4.3.3.2. *Effects at 48 hours*

At 48 hours *in vitro*, MVV tat peptide, ovalbumin peptide and a medium change caused significant differences in LDH release between treatments (one-way ANOVA, $p<0.01$, Fig. 4.4). Indeed, LDH release rose to 26% in neurons treated with MVV tat peptide and to 21% in cells treated with ovalbumin peptide. The average background level of cell death in wells receiving only a medium change approximated 19%. Post-hoc analysis showed that treatment with MVV tat peptide caused greater LDH release, and thus cell death, than treatment with ovalbumin peptide or a medium change alone (Modified LSD [Bonferroni's] test, $p<0.05$).

In similar experiments using the MTS assay as an indicator of cell death, a one-way ANOVA revealed a significant effect of treatment on MTS reduction ($p<0.001$, Fig.4.5). Neuronal cell death in wells treated with MVV tat peptide rose by 25%, whereas cell death in wells treated with ovalbumin peptide increased to 18%, as compared to control cells receiving a medium change, where the average value of cell death was 14%. Post-hoc analysis also showed that treatment of cells with MVV tat peptide caused greater LDH release than both the control ovalbumin peptide and medium change groups (Modified LSD [Bonferroni's] test, $p<0.05$). These results strongly suggest that MVV tat peptide is exerting a neurotoxic effect on neurons after 48 hours incubation *in vitro*.

4.3.3.3. *Effects at 72 hours*

After 72 hours incubation, a single factor ANOVA revealed a significant effect of treatment on neuronal LDH release ($p<0.001$, Fig. 4.6). MVV tat peptide treatment caused an increase in LDH release to 19% as compared to 14% in wells receiving the control ovalbumin peptide, and 13% in wells receiving only a medium change. Subsequent post-hoc data analysis showed that LDH release, and therefore cell death,

was significantly increased in cells receiving MVV tat peptide as compared to those receiving ovalbumin peptide, or a medium change alone (Modified LSD [Bonferroni's] test, $p < 0.05$).

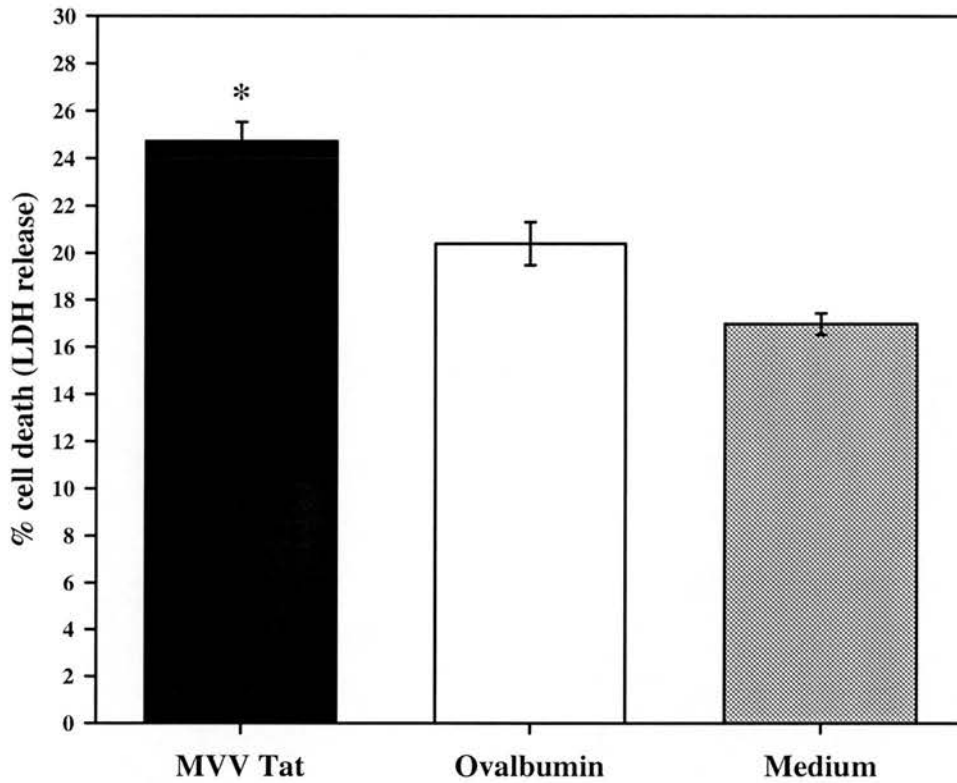


Fig. 4.2: *In vitro* effect of MVV tat peptide on neuronal LDH release at 24 hours.

Results: Mean \pm SEM. Cell death was measured using the LDH assay, 24 hours after application of MVV tat peptide (n=24), ovalbumin peptide (n=24) or a medium change (n=24) to RCC. A single factor ANOVA revealed a significant effect of treatment on LDH release ($p < 0.001$). Post-hoc analysis showed LDH release in the MVV tat peptide group was significantly greater than in both the ovalbumin and medium groups (Modified LSD [Bonferroni's] test, $*p < 0.05$).

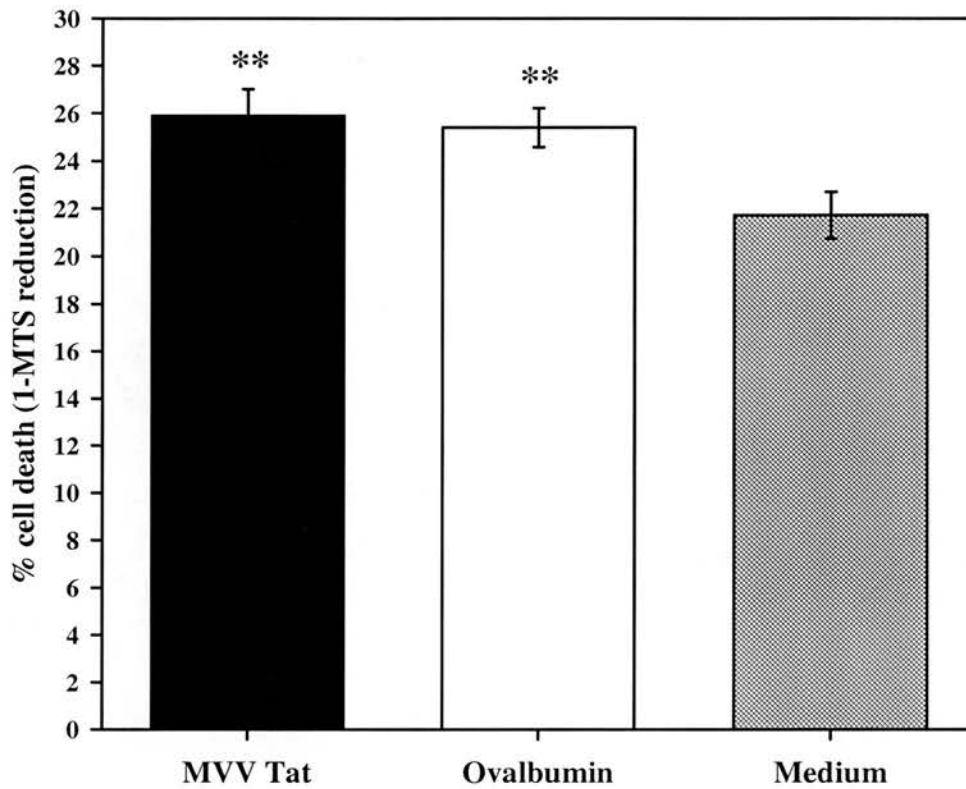


Fig. 4.3: *In vitro* effect of MVV tat peptide on neuronal MTS reduction at 24 hours.

Cell viability was measured using the MTS assay, 24 hours after application of MVV tat peptide (n=24), ovalbumin peptide (n=24) or a medium change (n=24) to RCC. A single factor ANOVA revealed a significant effect of treatment on MTS reduction ($p < 0.01$). Post-hoc analysis showed that treatment with MVV tat peptide did not cause significantly greater cell death than treatment with ovalbumin peptide, but both these treatments did cause significantly greater cell death than a medium change alone (Modified LSD [Bonferroni's] test, $**p < 0.05$). Results: Mean \pm SEM.

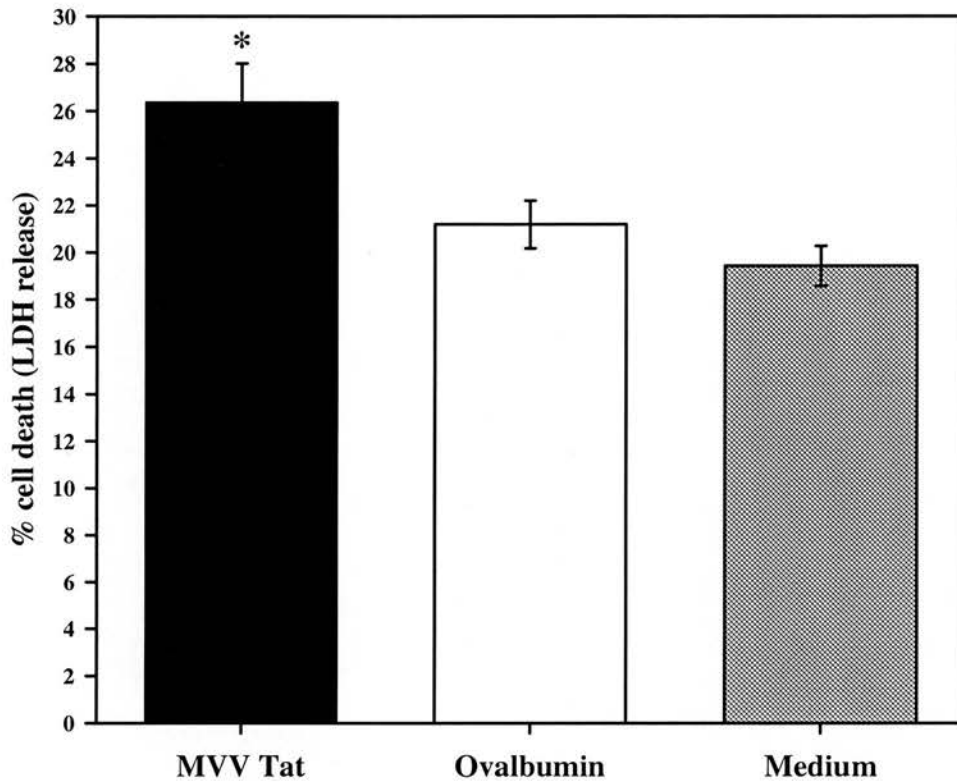


Fig. 4.4: *In vitro* effect of MVV tat peptide on neuronal LDH release at 48 hours.

Cell death was measured using the LDH assay, 48 hours after the application of the MVV tat peptide (n=24), ovalbumin peptide (n=24) or a medium change (n=22) to RCC. A single factor ANOVA revealed an effect of treatment on LDH release ($p < 0.001$). Post-hoc analysis showed LDH release in the MVV tat peptide group was significantly greater than in both the ovalbumin and medium groups (Modified LSD [Bonferroni's] test, $*p < 0.05$). Results: Mean \pm SEM.

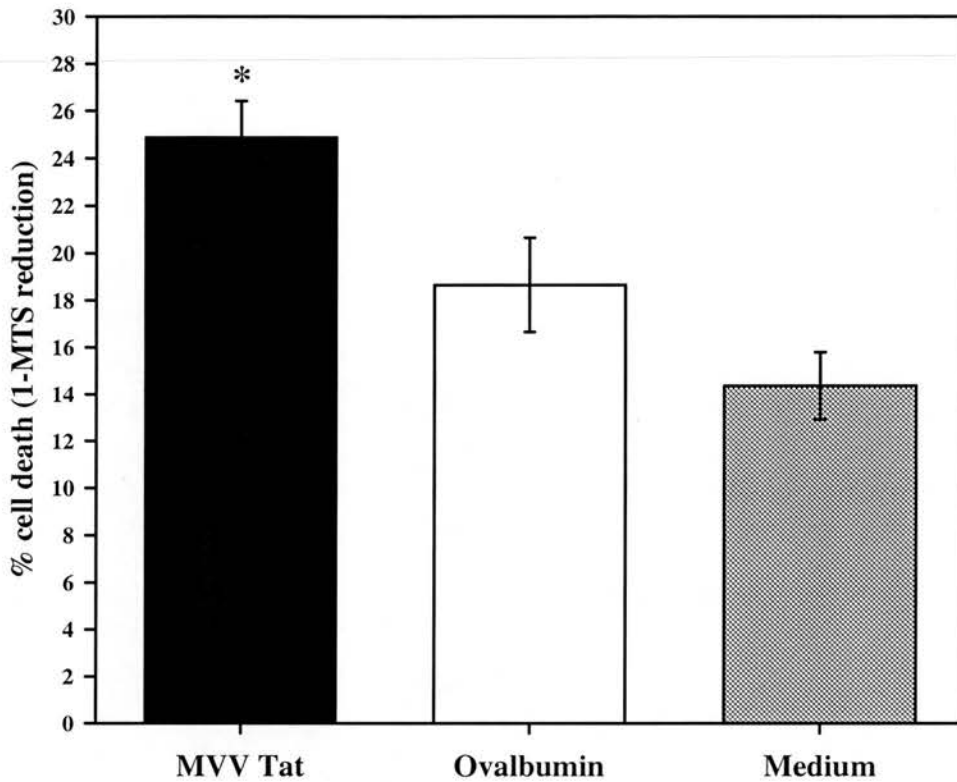


Fig. 4.5: *In vitro* effect of MVV tat peptide on neuronal MTS reduction at 48 hours.

Cell viability was measured using the MTS assay, 48 hours after the application of MVV tat peptide (n=24), ovalbumin peptide (n=24) or a medium change (n=24) to RCC. A single factor ANOVA ($p < 0.001$) revealed a significant effect of treatment on MTS reduction. Post-hoc analysis showed that MTS reduction in the MVV tat peptide group was significantly less than in both the ovalbumin and medium groups (Modified LSD [Bonferroni's] test, $*p < 0.05$). Results: Mean \pm SEM.

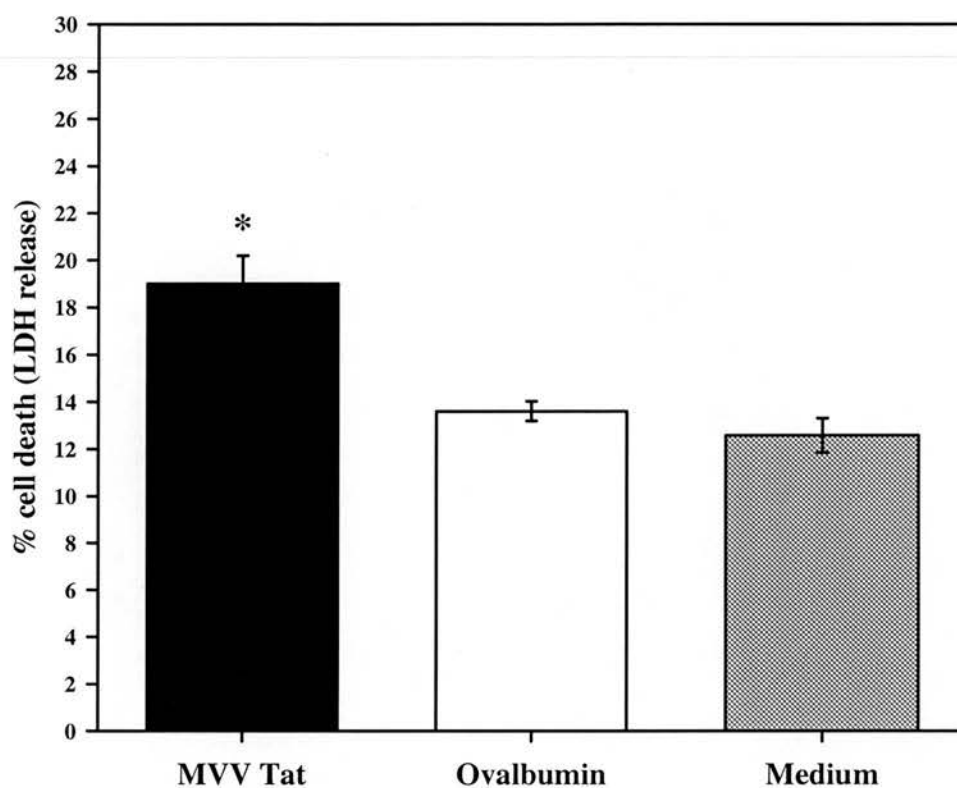


Fig. 4.6: *In vitro* effect of MVV tat peptide on neuronal LDH release at 72 hours.

Cell death was measured using the LDH assay 72 hours after treatment of cells with MVV tat peptide (n=12), ovalbumin peptide (n=12) or a medium change (n=12). A single factor ANOVA revealed a significant effect of treatment on LDH release ($p < 0.001$). Post-hoc analysis showed that LDH release in the MVV tat peptide group was significantly greater than in both the ovalbumin and medium groups (Modified LSD [Bonferroni's] test, $*p < 0.05$). Results: Mean \pm SEM.

4.4. DISCUSSION

The current experiments suggest that supernatant obtained from MVV infected macrophages is more neurotoxic than supernatant derived from uninfected macrophages after 24 hours application to neurons *in vitro*. The experiments carried out here also suggest that MVV tat peptide is neurotoxic to cultured neurons. This effect begins at 24 hours and is definite by 72 hours.

The aim of these experiments was to test the possible neurotoxicity of macrophage supernatants and that of an MVV tat peptide. Although macrophages infected with MVV did not cause any noticeable neuronal cell death in *scid* mice, as mentioned previously, the investigation of any neurotoxicity, in a different experimental setting, was deemed worthwhile. The subsequent finding that MVV infected macrophages supernatant causes greater toxicity to neurons than uninfected macrophage supernatant lends support to the neurodegenerative potential of products released from lentivirally infected macrophages. Lentiviral Tat protein has been shown to be released from infected cells and may move transcellularly (Frankel *et al.*, 1988). MVV Tat protein may therefore also be released from infected macrophages. Peptides derived from MVV Tat protein have previously been shown to be neurotoxic *in vitro* and *in vivo* (Hayman *et al.*, 1993; Strijbos *et al.*, 1995), and the current experiments confirm this. Furthermore, these experiments suggest an acute neurotoxic action of MVV tat peptide. This peptide exerts its effects rapidly, as some neurotoxicity is apparent in neurons incubated with the peptide after 24 hours. At 48 hours incubation, MVV tat peptide exerts definite neurotoxicity, both by measurement of total cell death and total cell viability.

However, it should not be inferred from these experiments that MVV Tat is considered here to be the only mediator possibly present in MVV infected macrophage supernatant that may be neurotoxic. Other mediators, for example cytokines or other viral proteins, may also be contributing to neurotoxicity. These experiments do serve to prove however, the neurotoxicity of a lentiviral peptide, putatively released from MVV infected macrophages, and can justify the subsequent testing of this peptide *in vivo*.

**CHAPTER 5: *IN VIVO* NEUROTOXICITY OF
LENTIVIRAL TAT.**

5.1. INTRODUCTION

The neurotoxic capability of lentiviral Tat has previously been documented *in vitro* and *in vivo*. However, no studies have been conducted on the acute neurotoxic potential of MVV tat peptide. In an effort to investigate any neurodegenerative effects of the MVV tat peptide in the short term, MVV tat peptide was administered *in vivo*, and its effects studied at short time courses. The long term effects of MVV tat peptide *in vivo* have been attributed to NO mediated glutamate neurotoxicity. Neuroprotection studies were therefore also carried out to investigate whether the same neurotoxic mechanisms operate acutely.

5.2. EXPERIMENTAL DESIGN.

The *in vivo* neurotoxic ability of HIV and MVV tat peptides was assessed by the stereotaxic injection of these into rat striatum. Neuronal loss, and activation of astrocytes and microglial cells were measured by immunocytochemical detection and morphometric image analysis of the lesion incurred at 30 minutes, 1 hour and 2 hours after injection. Some animals were also examined at later time points. The mechanisms of neurotoxic action of MVV tat peptide were then probed through the use of glutamate receptor antagonists, a NOS inhibitor and a TNF α antagonist.

5.3. RESULTS.

5.3.1. Lesion characteristics

MVV and HIV tat peptides (20 μ g in 1 μ l) were injected into rat striata, which were then recovered and examined at 30 minutes, 1 or 2 hours after the time of injection. An acute lesion was induced by MVV tat peptide as early as 30 minutes post-operatively. Furthermore, the appearance of this lesion was very distinctive and unusual. The lesion profile was the same at all the acute time intervals, and was similar for the HIV tat peptide.

NeuN immunocytochemical staining of rat striatum, injected with MVV tat peptide and recovered 1 hour post-surgery, showed neuronal loss. Normal NeuN

staining of rat striatum shows positive cells distributed homogeneously throughout the striatum (Fig. 5.1.A). Injection of control substances showed disruption of the normal organisation of NeuN staining, but this was confined to the needle tract (Fig. 5.1.B). Administration of 1 μ l MVV tat peptide caused widespread disruption in NeuN staining. At the centre of the lesion, NeuN positive cells appeared darkened and distorted (Fig. 5.1.C). Surrounding this area a 'halo' effect was observed of tissue devoid of staining (Fig. 5.1.D). At a higher magnification, NeuN staining revealed neuronal loss both at the centre of the lesion (Fig. 5.2.A) and in the 'halo' area (Fig. 5.2.B).

This same unusual pattern was evident on GFAP stained sections recovered from animals injected with 1 μ l MVV tat peptide and sacrificed at 1 hour. Injection of control substances into rat striatum showed few GFAP positive cells at the injection site 1 hour post-surgery (Fig. 5.3.A). Injection of 1 μ l MVV tat peptide, however, caused the appearance of GFAP positive cells at the centre of the injection site, surrounded by tissue devoid of staining (Fig. 5.3.B). Astrocytes therefore appear activated at the centre of the lesion, but are not evident in the 'halo' area surrounding the centre of the lesion.

Immunocytochemistry for activated microglia also showed a similar lesion profile in MVV tat peptide injected animals recovered 1 hour post-operatively, although this was much less striking than for the NeuN and GFAP stains. Injection of control substances caused microglial activation one hour post-surgery (Fig. 5.4.B). The injection of MVV tat peptide also caused microglial activation, but the pattern of staining revealed the same 'halo' effect as staining for NeuN and GFAP (Fig. 5.4.A). When compared to sections recovered 3 days post-injection, microglial activation at the shorter time points appeared minimal.

Histochemistry for diaphorase positive, NOS neurons also revealed a lesion caused by MVV tat peptide 1 hour post-operatively. Normal diaphorase staining reveals NOS positive neurons with long processes throughout the striatum (Fig. 5.5.C). In animals injected with ibotenic acid, some disruption of diaphorase staining was evident 1 hour post-operatively, but this was confined to the needle tract (Fig. 5.5.B). In animals injected with MVV tat peptide, diaphorase staining was absent over a large area, although some cell bodies were still recognisable (Fig. 5.5.A). The administration of L-NAME also caused the disappearance of diaphorase positive neurons, perhaps due to its inhibition of NOS.

In animals left to recover for 3 days or one week post-injection, NeuN staining

was absent at the centre of the lesion, but did not reveal the same pattern as the acute lesions. GFAP staining revealed astrocyte activation, but, as for NeuN, the distinctive lesion profile observed at short time intervals post-surgery was absent. In these animals astrocytosis was more diffuse, with no disappearance of GFAP immunoreactivity. Diaphorase staining was also reduced as was staining for PV and ChAT neurons (Figs. 5.6 and 5.7). The OX42 response also showed extensive microglial activation at 3 days, but this was decreased at one week.

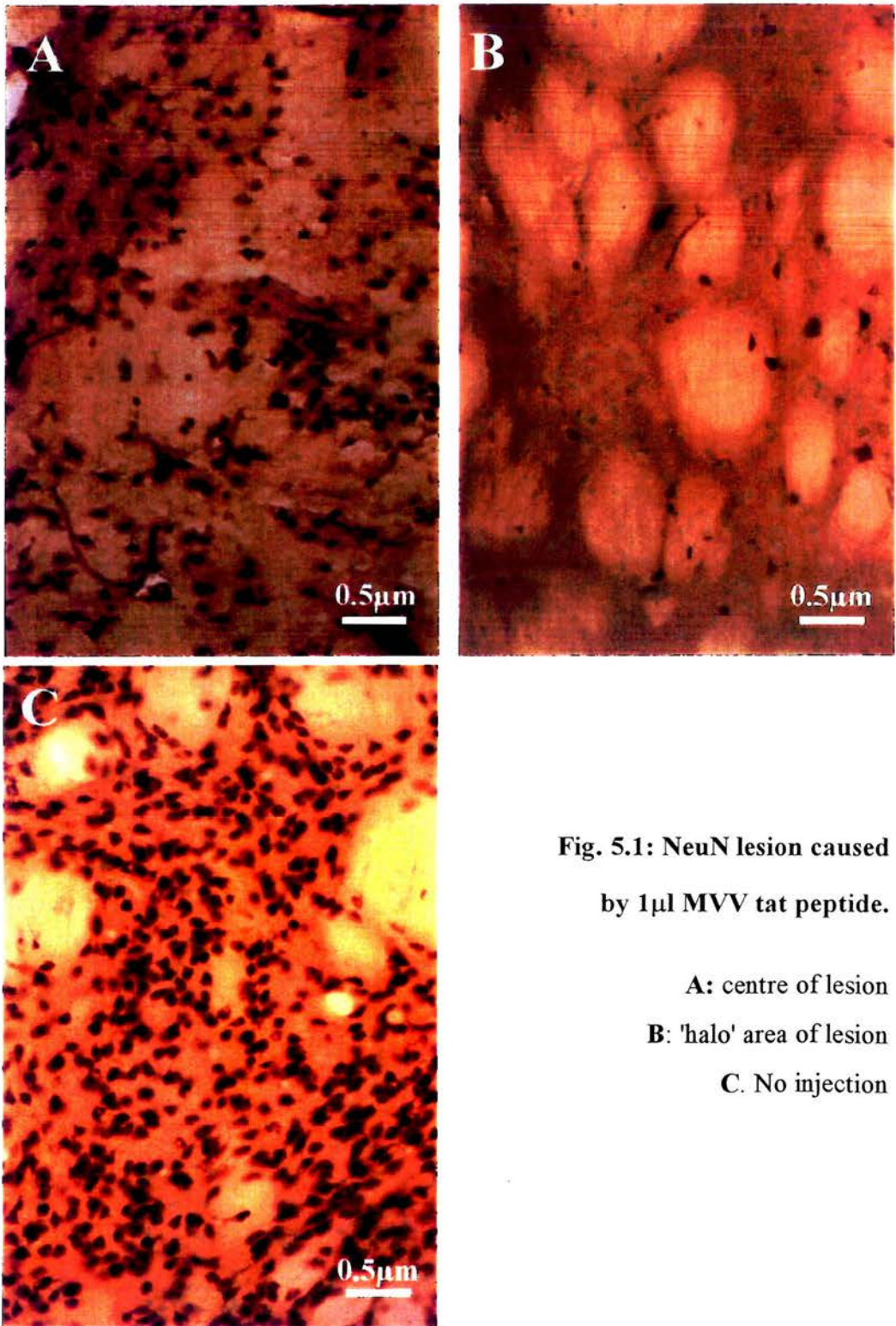


Fig. 5.1: NeuN lesion caused by 1 μl MVV tat peptide.

A: centre of lesion

B: 'halo' area of lesion

C: No injection

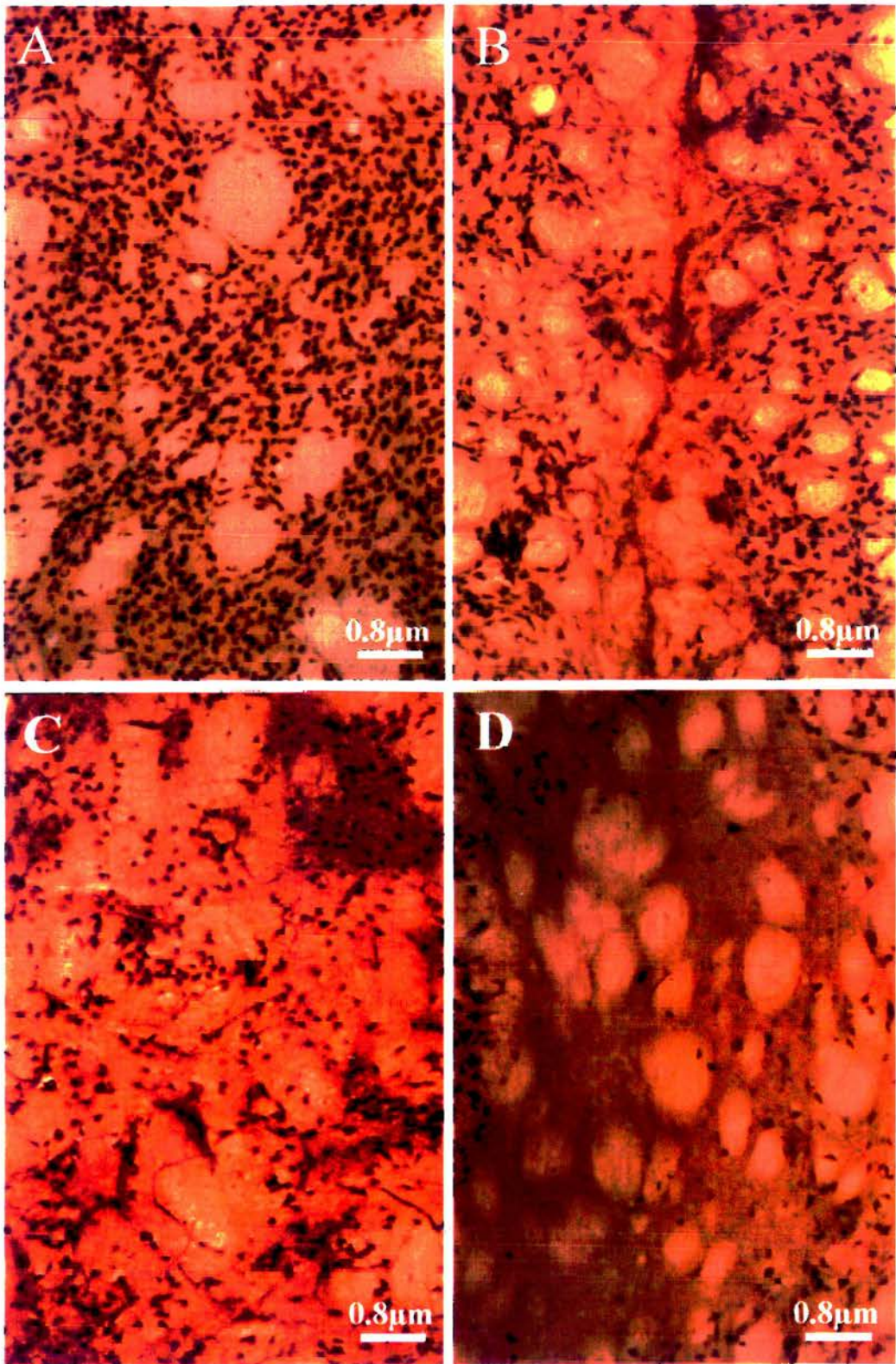


Fig. 5.2: NeuN staining of rat striatum

A: no injection, **B:** injection of 1µl L-NAME,
C: centre of lesion caused by 1µl MVV tat peptide
D: 'halo' area of lesion

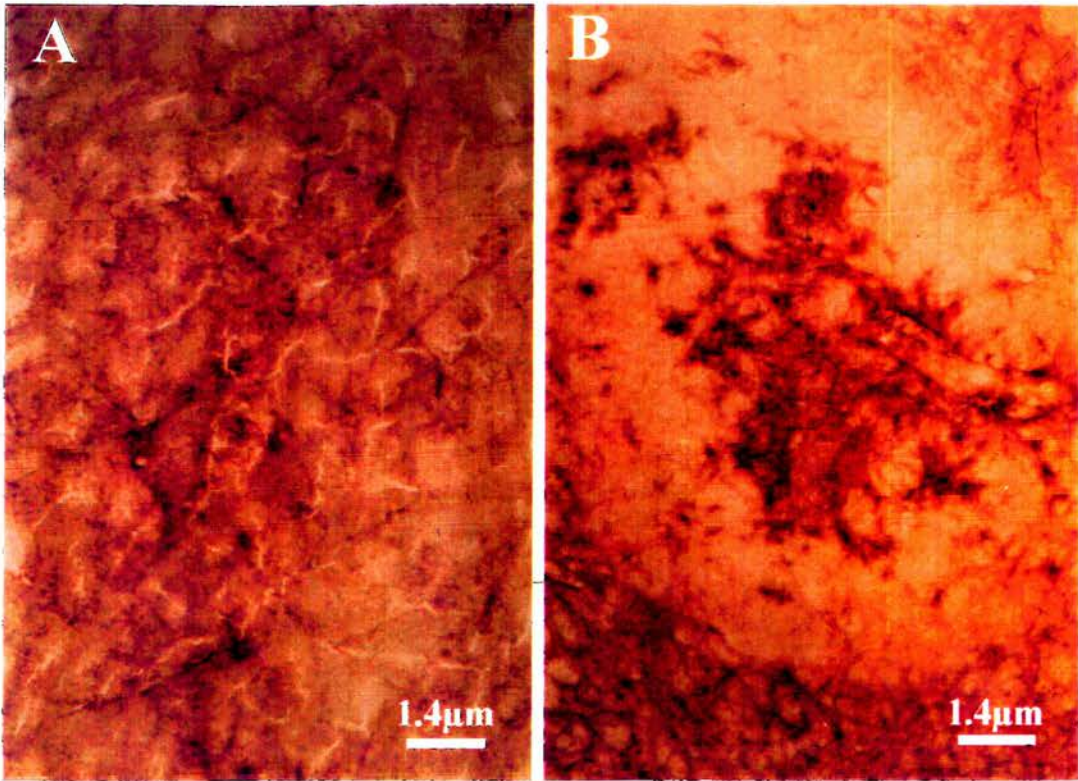


Fig. 5.3: GFAP induction by MVV tat peptide

A. Injection of 1µl saline **B.** Injection of 1µl MVV tat peptide. Injection of MVV tat peptide caused astrocyte activation at the centre of the injection site, but a disappearance of GFAP positive cells surrounding the lesion site.

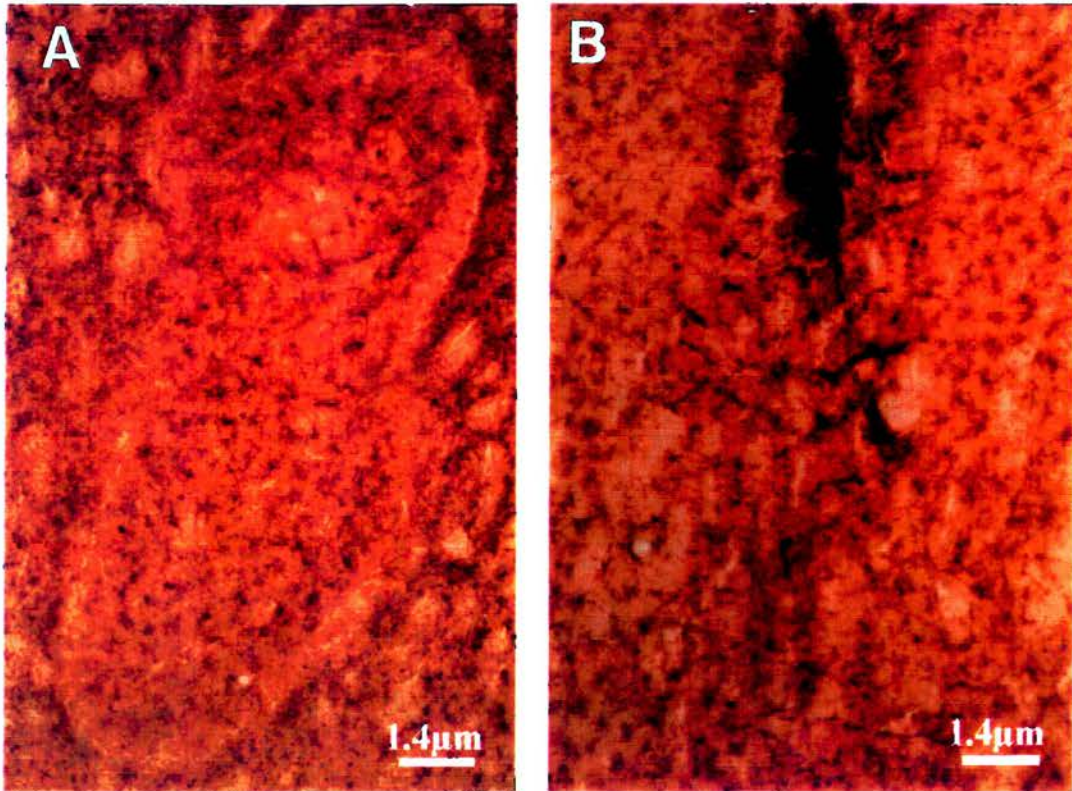


Fig. 5.4: OX42 induction by MVV tat peptide

A. Injection of 1 μ l MVV tat peptide **B.** Injection of 1 μ l ovalbumin peptide. The injection of MVV tat peptide caused microglial activation as did the injection of ibotenic acid. However, the pattern of microglial activation caused by MVV tat peptide was similar to the lesion profile seen with NeuN and GFAP staining.

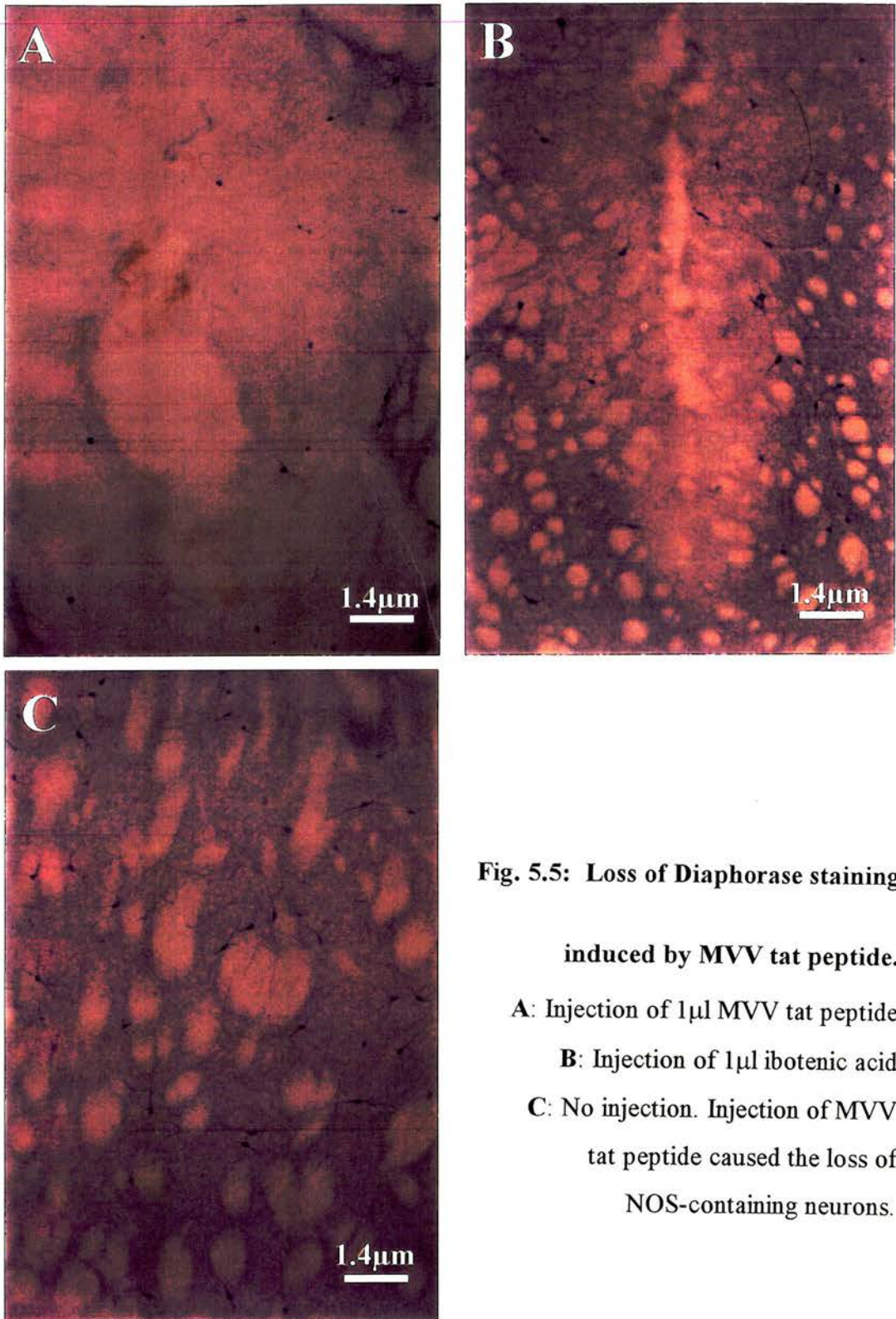


Fig. 5.5: Loss of Diaphorase staining

induced by MVV tat peptide.

A: Injection of 1 μl MVV tat peptide

B: Injection of 1 μl ibotenic acid

C: No injection. Injection of MVV tat peptide caused the loss of NOS-containing neurons.

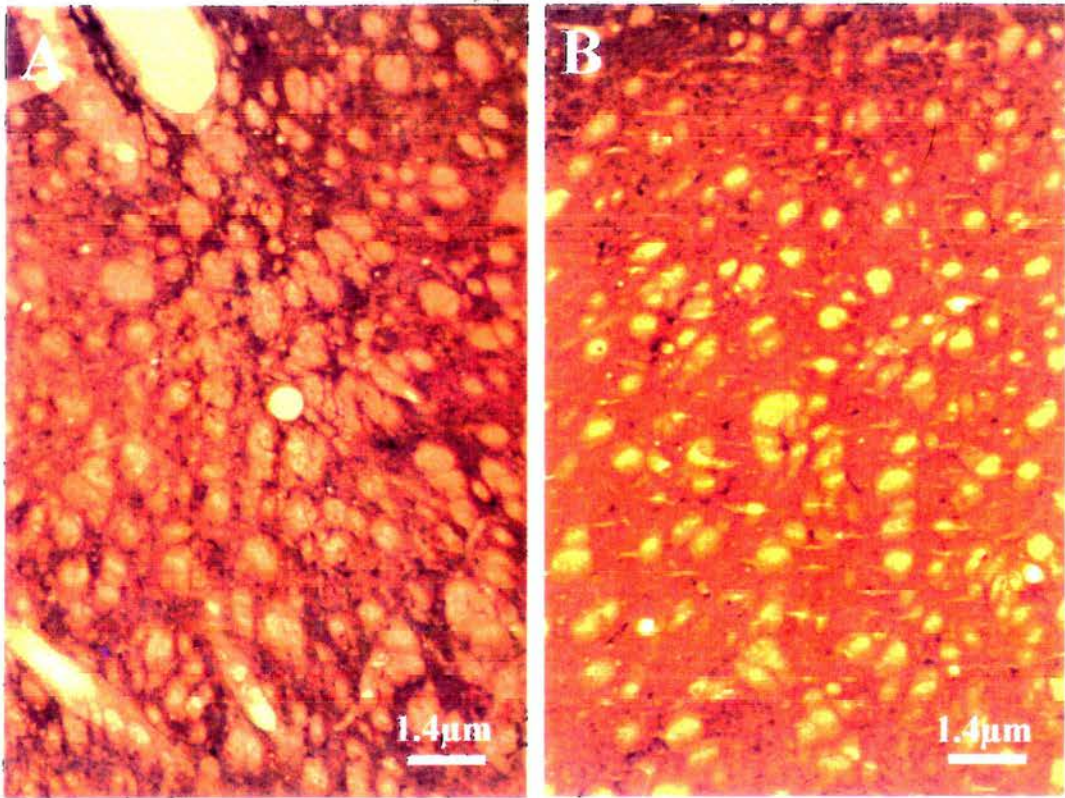


Fig. 5.6: Loss of PV immunoreactive neurons induced by MVV tat peptide

A. Injection of 1 μ l MVV tat peptide **B.** No injection. Some non-specific staining is observed surrounding the lesion area in the tat peptide injected striatum. Parvalbumin positive cells are not as readily observed in the MVV tat peptide injected striatum as compared to the uninjected striatum.

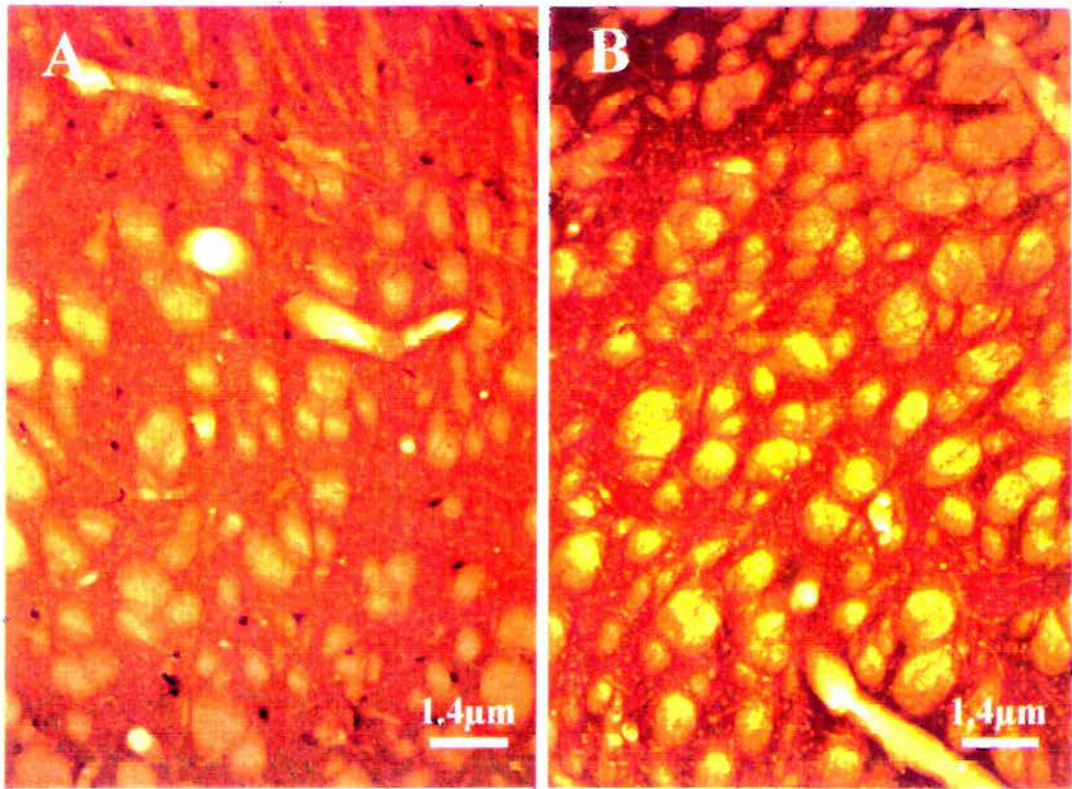


Fig. 5.7: Loss of ChAT immunoreactive neurons induced by MVV tat peptide
A. No injection **B.** Injection of 1µl MVV tat peptide. ChAT immunoreactive neurons are absent in the MVV tat peptide injected striatum.

5.3.2. Morphometric analysis.

The administration of control substances, saline, ovalbumin peptide and ibotenic acid, did not cause any lesions at 30 minutes post-surgery, as measured by the amount of NeuN staining and compared to the volume of the lesion caused by MVV tat peptide (Fig. 5.8). A one-way ANOVA revealed a significant effect of treatment on lesion volume ($p < 0.05$). Post-hoc analysis showed that the MVV tat peptide treated group caused a significantly greater NeuN lesion than any of the control groups (Duncan test, $p < 0.05$). Similarly, the GFAP activation caused by the injection of MVV tat peptide was greater than that caused by the injection of control substances at 30 minutes (One-way ANOVA, $p < 0.005$, and post-hoc Duncan test, $p < 0.05$, Fig. 5.9). However, no visible differences in OX42 staining were observed with the injection of control substances 30 minutes after administration. The HIV tat peptide group was omitted from statistical analysis due to the small number of experimental animals.

At 1 hour post-injection, the administration of a control substance, L-NAME, caused a significantly smaller NeuN lesion than the administration of MVV tat peptide (Student's t-test, $p < 0.05$, Fig. 5.10). The injection of L-NAME into rat striatum did not cause any measurable GFAP lesion, but both the MVV and HIV tat peptide groups caused a large GFAP lesion (Fig. 5.11). L-NAME did, however cause the disappearance of diaphorase positive neurons, due to its inhibition of NOS. No significant changes in OX42 immunoreactivity were observed with any of the control substances.

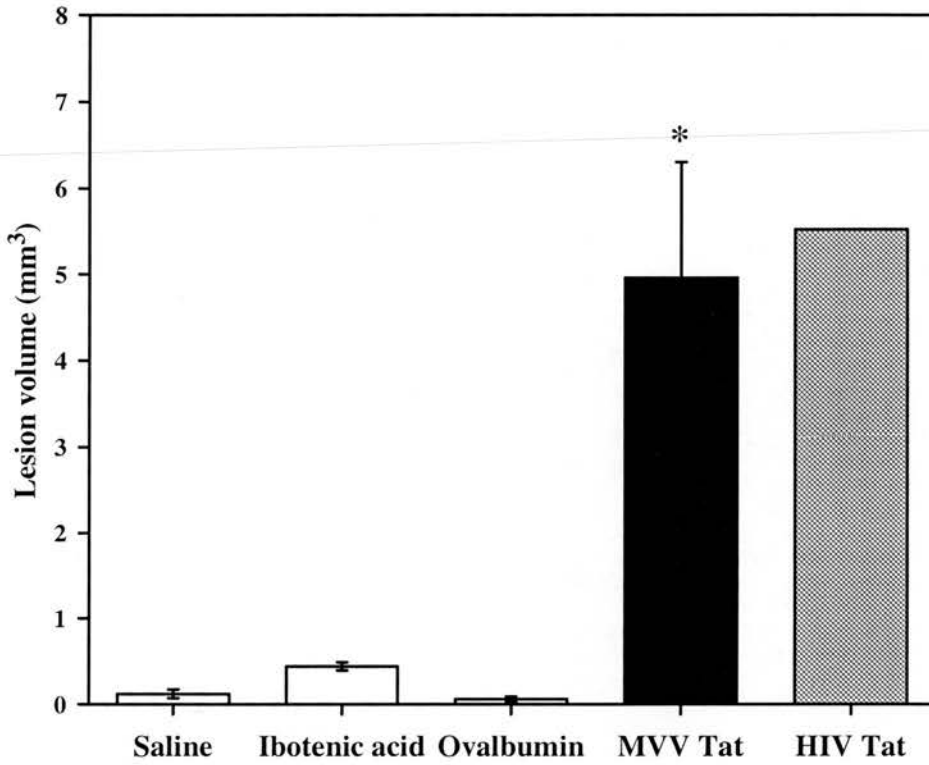


Fig. 5.8: Effect of intra-striatal injection of lentiviral tat peptides on NeuN staining at 30 minutes.

Treatment had a significant effect on lesion volume (one-way ANOVA, $p < 0.05$), and the MVV tat peptide lesion ($n=3$) was significantly greater than the application of saline ($n=2$), ibotenic acid ($n=2$) and ovalbumin peptide ($n=2$) control substances (post-hoc Duncan test, $*p < 0.05$). The HIV tat peptide group is illustrated from one animal and was omitted from statistical analysis. Results: Mean \pm SEM.

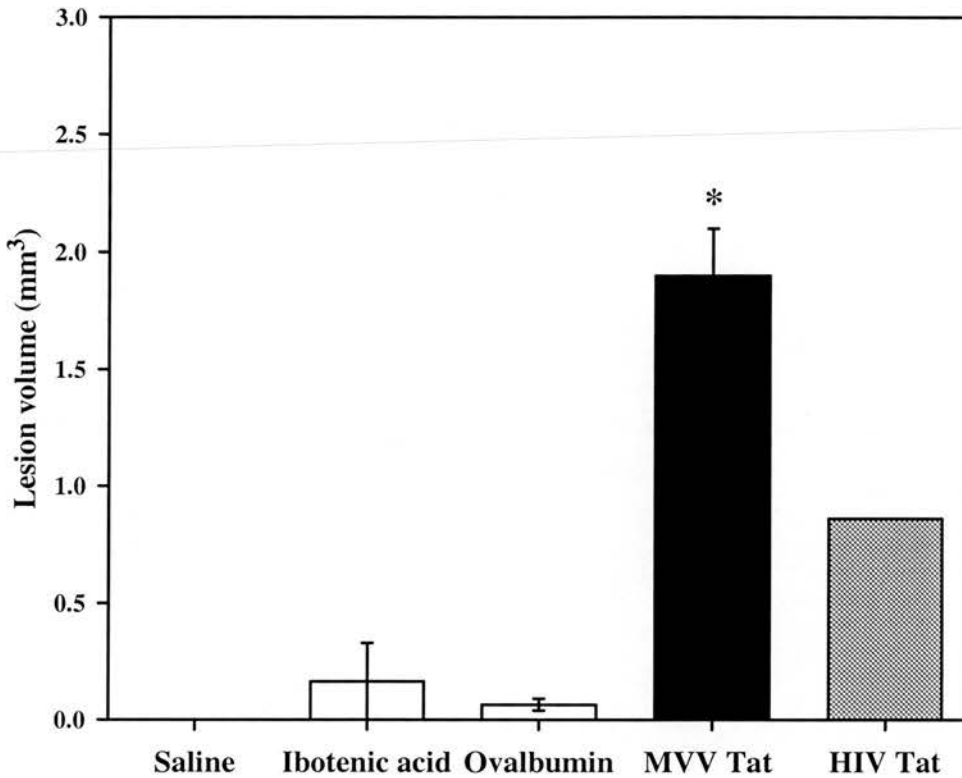


Fig. 5.9: Effect of intra-striatal injection of lentiviral tat peptides on GFAP staining at 30 minutes.

MVV tat peptide (n=3) caused a significantly greater lesion than the saline (n=3), ibotenic acid (n=2) and ovalbumin peptide (n=2) control groups (one-way ANOVA, * $p < 0.005$, post-hoc Duncan test $p < 0.05$). The HIV tat peptide group is illustrated from one animal and was omitted from statistical analysis. Results: Mean \pm SEM.

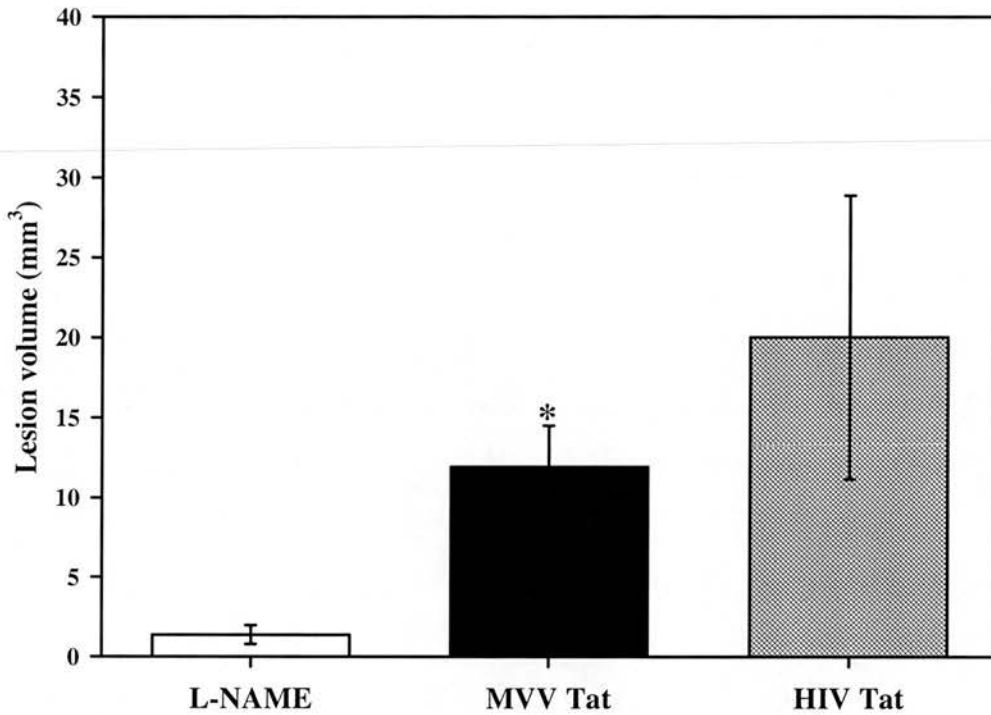


Fig. 5.10: Effect of intra-striatal injection of lentiviral tat peptides on NeuN staining at 1 hour

The L-NAME (n=5) control group was significantly different from the MVV tat peptide group (n=18) and the HIV tat peptide group (n=3, one-way ANOVA and post-hoc Duncan test, $*p<0.05$). Results: Mean \pm SEM.

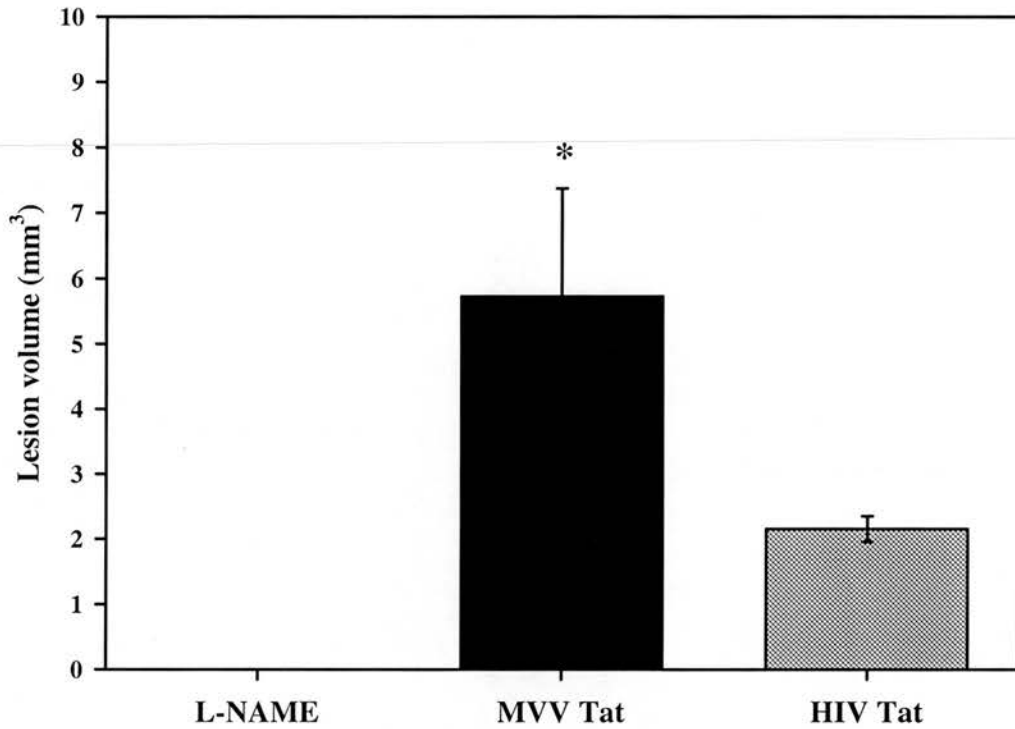


Fig. 5.11: Effect of intra-striatal injection of lentiviral tat peptides on GFAP staining at 1 hour.

The control substance, L-NAME (n=5), did not cause any measurable GFAP lesion. Both the MVV tat peptide (n=18) and the HIV tat peptide (n=3) caused significant lesions. Results: Mean \pm SEM.

5.3.2.2. Time course

Administration of MVV tat peptide induced a lesion in the striatum, visible with NeuN and GFAP staining, as early as 0.5 hours post-operatively. The amount of neuronal loss, as measured by the NeuN lesion volume, increased over a period of 24 hours (Fig. 5.12). Statistical analysis revealed that the lesions caused by MVV tat peptide at 1 and 24 hours were significantly greater than that at 30 minutes (one-way ANOVA and post-hoc Duncan test, $p < 0.05$). The lesion visible at 24 hours, approximately 15mm^3 , was of the same order of magnitude as that observed at one week as previously documented. Similarly, the GFAP lesion caused by the injection of MVV tat peptide increased significantly between 30 minutes and 24 hours (one-way ANOVA and post-hoc Duncan test, $p < 0.05$, Fig. 5.13).

5.3.2.3. Neuroprotection experiments

The effects of various putative neuroprotectants on the lesion caused by the MVV tat peptide was assessed by their prior or co-administration with the peptide. Since the MVV tat peptide lesion approximated maximal proportions at 1 hour, substances were tested at this time point. The NMDA receptor antagonist MK801, and the AMPA receptor antagonist NBQX, were injected intraperitoneally 1 hour prior to the intra-striatal injection of MVV tat peptide. L-NAME, an NOS inhibitor, and αMSH , a $\text{TNF}\alpha$ inhibitor were co-injected with the peptide. Preliminary investigations did not reveal any effects of NBQX and αMSH . However, the administration of MK801 reduced the volume of the NeuN lesion caused by the MVV tat peptide (Fig. 5.14). The administration of L-NAME seemed to slightly increase the volume of the MVV tat peptide induced NeuN lesion. A one-way ANOVA revealed a significant effect of the administration of treatment on the MVV tat peptide induced NeuN lesion volume ($p < 0.05$). Post-hoc analysis showed the injection of MK801 caused a reduction in the lesion volume caused by the MVV tat peptide (Duncan test, $p < 0.05$). The administration of L-NAME, however, had no significant effect. Similarly, MK801 reduced the volume of the GFAP lesion caused by the MVV tat peptide (one-way ANOVA and post-hoc Duncan test, $p < 0.05$, Fig. 5.15), whilst the administration of L-NAME had no significant effect.

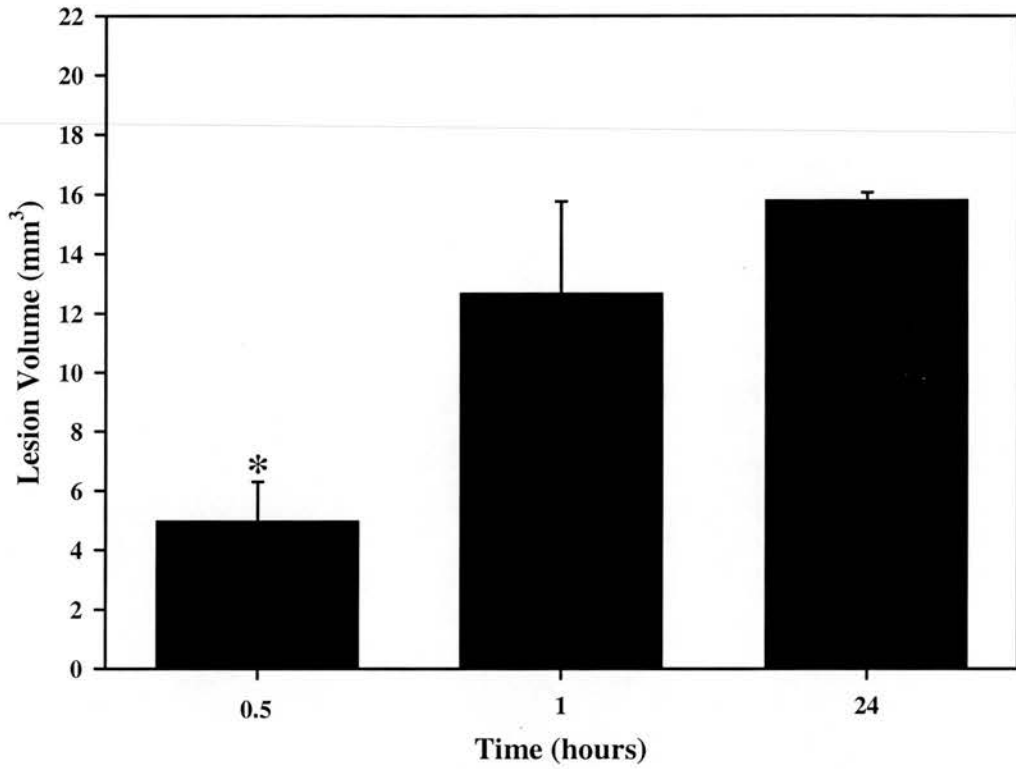


Fig. 5.12: Progress over time of the NeuN lesion induced by MVV tat peptide.

The lesion caused by the MVV tat peptide increased consistently over time, being significantly greater at 1 (n=18) and 24 hours (n=2) than at 30 minutes (n=3; one-way ANOVA and post-hoc Duncan test, * $p < 0.05$). Results: Mean \pm SEM.

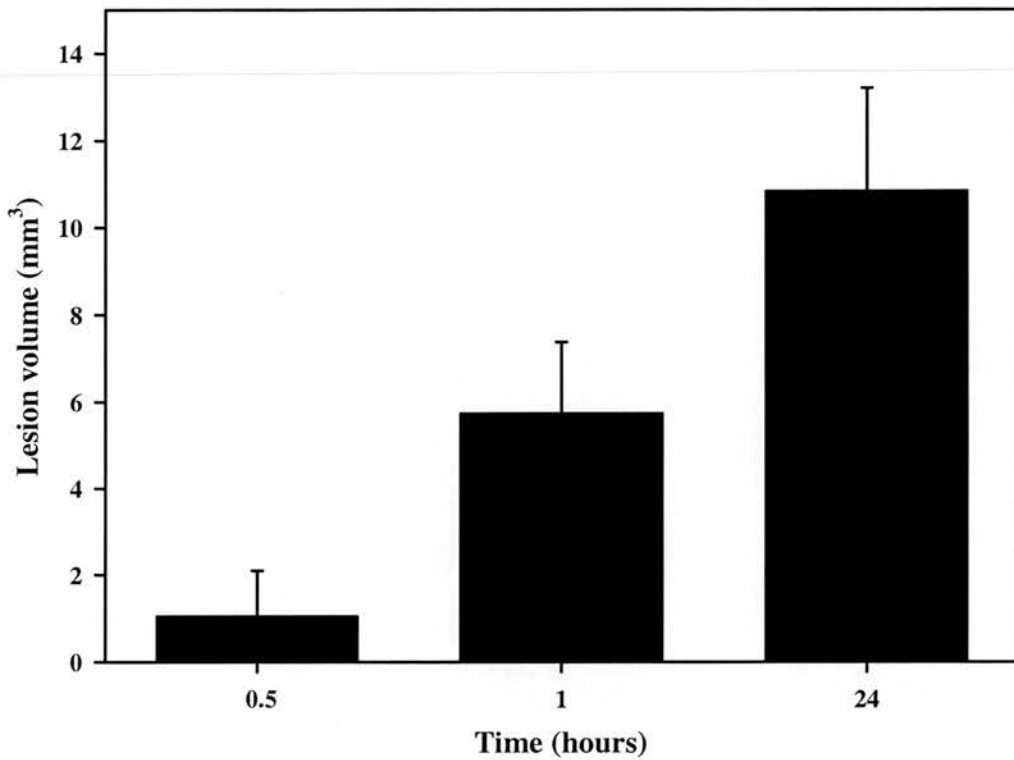


Fig. 5.13: Progress over time of the GFAP lesion caused by MVV tat peptide

The GFAP lesion caused by the MVV tat peptide increased significantly over time between 30 minutes (n=3), and 24 hours (n=2; one-way ANOVA and post-hoc Duncan test, $p < 0.05$). Results: Mean \pm SEM.

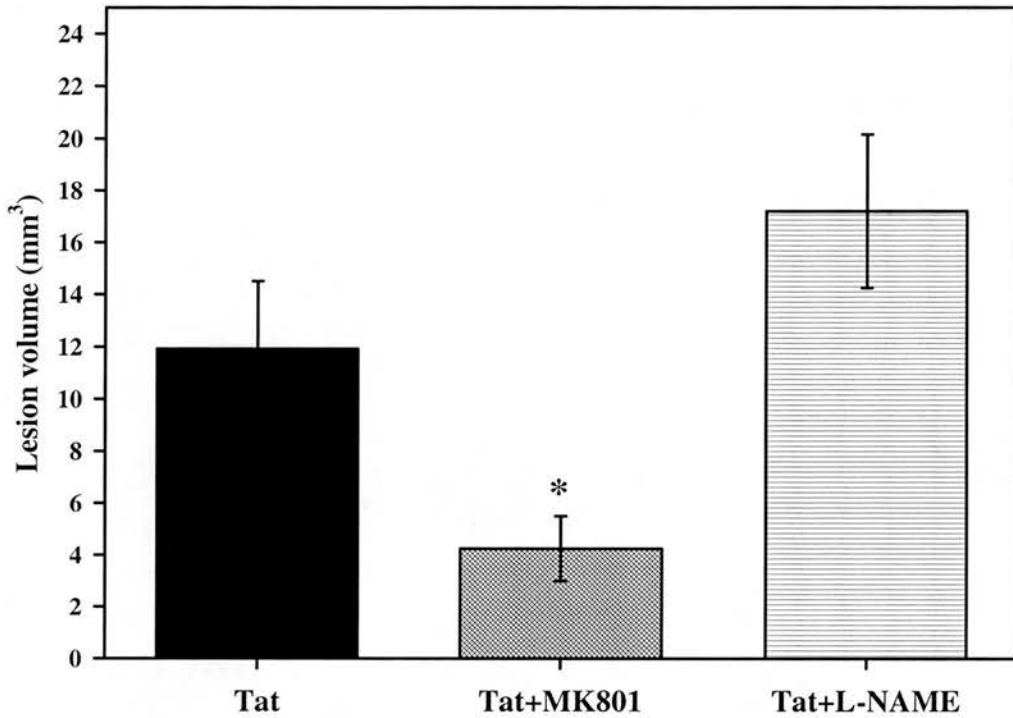


Fig. 5.14: Effect of neuroprotectants on the MVV tat peptide induced NeuN lesion at 1 hour.

Statistical analysis using a one-way ANOVA revealed a significant effect of treatment on lesion volume ($p < 0.05$). Post-hoc analysis showed the administration of MK801 ($n=7$) to significantly reduce the volume of the lesion caused by the MVV tat peptide ($n=18$, Duncan test, $*p < 0.05$), but the administration of L-NAME ($n=5$) did not. Results: Mean \pm SEM.

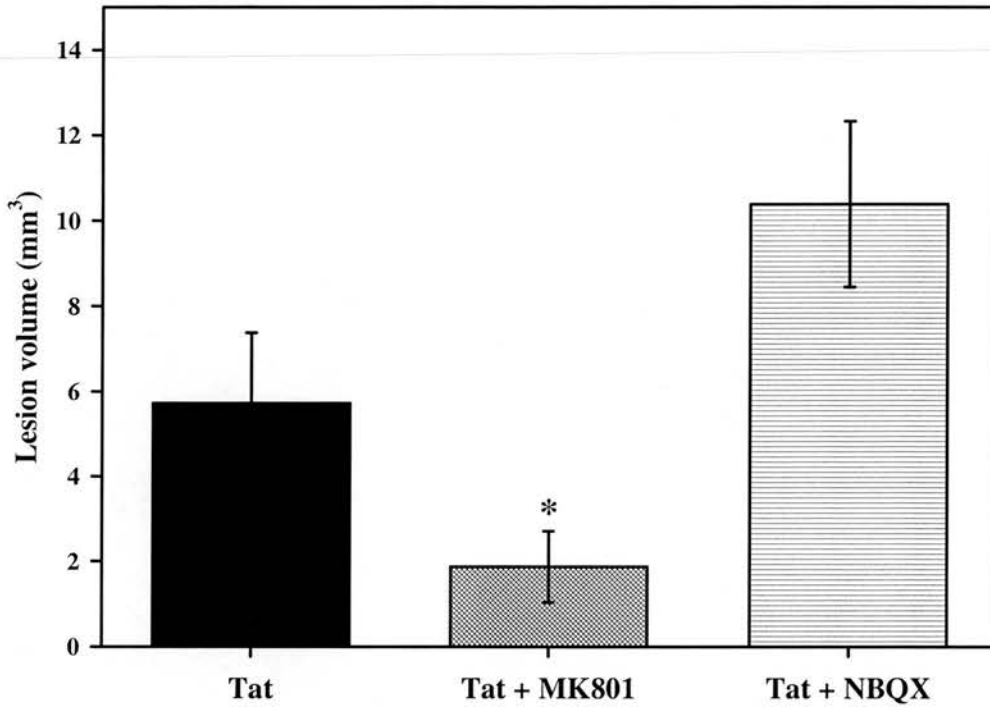


Fig. 5.15: Effect of neuroprotectants on the MVV tat peptide induced GFAP lesion at 1 hour.

The administration of MK801 (n=7) significantly reduced the volume of the GFAP lesion caused by the injection of MVV tat peptide (n=12, one-way ANOVA and post-hoc Duncan test, * $p < 0.05$). The administration of L-NAME (n=5) did not cause any significant difference to the lesion volume. Results: Mean \pm SEM.

5.3.3. Electron Microscopy

Observation at the ultrastructural level of the lesion induced by the MVV tat peptide at one hour revealed necrosis, but no apoptotic cells. Apoptosis and necrosis are readily distinguishable by the morphological characteristics of dying cells. Necrosis causes an increase in cell volume, swelling of intracellular organelles, and eventual lysis. In contrast, apoptotic cells gradually become digested. Endogenous proteases are activated, causing cytoskeletal disruption, cell shrinkage and membrane blebbing. Mitochondrial function is also lost. Endonucleases are activated to degrade DNA into oligonucleosomal fragments, and the nuclear chromatin becomes condensed. Throughout this process, membrane integrity is preserved until the cell is phagocytosed. Inspection of neurons at the centre of the lesion, revealed no chromatin condensation in the nucleus or membrane blebbing (Fig. 5.16). In the 'halo' area surrounding the centre of the lesion, massive tissue disruption was evident and no recognisable cell types could be identified. Glia at the centre of the MVV tat peptide lesion presented vacuolated and disrupted cytoplasm (Fig. 5.17).

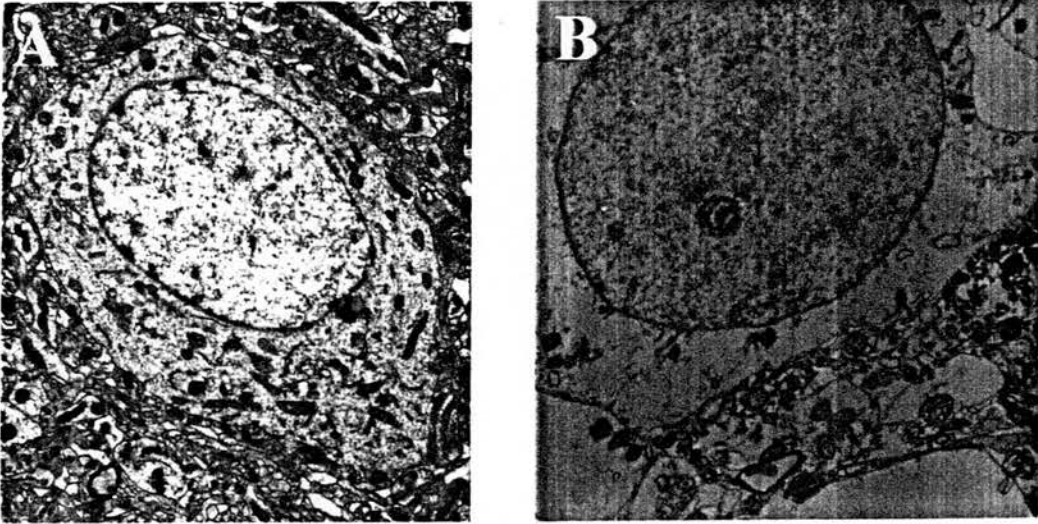


Fig. 5.16: Electron microscopy of neurons at the site of the lesion caused by MVV tat peptide.

A. No lesion **B.** Injection of 1 μ l MVV tat peptide. The cytoplasm of neurons in the striatum injected with MVV tat peptide is disrupted, but there is no evidence of chromatin condensation of the nucleus, or of membrane blebbing.

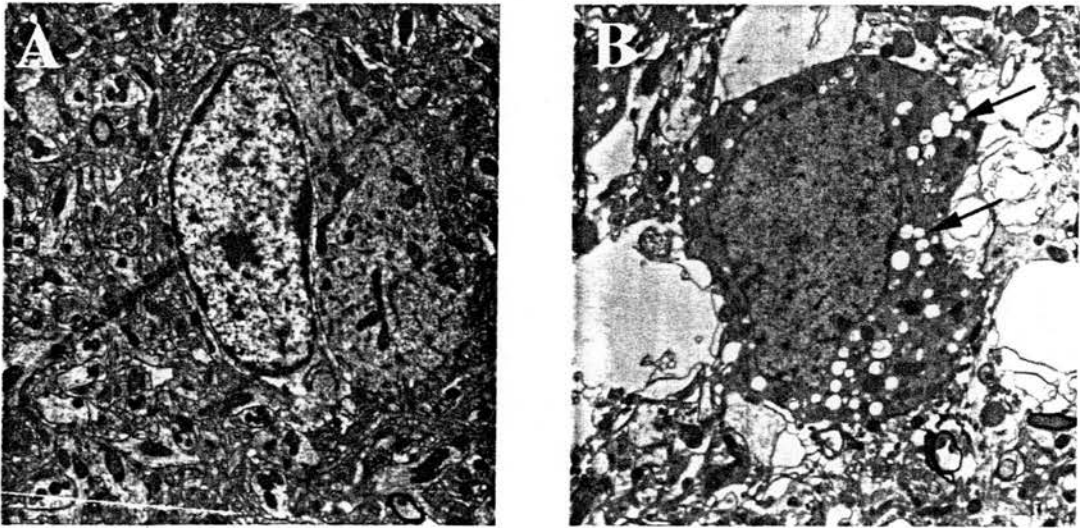


Fig. 5.17: Electron microscopy of glial cells at the site of the lesion caused by MVV tat peptide.

A. Normal striatum **B.** Injection of 1 μl MVV tat peptide. In the injected striatum, glia present vacuolated cytoplasms (arrows).

5.4. DISCUSSION.

The present experiments demonstrate the acute *in vivo* neurotoxicity of a peptide derived from the basic region of the MVV transactivating protein Tat. Lentiviral Tat and related peptides have previously found to be neurotoxic *in vitro* and *in vivo* (Gourdou *et al.*, 1990, Sabatier *et al.*, 1991, Hayman *et al.*, 1993, Strijbos *et al.*, 1995, New *et al.*, 1997), although their effects have not been studied at the short time courses investigated here. The current experiments therefore provide further evidence for the neurotoxic potential of this viral protein. Although the doses investigated here may be deemed high, Tat has been shown to be released in the vicinity of infected cells (Frankel and Pabo, 1988), and its levels may become elevated in the neighbourhood of the many infected cells, commonly surrounding glial nodules.

MVV tat peptide exerts, in these experiments, a very rapid disruption of neurons and astrocytes. It is possible that the lack of staining with NeuN does not in fact reflect the loss of neurones, although there are experiments which certainly indicate that it is a sensitive marker for healthy neurons (Wolf *et al.*, 1996). It is possible that some form of rapid degradation of the nuclear marker has reduced the staining, perhaps by some loss of access to the epitope recognised by the monoclonal antibody due to some modification of the antigen or neighbouring proteins in the nucleus. Nevertheless, the size of the lesions observed with this method and with the markers for gliosis in the same sections is very similar. Perhaps more strikingly, the volumes of the lesion detected by different methods in earlier work (Hayman *et al.*, 1993), are very similar to those detected by the loss of NeuN staining. Together these observations suggest that the lack of staining leads to, even if it does not immediately represent, the loss of viable neurones. MVV tat peptide causes a significantly greater acute NeuN lesion than the control substances saline, ibotenic acid, ovalbumin peptide and L-NAME. Similarly, MVV tat peptide causes significantly greater astrocytosis in the striata of injected rats than any of the control substances. These lesions increase consistently over time between 30 minutes and 24 hours after administration, and approximate the size of lesions observed one week post-operatively. Overall, the astrocytic lesion remains smaller than the neuronal lesion, and this may reflect a greater sensitivity of neurons to the MVV tat peptide, or may indicate a slower initiation of astroglial responses.

The lack of a lesion after injection of the well-known neurotoxin, ibotenic acid,

points to the dramatically short time course of these experiments. At one week after the injection of the same dose of ibotenic acid caused a lesion almost double the size of that seen after the dose of MVV tat peptide used in these experiments (Hayman *et al.*, 1993). Yet the peptide induced damage is almost as large at 1 hr as it is at one week. Preliminary tests with injections of endothelin close to the middle cerebral artery, which cause large lesions after 24 hr (Sharkey and Butcher, 1998), also show the damage after MVV tat peptide to occur more rapidly than the anoxic damage following arterial occlusion (Sharkey, Starling, Arbuthnott – unpublished).

The unusual profile of the lesion caused by the MVV tat peptide, with a surrounding 'halo' lacking neuronal staining, may be due to a number of actions of the peptide. Oedema surrounding the injection site is one possible explanation. The actions of the MVV tat peptide may also be amplified at distant sites due to neuronal glutamate release and increased receptor occupation. This may cause a greater number of neurons to die at the edges of the injection site. Indeed, lentiviral Tat has been shown to depolarise neurons (Magnusson *et al.*, 1994), and may exert its neurotoxic effects via an overstimulation of calcium entry through glutamate receptors, to cause excitotoxicity (Strjibos *et al.*, 1995, Hayman *et al.*, 1993). The present experiments also support this, as the administration of MK801, an NMDA glutamate receptor antagonist, reduces the volume of the lesion caused by the MVV tat peptide at 1 hour. The administration of L-NAME did not cause any reduction in MVV tat peptide induced lesion volume in these acute experiments, and the testing of an AMPA receptor antagonist and a TNF α inhibitor did not reveal any conclusive actions of these molecules on the lesion volume. Therefore, in the short term at least, the neurotoxic mechanisms of the MVV tat peptide appear to be mediated by actions at glutamate receptors on neurons. In the longer term, however, the detrimental actions of this peptide on neurons may involve other mediators such as NO and cytokines.

In an early description of the disease caused in sheep by MVV infection Georgsson (1977) describes neuronal damage in areas of liquefactive necrosis as early as one month after the infection. Although the doses we have used are large, these doses were effective in producing large lesions in the longer-term studies (Hayman *et al.*, 1993). The aim of these experiments was less to model the disease than to examine the dynamics of neuronal damage by this agent. If this peptide has any role in the generation of the neurotoxicity in the disease then it will only be after the toxin has

accumulated in the region of glial nodules containing infected cells. Should the peptide be made in any quantity during the metabolism of Tat released from such accumulations of infected cells, then rapid and permanent neuronal damage seems inevitable.

CHAPTER 6: DISCUSSION

The present experiments allow some limited conclusions regarding neuropathological mechanisms in MVV infection to be drawn. The aims of the work carried out here were i) to investigate whether macrophages infected with MVV caused any neural changes after injection *in vivo*, in the absence of other cell mediated immune effectors, ii) to test the neurotoxic potential of MVV infected macrophage products *in vitro*, and iii) to probe the acute *in vivo* neurotoxic effects of a peptide derived from lentiviral Tat protein.

6.1. EFFECTS OF MVV INFECTED MACROPHAGES ON *SCID* CNS.

The effects of MVV on the CNS of infected sheep have been attributed to the actions of mediators arising from circulating immune cells. To investigate any possible role of MVV infected macrophages on neural cells, immunodeficient (*scid*) mice were used, thus eliminating the contribution of cell-mediated immune responses.

The injection of live macrophages into *scid* mouse paranchyma caused significant short term astrogliosis and microgliosis, as well as significant longer term microgliosis. This was measured by estimating the extent of GFAP and F4/80 induction, and was replicated in experiments where macrophages were removed from their culture vessel by two different methods. GFAP induction was measurable one week after the delivery of MVV infected macrophages to *scid* mouse striatum. However, 3 weeks post-operatively the amount of GFAP staining induced by MVV infected macrophages was not significantly different from that incurred by uninfected macrophages. F4/80 induction at this time point, however, remained significantly more elevated when MVV infected macrophages, as opposed to uninfected macrophages, were injected. These results strongly suggest that MVV infected macrophages cause short term astrogliosis and long term microgliosis. These two events can be considered markers for inflammation within the CNS, and are characteristic of natural MVV infection of sheep (Georgsson *et al.*, 1977). Of the two events, the prolonged microgliosis is suggested here as the more important phenomenon. Although the experimental *scid* mouse model described in this thesis is removed from the natural disease, it allows the plausible speculation that the invasion of macrophages in the CNS of MVV diseased sheep may account, either in whole or in part, for the establishment of microgliosis in CNS lesions. Indeed, it has also been

recently independantly reported that MHC antigen expression on microglia correlates with the severity of lesions in experimentally MVV infected sheep (Bergsteinsdottir *et al.*, 1998).

Certain technical considerations regarding the transplantation of macrophages into *scid* mouse CNS were deemed problematic. Firstly, the possibility that macrophages had become lysed during removal from their culture flask and before injection into *scid* mice was taken into consideration. Experiments were carried out using deliberately lysed macrophage injections into *scid* mouse CNS, to investigate whether these had the same effects as live macrophages. These experiments showed that lysed macrophages were, in fact, able to cause F4/80 up-regulation, but not GFAP up-regulation. However, lesion volumes obtained with killed macrophages were smaller than those caused by live macrophages. This suggests that killed macrophages may have a slight effect on the induction of microgliosis, but, overall, have a lesser effect on *scid* parenchyma than live macrophages.

Up-regulation of F4/80 staining by lysed macrophages may be due to the spillage of cellular contents into the injection medium. The effects of many macrophage cellular components on brain parenchyma are not documented and therefore any conclusions as to the method of action of lysed macrophages on F4/80 induction are impossible. If one infers, however, that some lysed macrophages were contained within the cell preparations of macrophages scraped off the tissue culture flasks, then the effect of the live macrophages may be combined with the effect of lysed macrophages in causing F4/80 induction.

However, experiments using macrophages which were removed from their culture flask using warm versene, a less disruptive procedure, showed similar results to experiments where macrophages were gently scraped off their culture vessel. Versene-removed macrophages caused significantly more GFAP and F4/80 staining when they were MVV infected as compared to when they were uninfected. The extent of GFAP and F4/80 activation was comparable between macrophages removed from culture flasks with versene, and those removed by gentle scraping. This result reinforces the putative causative effect of live MVV infected macrophages on astrocytosis and microgliosis.

Astrocytosis and microgliosis are characteristics of the natural MVV disease in sheep (Georgsson *et al.*, 1977), and macrophages infiltrate the CNS in experimental infection (Georgsson *et al.*, 1979). The short lived increase in GFAP expression observed here probably corresponds to changes in astrocyte morphology and number, in response to changes in the local brain microenvironment. These changes have been found to occur in response to several different types of injury within the CNS (Landis 1994). The return of GFAP expression to background levels 3 weeks after the injection of MVV infected macrophages, may reflect the dynamics of astrocytes returning to steady-state functions. Changes in F4/80 expression reflect the activation of microglia. As with astrocytes, activation of these cells results in an altered physiological state, resulting in the upregulated expression of several inflammatory mediators. Increases in F4/80 induction may also reflect increased recruitment of monocytes from the circulation. In other models of injury to the CNS, monocytes are recruited, after a delay, to the site of injury (Marty *et al.*, 1991). This recruitment is the result of a chemokine signal attracting fresh monocytes to the area. This chemokine agent may be released by activated microglia or by the injected macrophages. Therefore, MVV infected macrophages may play a role in the establishment of the astrocytosis and microgliosis observed in MVV infection. However, this is not to assume that they are the sole effectors causing this pathology in MVV infection, although these experiments support this possible role.

The lack of significant effects of free virus on GFAP and F4/80 expression would seem to suggest the presence of a mediator released by MVV infected macrophages to cause astrocytosis and microgliosis, as opposed to a direct effect of the virus. p25 immunostaining did not localise MVV either when this was injected alone, or in MVV infected macrophages. The lack of p25 staining would suggest that the virus was no longer present within the striata of *scid* mice. Antibodies directed against ovine CD14, however, did reveal the presence of injected macrophages within the striatum of *scid* mice. Several suggestions are possible to explain the lack of p25 staining. For the injections of free virus alone, MVV may have been cleared from *scid* striatum, perhaps through extracellular fluid drainage. Another possibility is that MVV has become latent in *scid* tissue. Productive MVV replication is readily observed in cells *in vitro*, but *in vivo* environments have been observed to down

regulate the activity of MVV replication. For example, MVV injected into sheep joints, in models of the arthritic aspects of the disease, can be detected at short intervals post-injection, but the detection rate decreases with time, although pathology still becomes manifest. Similarly here, replication of MVV in *in vivo* environments may become latent. This would account for the lack of p25 staining in both the free virus injected animals and the MVV infected macrophage injected animals. Furthermore, in several accounts of the naturally occurring MVV disease, neuropathology is observed without the detection of specific viral antigens (Georgsson *et al.*, 1977; Georgsson *et al.*, 1982; Bergsteinsdottir *et al.*, 1998).

A more reliable predictor of cellular activation following MVV infection resides in the cytokine profile of infected cells. Infection of alveolar macrophages results in increased levels of IL-8 and IL-1 β mRNA *in vitro* (Legastelois *et al.*, 1998), and elevated levels of IL-8 mRNA and TGF β expression *in vivo* (Moreno *et al.*, 1998). Other investigators report augmented levels of TNF α mRNA in MVV infected microglia and macrophages (B. Ebrahimi, personal communication; Zhang *et al.*, in preparation). RT-PCR performed on the blood borne macrophages destined for injection into *scid* mice, found a threefold increase in IL-1 β mRNA levels when these were infected with MVV *in vitro*. This is taken to signify that these cells were in a state of activation after infection with MVV and at the time of transplantation into *scid* mice. This activation may also serve to explain the dichotomy between the effects of macrophages in *scid* parenchyma and the lack of staining for viral antigens.

The increased synthesis of IL-1 β mRNA in MVV infected macrophages may also represent a pro-inflammatory mediator released from MVV infected macrophages to cause astrocytosis and microgliosis in *scid* mouse brain. The pro-inflammatory effects of IL-1 β both in the CNS and in the periphery are well documented. Although this is an attractive hypothesis, further experiments would be needed to detect any ovine IL-1 β in *scid* parenchyma following injection of MVV infected macrophages. Furthermore, the putative species specificity of ovine and murine cytokines would need to be addressed.

Many other mediators have been proposed as neurodegenerative effectors in lentiviral infections. These include viral proteins. Of these, the lentiviral protein Tat has been shown to be released from HIV infected cells (Frankel and Pabo, 1988), and

has been shown to cause seizures *in vivo* in mice, accompanied by astrocytosis and neuronal loss (Philippon *et al.*, 1994). Recently also, HIV Tat has been proposed as a chemokine (Conant *et al.*, 1998). Speculation might allow the proposal that Tat may be released from MVV infected macrophages, to cause astrocytosis and microgliosis, as well as act as a chemoattractant for monocytes circulating in the periphery. It is also possible that MVV Tat may attract other monocyte/macrophage cells to the CNS of *scid* mice, and that the presence of these is required for any neuroinflammation. However, the effects of macrophages in the absence of other cell mediated immune responses on astrocytes and microglia, suggest a contributory role for these cells and their released products in the neuropathology of MVV infection.

6.2. EFFECTS OF MACROPHAGE PRODUCTS AND MVV TAT PEPTIDE ON NEURONS *IN VITRO*.

Injection of MVV infected macrophages did not cause any obvious neuronal or myelin loss in *scid* mice. The aim of testing macrophage supernatant on neuronal cultures was to investigate whether macrophage products could exert any neurotoxic action in a different experimental setting. The results showed that, indeed, supernatant obtained from MVV infected macrophages was significantly more neurotoxic than supernatant obtained from uninfected macrophage cultures.

Many molecules may be responsible for exerting this neurotoxic action. As previously mentioned, the cytokine release profile of MVV infected macrophages may be altered in MVV infection. MVV infection has been shown to increase TNF α mRNA expression in alveolar macrophages and microglia (B. Ebrahimi, personal communication; Zhang *et al.*, in preparation), as well as IL-8 mRNA and TGF β expression *in vivo* (Legastelois *et al.*, 1998; Moreno *et al.*, 1998). MVV infected macrophage supernatant may also contain many other mediators responsible for the observed neurotoxicity. Among these are viral proteins such as envelope glycoproteins and Tat protein.

Lentiviral Tat has been shown to be released from infected cells (Frankel and Pabo, 1988), and bears some sequence homology to snake venom neurotoxins (Garry and Koch, 1992). Peptides derived from the MVV Tat protein have previously been found to be neurotoxic *in vitro* (Strijbos *et al.*, 1995). In an effort to evaluate the time

course of MVV tat peptide neurotoxicity *in vitro*, MVV tat peptides were synthesized and applied to rat cortical neurons. Neurotoxicity was evaluated based on both total cell viability and total cell death. The results revealed that MVV tat peptide begins to exert neurotoxic actions after 24 hours incubation with neurons. This was suggested by the increase in LDH release, but was not similarly reflected by decreased MTS reduction in neuronal cultures. It must therefore be emphasised that a neurotoxic action of MVV tat peptide is only suspected at this time point. However, by 48 and 72 hours, a definite neurotoxic effect of MVV tat peptide is evident, as the peptide causes both significantly increased LDH release and decreased MTS reduction, when compared to a control proteinaceous compound and a medium change alone. These represent new observations, in particular the observed neurotoxicity at 48 hours, as previous experiments only document MVV tat peptide toxicity at 72 hours (Strijbos *et al.*, 1995). However, whilst these experiments point to a neurotoxic action of MVV tat peptide, they cannot confirm the existence of this peptide in the supernatant of MVV infected macrophages. It is possible that MVV Tat protein is present in the supernatant of MVV infected macrophages, but a detailed chemical analysis of this supernatant would be necessary in order to ascertain its composition.

Previous experiments have attributed the neurotoxicity of MVV tat peptide *in vitro* to an action occurring through NMDA receptors and involving excessive calcium influx at 72 hours (Strijbos *et al.*, 1995). Femtomolar concentrations of HIV Tat have also recently been reported as causing depolarisations to neurons in culture, possibly via an action on AMPA receptors (Cheng *et al.*, 1998). These experiments suggest a rapid action of MVV tat peptide in causing neurotoxicity. In an effort to further investigate this action, and underlying mechanisms, toxicity studies were carried out *in vivo*.

6.3 EFFECTS OF LENTIVIRAL TAT PEPTIDES *IN VIVO*.

MVV tat peptide has previously been found to be neurotoxic to rat striatum *in vivo* as have HIV tat peptides (Gourdou *et al.*, 1990; Hayman *et al.*, 1993; Philippon *et al.*, 1994). Most of these reports document a neurotoxicity occurring one week after the administration of peptides *in vivo*. The previous experiments carried out here point to a neurotoxic action of MVV tat peptide occurring rapidly *in vitro*. The effects of MVV

tat peptide application *in vivo* have not been investigated at short time courses. Although the relevance of MVV tat peptide neurotoxicity to the naturally occurring disease has previously been thought of as limited, lentiviral Tat has been implicated as a contributory agent to neuronal demise in other lentiviral infections, notably HIV (Lipton 1992a). If Tat were to have a role in the establishment of lentiviral neuropathologies, then the dynamics of this agent are of interest. The aim of these experiments was therefore to investigate the time course of the neurotoxicity of MVV tat peptide *in vivo* as well as its possible mechanisms of neurotoxicity. The results suggest that MVV tat peptide may play a role in the neuropathology of the naturally occurring disease.

The application of MVV tat peptide to rat striatum caused neurotoxicity rapidly, within 30 minutes of application. This was assessed by decreased NeuN staining. NeuN is a relatively unconventional neuronal marker but has been reliably proven to stain neurons (Wolf *et al.*, 1996). GFAP induction was also caused by MVV tat peptide 30 minutes post-operatively. These results were replicated 1 hour after administration, and caused significantly larger effects than the application of control substances. After 24 hours recovery, animals injected with MVV tat peptide developed a neuronal lesion of the same order of magnitude as that observed one week post-operatively (Hayman *et al.*, 1993). All neuronal subtypes were affected by the administration of MVV tat peptide, including cholinergic interneurons, parvalbumin positive neurons, and diaphorase positive neurons.

The appearance of the NeuN lesion was distinctive with intense neuronal disruption at the centre of the injection site, surrounded by an area lacking staining. This may reflect oedema surrounding the injection site, or an increased vulnerability of neurons at sites more distant from the injection site. If MVV tat peptide is exerting its actions through a specific receptor on neurons, the mechanisms of this vulnerability may reflect receptor occupancy effects. It is possible that at the centre of the lesion, receptor sites may become saturated, whilst at the edges of the lesion the action of MVV tat peptide may be amplified by neuronal glutamate release. Similar lesions were observed with GFAP staining, and may reflect similar dynamics. The GFAP induction was smaller in size than the NeuN lesion and may reflect a greater vulnerability of neurons to this neurotoxic agent, or a slower activation of GFAP. The

doses of MVV tat peptide used in these experiments were high. The minimum amount of MVV tat peptide shown to cause neurotoxicity *in vivo* has previously been shown to be 0.5nmol (Hayman *et al.*, 1993). However, the doses used here represent effective amounts to cause neurotoxicity, as previously determined. Moreover, comparable amounts of ibotenic acid, a known neurotoxin, do not cause neurotoxicity *in vivo* at the short time courses studied here. It is also plausible to comment that large amounts of MVV Tat protein may be released in the vicinity of MVV infected cells within the CNS of diseased sheep. The release of this agent and its accumulation may cause eventual neurotoxicity.

The neurotoxic mechanisms of MVV tat peptide have been ascribed to NO-mediated glutamate actions, one week post-operatively *in vivo* (Hayman *et al.*, 1993). Cytokines, in particular TNF α , have also been implicated as mediators contributing to MVV tat peptide mediated neurotoxicity (Philippon *et al.*, 1994). In an effort to ascertain whether any of these mechanisms may be operating at the time points studied here, neuroprotection experiments were carried out using MK801, an NMDA receptor antagonist, NBQX, an AMPA receptor antagonist, L-NAME, a NOS inhibitor, and α MSH, a TNF α inhibitor. Since the NeuN lesion observed at 1 hour post-injection to the striatum was comparable in magnitude to that seen at 24 hours and 1 week, this time point was chosen for the neuroprotection studies. Preliminary experiments using NBQX and α MSH did not reveal any significant effects of these agents on the MVV tat peptide induced neuronal lesion, although NBQX did seem to reduce the volume slightly. MK801 did, however, significantly reduce both the amount of neuronal loss and GFAP induction. This points to an action of MVV tat peptide on NMDA receptors to cause neurotoxicity. However, the role of cytokines, AMPA receptors and NO in aiding this neurotoxicity was not confirmed. This is not to say that these agents do not contribute to any observed neurotoxicity at later time points.

Limited experiments were carried out with HIV tat peptide. This agent caused the same lesion profile as MVV tat peptide, notably the disappearance of NeuN staining surrounding the injection site. Experimental animal numbers were small, due to the limited availability of the HIV tat peptide, and were thus omitted from statistical analysis.

6.4. CONCLUSIONS AND FUTURE DIRECTIONS

The present experiments permit certain conclusions. Firstly, macrophages may contribute to the establishment of neuropathology in MVV infection. This may be suggested by the actions of MVV infected macrophages on astrocytes and microglia in *scid* mice. Secondly, MVV tat peptide is rapidly neurotoxic to neurons *in vitro* and *in vivo*, and its actions can be inhibited by the glutamate receptor antagonist MK801. Although these experiments cannot suggest a link between the actions of macrophages on *scid* tissue and the neurotoxicity of MVV tat peptide, it may be plausible to suggest that MVV Tat is released from MVV infected macrophages to contribute to neurodegeneration. This molecule may also act as a chemokine to attract other cells to the CNS. However, this was not examined in the present experiments.

Future experiments would be needed to clarify the presence of MVV within *scid* CNS at differing time points. Although no virions were detected by the monoclonal antibody to p25 within the CNS of *scid* mice one week after the administration of MVV infected macrophages, they may be present at earlier time points. Also, although no neuronal loss was evident in *scid* mice in these experiments, the possibility of this occurrence may be explored at later time points, using more quantitative methods. A more detailed chemical analysis of macrophage supernatants would be essential for the determination of the presence of putative inflammatory mediators and neurodegenerative molecules such as Tat protein, gp135, NTox, PAF, NO and numerous others. Further experiments would also be carried out involving the MVV tat peptide. Neuronal excitatory properties should be investigated, possibly by using patch-clamping techniques, and the ability of other, more specific, agents to block the effects of this peptide may clarify the mechanism of action of this neurotoxic agent.

BIBLIOGRAPHY

- Aggoun-Zouaoui, D., Charriaud-Marlangue, C., Rivera, S., Jorquera, I., Ben-Ari, Y., Represa, A. The HIV-1 envelope protein gp120 induces neuronal apoptosis in hippocampal slices. *NeuroR*. 1996; **7**: 433-6.
- Anderson, A.A., Harkiss, G.D., Watt, N.J. Quantitative analysis of immunohistochemical changes in the synovial membrane of sheep infected with Maedi-Visna virus. *Clin. Immunol. Immunopathol*. 1994; **72**: 21-9.
- Andiman, W.A., Eastman, R., Martin, K., Katz, B.Z., Rubinstein, A., Pitt, J., Pahwa, S., Miller, G. Opportunistic lymphoproliferations associated with Epstein-Barr viral DNA in infants and children with AIDS. *Lancet*. 1985; **2**: 1390-3.
- Araujo, D.M., Cotman, C.W. Trophic effects of interleukin-4, -7 and -8 on hippocampal neuronal cultures: potential involvement of glial-derived factors. *Brain Res*. 1993; **600**: 49-55.
- Arya, S.K., Guo, C., Josephs, S.F., Wong-Staal, F. Trans-activator gene of human T-lymphotropic virus type III (HTLV-III). *Science* 1985; **229**: 69-73.
- Arya, S.K., Beaver, B., Jagodzinski, L., Ensoli, B., Kanki, P.J., Albert, J., Fenyo, E., Biberfeld, G., Zagury, J.F., Laure, F., *et al*. New human and simian HIV related retroviruses possess functional transactivator (tat) gene. *Nature* 1987; **328**: 548-50.
- Bagasra, O., Lavi, E., Bobroski, L., Khalili, K., Pestaner, J.P., Tawadros, R., Pomerantz, R.J. Cellular reservoirs of HIV-1 in the central nervous system of infected individuals: identification by the combination of *in situ* polymerase chain reaction and immunohistochemistry. *AIDS* 1996; **10**: 573-85.
- Bagasra, O., Bobroski, L., Sarker, a., Bagasra, A., Siakumari, P., Pomerantz, J. Absence of the inducible form of nitric oxide synthase in the brains of patients with the acquired immunodeficiency syndrome. *J. Neurovirol*. 1997; **3**: 153-67.
- Bagetta, G., Corasaniti, T.M., Finazzi-Agro, A., Nistico, G. Does the HIV-1 coat protein gp120 produce brain damage? *TIPS* 1994; **15**: 362-3.
- Baldeweg, T., Soorana, S., Das, I., Catalan, J., Gazzard, B. Serum nitrite concentration suggests a role for nitric oxide in AIDS. *AIDS* 1996; **10**: 451-2.
- Banati, R.B., Gehrman, J., Schubert, P., Kreutzberg, G.W. Cytotoxicity of microglia. *Glia* 1993; **7**: 111-8.
- Barbour, B., Brew, H., Attwell, D. Electrogenic glutamate uptake in glial cells is activated by intracellular potassium. *Nature* 1988; **335**: 433-5.
- Barger, S.W., Horster, D., Furukawa, K., Goodman, Y., Kriegelstein, J., Mattson, M.P. Tumour necrosis factor α and β protect neurons against amyloid β -peptide toxicity: evidence for involvement of a kB-binding factor and attenuation of peroxide and Ca^{2+}

accumulation. *Proc. Natl. Acad. Sci. USA* 1995; **92**: 9328-32.

Barna, B.P., Estes, M.L., Jacobs, B.S., Hudson, S., Ransohoff, R.M. Human astrocytes proliferate in response to tumor necrosis factor alpha. *J. Neuroimmunol.* 1990; **30**: 239-43.

Belman AL, Lantos G, Houroupan D, Novick BE, Ultmann MH, Dickson DW, and Rubinstein A. AIDS: Calcification of the basal ganglia in infants and children. *Neurol.* 1986;361192-9.

Benos, D.J., Hahn, B.H., Shaw, G.M., Bubien, J.K., Benveniste, E.N. Gp120-mediated alterations in astrocyte ion transport. *Adv. Neuroimmunol.* 1994; **4**: 175-9.

Benveniste, E.N., Kwon, J., Chung, W.J., Sampson, J., Pandya, K., Tang, L.P. Differential modulation of astrocyte cytokine gene expression by TGF- β 1. *J. Immunol.* 1994; **153**: 5210-21.

Bergsteinsdottir, K., Arnadottir, S., Torsteinsdottir, S., Agnarsdottir, G., Andresdottir, V., Petursson, G., Georgsson, G. Constitutive and visna virus induced expression of class I and II major histocompatibility complex antigens in the central nervous system of sheep and their role in the pathogenesis of visna lesions. *Neuropath. Appl. Neurobiol.* 1998; **24**: 224-32.

Berman, A., Espinoza, L.R., Diaz, J.D., Aguilar, J.L., Rolando, T., Vasey, F.B., Germain, B.F., Lockey, R.F. Rheumatic manifestations of human immunodeficiency virus infection. *Am. J. Med.* 1988; **85**: 59-64.

Bevilacqua, M.P., Pober, J.S., Mendrick, D.L., Cotran, R.S., Gimbrone, M.A. Identification of an inducible endothelial-leukocyte adhesion molecule. *Proc.Natl.Acad.Sci.USA* 1987; **84**: 9238-42.

Bevilacqua, M.P., Nelson, R.M. Selectins. *J. Clin. Invest.* 1993; **91**: 379-87.

Bezzi, P., Carmignoto, G., Pasti, L., Vesce, S., Rossi, D., Rizzini, B.L., Pozzan, T., Volterra, A. Prostaglandins stimulate calcium-dependant glutamate release in astrocytes. *Nature* 1998; **391**: 281-4.

Black, K.L., Hoff, J.T. Leukotrienes increase the blood-brain barrier permeability following intraparenchymal injections in rats. *Ann. Neurol.* 1985; **18**: 349-51.

Blumberg, B.M., Gelbard, H.A., Epstein, L.G. HIV-1 infection of the developing nervous system: central role of astrocytes in pathogenesis. *Virus Res.* 1994; **32**: 253-67.

Bochner, B.S., Luscinskas, F.W., Gimbrone, M.A.J., Newman, W., Sterbinsky, S., Derse-Anthony, C.P., Klunk, D., Schleimer, R.P. Adhesion of human basophils, eosinophils, and neutrophils to interleukin 1-activated human vascular endothelial cells: contributions of endothelial cell adhesion molecules. *J. Exp. Med.* 1991; **173**: 1553-6.

Bolam, J.P., Wainer, B.H., Smith, A.D. Characterization of cholinergic neurons in the rat neostriatum A combination of choline acetyltransferase immunocytochemistry,

Golgi-impregnation and electron microscopy. *Neurosci.* 1984; **12**: 711-8.

Bourdiol, F., Toulmond, S., Serrano, A., Benavides, J., Scatton, B. Increase in ω 3 (peripheral type benzodiazepine) binding sites in the rat cortex and striatum after local injection interleukin-1, tumour necrosis factor- α and lipopolysaccharide. *Brain Res.* 1991; **543**: 194-200.

Bowman, C.L., Kimelberg, H.K. Excitatory amino acids directly depolarize rat brain astrocytes in primary culture. *Nature* 1984; **311**: 656-9.

Brahic, M., Filippi, P., Vigne, R., Haase, A.T. Visna virus RNA synthesis. *J. Virol.* 1977; **24**: 74-81.

Braun, M.J., Clements, J.E., Gonda, M.A. The visna virus genome, evidence for a hyper variable site in the *env* gene and sequence homology among lentivirus envelope proteins. *J. Virol.* 1987; **61**: 4046-54.

Brenneman, D.E., Westbrook, G.L., Fitzgerald, S.P., Ennist, D.L., Elkins, K.L., Ruff, M.R., Pert, C.B. Neuronal cell killing by the envelope glycoprotein of HIV and its prevention by vasoactive intestinal peptide. *Nature* 1988; **335**: 639-42.

Brenneman, D.E., McCune, S.K., Mervis, R.F., Hill, J.M. Gp120 as an etiologic agent for NeuroAIDS: neurotoxicity and model systems. *Adv. Neuroimmunol.* 1994; **4**: 157-65.

Brew, H., Attwell, D. Electrogenic glutamate uptake is a major current carrier in the membrane of axolotl retinal ganglion cells. *Nature* 1987; **327**: 707-9.

Brosnam, C.F., Selmaj, K., Raine, C.S. Hypothesis: a role for tumor necrosis alpha in immune mediated demyelination and its relation to Multiple Sclerosis. *J. Neuroimmunol.* 1988; **18**: 87-94.

Bruce, A.J., Boling, W., Kindy, M.S., Peschon, J., Kraemer, P.J., Carpenter, M.K., Holtsberg, F.W., Mattson, M.P. Altered neuronal and microglial responses to excitotoxic and ischemic brain injury in mice lacking TNF receptors. *Nature Med.* 1996; **2**: 788-94.

Budka, H. Multinucleated giant cells in brains: a hallmark of the acquired immunodeficiency syndrome. *Acta Neuropath.* 1986; **69**: 253-8.

Budka, H. Neuropathology of human immunodeficiency virus infection. *Brain Pathol.* 1991; **1**: 163-75.

Bukrinsky, M.I., Nottet, H.S.L.M., Schmidtayerova, H., Dubrovsky, L., Flanagan, C.R., Mullins, M.E., Lipton, S.A., Gendelman, H.E. Regulation of nitric oxide synthase activity in Human Immunodeficiency Virus Type 1 (HIV-1)-infected monocytes: implications for HIV-associated neurological disease. *J. Exp. Med.* 1995; **181**: 735-45.

Buonaguro, L., Barillari, G., Chang, H.K., Bohan, C.A., Kao, V., Morgan, R., Gallo, R.C., Ensoli, B. Effects of the Human Immunodeficiency Virus Type 1 on the

expression of inflammatory cytokines. *J. Virol.* 1992; **66**: 7159-67.

Buskila, D., Gladman, D. Musculoskeletal manifestations of infection with human immunodeficiency virus. *Rev. Infect. Dis.* 1990; **12**: 223-35.

Buttini, M., Appel, K., Sauter, A., Gebicke-Haerter, P., Boddeke, H.W.G.M. Expression of tumor necrosis factor alpha after focal cerebral ischaemia in the rat. *Neurosci.* 1996; **71**: 1-16.

Campbell, I.L., Abraham, C.R., Masliah, E., Kemper, P., Inglis, J.D., Oldstone, M.B.A., Mucke, L. Neurologic disease induced in transgenic mice by cerebral overexpression of interleukin 6. *Proc. Natl. Acad. Sci. USA* 1993; **90**: 10061-5.

Carey, N., Dalziel, R.G. The biology of Maedi Visna Virus-an overview. *Br. Vet. J.* 1993; **149**: 437

Carlos, T., Kovach, N., Schwartz, B., Rosa, M., Newman, B., Wayner, e., Benjamin, C., Osborn, L., Lobb, R., Harlan, J. Human monocytes bind to two cytokine-induced adhesive ligands on cultured human endothelial cells: endothelial-leukocyte adhesion molecule-1 and vascular cell adhesion molecule-1. *Blood* 1991; **77**: 2266-71.

Carruth, L.M., Hardwick, J.M., Morse, B.A., Clements, J.E. Visna virus tat protein: a potent transcription factor with both activator and suppressor domains. *J. Virol.* 1994; **68**: 6137-46.

Chakrabarti, L., Hurtrel, M., Maire, M., Vazeux, R., Dormont, D., Montagnier, L., Hurtrel, B. Early viral replication in the brain of SIV-infected rhesus monkeys. *Am. J. Path.* 1991; **139**: 1273-80.

Chao, C.C., Hu, S., Kravitz, F.H., Tsang, M., Anderson, W.R., Peterson, P.K. Transforming Growth Factor β protects human neurons against β -amyloid-induced injury. *Mol. Chem. Neuropathol.* 1994; **23**: 159-78.

Chao, C.C., Hu, S., Sheng, W.S., Bu, D., Bukrinsky, M.I., Peterson, P.K. Cytokine stimulated astrocytes damage human neurons via a nitric oxide mechanism. *Glia* 1996; **16**: 276-84.

Charles, A.C., Merrill, J.E., Dirksen, E.R., Sanderson, M.J. Intercellular signaling in glial cells: calcium waves and oscillations in response to mechanical stimulation and glutamate. *Neuron* 1991; **6**: 983-92.

Cheng, B., Christakos, S., Mattson, M.P. Tumour necrosis factors protect neurons against metabolic-excitotoxic insults and promote maintenance of calcium homeostasis. *Neuron* 1994; **12**: 139-53.

Cheng, J., Nath, A., Knudsen, B., Hochman, S., Geiger, J.D., Ma, M., Magnuson, D.S.K. Neuronal excitatory properties of human immunodeficiency virus type 1 *tat* protein. *Neurosci.* 1998; **82**: 97-106.

Cheng-Mayer, C., Rutka, J.T., Rosenblum, M.L., McHugh, T., Stites, D.P., Levy, J.A.

- Human immunodeficiency virus can productively infect cultured human glial cells. *Proc. Natl. Acad. Sci. USA* 1987; **84**: 3526-30.
- Chiodi, F., Fuerstenberg, S., Gidlund, M., Asjo, B., Fenyo, E.M. Infection of brain-derived cells with the human immunodeficiency virus. *J. Virol.* 1987; **61**: 1244-7.
- Chung, I.L., Benveniste, E.N. Tumor necrosis factor- α production by astrocytes. *J. Immunol.* 1990; **144**: 2999-3007.
- Clouse, K.A., Cosentino, M.L., Weih, K.A., Pyle, S.W., Robbins, P.B., Hochstein, H.D., Natarajan, V., Farrar, W.L. The HIV-1 gp120 envelope glycoprotein has the intrinsic capacity to stimulate monokine secretion. *J. Immunol.* 1991; **147**: 2892-901.
- Colton, C.A., Gilbert, D.L. Production of superoxide anions by a CNS macrophage, the microglia. *FEBS* 1987; **223**: 284-8.
- Conant, K., Garzino-Demo, A., Nath, A., McArthur, J.C., Halliday, W., Power, C., Gallo, R.C., Major, E.O. Induction of monocyte chemoattractant protein-1 in HIV-1 Tat-stimulated astrocytes and elevation in AIDS dementia. *Proc. Natl. Acad. Sci. (USA)* 1998; **95**: 3117-21.
- Corasaniti, M.T., Melino, G., Navarra, M., Garaci, E., Finazzi-Agrò, A., Nisticò, G. Death of cultured human neuroblastoma cells induced by HIV-1 gp120 is prevented by NMDA receptor antagonists and inhibitors of nitric oxide and cyclooxygenase. *Neurodegen.* 1995; **4**: 315-21.
- Cornell-Bell, A.H., Finkbeiner, S.M., Cooper, M.S., Smith, S.J. Glutamate induces calcium waves in cultured astrocytes: long-range glial signaling. *Science* 1990a; **247**: 470-3.
- Cornell-Bell, A., Thomas, P.G., Smith, S.J. The excitatory neurotransmitter glutamate causes filopodia formation in cultured hippocampal astrocytes. *Glia* 1990b; **3**: 322-34.
- Crane, S.E., Kanda, P., Clements, J.E. Identification of the fusion domain in the visna virus transmembrane protein. *Virol.* 1991; **185**: 488-92.
- Crawford, T.B., Adams, D.S. Caprine Arthritis encephalitis: clinical features and presence of antibody in selected goat populations. *JAVMA* 1981; **178**: 713-9.
- Cutlip, R.C., Lehmkuhl, H.D., Brogden, K.A., McClurkin, A.W. Vasculitis associated with ovine progressive pneumonia virus infection in sheep. *Am. J. Vet. Res.* 1985; **46**: 61-8.
- da Cunha, A., Vitkovic, L. Transforming growth factor-beta 1(TGF- β 1) expression and regulation in rat cortical astrocytes. *J. Neuroimmunol.* 1992; **36**: 157-69.
- da Cunha, A., Jefferson, J.A., Jackson, R.W., Vitkovic, L. Glial cell-specific mechanisms of TGF- β 1 induction by IL-1 in the cerebral cortex. *J. Neuroimmunol.* 1993a; **42**: 71-86.

da Cunha, A., Jefferson, J.J., Tyor, W.R., Glass, J.D., Jannotta, F.S., Vitkovic, L. Control of astrocytosis by interleukin-1 and transforming growth factor- β 1 in human brain. *Brain Res.* 1993b; **631**: 39-45.

da Cunha, A., Jackson, R.W., Vitkovic, L. HIV-1 non-specifically stimulates production of transforming growth factor- β 1 transfer in primary astrocytes. *J. Neuroimmunol.* 1995; **60**: 125-33.

Dalton, A.D.A., Harcourt-Webster, J.N., Keat, A.C.S. Synovium in AIDS: a postmortem study. *BMJ* 1990; **300**: 1239-40.

Dalziel, R.G., Hopkins, J., Watt, N.J., Dutia, B.M., Clarke, H.A.K., McConnell, I. Identification of a putative cellular receptor for the lentivirus visna virus. *J. Gen. Virol.* 1991; **72**: 1905-11.

Dani, J.W., Chernjavsky, A., Smith, S.J. Neuronal activity triggers calcium waves in hippocampal astrocyte networks. *Neuron* 1992; **8**: 429-40.

Davis, J.L., Clements, J.E. Characterisation of a cDNA clone encoding the visna virus transactivating protein. *Proc. Natl. Acad. Sci. USA* 1989; **86**: 414-8.

Dawson, M. Maedi/visna: a review. *Vet. Rec.* 1980; **106**: 212-6.

Dawson, T.M., Bredt, D.S., Fotuhi, M., Hwang, P.M., Snyder, S.H. Nitric oxide synthase and neuronal NADPH diaphorase are identical in brain and peripheral tissues. *Proc. Natl. Acad. Sci. USA* 1991; **88**: 7797-801.

Dawson, T.M., Dawson, V.L. Gp120 neurotoxicity in primary cortical cultures. *Adv. Neuroimmunol.* 1994; **4**: 167-73.

Dawson, V.L., Dawson, T.M., Uhl, G.R., Snyder, S.H. Human immunodeficiency type 1 coat protein neurotoxicity mediated by nitric oxide in primary cortical cultures. *Proc. Natl. Acad. Sci. USA* 1993; **90**: 3256-9.

Denis-Donini, S., Glowinski, J., Prochiantz, A. Glial heterogeneity may define the three-dimensional shape of mouse mesencephalic dopaminergic neurones. *Nature* 1984; **307**: 641-3.

Derse, D., Carvalho, M., Carroll, R., Peterlin, B.M. A minimal lentivirus tat. *J. Virol.* 1991; **65**: 7012-5.

Derynck, R. TGF- β receptor-mediated signaling. *TIBS* 1994; **19**: 548-53.

Dewhurst, S., Sakai, K., Bresser, J., Stevenson, M., Evinger-Hodges, M.J., Volsky, D.J. Persistent productive infection of human glial cells by human immunodeficiency virus (HIV) and by infectious molecular clones of HIV. *J. Virol.* 1987; **61**: 3774-82.

Dickson, D.W. Multinucleated giant cells in acquired immunodeficiency syndrome. *Arch. Pathol. Lab. Med.* 1986; **110**: 967-8.

Dickson, D.W., Belman, A.L., Kim, T.S., Houroupan, D.S., Rubinstein, A. Spinal cord pathology in pediatric acquired immunodeficiency syndrom. *Neurol.* 1989; **39**: 227-35.

Dobrina, A., Menegazzi, R., Carlos, T.M., Nardon, E., Cramer, R., Zacchi, T., Harlan, J.M., Patriarca, P. Mechanisms of eosinophil adherence to cultured vascular endothelial cells. *J. Clin. Invest.* 1991; **88**: 20-6.

Ebrahimi, B., Roy, D.J., Bird, P., Sargan, D.R. Cloning, sequencing and expression of the ovine interleukin 6 gene. *Cytokine* 1995; **7**: 232-6.

Egg, D., Herold, M., Rimpl, E., Gunther, R. Prostaglandin F_{2α} levels in human cerebrospinal fluid in normal and pathological conditions. *J. Neurol.* 1980; **222**: 239-48.

Eilbott, D.J., Peress, N., Burger, H., LaNeve, D., Orenstein, J., Gendelman, H.E., Seidman, R., Weiser, B. Human immunodeficiency type 1 in spinal cords of acquires immunodeficiency syndrme patients with myelopathy: expression and replication in macrophages. *Proc. Natl. Acad. Sci. USA* 1989; **86**: 3337-41.

Elices, M.J., Osborn, L., Takada, Y., Crouse, C., Luhowskyj, S., Hemler, M.E., Lobb, R.R. VCAM-1 on activated endothelium interacts with the leukocyte integrin VLA-4/fibronectin binding site. *Cell* 1990; **60**: 577-84.

Ensoli, B., Barillari, G., Salahuddin, S.Z., Gallo, R.C., Wong-Staal, F. Tat protein of HIV-1 stimulates growth of cells derived from Kaposi's sarcoma lesions of AIDS patients. *Nature* 1990; **345**: 84-6.

Epstein, L.G., Sharer, L.R., Joshi, V.V., Fojas, M.M., Koenigsberger, M.R., Oleske, J.M. Progressive encephalopathy in children with acquired immunodeficiency syndrome. *Ann. Neurol.* 1985; **17**: 488-96.

Espinoza, L.R., Aguilar, J.L., Espinoza, C.G., Berman, A., Gutierrez, F., Vasey, F.B., Germain, B.F. HIV associated arthropathy: HIV antigen demonstration in the synovial membrane. *J. Rheumatol.* 1990; **17**: 1195-201.

Everall, I, Luthert, P.J., Lantos, P.L. Neuronal loss in the frontal cortex in HIV infection. *Lancet* 1991; **337**: 1119-21.

Fagan, A.M., Gage, F.H. Cholinergic sprouting in the hippocampus: a proposed role for IL-1. *Exp. Neurol.* 1990; **110**: 105-20.

Fiala, M., Rhodes, R.H., Shapshack, P., Negano, I., Martinez-Maza, O., Diagne, A., Baldwin, G., Graves, M. Regulation of HIV-1 infection of astrocytes: expression of Nef, TNF and IL-6 is enhanced in co-cultures of astrocytes with macrophages. *J. Neurovirol.* 1996; **2**: 158-66.

Fillit, H., Leveugle, B. Disorders of the extracellular matrix and the pathogenesis of senile dementia of the Alzheimer's type. *Lab. Invest.* 1995; **72**: 249-53.

Finch, C.E., Laping, N.J., Morgan, T.E., Nichols, N.R., Pasinetti, G.M. TGF-β1 is an organiser of responses to neurodegeneration. *J. Cell. Biochem.* 1993; **53**: 314-22.

Frankel, A.D., Pabo, C.O. Cellular uptake of the tat protein from human immunodeficiency virus. *Cell* 1988; **55**: 1189-93.

Fuchs, D., Chiodi, F., Albert, J., Asjo, B., Hagberg, L., Hausen, A., Norkrans, G., Reibnegger, G., Werner, E.R., Wachter, H. Neopterin concentrations in cerebrospinal fluid and serum of individuals infected with HIV-1. *AIDS* 1989; **3**: 285-8.

Fuchs, D., Murr, C., Reibnegger, G., Weiss, G., Werner, E.R., Werner-Felmayer, G., Wachter, H. Nitric oxide synthase and antimicrobial armature of human macrophages. *J. Infect. Dis.* 1994; **169**: 224-5.

Fuchs, D., Baier-Bitterlich, G., Wachter, H. Nitric oxide and AIDS dementia. *N. Engl. J. Med.* 1995; **333**: 521-2.

Funke, I., Hahn, A., Rieber, E.P., Weiss, E., Riethmuller, G. The cellular receptor (CD4) of the human immunodeficiency virus is expressed on neurons and glial cells in human brain. *J. Exp. Med.* 1987; **165**: 1230-5.

Gabuzda, D.H., Hess, J.L., Small, J.A., Clements, J.E. Regulation of the visna virus long terminal repeat in macrophages involves cellular factors that bind sequences containing AP-1 sites. *Mol. Cell. Biol.* 1989; **9**: 2728-33.

Gallo, P., Frei, K., Rordorf, C., Lazdins, J., Tavolato, B., Fontana, A. Human immunodeficiency virus type 1 (HIV-1) infection of the central nervous system: an evaluation of cytokines in cerebrospinal fluid. *J. Neuroimmunol.* 1989; **23**: 109-16.

Gardner-Medwin, A.R. Analysis of potassium dynamics in mammalian brain tissue. *J. Physiol.* 1983; **335**: 393-426.

Garry, R.F., Koch, G. Tat contains a sequence related to snake venom neurotoxins. *AIDS* 1992; **6**: 1541-2.

Gehrmann, J., Mies, G., Bonnekoh, P., Banati, R., Iijima, T., Kreutzberg, G.W., Hossmann, K. Microglial reaction in the rat cerebral cortex induced by cortical spreading depression. *Brain Pathol.* 1993; **3**: 11-7.

Gelbard, H.A., Dzenko, K.A., DiLoreto, D., del Cerro, C., del Cerro, M., Epstein, L.G. Neurotoxic effects of tumor necrosis alpha in primary human neuronal cultures are mediated by the activation of the glutamate AMPA receptor subtype: implications for AIDS neuropathogenesis. *Dev. Neurosci.* 1993; **15**: 417-22.

Gelbard, H.A., Nottet, H.S.L.M., Swindells, S., Jett, M., Dzenko, K.A., Genis, P., White, R., Wang, L., Choi, Y., Zhang, D., et al. Platelet activating factor: a candidate for human immunodeficiency virus type 1 induced neurotoxin. *J. Virol.* 1994; **68**: 4628-35.

Gendelman, H.E., Narayan, O., Molineaux, S., Clements, J.E., Ghotbi, Z. Slow, persistent replication of lentiviruses: role of tissue macrophages and macrophage precursors in bone marrow. *Proc. Natl. Acad. Sci. USA* 1985; **82**: 7086-90.

Gendelman, H.E., Narayan, O., Kennedy-Stoskopf, S., Kennedy, P.G.E., Ghotbi, Z., Clements, J.E., Stanley, J., Pezeshkpour, G. Tropism of sheep lentiviruses for monocytes: susceptibility to infection and virus gene expression increase during maturation of monocytes to macrophages. *J. Virol.* 1986; **58**: 67-74.

Genis, P., Jett, M., Bernton, E.W., Boyle, T., Gelbard, H.A., Dzenko, K., Keane, R.W., Resnick, L., Mizrachi, Y., Volsky, D.J., *et al.* Cytokines and arachidonic acid metabolites produced during human immunodeficiency virus (HIV)-infected macrophage-astroglia interaction: implications for the pathogenesis of HIV disease. *J. Exp. Med.* 1992; **176**: 1703-18.

Georgsson, G., Palsson, P.A., Panitch, H., Nathanson, N., Petursson, G. The ultrastructure of early visna lesions. *Acta Neuropath.* 1977; **37**: 127-35.

Georgsson, G., Martin, J.R., Palsson, P.A., Nathanson, N., Benediksdottir, E., Petursson, G. An ultrastructural study of the cerebrospinal fluid in visna. *Acta Neuropath.* 1979; **48**: 39-43.

Georgsson, G., Martin, J.R., Klein, J., Palsson, P.A., Nathanson, N., Petursson, G. Primary demyelination in visna - an ultrastructural study of Icelandic sheep with clinical signs following experimental infection. *Acta Neuropath.* 1982; **57**: 171-8.

Giulian, D., Vaca, K., Noonan, C.A. Secretion of neurotoxins by mononuclear phagocytes infected with HIV-1. *Science* 1990; **250**: 1593-5.

Giulian, D., Wendt, E., Vaca, K., Noonan, C.A. The envelope glycoprotein of human immunodeficiency virus type 1 stimulates the release of neurotoxins from monocytes. *Proc. Natl. Acad. Sci. USA* 1993; **90**: 2769-73.

Giulian, D., Yu, J., Li, X., Tom, D., Li, J., Wendt, E., Lin, S., Schwarcz, R., Noonan, C. Study of receptor mediated neurotoxins released by HIV-1 infected mononuclear phagocytes found in human brain. *J. Neurosci.* 1996; **16**: 3139-53.

Glowa, J.R., Panlilio, L.V., Brenneman, D.E., Gozes, I., Fridkin, M., Hill, J.M. Learning impairment following intracerebral administration of the envelope glycoprotein gp120 or a VIP antagonist. *Brain Res.* 1992; **570**: 49-53.

Goncalves, J., Korin, Y., Zack, J., Gabuzda, D. Role of Vif in human immunodeficiency virus type 1 reverse transcription. *J. Virol.* 1996; **70**: 8701-9.

Gourdou, I., Mazarin, V., Quercat, G., Sauze, N., Vigne, R. The open reading frame S of visna virus genome is a transactivating gene. *Virol.* 1989; **171**: 170-8.

Gourdou, I., Mabrouk, K., Harkiss, G., Marchot, P., Watt, N., Hery, F., Vigne, R. Neurotoxicite chez la souris de portions riches en cysteines des proteines Tat du virus visna et de VIH-1. *Comptes Rendus de l'Academie des Sciences - Serie Iii, Sciences de la vie.* 1990; **311** : 149-55.

Graeber, M.B., Tatzlaff, W., Streit, W.J., Kreutzberg, G.W. Microglial cells but not

- astrocytes undergo mitosis following rat facial nerve axotomy. *Neurosci. Lett.* 1988; **85**: 317-21.
- Gray, C.W., Patel, A.J. Regulation of β -amyloid precursor protein isoform mRNAs by transforming growth factor- β 1 and interleukin-1 β in astrocytes. *Mol. Brain Res.* 1993; **19**: 251-6.
- Gray, F., Lescs, M., Keohane, C., Paraire, F., Marc, B., Durigon, M., Gherardi, R. Early brain changes in HIV infection: neuropathological study of 11 seropositive, non-AIDS cases. *J. Neuropath. Exp. Neurol.* 1992; **51**: 177-85.
- Gray, F., Scaravilli, F., Everall, I., Chretien, F., An, S., Boche, D., Adle-Biassette, H., Wingertsmann, L., Durigon, M., Hurtrel, B., et al. Neuropathology of early HIV-1 infection. *Brain Pathol.* 1996; **6**: 1-15.
- Green, I.R., Fiskerstrand, C., Bertoni, G., Roy, D.J., Peterhans, E., Sargan, D.R. Expression and characterization of bioactive recombinant TNF-alpha: some species specificity in cytotoxic response to TNF. *Cytokine* 1993; **5**: 213-23.
- Griffin, D.E., Wesselingh, S.L., McArthur, J.C. Elevated central nervous system prostaglandins in human immunodeficiency virus-associated dementia. *Ann. Neurol.* 1994; **35**: 592-7.
- Griffin, W.S.T., Stanley, L.C., Ling, C., White, L., MacLeod, V., Perrot, L.J., White, C.A., Araoz, C. Brain interleukin 1 and S-100 immunoreactivity are elevated in Down syndrome and Alzheimer's disease. *Proc. Natl. Acad. Sci. USA* 1989; **86**: 7611-5.
- Grimaldi, L.M.E., Martino, G.V., Franciotta, D.M., Brustia, R., Castagna, A., Pristera, R., Lazzarin, A. Elevated alpha tumour necrosis factor levels in spinal fluid from HIV-1 infected patients with central nervous system involvement. *Ann. Neurol.* 1991; **29**: 21-5.
- Gudnadottir, M., Palsson, P.A. Transmission of Maedi by inoculation of a virus from Maedi affected lungs. *J. Infect. Dis.* 1966; **117**: 1-7.
- Gyorkey, F., Melnick, J.L., Gyorkey, P. Human immunodeficiency virus in brain biopsies of patients with AIDS and progressive encephalopathy. *J. Infect. Dis.* 1987; **155**: 870-6.
- Haase, A.T., Varmus, H.E. Demonstration of DNA provirus in the lytic growth of visna virus. *Nature New Biol.* 1973; **245**: 237-9.
- Hakkert, B.C., Kuijpers, T.W., Leeuwenberg, J.F.M., van Mourik, J.A., Roos, D. Neutrophil and monocyte adherence to and migration across monolayers of cytokine-activated endothelial cells: the contribution of CD18, ELAM-1 and VLA-4. *Blood* 1991; **78**: 2721-7.
- Hallermeyer, K., Hamprecht, B. Cellular heterogeneity in primary cultures of brain cells revealed by immunocytochemical localization of glutamine synthetase. *Brain Res.* 1984; **295**: 1-11.

- Halprin, G.M., Ramirez, J., Pratt, P.C. Lymphoid interstitial pneumonia. *Chest* 1972; **72**: 418-23.
- Harmache, A., Vitu, C., Russo, P., Bouyac, M., Hieblot, C., Peveri, P., Vigne, R., Suzan, M. The Caprine Arthritis Encephalitis virus tat gene is responsible for efficient viral replication *in vitro* and *in vivo*. *J. Virol.* 1995; **69**: 5445-54.
- Harouse, J.M., Kunsch, C., Hartle, H.T., Laughlin, M.A., Hoxie, J.A., Wigdahl, B., Gonzalez-Scarano, F. CD4 independent infection of human neural cells by human immunodeficiency virus type 1. *J. Virol.* 1989; **63**: 2527-33.
- Harouse, J.M., Bhat, S., Spitalnik, S.L., Laughlin, M., Stefano, K., Silberberg, D.H., Gonzalez-Scarano, F. Inhibition of entry of HIV-1 in neural cell lines by antibodies against galactosyl ceramide. *Science* 1991; **253**: 320-3.
- Hartung, H. Immune mediated demyelination. *Ann. Neurol.* 1993; **33**: 563-7.
- Hatten, M.E. Neuronal regulation of astroglial morphology and proliferation *in vitro*. *J. Cell Biol.* 1985; **100**: 384-96.
- Hatton, G.I. Emerging concepts of structure-function dynamics in adult brain: the hypothalamo-neurohypophyseal system. *Prog. Neurobiol.* 1990; **34**: 437-504.
- Hayman, M., Arbuthnott, G.W., Harkiss, G., Brace, H., Filippi, P., Philippon, V., Thomson, D., Vigne, R., Wright, A.K. Neurotoxicity of peptide analogues of the transactivating protein tat from Maedi-Visna virus and Human Immunodeficiency Virus. *Neurosci.* 1993; **53**: 1-6.
- He, J., Chen, Y., Farzan, M., Choe, H., Ohagen, A., Gartner, S., Busciglio, J., Yang, X., Hofmann, W., Newman, W., et al. CCR3 and CCR5 are co-receptors for HIV-1 infection of microglia. *Nature* 1997; **385**: 645-9.
- Helland, D.E., Welles, J.L., Caputo, A., Haseltine, W.A. Transcellular transactivation by the human immunodeficiency virus type 1 tat protein. *J. Virol.* 1991; **65**: 4547-9.
- Hertz, L., McFarlin, D.E., Waksman, B.H. Astrocytes: auxiliary cells for immune responses in the central nervous system. *Immunol. Today* 1990; **11**: 265-8.
- Heyes, M.P., Brew, B.J., Saito, K., Quearry, B.J., Price, R.W., Lee, K., Bhalla, R.B., Der, M., Markey, S.P. Inter-relationships between quinolinic acid, neuroactive kynurenines, neopterin and microglobulin in cerebrospinal fluid and serum of HIV-1 infected patients. *J. Neuroimmunol.* 1992; **40**: 71-80.
- Hill, J.M., Mervis, R.F., Avidor, R., Moody, T.W., Brenneman, D.E. HIV envelope protein induced neuronal damage and retardation of behavioural development in rat neonates. *Brain Res.* 1993; **603**: 222-33.
- Holzwarth, J.A., Gibbons, S.J., Brorson, J.R., Philipson, L.H., Miller, R.J. Glutamate receptor agonists stimulate diverse calcium responses in different types of cultured rat cortical glial cells. *J. Neurosci.* 1994; **14**: 1879-91.

Hopkins, S.J., Rothwell, N.J. Cytokines and the nervous system: expression and recognition. *TINS* 1995; **18**: 83-8.

Houwens, D.J., Schaake, J.J., de Boer, G.F. Maedi-Visna control in sheep II. Half-yearly serological testing with culling of positive ewes and progeny. *Vet. Microbiol.* 1984; **9**: 445-51.

Hurtrel, B., Chakrabarti, L., Hurtrel, M., Maire, M.A., Dormont, D., Montagnier, L. Early SIV encephalopathy. *J. Med. Primatol.* 1991; **20**: 159-66.

Ishihara, A., Saito, H., Abe, K. Transforming growth factor- β 1 and - β 2 promote neurite sprouting and elongation of cultured rat hippocampal neurons. *Brain Res.* 1994; **639**: 21-5.

Jackson, G.R., Werrback-Perez, K., Perez-Polo, J.R. Role of nerve growth factor in oxidant-antioxidant balance and neuronal injury. II. A conditioning lesion paradigm. *J. Neurosci. Res.* 1990; **25**: 369-74.

Johns, L.D., Babcock, G., Green, D., Freedman, M., Sriram, S., Ransohoff, R.M. Transforming growth factor- β 1 differentially regulates proliferation and MHC class-II expression in forebrain and brainstem astrocyte primary cultures. *Brain Res.* 1992; **585**: 229-36.

Jolly, P.E., Huso, D.L., Sheffer, D., Narayan, O. Modulation of virus replication by antibodies: Fc portion of immunoglobulin molecule is essential for enhancement of binding, internalisation and neutralization of visna virus in macrophages. *J. Virol.* 1989; **63**: 1811-3.

Jordan, C.A., Watkins, B.A., Kufta, K., Dubois-Dalcq, M. Infection of brain microglial cells by human immunodeficiency virus type 1 is CD4 dependant. *J. Virol.* 1991; **65**: 736-42.

Kettenman, H., Orkand, R.K., Schachner, M. Coupling unidentified cells in mammalian nervous system cultures. *J. Neurosci.* 1983; **3**: 506-16.

Kettenman, H., Hoppe, D., Gottmann, K., Banati, R., Kreutzberg, G. Cultured microglial cells have a distinct pattern of membrane channels different from peritoneal macrophages. *J. Neurosci. Res.* 1990; **26**: 278-87.

Kettenman, H., Banati, R., Walz, W. Electrophysiological behaviour of microglia. *Glia* 1993; **7**: 93-101.

Kiefer, R., Lindholm, D., Kreutzberg, G.W. Interleukin-6 and transforming growth factor- β 1 mRNAs are induced in rat facial nucleus following motoneuron axotomy. *Eur. J. Neurosci.* 1993; **5**: 775-81.

Kim, J.P., Choi, D.W. Quinolate neurotoxicity in cortical cell culture. *Neurosci.* 1987; **25**: 423-32.

Kimelberg, H.K., Goderie, S.K., Higman, S., Pang, S., Waniewski, R.A. Swelling-induced release of glutamate, aspartate and taurine from astrocyte cultures. *J. Neurosci.* 1990; **10**: 1583-91.

Kimes, A.S., London, E.D., Szabo, G., Raymon, L., Tabakoff, B. Reduction of cerebral glucose utilisation by the HIV envelope glycoprotein gp120. *Exp. Neurol.* 1991; **112**: 224-8.

Kita, H., Kosaka, T., Heizmann, C.W. Parvalbumin-immunoreactive neurons in the rat neostriatum: a light and electron microscopic study. *Brain Res.* 1990; **536**: 1-15.

Kohleisen, B., Neumann, M., Herrmann, R., Brack-Werner, R., Krohn, K.J., Ovod, V., Ranki, A., Erfle, V. Cellular localization of Nef expressed in persistently HIV-1 infected low-producer astrocytes. *AIDS* 1992; **6**: 1427-36.

Koka, P., He, K., Zack, J.A., Kitchen, S., Peacock, W., Fried, I., Tran, T., Yashar, S.S., Merrill, J.E. Human immunodeficiency virus 1 envelope proteins induce interleukin 1, tumour necrosis factor alpha, and nitric oxide in glial cultures derived from fetal, neonatal and adult human brain. *J. Exp. Med.* 1995; **182**: 941-52.

Kolson, D.L., Buchhalter, J., Collman, R., Hellmig, B., Farrell, C.F., Debouck, C., Gonzalaz-Scarano, F. HIV-1 Tat alters normal organisation of neurons and astrocytes in primary rodent brain cell cultures: RGD sequence dependence. *AIDS Res. Hum. Retro.* 1993; **9**: 677-85.

Kraig, R.P., Chesler, M. Astrocytic acidosis in hyperglycemic and complete ischemia. *J. Cereb. Blood Flow Metab.* 1990; **10**: 104-14.

Kriegelstein, K., Suter-Crazzolaro, C., Fischer, W.H., Unsicker, K. TGF- β superfamily members promote survival of midbrain dopaminergic neurons and protect them against MPP⁺ toxicity. *EMBO J.* 1995; **14**: 736-42.

Kunsch, C., Hartle, H.T., Wigdahl, B. Infection of human dorsal root ganglion glial cells with human immunodeficiency type 1 involves an entry mechanism independent of the CD4 T4A epitope. *J. Virol.* 1989; **63**: 5054-61.

Kure, K., Lyman, W.D., Weidenheim, K.M., Dickson, D.W. Cellular localisation of an HIV-1 antigen in subacute AIDS encephalitis using an improved double labeling immunohistochemical method. *Am. J. Path.* 1990a; **136**: 1085-92.

Kure, K., Weidenheim, K.M., Lyman, W.D., Dickson, D.W. Morphology and distribution of HIV-1 gp41 positive microglia in subacute AIDS encephalitis. *Acta Neuropath.* 1990b; **80**: 393-400.

Landis, D.M.D., Reese, T.S. Arrays of particles in freeze-fractured astrocytic membranes. *J. Cell Biol.* 1974; **60**: 316-20.

Landis, D.M.D. Membrane structure in mammalian astrocytes: a review of freeze-fracture studies on adult, developing, reactive and cultured astrocytes. *J. Exp. Biol.* 1981; **95**: 35-48.

Landis, D.M.D. The early reactions of non-neuronal cells to injury. *Ann. Rev. Neurosci.* 1994; **17**: 133-51.

Landis, T.M., Reese, T.S. Regional organization of astrocytic membranes in cerebellar cortex. *Neurosci.* 1982; **7**: 937-50.

Langosch, J.M., Gebicke-Haerter, P.J., Norenberg, W., Illes, P. Characterization and transduction mechanisms of purinoreceptors in activated rat microglia. *Br. J. Pharmacol.* 1994; **113**: 29-34.

Lapchak, P.A., Araujo, D.M., Hefti, F. Systemic interleukin-1 β decreases brain-derived neurotrophic factor messenger RNA expression in the rat hippocampal formation. *Neurosci.* 1993; **53**: 297-301.

Lawson, L.J., Perry, V.H., Dri, P., Gordon, S. Heterogeneity in the distribution and morphology of microglia in the normal adult mouse brain. *Neurosci.* 1990; **39**: 151-70.

Lee, S.C., Liu, W., Dickson, D.W., Brosnan, C.F., Berman, J.W. Cytokine production by human fetal microglia and astrocytes. *J. Immunol.* 1993; **150**: 2659-67.

Legastelois, I., Levrey, H., Greenland, T., Mornex, J.F., Cordier, G. Visna-maedi virus induces interleukin-8 in sheep alveolar macrophages through a tyrosine-kinase signalling pathway. *Am. J. Resp. Cell Mol. Biol.* 1998; **18**: 532-7.

Lenhardt, T.M., Super, M.A., Wiley, C.A. Neuropathological changes in an asymptomatic HIV seropositive man. *Ann. Neurol.* 1988; **23**: 209-10.

Levi, G., Patriozi, M., Bernardo, A., Petrucci, T.C., Agresti, C. Human immunodeficiency virus coat protein gp120 inhibits the β -adrenergic regulation of astroglial and microglial functions. *Proc. Natl. Acad. Sci. USA* 1993; **90**: 1541-5.

Licinio, J., Wong, M., Gold, P.W. Localization of interleukin-1 receptor antagonist mRNA in rat brain. *Endocrinol.* 1991; **129**: 562-4.

Lin, F.H., Thormar, H. Ribonucleic acid dependant deoxyribonucleic acid polymerase in visna virus. *J. Virol.* 1970; **6**: 702-4.

Lin, F.H., Thormar, H. Characterization of ribonucleic acid from visna virus. *J. Virol.* 1971; **7**: 582-7.

Lindholm, D., Castren, E., Kiefer, R., Zafra, F., Thoenen, H. Transforming growth factor- β 1 in the rat brain: increase after injury and inhibition of astrocyte proliferation. *J. Cell Biol.* 1992; **117**: 395-400.

Lipsky, R.H., Silverman, S.J. Effects of mycophenolic acid on detection of glial filaments in human and rat astrocytoma cultures. *Cancer Res.* 1987; **47**: 4900-4.

Lipton, S.A. Calcium channel antagonists and Human Immunodeficiency Virus coat protein-mediated neuronal injury. *Ann. Neurol.* 1991; **30**: 110-4.

Lipton, S.A. Models of neuronal injury in AIDS: another role for the NMDA receptor? *TINS* 1992a; **15**: 75-9.

Lipton, S.A. Requirement for macrophages in neuronal injury induced by HIV envelope protein gp120. *NeuroR.* 1992b; **3**: 913-5.

Lipton, S.A. Neuronal injury associated with HIV-1 and potential treatment with calcium-channel and NMDA antagonists. *Dev. Neurosci.* 1994; **16**: 145-51.

Lipton, S.A., Brenneman, D.E., Silverstein, F.S., Masliah, E., Mucke, L. Gp120 and neurotoxicity *in vivo*. *TIPS* 1995; **16**: 122

Liu, J., Marino, M.W., Wong, G., Grail, D., Dunn, A., Bettadapura, J., Slavin, A.J., Old, L., Bernard, C.C.A. TNF is a potent anti-inflammatory cytokine in autoimmune-mediated demyelination. *Nature Med.* 1998; **4**: 78-83.

Liu, T., Clark, R.K., McDonnell, P.C., Young, P.R., White, R.F., Barone, F.C., Feuerstein, G.Z. Tumor necrosis factor- α expression in ischemic neurons. *Stroke* 1994; **25**: 1481-8.

Liuzzi, F.J., Lasek, R.J. Astrocytes block axonal regeneration in mammals by activating the physiological stop pathway. *Science* 1987; **237**: 642-5.

Lo, T., Fallert, C.J., Piser, T.M., Thayer, S.A. HIV-1 envelope glycoprotein evokes intracellular calcium oscillations in rat hippocampal neurons. *Brain Res.* 1992; **594**: 189-96.

Luheshi, G., Hopkins, S.J., Lefevre, R.A., Dascombe, M.J., Chiara, P., Rothwell, N.J. Importance of brain IL-1 type II receptors in fever and thermogenesis in the rat. *Am. J. Physiol.* 1993; **265**: E585-91.

Ma, M., Geiger, J.D., Nath, A. Characterisation of a novel binding site for the human immunodeficiency virus type 1 envelope protein gp120 on human fetal astrocytes. *J. Virol.* 1994; **68**: 6824-8.

Ma, X., Sova, P., Chao, W., Volsky, D.J. Cysteine residues in the vif protein of human immunodeficiency virus type 1 are essential for viral infectivity. *J. Virol.* 1994; **68**: 1714-20.

Mabrouk, K., Van Rietschoten, J.V., Vives, E., Darbon, H., Rochat, H., Sabatier, J. Lethal neurotoxicity in mice of the basic domains of HIV and SIV Rev proteins. *FEBS* 1991; **289**: 13-7.

MacDonald, M.C., Robertson, H.A., Wilkinson, M. Age- and dose-related NMDA induction of Fos-like immunoreactivity and c-fos mRNA in the arcuate nucleus of immature female rats. *Dev. Brain Res.* 1993; **73**: 193-8.

Magnuson, D.S.K., Knudsen, B.E., Geiger, J.D., Brownstone, R.M., Nath, A. Human Immunodeficiency Virus Type 1 Tat Activates Non-N-Methyl-D-Aspartate Excitatory

Amino Acid Receptors and Causes Neurotoxicity. *Ann. Neurol.* 1995; **37**: 373-80.

Mann, D.A., Frankel, A.D. Endocytosis and targeting of exogenous HIV-1 Tat protein. *EMBO J.* 1991; **10**: 1733-9.

Marcuzzi, A., Lowy, I., Weinberger, O.K. Transcellular transactivation of the human immunodeficiency virus type 1 long terminal repeat in T lymphocytes requires CD4-gp120 binding. *J. Virol.* 1992a; **66**: 4536-9.

Marcuzzi, A., Weinberger, J., Weinberger, O.K. Transcellular activation of the human immunodeficiency virus type 1 long terminal repeat in cocultured lymphocytes. *J. Virol.* 1992b; **66**: 4228-32.

Martinou, J., Le Van Thai, A., Valette, A., Weber, M.J. Transforming growth factor β 1 is a potent survival factor for rat embryo motoneurons in culture. *Dev. Brain Res.* 1990; **52**: 175-81.

Marty, S., Dusart, I., Peschanski, M. Glial changes following an excitotoxic lesion in the CNS - I. Microglia/macrophages. *Neurosci.* 1991; **45**: 529-39.

Masliah, E., Ge, N., Morey, M., DeTeresa, R., Terry, R.D., Wiley, C.A. Cortical dendritic pathology in human immunodeficiency virus encephalitis. *Lab. Invest.* 1992; **66**: 285-91.

Mazarin, V., Gourdou, I., Querat, G., Sauze, N., Audoly, G., Vitu, C., Russo, P., Rousselot, C., Filippi, P., Vigne, R. Subcellular location of *rev* gene product in visna virus infected cells. *Virol.* 1990; **178**: 305-10.

McArthur, J.C., Scott Becker, P., Parisi, J.E., Trapp, B., Selnes, O.A., Cornblath, D.R., Balakrishnan, J., Griffin, J.W., Price, D. Neurpathological changes in early HIV-1 dementia. *Ann. Neurol.* 1989; **26**: 681-4.

McNeill, H., Williams, C., Guan, J., Dragunow, M., Lawlor, P., Sirimanne, E., Nikolics, K., Gluckman, P. Neuronal rescue with transforming growth factor- β 1 after hypoxic-ischaemic brain injury. *NeuroR.* 1994; **5**: 901-4.

McQueen, J., Wright, A.K., Arbuthnott, G.W., Fink, G. Glial fibrillary acidic protein (GFAP)-immunoreactive astrocytes are increased in the hypothalamus of androgen-insensitive testicular feminized (Tfm) mice. *Neurosci. Lett.* 1990; **118**: 77-81.

Mearow, K.M., Mill, J.F., Vitkovic, L. The ontogeny and localization of glutamine synthetase gene expression in rat brain. *Mol. Brain Res.* 1989; **6**: 223-32.

Mennerick, S., Zorumski, C.F. Glial contributions to excitatory neurotransmission in cultured hippocampal cells. *Nature* 1994; **368**: 59-62.

Merrill, J.E., Gerner, R.H., Myers, L.W., Ellison, G.W. Regulation of natural killer cell cytotoxicity by prostaglandin E in the peripheral blood and cerebrospinal fluid of patients with multiple sclerosis and other neurological diseases. Part 1. Association between amount of prostaglandin produced, natural killer and endogenous interferon. *J.*

Neuroimmunol. 1983; **4**: 223-37.

Merrill, J.E., Koyanagi, Y., Chen, I.S.Y. Interleukin 1 and tumour necrosis factor alpha can be induced from mononuclear phagocytes by human immunodeficiency virus type 1 binding to the CD4 receptor. *J. Virol.* 1989; **63**: 4404-8.

Meucci, O., Miller, R.J. gp120 induced neurotoxicity in hippocampal pyramidal neurons cultures: protective action of TGFb1. *J. Neurosci.* 1996; **16**: 4080-8.

Miller, M.A., Garry, R.F., Jaynes, J.M., Montelaro, R.C. A structural correlation between lentivirus transmembrane proteins and natural cytolytic peptides. *AIDS Res. Hum. Retro.* 1991; **7**: 511-9.

Milstien, S., Sakai, N., Brew, B.J., Krieger, C., Vickers, J.H., Saito, K., Heyes, M.P. Cerebrospinal fluid nitrite/nitrate levels in neurologic diseases. *J. Neurochem.* 1994; **63**: 1178-80.

Minami, M., Kuraishi, Y., Yabuuchi, K., Yamazaki, A., Satoh, M. Induction of interleukin-1 β mRNA in rat brain after transient forebrain ischemia. *J. Neurochem.* 1992; **58**: 390-2.

Miyake, T., Okada, M., Kitamura, T. Reactive proliferation of astrocytes studied by immunohistochemistry for proliferating cell nuclear antigen. *Brain Res.* 1992; **590**: 300-2.

Miyazono, K., ten Dijke, P., Yamashita, H., Heldin, C. Signal transduction via serine/threonine kinase receptors. *Sem. Cell Biol.* 1994; **5**: 389-98.

Molina, J., Scadden, D.T., Byrn, R., Dinarello, C.A., Groopman, J.E. Production of tumour necrosis factor alpha and interleukin1 beta by monocytic cells infected with human immunodeficiency virus. *J. Clin. Invest.* 1989; **84**: 733-7.

Moore, G.R.W., Traugott, U., Scheinberg, L.C., Raine, C.S. Tropical spastic paraparesis: a model of virus induce, cytotoxic T cell mediated demyelination. *Ann. Neurol.* 1989; **26**: 523-30.

Moreno, B., Woodall, C.J., Watt, N.J., Harkiss, G.D. Transforming growth factor-beta 1 expression in ovine lentivirus-induced lymphoid interstitial pneumonia. *Clin. Exp. Immunol.* 1998 **112**: 74-83.

Moses, A.V., Nelson, J.A. HIV infection of human brain capillary endothelial cells - implications for AIDS dementia. *Adv. Neuroimmunol.* 1994; **4**: 239-47.

Mucke, L., Abraham, C.R., Ruppe, M.D., Rockenstein, E.M., Toggas, S.M., Mallory, M., Alford, M., Masliah, E. Protection against HIV-1 gp120 induce brain damage by neuronal expression of human amyloid precursor protein. *J. Exp. Med.* 1995; **181**: 1551-6.

Mullen, R.J., Buck, C.R., Smith, A.M. NeuN, A neuronal specific nuclear-protein in vertebrates. *Development* 1992; **116**: 201-11.

- Muller, W.E.G., Schroder, H.C., Ushijima, H., Dapper, J., Bormann, J. Gp120 of HIV-1 induces apoptosis in rat cortical cell cultures: prevention by memantine. *Eur. J. Pharmacol.* 1992; **226**: 209-14.
- Murphy, S., Pearce, B. Functional receptors for neurotransmitters on astroglial cells. *Neurosci.* 1987; **22**: 381-94.
- Murray, M., Wang, S., Goldberger, M.E., Levitt, P. Modification of astrocytes in the spinal cord following dorsal root or peripheral nerve lesions. *Exp. Neurol.* 1990; **110**: 248-57.
- Narayan, O., Wolinsky, J.S., Clements, J.E., Stradberg, J.D., Griffin, D.E., Cork, L.C. Slow virus replication: the role of macrophages in the persistence and expression of visna viruses of sheep and goats. *J. Gen. Virol.* 1982; **59**: 345-56.
- Narayan, O., Cork, L.C. Lentiviral diseases of sheep and goats: chronic pneumonia leukoencephalitis and arthritis. *Rev. Infect. Dis.* 1985; **7**: 89-98.
- Narayan, O., Zink, M.C., Gorrell, M., Crane, S., Huso, D., Jolly, P., Satarelli, M., Adams, R.J., Clements, J.E., in Levy, J.A. editor, *The Retroviridae*, Plenum Press: New York, 1993. The lentiviruses of sheep and goats, p 229-55.
- Nathanson, N., Panitch, H., Palsson, P.A., Petursson, G., Georgsson, G. Pathogenesis of visna II: effect of immunosuppression upon early central nervous system lesions. *Lab. Invest.* 1976; **35**: 444-51.
- Navia, B.A., Jordan, B.D., Price, R.W. The AIDS dementia complex: I. Clinical features. *Ann. Neurol.* 1986; **19**: 517-24.
- Nedergaard, M. Direct signaling from astrocytes to neurons in cultures of mammalian brain cells. *Science* 1994; **263**: 1768-71.
- New, D.R., Ma, M., Epstein, L.G., Nath, A., Gelbard, H.A. Human Immunodeficiency Virus type I Tat protein induces death by apoptosis in human neuron cultures. *J. Neurovirol.* 1997; **2**: 168-73.
- Norenberg, M.D. Astrocyte responses to CNS injury. *J. Neuropath. Exp. Neurol.* 1994; **53**: 213-20.
- Noris, J.G., Tang, L., Sparacio, S.M., Benveniste, E.N. Signal transduction pathways mediating astrocyte IL-6 induction by IL-1 β and tumor necrosis factor- α . *J. Immunol.* 1994; **152**: 841-50.
- Nottet, H.S.L.M., Gendelman, H.E. Unravelling the neuroimmune mechanisms for the HIV-1-associated cognitive/motor complex. *Immunol. Today* 1995a; **16**: 441-8.
- Nottet, H.S.L.M., Jett, M., Flanagan, C.R., Zhai, Q., Persidsky, Y., Rizzino, A., Bernton, E.W., Genis, P., Baldwin, T., Schwartz, J., *et al.* A regulatory role for astrocytes in HIV-1 encephalitis. *J. Immunol.* 1995b; **154**: 3567-81.

Nottet, H.S.L.M., Flanagan, E.M., Flanagan, C.R., Gelbard, H.A., Gendelman, H.E., Reinhard, J.F. The regulation of quinolinic acid in human immunodeficiency virus infected monocytes. *J. Neurovirol.* 1996a; **2**: 111-7.

Nottet, H.S.L.M., Persidsky, Y., Sasseville, V.G., Nukuna, A.N., Bock, P., Zhai, Q., Sharer, L.R., McComb, R.D., Swindells, S., Soderland, C., et al. Mechanisms for the transendothelial migration of HIV-1 infected monocytes into brain. *J. Immunol.* 1996b; **156**: 1284-95.

Nuovo, G.J., Alfieri, M.L. AIDS dementia is associated with massive, activated HIV-1 infection and concomittant expression of several cytokines. *Mol. Med.* 1996; **2**: 358-66.

Ognibene, F.P., Masur, H., Rogers, P., Travis, W.D., Suffredini, A.F., Feuerstein, I., Gill, V.J., Baird, B.F., Carrasquillo, J.A., Parrillo, J.E. Nonspecific interstitial pneumonitis without evidence of *Pneumocystis carinii* in asymptomatic patients infected with human immunodeficiency virus (HIV). *Ann. Int. Med.* 1988; **109**: 874-9.

Oliver, R.E., Gorham, J.R., Parish, S.F., Hadlow, W.J., Narayan, O. Ovine progressive pneumonia: pathologic and virologic studies on the naturally occurring disease. *Am. J. Vet. Res.* 1981a; **42**: 1554-9.

Oliver, R.E., Gorham, J.R., Perryman, L.E., Spencer, G.R. Ovine progressive pneumonia: experimental intrathoracic, intracerebral and intra-articular infections. *Am. J. Vet. Res.* 1981b; **42**: 1560-4.

Olsson, T., Maehlen, J., Love, A., Norrby, E., Kristensson, K. Induction of class I and class II transplantation antigens in rat brain during fatal and non-fatal measles virus infection. *J. Neuroimmunol.* 1987; **16**: 215-24.

Osborn, L., Hession, C., Tizard, R., Vassallo, C., Luhowskyj, S., Chi-Rosso, G., Lobb, R. Direct expression cloning of vascular cell adhesion molecule 1, a cytokine-induced endothelial protein that binds to lymphocytes. *Cell* 1989; **59**: 1203-11.

Pallansch, L.A., Lackman-Smith, C.S., Gonda, M.A. Bovine immunodeficiency-like virus encodes factors which transactivate the long terminal repeat. *J. Virol.* 1992; **66**: 2647-52.

Palsson, P.A. in Kimberlin, R.H. editor, *Slow virus diseases of animals and man*. Amsterdam: North-Holland Publishing, 1976; Visna-Maedi. p. 17-43.

Paulson, O.B., Newman, E.A. Does the release of potassium from astrocyte endfeet regulate cerebral blood flow? *Science* 1987; **237**: 897-8.

Paxinos G, Watson C. *The Rat Brain in Stereotaxic Coordinates*. 2nd ed. New York: Academic Press; 1986;

Peluso, R., Haase, A., Stowring, L., Edwards, M., Ventura, P. A Trojan Horse mechanism for the spread of visna virus in monocytes. *Virol.* 1985; **147**: 231-6.

- Perrella, O., Carrieri, P.B., Guarnaccia, D., Soscia, M. Cerebrospinal fluid cytokines in AIDS dementia complex. *J. Neurol.* 1992; **239**: 387-8.
- Perry, V.H., Hume, D.A., Gordon, S. Immunohistochemical localisation of macrophages and microglia in the adult and developing mouse brain. *Neurosci.* 1985; **15**: 313-26.
- Perry, V.H., Lawson, L.J., Reid, D.M. Biology of the mononuclear phagocyte system of the central nervous system and HIV infection. *J. Leuk. Biol.* 1994; **56**: 399-406.
- Persidsky, Y., Limoges, J., McComb, R., Bock, P., Baldwin, T., Tyor, W., Patil, M., Nottet, H.S.L.M., Epstein, L., Gelbard, H., *et al.* Human Immunodeficiency virus encephalitis in *scid* mice. *Am. J. Path.* 1996; **149**: 1027-53.
- Persidsky, Y., Buttini, M., Limoges, J., Bock, P., Gendelman, H.E. An analysis of HIV-1-associated inflammatory products in brain tissue of humans and *scid* mice with HIV-1 encephalitis. *J. Neurovirol.* 1997; **3**: 401-16.
- Petito, C.K., Navia, B.A., Cho, E., Jordan, B.D., George, D.C., Price, R.W. Vacuolar myelopathy pathologically resembling subacute combined degeneration in patients with the acquired immunodeficiency syndrome. *New Engl. J. Med.* 1985; **312**: 874-9.
- Philippon, V., Vellutini, C., Gambarelli, D., Harkiss, G., Arbuthnott, G., Metzger, D., Roubin, R., Filippi, P. The basic domain of the lentiviral Tat protein is responsible for damages in mouse brain: involvement of cytokines. *Virol.* 1994; **205**: 519-29.
- Pietraforte, D., Tritarelli, E., Testa, U., Minetti, M. Gp120 HIV envelope glycoprotein increases the production of nitric oxide in human monocyte-derived macrophages. *J. Leuk. Biol.* 1994; **55**: 175-82.
- Prehn, J.H., Backhaub, C., Krieglstein, J. Transforming growth factor- β 1 prevents glutamate neurotoxicity in rat neocortical cultures and protects mouse neocortex from ischemic injury *in vivo*. *J. Cereb. Blood Flow Met.* 1993; **13**: 521-5.
- Price, R.W., Brew, B., Sidtis, J., Rosenblum, M., Scheck, A.C., Cleary, P. The Brain in AIDS: central nervous system HIV-1 infection and AIDS dementia complex. *Science* 1988; **23**: 586-92.
- Priller, J., Haas, C.A., Reddington, M., Kreutzberg, G.W. Calcitonin gene-related peptide and ATP induce immediate early gene expression in cultured rat microglial cells. *Glia* 1995; **15**: 447-57.
- Privat, A., Rataboul, P. in Federoff, S., Vernadakis, A. editors, *Astrocytes*. New York: Academic, 1986; Fibrous and protoplasmic astrocytes. p. 105-29.
- Pulliam, L., West, D., Haigwood, N., Swanson, R.A. HIV-1 envelope gp120 alters astrocytes in human brain cultures. *AIDS Res. Hum. Retro.* 1993; **9**: 439-44.
- Pumarole-Sune, T., Navia, B.A., Cordon-Cardo, C., Cho, E., Price, R.W. HIV antigens in the brains of patients with the AIDS demementia complex. *Ann. Neurol.* 1987; **21**: 490-

6.

Qiu, Z., Parsons, K.L., Gruol, D.L. Interleukin-6 selectively enhances the intracellular calcium response to NMDA in developing CNS neurons. *J. Neurosci.* 1995; **15**: 6688-99.

Querat, G., Audoly, G., Sonigo, P., Vigne, R. Nucleotide sequence analysis of SA-OMVV, a visna related ovine lentivirus : Phylogenetic history of lentiviruses. *Viol.* 1990; **175**: 434-47.

Raff, M.C. Glial cell diversification in the rat optic nerve. *Science* 1989; **243**: 1450-5.

Ranki, A., Nyberg, M., Ovod, V., Haltia, M., Elovaara, I., Raininko, H., Krohn, K. Abundant expression of HIV nef and rev proteins in brain astrocytes *in vivo* is associated with dementia. *AIDS* 1995; **9**: 1001-8.

Robbins, D.S., Shirazi, Y., Drysdale, B.E., Lieberman, A., Shin, H.S., Shin, M.L. Production of a cytotoxic factor for oligodendrocytes by stimulated astrocytes. *J. Immunol.* 1987; **139**: 2593-7.

Robinson, A.P., White, T.M., Mason, D.W. Macrophage heterogeneity in the rat as delineated by two monoclonal antibodies MRC OX41 and MRC OX42, the latter recognising the complement receptor type 3. *Immunol.* 1986; **57**: 239-47.

Rollins, B.J., Yoshimura, T., Leonard, E.J., Pober, J.S. Cytokine-activated human endothelial cells synthesise and secrete a monocyte chemoattractant, MCP-1/JE. *Am. J. Path.* 1990; **136**: 1229-33.

Rothwell, N.J., Relton, J.K. Involvement of cytokines in acute neurodegeneration in the CNS. *Neurosci. Biobehav. Rev.* 1993; **17**: 217-27.

Sabatier, J.-M., Vives, E., Mabrouk, K., Benjouad, A., Rochat, H., Duval, A., Hue, B., Bahraoui, E. Evidence for neurotoxic activity of tat from human immunodeficiency virus type 1. *J. Virol.* 1991; **65**: 961-7.

Saito, Y., Sharer, L.R., Epstein, L.G., Michaels, J., Mintz, M., Louder, M., Golding, K., Cvetkovich, T.A., Blumberg, B.M. Overexpression of nef as a marker for restricted HIV-1 infection of astrocytes in post-mortem pediatric central nervous tissues. *Neurol.* 1994; **44**: 474-80.

Sargan, D.R., Bennet, I.D., Cousens, C., Roy, D.J., Blacklaws, B., Dalziel, R.G., Watt, N.J., McConnell, I. Nucleotide sequence of EV-1, a British isolate of Maedi Visna virus. *J. Gen. Virol.* 1991; **72**: 1893-903.

Sawada, M., Itoh, Y., Suzumura, A., Marnnouchi, T. Expression of cytokine receptors in cultured neuronal cells and glial cells. *Neurosci. Lett.* 1993; **160**: 131-4.

Schmidtmayerova, H., Nottet, H.S.L.M., Nuovo, G., Raabe, T., Flanagan, C.R., Dubrovsky, L., Gendelman, H.E., Cerami, A., Bukrinsky, M., Sherry, B. Human immunodeficiency virus type 1 infection alters chemokine beta peptide expression in

- human monocytes: implications for recruitment of leukocytes into brain and lymph nodes. *Proc. Natl. Acad. Sci. USA* 1996; **93**: 700-4.
- Schneider, R.F. Lymphocytic interstitial pneumonitis and nonspecific interstitial pneumonitis. *Clinics Chest Med.* 1996; **17**: 763-6.
- Schobitz, B., Voorhuis, D.A.M., Ronald de Kloet, E. Localization of interleukin 6 mRNA and interleukin 6 receptor mRNA in rat brain. *Neurosci. Lett.* 1992; **136**: 189-92.
- Schwarcz, R., Whetsell, W.O., Jr., Mangano, R.M. Quinolinic acid: An endogenous metabolite that produces axon-sparing lesions in rat brain. *Science* 1983; **219**: 316-8.
- Selmaj, K.W., Raine, C.S. Tumour necrosis factor alpha mediates myelin and oligodendrocyte damage in vitro. *Ann. Neurol.* 1988; **23**: 339-46.
- Sharer, L.R., Epstein, L.G., Cho, E.S., Joshi, V.V., Meyenhofer, M.F., Rankin, L.F., Petito, C.K. Pathologic features of AIDS encephalopathy in children: evidence for LAV/HTLV III infection of brain. *Hum. Pathol.* 1986; **17**: 271-84.
- Shimizu, Y., Shaw, S., Graber, N., Venkat Gopal, T., Horgan, K.J., Van Seventer, G.A., Newman, W. Activation-independent binding of human memory T cells to adhesion molecule ELAM-1. *Nature* 1991; **349**: 799-802.
- Shinoda, H., Marini, A.M., Cosi, C., Schwartz, J.P. Brain region and gene specificity of neuropeptide gene expression in cultured astrocytes. *Science* 1989; **245**: 415-7.
- Sigurdsson, B. Rida, a chronic encephalitis of sheep. *Br. Vet. J.* 1954a; **110**: 341-54.
- Sigurdsson, B. Maedi, a slow progressive pneumonia of sheep: an epizootological and a pathological study. *Br. Vet. J.* 1954b; **110**: 255-70.
- Sims, J.E., Gayle, M.A., Slack, J.L., Anderson, M.R., Bird, T.A., Giri, J.G., Colotta, F., Re, F., Mantovani, A., Shanebeck, K., et al. IL-1 signalling occurs exclusively via the type I receptor. *Proc. Natl. Acad. Sci.* 1993; **90**: 6155-9.
- Sinclair, E., Barbosa, P., Feinberg, M.B. The *nef* gene products of both simian and human immunodeficiency viruses enhance virus infectivity and are functionally interchangeable. *J. Virol.* 1997; **71**: 3641-51.
- Smith, C.A., Farrah, T., Goodwin, R.G. The TNF receptor superfamily of cellular and viral proteins: activation, costimulation and death. *Cell* 1994; **76**: 959-62.
- Smith, R.A., Baglioni, C. Characterisation of TNF receptors. *Immunol. Ser.* 1992; **56**: 149-60.
- Sonigo, P., Alizon, M., Staskus, K., Klatzmann, D., Cole, S., Danos, O., Retzel, E., Tiollais, P., Haase, A., Wain-Hobson, S. Nucleotide sequence of the visna lentivirus: relationship to the AIDS virus. *Cell* 1985; **42**: 369-82.

- Sparger, E.E., Shacklett, B.L., Renshaw-Gegg, L., Barry, P.A., Pedersen, N.C., Elder, J.H., Luciw, P.A. Regulation of gene expression directed by the long terminal repeat of the feline immunodeficiency virus. *Viol.* 1992; **187**: 165-77.
- Staskus, K.A., Retzel, E.F., Lewis, E.D., Silsby, J.L., St.Cyr, S., Rank, J.M., Wietgreffe, S.W., Haase, A.T., Cook, R., Fast, D., *et al.* Isolation of replication competent molecular clones of visna virus. *Viol.* 1991; **181**: 228-40.
- Staub, F., Baethmann, A., Peters, J., Weigt, H., Kempfski, O. Effects of lactacidosis on glial cell volume and viability. *J. Cereb. Blood Flow Metab.* 1990; **10**: 866-76.
- Staunton, D.E., Marlin, S.D., Stratowa, C., Dustin, M.L., Springer, T.A. Primary structure of ICAM-1 demonstrates interaction between members of the immunoglobulin and integrin supergene families. *Cell* 1988; **52**: 925-33.
- Steffy, K., Wong-Staal, F. Genetic regulation of the human immunodeficiency virus. *Microbiol. Rev.* 1991; **55**: 193-205.
- Stoler, M.H., Eskin, T.A., Benn, S., Angerer, R.C., Angerer, L.M. Human T-cell lymphotropic virus type III infection of the central nervous system. *J. Am. Med. Ass.* 1986; **256**: 2360-4.
- Stowring, L., Haase, A.T., Petursson, G., Georgsson, G., Palsson, P.A., Lutley, R., Roos, R., Szuchet, S. Detection of visna virus antigens and RNA in glial cells in foci of demyelination. *Viol.* 1985; **141**: 311-8.
- Strauss, S., Bauer, J., Ganter, U., Jonas, U., Berger, M., Volk, B. Detection of interleukin-6 and α 2-macroglobulin immunoreactivity in cortex and hippocampus of Alzheimer's disease patients. *Lab Invest* 1992; **66**: 223-9.
- Streit, W.J., Graeber, M.B., Kreutzberg, G.W. Functionnal plasticity of microglia: a review. *Glia* 1988a; **1**: 301-7.
- Streit, W.J., Kreutzberg, G.W. Response of endogenous glial cells to motor neuron degeneration induced by toxic ricin. *J. Comp. Neurol.* 1988b; **268**: 248-63.
- Streit, W.J., Graeber, M.B., Kreutzberg, G.W. Expression of Ia antigen on perivascular and microglial cells after sublethal and lethal motor neuron injury. *Exp. Neurol.* 1989; **105**: 115-26.
- Strijbos, P.J.L.M., Rothwell, N.J. Interleukin 1 beta attenuates excitatory amino acid induced neurodegeneration in vitro: involvement of nerve growth factor. *J. Neurosci.* 1995a; **15**: 3468-74.
- Strijbos, P.J.L.M., Zamani, M.R., Rothwell, N.J., Arbuthnott, G., Harkiss, G. Neurotoxic mechanisms of transactivating protein Tat of Maedi-Visna virus. *Neurosci. Lett.* 1995b; **197**: 215-8.
- Suda, T., Takahashi, T., Golstein, P., Nagata, S. Molecular cloning and expression of the Fas ligand, a novel member of the tumor necrosis factor family. *Cell* 1993; **75**: 1169-78.

Sutton, K.A., Lin, C., Harkiss, G.D., McConnell, I., Sargan, D.R. Regulation of the long terminal repeat in visna virus by a transcription factor related to the AML/PEBP2/CBF superfamily. *Virology*. 1997; **229**: 240-50.

Suzumura, A., Lavi, E., Weiss, S.R., Silberberg, D.H. Coronavirus infection induces H-2 antigen expression on oligodendrocytes and astrocytes. *Science* 1986; **232**: 991-3.

Suzumura, A., Sawada, M., Yamamoto, H., Marunouchi, T. Transforming growth factor- β suppresses activation and proliferation of microglia *in vitro*. *J. Immunol.* 1993; **151**: 2150-8.

Sweetnam, P.M., Saab, O.H., Wroblewski, J.T., Price, C.H., William Karbon, E., Ferkany, J.W. The envelope glycoprotein of HIV-1 alters NMDA receptor function. *Eur. J. Neurosci.* 1993; **5**: 276-83.

Swingler, S., Easton, A., Morris, A. Cytokine augmentation of HIV-1 LTR-driven gene expression in neural cells. *AIDS Res. Hum. Retro.* 1992; **8**: 487-93.

Taga, T., Hirata, Y., Yamasaki, K., Yasukawa, K., Matsuda, T., Hirano, T., Kishimoto, T. IL-6 triggers the association of its receptor with a possible signal transducer gp130. *Cell* 1989; **58**: 573-81.

Takao, T., Tracey, D.E., Mitchell, W.M., De Souza, E.B. IL-1 receptors in mouse brain: characterisation and neuronal localization. *Endocrinol.* 1990; **127**: 3070-8.

Talley, A.K., Dewhurst, S., Perry, S.W., Dollard, S.C., Gummuluru, S., Fine, S.M., New, D., Epstein, L.G., Gendelman, H.E., Gelbard, H.A. Tumour necrosis factor alpha induced apoptosis in human neuronal cells: protection by the antioxidant N-acetylcysteine and the genes bcl-2 and crmA. *Mol. Cell. Biol.* 1995; **15**: 2359-66.

Tang, C., Orkand, R.K. Glutamate depolarization of glial cells in *Necturus* optic nerve. *Neurosci. Lett.* 1986; **63**: 300-4.

Tartaglia, L.A., Weber, R.F., Figari, I.S., Reynolds, C., Palladino, M.A.J., Goeddel, D.V. The two different receptors for tumor necrosis factor mediate distinct cellular responses. *Proc. Natl. Acad. Sci. USA* 1991; **88**: 9292-6.

Taupin, V., Renno, T., Bourbonniere, L., Peterson, A.C., Rodriguez, M., Owens, T. Increased severity of experimental autoimmune encephalomyelitis, chronic macrophage/microglial reactivity, and demyelination in transgenic mice producing tumor necrosis factor alpha in the central nervous system. *Eur. J. Immunol.* 1997; **27**: 905-13.

Tiley, L.M., Brown, P.H., Le, S., Maizel, J.V., Clements, J.E., Cullen, B.R. Visna virus encodes a post-transcriptional regulator of viral structural gene expression. *Proc. Natl. Acad. Sci. USA* 1990; **87**: 7497-501.

Toggas, S.M., Masliah, E., Rockenstein, E.M., Rall, G.F., Abraham, C.R., Mucke, L. Central nervous system damage produced by the expression of the HIV-1 coat protein

gp120 in transgenic mice. *Nature* 1994; **367**: 188-93.

Toohy, K.L., Haase, A.T. The *rev* gene of visna virus is required for productive infection. *Viol.* 1994; **200**: 276-80.

Tornatore, C., Meyers, K., Atwood, W., Conant, K., Major, E. Temporal patterns of human immunodeficiency type 1 transcripts in human fetal astrocytes. *J. Virol.* 1994; **68**: 93-102.

Torre, D., Ferrario, G., Bonetta, G., Speranza, F., Zeroli, C. Production of nitric oxide from peripheral blood mononuclear cells and polymorphonuclear leukocytes of patients with HIV-1. *AIDS* 1995; **9**: 979-80.

Torsteindottir, S., Georgsson, G., Gisladdottir, E., Rafnar, B., Palsson, P.A., Petursson, G. Pathogenesis of central nervous system lesions in visna: cell-mediated immunity and lymphocyte subsets in blood, brain and cerebrospinal fluid. *J. Neuroimmunol.* 1992; **41**: 149-58.

Totterdell, S., Ingham, C.A., Bolam, J.P. in Bolam, J.P. editor. *Experimental Neuroanatomy*. Oxford: Oxford University Press, 1992; Immunocytochemistry I: pre-embedding staining. p. 103-29.

Toulmond, S., Vige, X., Fage, D., Benavides, J. Local infusion of interleukin-6 attenuates the neurotoxic effects of NMDA on rat striatal cholinergic neurons. *Neurosci. Lett.* 1992; **144**: 49-52.

Travis, D.A., Fox, C.H., Devaney, K.O. Lymphoid pneumonitis in 50 adult patients infected with the human immunodeficiency virus : lymphocytic interstitial pneumonitis versus nonspecific interstitial pneumonitis. *Hum. Pathol.* 1992; **23**: 529-41.

Tyor, W.R., Glass, J.D., Griffin, J.W., Scott Becker, P., McArthur, J.C., Bezman, L., Griffin, D.E. Cytokine expression in the brain during the acquired immunodeficiency syndrome. *Ann. Neurol.* 1992; **31**: 349-60.

Ushijima, H., Ando, S., Kunisida, T., Schroder, H.C., Klocking, H., Kijoa, A., Muller, W.E.G. HIV-1 gp120 and NMDA induce protein kinase C translocation differentially in rat primary neuronal cultures. *J. AIDS* 1993; **6**: 339-43.

Van Snick, J. Interleukin-6: an overview. *Ann. Rev. Immunol.* 1990; **8**: 253-78.

Varki, A. Selectin ligands. *Proc. Natl. Acad. Sci. USA* 1994; **91**: 7390-7.

Vaseux, R., Brousse, N., Jarry, A., Henin, D., Marche, C., Vedrenne, C., Mikol, J., Wolff, M., Michon, C., Rozenbaum, W., *et al.* AIDS subacute encephalitis. *Am. J. Path.* 1987; **126**: 403-10.

Vigne, R., Filippi, P., Querat, G., Sauze, N., Vitu, C., Russo, P., Delori, P. Precursor polypeptides to structural proteins of visna virus. *J. Virol.* 1982; **42**: 1046-56.

Vitkovic, L., da Cunha, A., Tyor, W.R. in Price, R.W., Perry, S.W. editors, *HIV, AIDS*

and the brain. New York: Raven Press Ltd. 1994; Cytokine expression and pathogenesis in AIDS brain. p. 203-22.

Vitkovic, L., da Cunha, A. Role for astrocytosis in HIV-1 associated dementia. *Curr. Top. Microbiol. Immunol.* 1995; **202**: 105-16.

Wahl, L.M., Corcoran, M.L., Pyle, S.W., Arthur, L.O., Harel Bellan, A., Farrar, W.L. Human immunodeficiency virus glycoprotein (gp120) induction of monocyte arachidonic acid metabolites and interleukin-1. *Proc. Natl. Acad. Sci. USA* 1989; **86**: 621-31.

Wahl, S.M., Hunt, D.A., Wakefield, L.M., McCartney-Francis, N., Wahl, L.M., Roberts, A.B., Sporn, M.B. Transforming growth factor type β induces monocyte chemotaxis and growth factor production. *Proc. Natl. Acad. Sci. USA* 1987; **84**: 5788-92.

Wahl, S.M., Allen, J.B., McCartney-Francis, N., Morganti-Kossmann, M.C., Kossmann, T., Ellingsworth, L., Mai, U.E.H., Mergenhagen, S.E., Orenstein, J.M. Macrophage- and astrocyte-derived transforming growth factor β as a mediator of central nervous system dysfunction in acquired immunodeficiency syndroms. *J. Exp. Med.* 1991; **173**: 981-91.

Walz, W., Ilshmer, S., Ohlemeyer, C., Banati, R., Kettenman, H. Extracellular ATP activates a cation conductance and a K^+ conductance in cultured microglial cells from mouse brain. *J. Neurosci.* 1993; **13**: 4403-11.

Warner, B.B., Burhans, M.S., Clark, J.C., Wispe, J.R. Tumor necrosis factor alpha increases Mn-SOD expression: protection against oxidant injury. *Am. J. Physiol.* 1991; **260**: L296-301.

Watkins, B.A., Dorn, H.H., Kelly, W.B., Armstrong, R.C., Potts, B.J., Michaels, F., Kufta, C.V., Dubois-Dalcq, M. Specific tropism of HIV-1 for microglial cells in primary human brain cultures. *Science* 1990; **249**: 549-53.

Wekerle, H., Linington, C., Lassmann, H., Meyermann, R. Cellular immune reactivity within the CNS. *TINS* 1986; 271-7.

Weller, M., Stevens, A., Sommer, N., Melms, A., Dichgans, J., Wietholter, H. Comparative analysis of cytokine patterns in immunological, infectious and oncological neurologic disorders. *J. Neurol. Sci.* 1991; **104**: 215-21.

Werner, T., Ferroni, S., Saermark, T., Brack-Werner, R., Banati, R.B., Mager, R., Steinaa, L., Kreutzberg, G.W., Erfle, V. HIV-1 Nef protein exhibits structural and functional similarity to scorpion peptides interacting with K^+ channels. *AIDS* 1991; **5**: 1301-8.

Wesselingh, S.L., Power, C., Glass, J.D., Tyor, W.R., McArthur, J.C., Farber, J.M., Griffin, J.W., Griffin, D.E. Intracerebral cytokine messenger RNA expression in acquired immunodeficiency syndrome dementia. *Ann. Neurol.* 1993; **33**: 576-82.

Wesselingh, S.L., Glass, J., McArthur, J.C., Griffin, J.W., Griffin, D.E. Cytokine

dysregulation on HIV-associated neurological disease. *Adv. Neuroimmunol.* 1994; **4**: 199-206.

Westmoreland, S.V., Kolson, D., Gonzalez-Scarano, F. Toxicity of TNF and platelet activating factor for human NT2N neurons: a tissue culture model for human immunodeficiency virus. *J. Neurovirol.* 1996; **2**: 118-26.

White, D.A., Matthay, R.A. Noninfectious pulmonary complications of infection with the human immunodeficiency virus. *Am. Rev. Respir. Dis.* 1989; **140**: 1763-87.

Whittemore, E.R., Korotzer, A.R., Etebari, A., Cotman, C.W. Carbachol increases intracellular free calcium in cultured rat microglia. *Brain Res.* 1993; **621**: 59-64.

Wigdahl, B., Guyton, R.A., Sarin, P.M. Human immunodeficiency virus infection of the developing human nervous system. *Virol.* 1987; **159**: 440-5.

Wiley, C.A., Schrier, R.D., Nelson, J.A., Lampert, P.W., Oldstone, M.B.A. Cellular localisation of human immunodeficiency virus infection within the brains of acquired immunodeficiency syndrome patients. *Proc. Natl. Acad. Sci. USA* 1986; **83**: 7089-93.

Wilkin, G.P., Marriott, D.R., Cholewinski, A.J. Astrocyte heterogeneity. *TINS* 1990; **13**: 43-6.

Wolf, H.K., Buslei, R., Schmidtkasner, R., Schmidtkasner, P.K., Pietsch, T., Wiestler, O.D., Blumcke, I. NeuN – a useful neuronal marker for diagnostic histopathology. *J. Histochem. Cytochem.* 1996; **44**: 1167-1171.

Wyss-Coray, T., Feng, L., Masliah, E., Ruppe, M.D., Lee, H.S., Toggas, S.M., Rockenstein, E.M., Mucke, L. Increased extracellular matrix components and development of hydrocephalus in transgenic mice overexpressing transforming growth factor β 1. *Am. J. Path.* 1995; **147**: 53-67.

Yoshioka, M., Shapshak, P., Srivastava, A.K., Stewart, R.V., Nelson, S.J., Bradley, W.G., Berger, J.R., Rhodes, R.H., Sun, N.C.J., Nakamura, S. Expression of HIV-1 and interleukin-6 in lumbosacral dorsal root ganglia of patients with AIDS. *Neurol.* 1994; **44**: 1120-30.

43.3

ACTIVATION OF THE KYNURENINE PATHWAY IN THE BRAIN IN AIDS - A NEUROTOXIC MECHANISM?

A.M.Sardar, C.J.Eggett and G.P.Reynolds. Department of Biomedical Science, The University of Sheffield, Sheffield S10 2TN U.K.

HIV-associated dementia is a frequent consequence of HIV infection and is associated with neuronal deficits. HIV invasion of the brain is considered to be primarily via macrophages/microglia, that when activated produce soluble neurotoxic factors. Macrophage activation can lead to the induction of indoleamine-2,3-dioxygenase (IDO) that regulates tryptophan/kynurenine metabolism, and thus to the overproduction of two neurotoxins, 3-hydroxykynurenine (3HK) and quinolinic acid. We find that 3HK, like quinolinic acid, is able to induce neuronal cell damage in a chick embryo retina preparation. This effect is blocked by AP5, implicating NMDA receptors in the mechanism of 3HK toxicity. We have determined 3HK concentration and the activity of both IDO and the 3HK catabolic enzyme, 3HKase, in brain tissue taken post-mortem from the frontal cortex of HIV-positive individuals and matched control subjects. 3HK was increased in the AIDS group, an effect which is greatest in patients with dementia. 3HKase activity was similarly increased in the brain in AIDS. IDO was found to be increased in AIDS patients, but only reached significance in the group of patients with dementia. Thus we conclude that an activation of the kynurenine pathway in the brain in AIDS, as a consequence of the increase in IDO activity, is responsible for increased formation of 3HK and, presumably, quinolinic acid. These neurotoxins may well be responsible for the neuronal losses underlying HIV-associated dementia.

43.5

IMMEDIATE EARLY GENE EXPRESSION AND CELL DEATH IN THE IMMATURE RAT STRIATUM FOLLOWING AN EXCITOTOXIC LESION.

Carolyn A. Walker and Stephen W. Davies. Department of Anatomy and Developmental Biology, University College London, Gower Street, London, WC1E 6BT.

We have investigated the molecular mechanisms underlying excitotoxin-induced striatal cell death to determine any differences that might exist between the adult and the developing rat striatum. An injection of the excitotoxin kainic acid into the striatum of postnatal day 10 rats results in a contrasting pattern of cell death to that seen in the adult. There is a sparing of the NADPH-diaphorase striatal cell type coupled with a 75% loss of the cholinergic neuron; the opposite to that seen in the adult.

Using this model of excitotoxin-induced cell death we have examined by immunocytochemistry and *in situ* hybridisation the spatial and temporal expression of immediate early genes belonging to the AP-1 transcription factor complex, namely *c-fos*, *c-jun*, *fos-B*, *jun-B* and *jun-D*, to establish whether cell death is accompanied by an up-regulation of these genes. In the adult there is a rapid and transient expression of *c-fos* and *jun-B* within the 'peripheral shell' of the striatum which is followed by a delayed expression of *fos-B*, *c-jun*, and *jun-D* within the central lesioned 'core' of the striatum. However, in the developing striatum the immediate early gene expression contrasts that seen in the adult. Immediate early gene primary transcripts are minimally up-regulated and protein induction cannot be detected during development.

Furthermore, we have sought to define the means by which cells are dying in this model, whether necrotic or apoptotic. Using the technique of *in situ* nick end labelling it is possible to establish whether nuclear condensation is occurring and using agarose gel electrophoresis it is possible to observe DNA laddering, both characteristic features of apoptotic cell death. It is important to note that the effect of excitotoxin-induced cell death differs markedly during development and this may provide some insight into the mechanisms of cell death in neurodegenerative diseases.

CAW is in receipt of an MRC studentship.

43.4

ACUTE NEUROTOXICITY OF A PEPTIDE FROM MAEDI VISNA TAT.

I. Starling, S. Hunt, A.K. Wright, L. Nornie, G.W. Arbuthnott, G. Harkiss. MRC External Scientific Staff, University of Edinburgh Centre for Neuroscience, Preclinical Vet. Sciences, Department of Veterinary Pathology, Summerhall, Edinburgh, EH9 1QH.

A short peptide sequence which forms part of the tat protein synthesised by the sheep virus Maedi Visna, has been shown to be neurotoxic. Most of our measurements of its action so far have relied upon what we believed to be the glial response to the neuronal damage caused by the peptide. Indeed this is a common method for the assessment of neuronal damage by many agents, including excitatory amino acids for instance.

Our conclusion that the peptides were indeed neurotoxic was supported by the demonstration that a neurone specific antigen NeuN was absent in the region into which the peptide had been injected in rat brain, and by evidence of frank neuronal loss in the hippocampus after injection into mice.

To decide between a neuronal site of action and a glial one we have studied the effect of tat peptide injections shortly after their application. Within 30 min of the injection of the peptide into the striatum a significant action of the peptide is seen in the striatum. There is a 'halo' round the injection site which is free of staining. Within the circle formed by this 'halo' is an area where the morphology of the cells looks changed. The cell profiles seem shrunken and the staining a little darker. Over the following two hours this staining in the centre of the injection site fades and by three hours there is an area of no staining which is some 50% of the final volume of damage which we recorded by measuring the microglial response one week after the injection.

Although we do not at present have a clear idea of the mechanism of action of the peptide it is clear that the action occurs immediately and is, at least in the early stages neurotoxic. There are changes in glial staining in the short term animals but the glial proliferation which marks the full blown lesion takes three days to develop.

43.6

ABNORMAL NEURONAL NITRIC OXIDE SYNTHASE EXPRESSION IN NEURONES OF THE MUTANT MOUSE WOBBLER

G.J.Clowry¹ and S.McHanwell², Department of Child Health¹, Sir James Spence Institute, and Division of Neurobiology², Medical School, Framlington Place, Newcastle upon Tyne, NE2 4HH, United Kingdom.

Somatic motor neurones do not normally express nitric oxide synthase (NOS). However, axonal injury when it leads to cell death can induce expression of NOS in dying motor neurones^{1,2}. The wobbler mouse is an autosomal recessive mutant characterized by vacuolar degeneration and loss of motor neurones in the spinal cord and brainstem³. We have investigated the expression of neuronal NOS in the brainstem, spinal cord and cerebellum by NADPH diaphorase histochemistry in frozen sections of paraformaldehyde perfused tissues. Studies were made on younger wobbler mice aged from 5 to 8 weeks, when motor neurone death is actively occurring and in older mice from 10 months to 1 year when motor neurone death is largely completed. Unaffected littermates were used as controls. In the spinal cords of younger wobbler mice, but not unaffected littermates, large NOS positive swollen neurones with eccentric nuclei were found in the motor columns of the cervical and lumbar spinal cords. Abnormal neuronal profiles could also be seen in the vestibular nuclei of the younger wobblers. Such profiles were not found in the brainstem motor nuclei at any age or in the spinal cords of older animals. However, in the ventral horn of older animals unusually large numbers of NOS positive beaded axons were present often meeting in tangled foci in both white and grey matter. NOS staining in the cerebellum was abnormal at both ages examined being overexpressed in the granule cell layer of younger animals but underexpressed in older animals. This study demonstrates the complex pattern of neurodegeneration in a mutant often regarded simply as a model for motor neurone disease.

REFERENCES

1. Clowry (1993). *Neuroreport* **5**, 361-364.
2. Wu and Linx (1993). *Neurosci. Lett.*, **153** 121-124.
3. Pollin, McHanwell and Slater (1990). *J.Neurocytol* **19**, 29-38.

3rd. European Workshop on Ovine and Caprine Retroviruses
Jaca, Spain. 2nd-5th March, 1997

MAEDI VISNA VIRUS INDUCED NEUROINFLAMMATION: A SCID MOUSE MODEL

I. Starling (1), G. Harkiss (2) and G. Arbuthnott (1)

1) *Dept. of Preclinical Vet. Sci. Royal (Dick) School of Vet. Studies. Univ. of Edinburgh. U.K.*

2) *Dept. of Veterinary Pathology. Royal (Dick) School of Vet. Studies. Univ. of Edinburgh. U.K.*

In late stages on infection, Maedi Visna virus (MVV) causes ataxia and paralysis in sheep. The accompanying neuropathology shows demyelination, axonal lesions and reactive astrocytosis in both grey and white matter structures. Also characteristic is the invasion of monocytes along the ventricular system, followed by T cell infiltration. At present, it is not clear whether the neuroinflammation in MVV is caused by a direct action of the virus on neuronal cell types, possibly via the action of cytokines, or by an immune type response occurring within the CNS.

In order to investigate the potential causes of neuroinflammation occurring in MVV, severe combined immunodeficient (scid) mice were used. These lack T and B cells and are unable to mount any immune response, thus allowing investigation into a direct action of virus infected cells on neuronal cell types.

In the first set of experiments, scid mice were injected intra-atrially with mature macrophages infected with MVV. Immunocytochemistry for GFAP and F4/80 was then carried out on fixed brain tissue and the degree of astrocytosis was measured by image analysis.

Results show that at one week post-operatively, the degree of astrocytosis is significantly greater in those mice injected with virus infected macrophages as opposed to those injected with uninfected macrophages, suggesting that the virus infected macrophages are having a direct effect on the CNS.

In a second set of experiments, mononuclear cell preparations containing infected and uninfected monocytes have been injected into scid mice in the same manner as above, and the results are currently being collated in order to evaluate the role of the immune response in causing brain damage.

The current results seem to suggest the feasibility of a model of MVV encephalopathy in scid mice.



ELSEVIER

Brain Research 830 (1999) 285–291

BRAIN
RESEARCH

Research report

Acute in vivo neurotoxicity of peptides from Maedi Visna virus transactivating protein Tat

Isabella Starling^a, Ann Wright^b, Gordon Arbuthnott^{b,*}, Gordon Harkiss^c^a Division of Biomolecular Sciences, GKT Medical School, King's College London, Guy's Campus, St. Thomas Street, London SE1 9RT, UK^b Department of Preclinical Veterinary Sciences, R(D)SVS, University of Edinburgh, Summerhall, Edinburgh EH9 1QH, UK^c Department of Veterinary Pathology, R(D)SVS, University of Edinburgh, Summerhall, Edinburgh EH9 1QH, UK

Accepted 16 March 1999

Abstract

Lentiviruses such as Maedi Visna virus (MVV) in sheep, and human immunodeficiency virus (HIV) in man often cause a variety of neurological syndromes in later stages of infection. Neuropathological investigations reveal damage to myelin and astrogliosis in both white and grey matter. MVV infection induces axonal damage with some areas of necrosis while neuronal loss, and synaptic damage have been reported in HIV-1 infection. It is not clear, at present, how this neurodegeneration is mediated but, as these viruses do not directly infect neurons, an indirect neurotoxic action of the viruses is indicated. Previous experiments have shown that the intra-striatal injection in rats of a synthetic peptide derived from the basic region of the MVV transactivating protein Tat causes considerable neurotoxicity 1 week post-operatively. By in vivo stereotaxic injections of the same synthetic peptide, and subsequent immunocytochemical detection of neurons, astrocytes and microglia, we show that this neurotoxicity displays a distinctive and unusual lesion profile and is evident as rapidly as 0.5 h post-operatively. Furthermore, neuroprotection studies suggest that the early effects of the MVV tat peptide may involve glutamate neurotoxicity via the *N*-methyl-D-aspartate (NMDA) receptors since the application of dizolcipine (MK801) reduces the volume of the lesion seen at 1 h after the injection of neurotoxic peptide, while L-NAME is ineffective. The mechanism of this early neurotoxicity is thus different from the longer term actions already described. © 1999 Elsevier Science B.V. All rights reserved.

Keywords: Neurotoxicity; Lentivirus; Maedi Visna virus; Human immunodeficiency virus; Tat peptides; Rat

1. Introduction

Lentiviral infection of the central nervous system (CNS) causes damage of astrocytes, microglia and neurons. In Maedi Visna virus (MVV), post-mortem examination of the brains of affected sheep also reveals areas of liquefactive necrosis involving both neurones and glia in foci of infection [12]. In human immunodeficiency virus (HIV)-1 infection, neuronal loss is commonly observed in several areas including cortical regions and the basal ganglia [7,8]. Astrogliosis and some myelin damage are also characteristic features of both infections [2,11], although multinucleated giant cells are a hallmark of HIV infection [6]. Neither MVV nor HIV infect neurons, but HIV and MVV viral antigens have been co-localised with microglia, astrocytes and, occasionally oligodendrocytes [16,28,31]. Lentiviral

invasion of the CNS is believed to occur through the migration of infected macrophages across the blood brain barrier [23], although HIV may also penetrate the CNS via cell-free entry. Little cell free virus is usually present in lentiviral CNS infection. The neurotoxic capabilities of lentiviruses have therefore been attributed to indirect mechanisms.

Several lentiviral proteins have been proposed as neurotoxic candidates. The HIV envelope glycoprotein gp120 has been shown to be neurotoxic both in vivo and in vitro. In vitro, the neurotoxic mechanism of gp120 has been attributed to glutamate toxicity occurring at the *N*-methyl-D-aspartate (NMDA) receptor [18], aberrant calcium influx [17] or apoptotic mechanisms [1]. In vivo, gp120 causes neuronal damage [15], and transgenic mice overexpressing gp120 develop severe neurologic abnormalities [30].

The transactivating protein Tat of HIV and MVV is necessary for efficient lentiviral replication, although it only functions as a weak transactivator of MVV [3]. Lentiviral Tat contains amino acid sequences related to

* Corresponding author. Fax: +44-131-650-6177; E-mail: g.arbuthnott@ed.ac.uk

some snake venom neurotoxins [10] and has been shown to depolarise neurons [4,19]. Moreover, it is released from HIV infected cells and may move transcellularly [9]. HIV Tat protein and a peptide derived from the basic region of the protein have been found to be neurotoxic. Several investigators have documented this neurotoxicity in vitro and report HIV Tat to cause excitotoxic [26] or apoptotic [22] neuronal demise. Similarly, a peptide derived from the basic region of MVV Tat protein has been shown to be neurotoxic in vivo and in vitro. Its effects, in vitro, have been attributed to excessive calcium influx in neurons [29]. In vivo, the neurotoxic actions of MVV tat peptide, seen at 1 week after the injection, seemed to depend on nitric oxide mediated glutamate neurotoxicity [14], with the concomitant release of proinflammatory cytokines [24]. Here we report the rapidly developing neurotoxicity of the MVV tat peptide when administered in vivo to rat striatum, and conclude that although it is sensitive to NMDA antagonists at this early stage, nitric oxide synthesis inhibition does not protect striatal neurones during the first hour after the peptide injection.

2. Materials and methods

2.1. Stereotaxic injections

Fifty-two male Sprague–Dawley rats were anaesthetised with halothane and placed in a stereotaxic frame. The injection site was determined following the coordinates: 0.7 mm anterior to Bregma, 2.5 mm lateral and –5 mm ventral from the surface of the brain. Rats were either injected with 20 µg (9.6 nmol) MVV (22 rats) or 20 µg (9 nmol) HIV (4 rats) tat peptide dissolved in 1 µl sterile saline. The MVV tat peptide and a control ovalbumin peptide were synthesised by standard FMOC chemistry, desalted and purified, as previously described [14]. The HIV tat peptide was obtained from the MRC AIDS directed programme (Table 1).

In the neuroprotection experiments, 20 µg (25 nmol) L-NAME (Research Biochemicals International) was co-injected with the MVV tat peptide (6 rats). MK801 (Research Biochemicals International) was administered intraperitoneally at a dose of 0.01 mmol/kg 1 h before the injection of MVV tat peptide (9 rats).

Control injections were also made with 5 µg (56.8 nmol) ibotenic acid (Sigma) (2 rats), 0.9% sterile saline (2 rats), 100 µg (61.9 nmol) ovalbumin peptide (2 rats) and 20 µg (25 nmol) L-NAME (5 rats).

Table 1

Single letter amino acid code of the peptides used

Peptide	Amino acid code
MVV tat	(Ac)-MWKHKGAARRRNCGRCLC-(NH)
HIV tat	CFTTKALGISYGRKKRRRPPQGSQTHQVLSKQ
Ovalbumin	(Ac)-ISQAVHAAHAEINEAG-(NH)

(Ac): Acetylated.

(NH): Amidated position on the peptides synthesised *in house*.

HIV tat was obtained from the MRC AIDS directed programme.

Once the injection was made, the Hamilton syringe used was left in place for 5 min in order to minimise needle reflux. At the appropriate time after surgery, rats were injected intraperitoneally with a lethal dose of pentobarbitone (1 ml/kg, Sagatal) and transcardially perfused with 50 ml of warm saline containing 1000 units of heparin sulphate, followed by 300 ml of 4% paraformaldehyde, 0.05% glutaraldehyde in 0.1 M Phosphate buffer, pH 7.4. Their brains were dissected out and placed in a 50:50 solution of 20% sucrose and fixative overnight. Sections, 50 µm thick, were subsequently cut on a freezing microtome.

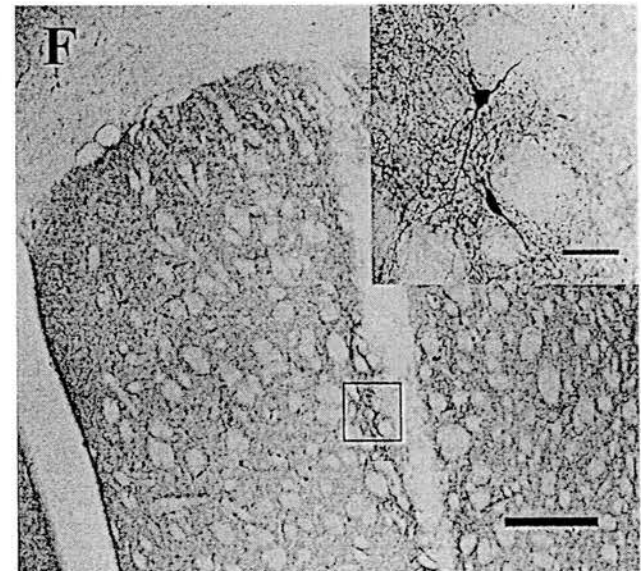
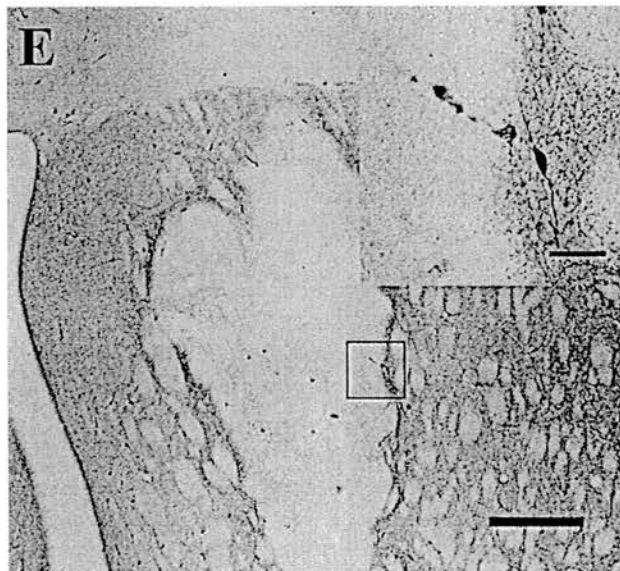
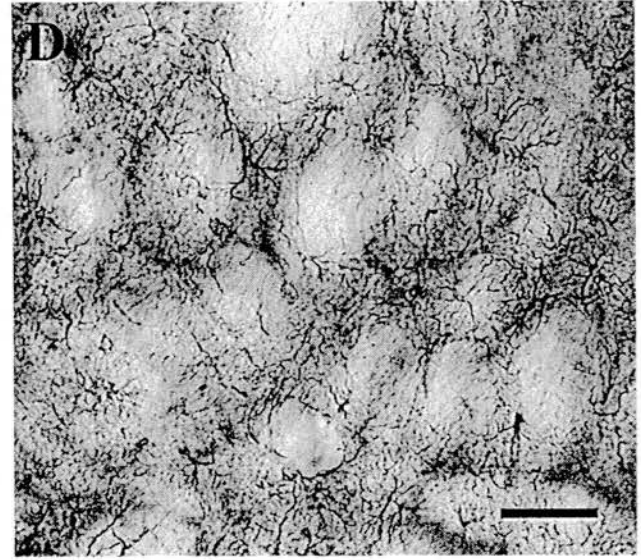
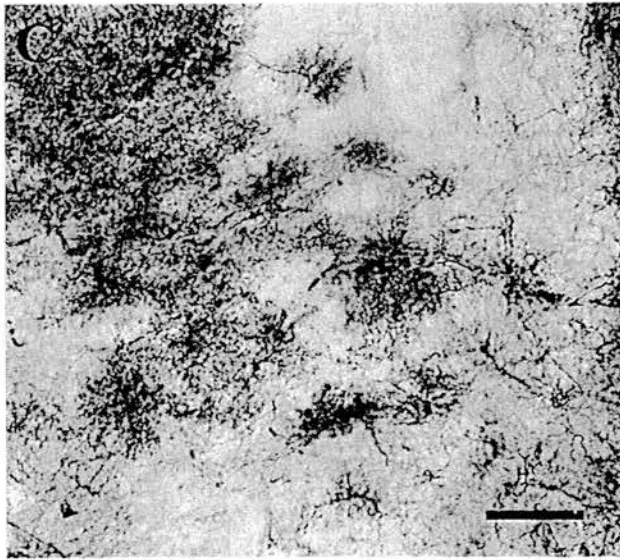
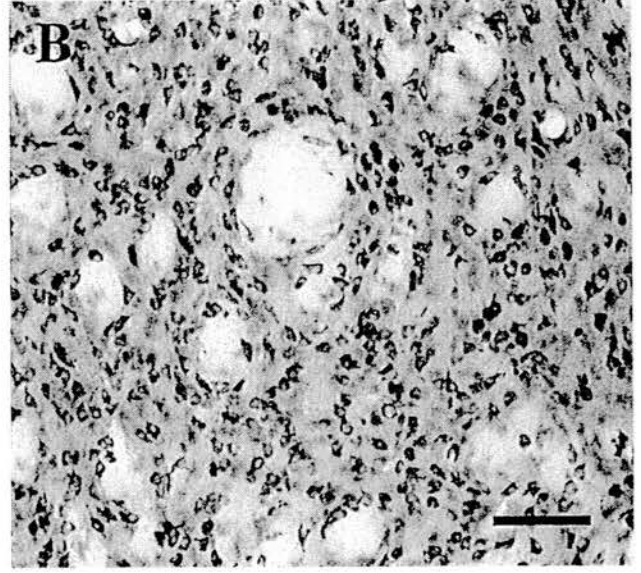
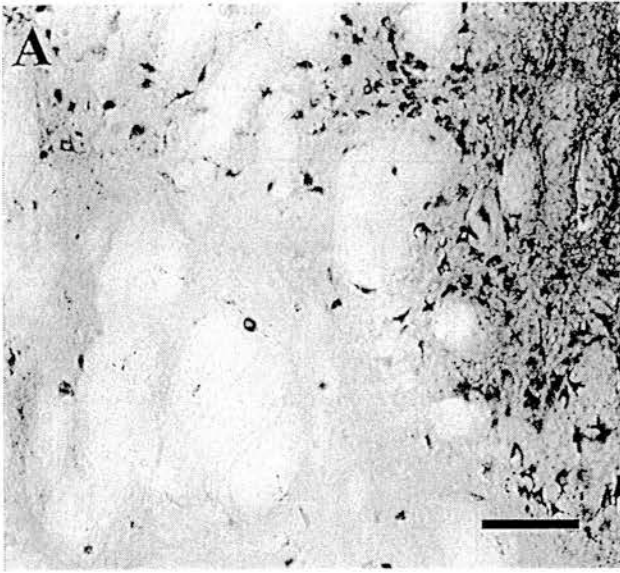
2.2. Immunocytochemistry

Free-floating sections were reacted histologically in multiwell plates. Immunocytochemistry was performed for Glial Fibrillary Acidic Protein (GFAP) to reveal astrocyte activation [20], the neuron specific nuclear protein NeuN to reveal possible neuronal damage [21,32], and the type 1 complement receptor (OX42) to estimate microglial activation [25]. The NADPH-Diaphorase method was also performed for the detection of NOS containing neurons [23]. The antibodies to GFAP (1:2000, Dako), OX42 (1:500, Serotec) and NeuN (1:500, a gift from Dr. R. Mullen) were revealed using the ABC method (Vectastain ABC and ABC Elite kits, respectively) with 3,3'-diaminobenzidine (Vector) as the chromogen.

2.3. Image analysis

Mounted sections were examined under the light microscope and camera lucida drawings were made of the entire lesioned area, including the pale area surrounding the injection site, in sections stained with NeuN. The volume of the lesioned area was measured by scanning the serial drawings of the lesioned area, and measuring the total area in the 'NIH Image' software package (<http://rsb.info.nih.gov/nih-image>). The total lesion volume was then calculated using the number of sections

Fig. 1. Immunocytochemical detection of the lesion caused by the MVV Tat peptide at 1 h. (A,C,E) injection of 1 µl MVV tat peptide, (B,D,F) injection of 1 µl control substances saline, ibotenic acid and ovalbumin, respectively. (A,B) NeuN immunocytochemistry shows a lack of staining in MVV tat peptide injected striatum (A) compared to control striatum (B). (C,D) Detection of GFAP in activated astrocytes shows an increase in GFAP activation at centre of the injection site with a halo devoid of staining surrounding the injection area (C). Some GFAP upregulation is visible with the injection of ibotenic acid (D). (E,F) Diaphorase histochemistry reveals a loss of NOS positive neurons and neuropile in MVV tat peptide injected striatum (E), minimal loss in control injected striatum (F), the insets in E and F show 10 × enlargements of the area within the boxes in the main pictures, to illustrate the cell morphology. Scale bar represents 100 µm in A, B, C, D, while in E and F the scale bars are 500 µm in the main picture, and 50 µm in the insets.



showing a lesion (n), the thickness of each section ($50 \mu\text{m}$), the number of immunocytochemical stains (δ) performed in the experiment (GFAP, NeuN, OX42 and Diaphorase) and the sum of the areas (x) of the drawings of lesion, according to the formula:

$$\text{lesion volume (mm}^3\text{)} = \sum x \times n \times 0.05 \times \delta$$

2.4. Stastical analysis

Areas of the lesions were compared with a one-way analysis of variance followed by Duncan's range test to indicate the source of any significant differences detected. We have used a significance level of $p < 0.05$ throughout.

3. Results

3.1. Lesion characteristics

The appearance of the lesion induced by the MVV tat peptide was distinctive and unusual. At the centre of the lesion, towards the location of the tip of the Hamilton syringe, cells appear darkened and distorted on sections processed for NeuN (Fig. 1A), GFAP (Fig. 1C) and OX42. On these same sections, the central area of the lesion was surrounded by a 'halo' of unstained cells. This profile was visible at all the short time intervals studied (0.5, 1 and 2

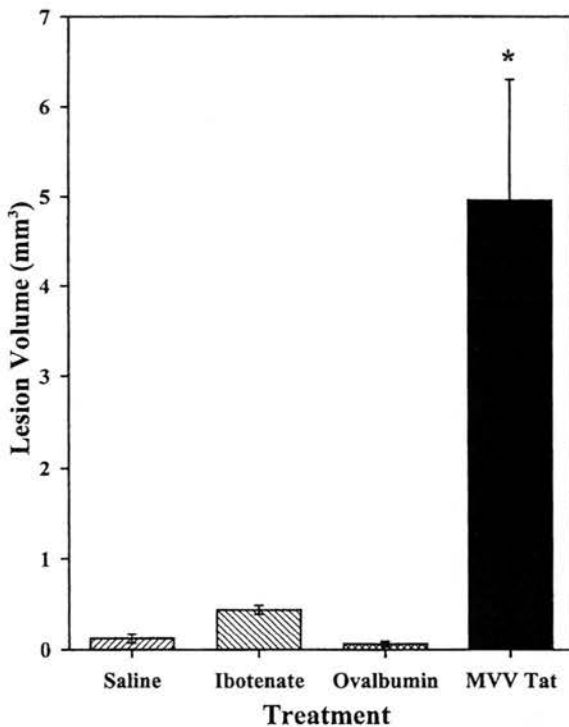


Fig. 2. Lesion volumes induced by the MVV tat peptide ($n = 3$), saline ($n = 2$), ibotenic acid ($n = 2$) and ovalbumin ($n = 2$) intra-striatal injections at 0.5 h. Values are mean \pm S.E.M. Control lesions were significantly smaller than the MVV tat peptide induced lesion (one-way ANOVA, $p < 0.05$; post hoc Duncan test, $*p < 0.05$).

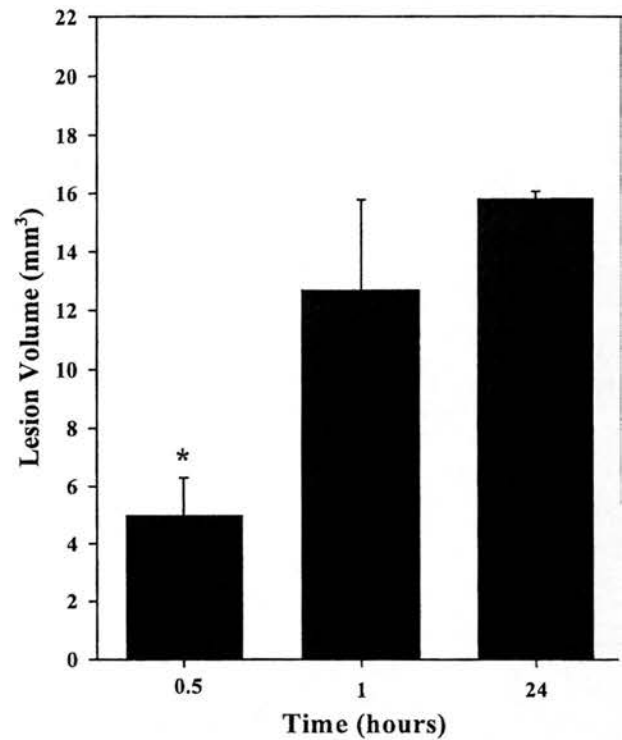


Fig. 3. Progress over time of the lesion caused by the MVV tat peptide. The lesion was measured according to disappearance of neuronal staining as revealed by immunocytochemistry for the NeuN antibody. The lesion occurs as rapidly as 0.5 h post-operatively ($n = 2$), is larger at 1 h ($n = 18$), and increases over a period of 24 h ($n = 2$). The lesion at 24 h which is of the same order of magnitude as that measured 1 week post-operatively, is significantly greater than that at 0.5 h (one-way ANOVA, $p < 0.05$; post hoc Duncan test, $*p < 0.05$).

h), although no 'halo' surrounded the older lesions studied previously [14]. The intracerebral injection of saline, ovalbumin, ibotenic acid and L-NAME did not cause a lesion as revealed by immunocytochemistry for neurons and astrocytes (Fig. 1B and D), but injection of HIV tat peptide had very similar effects to MVV tat peptide in the few animals on which we were able to test it (one rat perfused 0.5 h after the injection 3 at 1 h). On sections processed for Diaphorase histochemistry, the MVV tat peptide caused loss of staining of Diaphorase positive, NOS containing neurons at the injection site (Fig. 1E). It is interesting to note that the terminals of these cells were most affected, some cell bodies still being recognisable, even at the centre of the lesion. The injection of L-NAME is known to result in the disappearance of Diaphorase positive neurons [14]. None of the other control substances caused any alteration in Diaphorase staining. The state of microglial activation as revealed by OX42 staining, was minimal when compared to its optimal response, observed at 3 days post-operatively.

At 0.5 h, a one-way ANOVA revealed a significant effect of treatment on lesion volume. Post hoc analysis showed that the lesion volume caused by the MVV tat peptide was significantly different to that caused by t

three other control injections (Duncan test, $p < 0.05$, Fig. 2), HIV tat peptide produced a lesion of similar volume ($20.0 \pm 8.9 \text{ mm}^3$ at 1 h compared with $11.9 \pm 2.6 \text{ mm}^3$ for MVV tat at the same time point). At 1 h, the injection of L-NAME alone caused a reduction in Diaphorase staining that was significantly smaller than that following the injection of the MVV tat peptide (Duncan test, $p < 0.05$).

3.2. Time course

Administration of the MVV tat peptide induced a lesion in the striatum, visible with all the staining techniques used, as early as 0.5 h post-operatively (Fig. 3). The volume of the lesion induced by the MVV tat peptide increased over time between 0.5 and 24 h and was significantly greater at 1 and 24 h than at 0.5 h (one-way ANOVA and post hoc Duncan test, $p < 0.05$). The lesion visible at 24 h was of the same order of magnitude as that observed at 1 week.

3.3. Neuroprotection experiments

Since the lesion was nearly maximal 1 h after injection of the peptide, neuroprotective actions of two different treatments were tested at this timepoint. Administration of MK801 1 h before the peptide injection and co-injection of L-NAME with the peptide were tested. Statistical analysis revealed a reducing effect of MK801 on the volume of the lesion caused by the MVV tat peptide (one-way ANOVA

and post hoc Duncan test $p < 0.05$, Fig. 4), but the co-injection of L-NAME did not cause any significant difference in the volume of the lesion caused by the MVV tat peptide.

4. Discussion

We demonstrate here the acute in vivo neurotoxicity of a peptide derived from the basic region of the MVV transactivating protein Tat. Lentiviral Tat and related peptides have been previously found to be neurotoxic in vitro and in vivo [13,26,14,29,22], although their effects have not been studied at the short time courses investigated here. The current experiments therefore provide further evidence for the neurotoxic potential of this viral protein. Although the doses investigated here may be deemed high, Tat has been shown to be released in the vicinity of infected cells [9], and its levels may become elevated in the neighbourhood of many infected cells. Moreover, injections of similar doses of ibotenic acid, and a control peptide derived from ovalbumin, do not reveal any significant disruption to the brain parenchyma in vivo at this short time after the injection.

The lack of a lesion after injection of the well-known neurotoxin, ibotenic acid, points to the dramatically short time course of these experiments. At 1 week after the injection, the same dose of ibotenic acid caused a lesion almost double the size of that seen after the dose of MVV tat peptide used in these experiments [14]. Yet the peptide induced damage is almost as large at 1 h as it is at 1 week. Preliminary tests with injections of endothelin close to the middle cerebral artery, which cause large lesions after 24–72 h [27], also show the damage after tat peptide to occur more rapidly than the anoxic damage following arterial occlusion (Sharkey, Starling, Arbuthnott, unpublished).

The unusual profile of the lesion caused by the MVV tat peptide, with a surrounding 'halo' lacking neuronal staining, may be due to a number of actions of the peptide. Oedema surrounding the injection site is one possible explanation. The actions of the MVV tat peptide may also be amplified at distant sites due to neuronal glutamate release and increased receptor occupation. This may cause a greater number of neurons to die at the edges of the injection site. Indeed, lentiviral Tat has been shown to depolarise neurons [4,19] and may exert its neurotoxic effects via an overstimulation of calcium entry through glutamate receptors, to cause excitotoxicity [14,29]. Our present experiments also support this, as the administration of MK801, an NMDA glutamate receptor antagonist, reduces the volume of the lesion caused by the MVV tat peptide at 1 h.

It is possible that the lack of staining with NeuN does not in fact reflect the loss of neurones, although there are experiments which certainly indicate that it is a sensitive

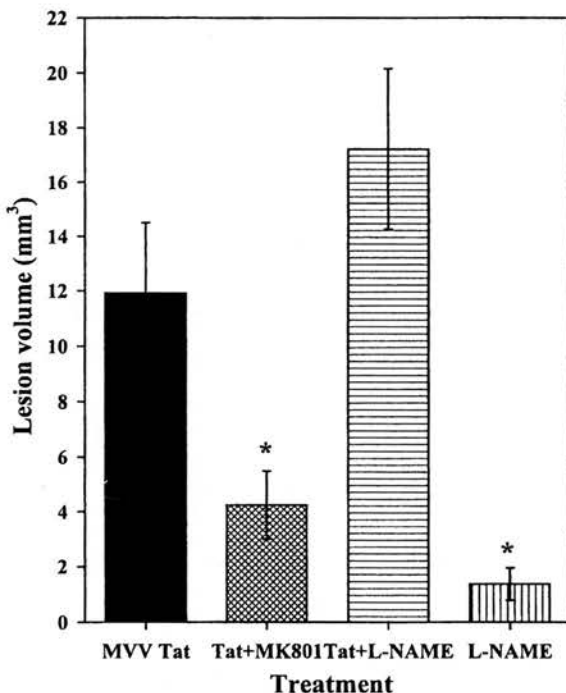


Fig. 4. Effect of MK801 and L-NAME on the MVV tat peptide induced lesion at 1 h. Values are mean \pm S.E.M. The volume of the lesion caused by the injection of the MVV tat peptide ($n = 18$) was reduced by the administration of MK801 ($n = 9$), but not by L-NAME ($n = 6$), (one-way ANOVA, $p < 0.05$; post hoc Duncan test, * $p < 0.05$).

marker for healthy neurons [32]. It is possible that some form of rapid degradation of the nuclear marker has reduced the staining, perhaps by some loss of access to the epitope recognised by the monoclonal antibody due to some modification of the antigen or neighbouring proteins in the nucleus. On the other hand, the size of the lesions observed with this method and with the markers for gliosis in the same sections is very similar. Perhaps more strikingly, the volumes of the lesion detected by different methods in the earlier work [14], are very similar to those detected by the loss of NeuN staining. Together these observations suggest that the lack of staining leads to, even if it does not immediately represent, the loss of viable neurones.

In an early description of the disease caused in sheep by MVV infection, Georgsson et al. [12] describes neuronal damage in areas of liquefactive necrosis as early as one month after the infection. Although the doses we have used are large, they were doses which were effective in producing large lesions in the longer-term studies [14]. Our aim was less to model the disease than to examine the dynamics of neuronal damage by this agent. We would expect that, if this peptide has any role in the generation of the neurotoxicity in the disease, then it will only be after the toxin has accumulated in the region of glial nodules containing infected cells. Should the peptide be made in any quantity, during the metabolism of tat released from such accumulations of infected cells, then rapid and permanent neuronal damage seems inevitable.

In conclusion, the MVV tat peptide exerts rapid neurotoxicity in vivo, which can be reduced by the administration of an NMDA receptor antagonist. This acute neurotoxicity, as well as the previously documented longer-term effects of lentiviral Tat, may offer insights into neuronal deficits in naturally occurring lentiviral diseases.

Acknowledgements

The work was supported by grants from the University of Edinburgh Faculty of Veterinary Medicine and AFRC. Stefan Hunt first alerted us to the very early actions of the tat peptide during the tenure of a Wellcome Trust summer studentship. Isabella Starling was an MRC Scholar in the Preclinical Veterinary Sciences Department. We are grateful to all our sponsors.

References

- [1] D. Aggoun-Zouaoui, C. Charriaud-Marlangue, S. Rivera, I. Jorquera, Y. Ben-Ari, A. Represa, The HIV-1 envelope protein gp120 induces neuronal apoptosis in hippocampal slices, *NeuroReport* 7 (1996) 433–436.
- [2] H. Budka, Neuropathology of human immunodeficiency virus infection, *Brain Pathol.* 1 (1991) 163–175.
- [3] L.M. Carruth, J.M. Hardwick, B.A. Morse, J.E. Clements, Visna virus tat protein: a potent transcription factor with both activator and suppressor domains, *J. Virol.* 68 (1994) 6137–6146.
- [4] J. Cheng, A. Nath, B. Knudsen, S. Hochman, J.D. Geiger, M. M. D.S.K. Magnuson, Neuronal excitatory properties of human immunodeficiency virus type 1 tat protein, *Neuroscience* 82 (1998) 97–107.
- [5] T.M. Dawson, D.S. Bredt, M. Fotuhi, P.M. Hwang, S.H. Snyder, Nitric oxide synthase and neuronal NADPH diaphorase are identical in brain and peripheral tissues, *Proc. Natl. Acad. Sci. USA* 88 (1991) 7797–7801.
- [6] D.W. Dickson, Multinucleated giant cells in acquired immunodeficiency syndrome, *Arch. Pathol. Lab. Med.* 110 (1986) 967–968.
- [7] I. Everall, P.J. Luthert, P.L. Lantos, Neuronal loss in the frontal cortex in HIV infection, *Lancet* 337 (1991) 1119–1121.
- [8] I. Everall, P.J. Luthert, P.L. Lantos, A review of neuronal damage in human immunodeficiency virus infection: its assessment, possible mechanism and relationship to dementia, *J. Neuropathol. Exp. Neurol.* 52 (1993) 561–566.
- [9] A.D. Frankel, C.O. Pabo, Cellular uptake of the tat protein from human immunodeficiency virus, *Cell* 55 (1988) 1189–1193.
- [10] R.F. Garry, G. Koch, Tat contains a sequence related to snake venom neurotoxins, *AIDS* 6 (1992) 1541–1542.
- [11] G. Georgsson, J.R. Martin, J. Klein, P.A. Palsson, N. Nathanson, C. Petrusson, Primary demyelination in visna—an ultrastructural study of Icelandic sheep with clinical signs following experimental infection, *Acta Neuropathol.* 57 (1982) 171–178.
- [12] G. Georgsson, P.A. Palsson, H. Panitch, N. Nathanson, G. Petrusson, The ultrastructure of early visna lesions, *Acta Neuropathol.* 5 (1977) 127–135.
- [13] I. Gourdou, K. Mabrouk, G. Harkiss, P. Marchot, N. Watt, F. Herberich, R. Vigne, Neurotoxicité chez la souris de portions riches en cytochromes des protéines Tat du virus visna et de VIH-1, *C.R. Acad. Sci. Paris* 311 (1990) 149–155, Series III.
- [14] M. Hayman, G.W. Arbuthnott, G. Harkiss, H. Brace, P. Filippi, V. Philippon, D. Thomson, R. Vigne, A.K. Wright, Neurotoxicity of peptide analogues of the transactivating protein tat from Maedi-Visna virus and human immunodeficiency virus, *Neuroscience* 53 (1993) 1–6.
- [15] J.M. Hill, R.F. Mervis, R. Avidor, T.W. Moody, D.E. Brenneman, HIV envelope protein induced neuronal damage and retardation of behavioural development in rat neonates, *Brain Res.* 603 (1992) 222–233.
- [16] K. Kure, W.D. Lyman, K.M. Weidenheim, D.W. Dickson, Cellular localisation of an HIV-1 antigen in subacute AIDS encephalitis using an improved double labeling immunohistochemical method, *Am. J. Pathol.* 136 (1990) 1085–1092.
- [17] S.A. Lipton, Calcium channel antagonists and Human Immunodeficiency Virus coat protein-mediated neuronal injury, *Ann. Neurol.* 30 (1991) 110–114.
- [18] S.A. Lipton, Models of neuronal injury in AIDS: another role for the NMDA receptor?, *Trends Neurosci.* 15 (1992) 75–79.
- [19] D.S.K. Magnuson, B.E. Knudsen, J.D. Geiger, R.M. Brownstone, A. Nath, Human immunodeficiency virus type 1 tat activates non-methyl-D-aspartate excitatory amino acid receptors and causes neurotoxicity, *Ann. Neurol.* 37 (1995) 373–380.
- [20] J. McQueen, A.K. Wright, G.W. Arbuthnott, G. Fink, Glial fibrillary acidic protein (GFAP)-immunoreactive astrocytes are increased in the hypothalamus of androgen-insensitive testicular feminized (Tfm) mice, *Neurosci. Lett.* 118 (1990) 77–81.
- [21] R.J. Mullen, C.R. Buck, A.M. Smith, NeuN: a neuronal specific nuclear-protein in vertebrates, *Development* 116 (1992) 201–211.
- [22] D.R. New, M. Ma, L.G. Epstein, A. Nath, H.A. Gelbard, Human immunodeficiency virus type 1 Tat protein induces death by apoptosis in human neuron cultures, *J. Neurovirol.* 2 (1997) 168–173.
- [23] R. Peluso, A. Haase, L. Stowring, M. Edwards, P. Ventura, Trojan Horse mechanism for the spread of visna virus in monocytic cells, *Virology* 147 (1985) 231–236.
- [24] V. Philippon, C. Vellutini, D. Gambarelli, G. Harkiss, G. Arbuthnott

- nott, D. Metzger, R. Roubin, P. Filippi, The basic domain of the lentiviral Tat protein is responsible for damages in mouse brain: involvement of cytokines, *Virology* 205 (1994) 519–529.
- [25] A.P. Robinson, T.M. White, D.W. Mason, Macrophage heterogeneity in the rat as delineated by two monoclonal antibodies MRC OX41 and MRC OX42, the latter recognising the complement receptor type 3, *Immunology* 57 (1986) 239–247.
- [26] J.-M. Sabatier, E. Vives, K. Mabrouk, A. Benjouad, H. Rochat, A. Duval, B. Hue, E. Bahraoui, Evidence for neurotoxic activity of tat from human immunodeficiency virus type 1, *J. Virol.* 65 (1991) 961–967.
- [27] J. Sharkey, S.P. Butcher, Characterization of an experimental model of stroke produced by intracerebral microinjection of endothelin-1 adjacent to the rat middle cerebral artery, *J. Neurosci. Meth.* 60 (1998) 125–131.
- [28] L. Stowring, A.T. Haase, G. Petursson, G. Georgsson, P.A. Palsson, R. Lutley, R. Roos, S. Szuchet, Detection of visna virus antigens and RNA in glial cells in foci of demyelination, *Virology* 141 (1985) 311–318.
- [29] P.J.L.M. Srijbos, M.R. Zamani, N.J. Rothwell, G. Arbuthnott, G. Harkiss, Neurotoxic mechanisms of transactivating protein Tat of Maedi-Visna virus, *Neurosci. Lett.* 197 (1995) 215–218.
- [30] S.M. Toggas, E. Masliah, E.M. Rockenstein, G.F. Rall, C.R. Abraham, L. Mucke, Central nervous system damage produced by the expression of the HIV-1 coat protein gp120 in transgenic mice, *Nature* 367 (1994) 188–193.
- [31] C. Tornatore, K. Meyers, W. Atwood, K. Conant, E. Major, Temporal patterns of human immunodeficiency type 1 transcripts in human fetal astrocytes, *J. Virol.* 68 (1994) 93–102.
- [32] H.K. Wolf, R. Buslei, R. Schmidtkastner, P.K. Schmidtkastner, T. Pietsch, O.D. Wiestler, I. Blumcke, NeuN—a useful neuronal marker for diagnostic histopathology, *J. Histochem. Cytochem.* 44 (1996) 1167–1171.